



Recovery of lipids from spent coffee grounds for use as a biofuel

Ioannis Efthymiopoulos

Submitted in partial fulfilment of the requirements
for the degree of Doctor of Philosophy
at University College London.

February 2018

I, Ioannis Efthymiopoulos confirm that the work presented in this thesis is my own. Where information has been derived from other sources, I confirm that this has been indicated in the thesis.

Dated:

Abstract

Spent coffee grounds (SCG) are the main residues of the coffee industry, and a potentially valuable source of lipids for sustainable biodiesel production. However, feedstock properties, such as the high SCG moisture content and the relatively high free fatty acid (FFA) content of recovered oil, can impact on the efficiency of the extraction and the quality of extracted oil and derived biodiesel, thus reducing the possible environmental benefits of producing biodiesel from this waste stream. Therefore, a better understanding of feedstock properties and processing steps is required to improve the efficiency of SCG valorization as a biodiesel feedstock and contribute to its future industrialization.

This work presents experimental studies including feedstock characterization of SCG, laboratory and pilot plant scale solvent extraction experiments and utilization of mechanical pressing for processing of coffee residues. The solvent extraction experiments investigated effects of solvent type, SCG moisture content and particle size, SCG-to-solvent ratio, and the duration, temperature and pressure of the extraction process on oil extraction efficiency and composition. Transesterification was performed with SCG oil containing high FFA content, and the combustion of derived biodiesel was investigated in a compression-ignition engine.

Instant SCG were found to possess higher lipid and FFA content than retail SCG. Solvent extraction experiments showed that longer durations, higher temperatures, low moisture presence and mixed size SCG particles generally improved extraction efficiency, while the impact of pressure depended on temperature. A correlation was observed between longer extraction durations and lower FFA content, while extraction temperature and solvent selection affected the oil composition. Pilot plant extraction showed reduced sensitivity to moisture, while mechanical pressing was efficient in removing a fraction of residual moisture. A two-step transesterification process achieved a biodiesel conversion yield of 86.7 % relative to initial oil weight. SCG biodiesel showed similar combustion and emissions characteristics to commercial soybean and rapeseed biodiesel.

Research impact statement

The present study has demonstrated that oil extracted from SCG can be successfully converted into biodiesel despite its high acidity, and that this biodiesel has combustion and emission characteristics comparable to commercial biodiesel samples. Extracting lipids from SCG and converting them into biodiesel adds a considerably greater value to processing this waste material relative to currently used practices that include drying and using SCG as solid fuel or compost.

This work has shown that mechanical pressing can be used as a less energy-intensive moisture removal method relative to thermal drying to obtain partially dried SCG, whereas experimentation with various solvents at conditions of elevated temperature and pressure proved that relatively high oil recoveries can be achieved from wet or partly dried SCG with polar solvents. Such findings can improve the sustainability of producing biodiesel from SCG, thus facilitating its future industrialization. The knowledge gained from this research has contributed to the undertaking of large scale production of SCG biodiesel from Bio-bean Ltd., and to its subsequent utilization as a fuel blend with fossil diesel in London buses.

This thesis is a comprehensive case study including all the processing steps required to transform SCG into a high value biofuel and an assessment of its performance in an engine. In particular, the present study demonstrates how moisture removal, oil extraction and transesterification techniques can be applied to a waste material like SCG, while several experimental aspects are investigated for the first time, such as the influence of elevated temperature and pressure on the efficiency of solvent extraction from SCG and the determination of combustion and emissions characteristics of the produced biodiesel. Other aspects are covered in significantly greater detail relative to previous works, for example the use of mechanical pressing for SCG processing.

To date, this work has resulted in the publication of three peer-reviewed journal papers:

- I. Efthymiopoulos, P. Hellier, N. Ladommatos, A. Kay, B. Mills-Lampzey, “Effect of Solvent Extraction Parameters on the Recovery of Oil From Spent Coffee Grounds for Biofuel Production” *Waste Biomass Valor* (2017), <https://doi.org/10.1007/s12649-017-0061-4>.
- I. Efthymiopoulos, P. Hellier, N. Ladommatos, A. Russo-Profili, A. Eveleigh, A. Aliev, A. Kay, B. Mills-Lampzey, “Influence of solvent selection and extraction temperature on yield and composition of lipids extracted from spent coffee grounds”, *Industrial Crops and Products*, Volume 119 (2018), <https://doi.org/10.1016/j.indcrop.2018.04.008>.
- I. Efthymiopoulos, P. Hellier, N. Ladommatos, A. Kay, B. Mills-Lampzey, “Integrated strategies for water removal and lipid extraction from coffee industry residues”. *Sustainable Energy Technologies and Assessments*, (2018), <https://doi.org/10.1016/j.seta.2018.06.016>.

In addition, a further two papers based on this work are currently under preparation. Finally, results obtained during this study were presented at the following international conferences:

- International Bioenergy Conference, Manchester, UK. March 22-23, 2017. Poster presentation, “Effect of solvent extraction parameters on the recovery of oil for biodiesel production from spent coffee grounds”.
- XXVI International Materials Research Congress, Cancun, Mexico. August 20-25, 2017. Oral presentation, “Impact of solvent properties with varying temperature and pressure for extraction of lipids from spent coffee grounds for biodiesel production”.

Acknowledgements

First and foremost, I wish to thank my PhD supervisor, Dr. Paul Hellier for his continuous support and guidance. His ideas, knowledge, technical expertise and practical assistance have been invaluable throughout the course of this project. I am also grateful to Professor Nicos Ladommatos, whose support, counsel and contributions to this research have been much appreciated.

I would like to thank my industrial collaborators for this PhD, Bio-Bean Ltd., for the financial contribution to the project and for providing several of the samples used in the experimental part of this work. Many thanks go to Mr. Arthur Kay and Dr. Ben Mills-Lamprey for their ideas and guidance and for offering me the opportunity to perform large scale experiments.

Thanks are due to Mr. Alessandro Russo Profili and Dr. Aaron Eveleigh for performing the spectroscopic analysis, and to Ms. Anastasia Papadopoulou for the viscosity measurement tests. I would also like to thank Dr. Rhianna Briars for her help with gas chromatography and Dr. Midhat Talibi for his assistance in solving various experimental issues throughout my PhD.

I thank all of my friends and colleagues with whom I have shared the UCL Thermodynamics Laboratory: Gokce, Maria, Viktor, Ahmad, Hamisu and Christopher. Thank you for making this experience much more pleasurable. To all those working in the UCL's Nanoengineered Systems Laboratory, thank you for your assistance and company and for tolerating my continuous presence while I was conducting experiments in the fume cupboard.

For their constant encouragement and support, I must express my gratitude to my parents, Mr Thomas Efthymiopoulos and Dr. Vasiliki Mousga, and to my friends. Finally, special thanks are due to Ms. Marion Kagka for her infinite support and patience.

Table of Contents

Abstract	3
Research impact statement	4
Aknowledgements	6
List of Figures	11
List of Tables	19
Nomenclature	21
1. Introduction	23
1.1 Thesis structure	26
2. Literature review	28
2.1 Availability of coffee.....	28
2.2 Processing of coffee beans within the beverage industry.....	31
2.2.1 Production of green coffee	31
2.2.2 Roasting of green coffee beans	35
2.2.3 Coffee brewing.....	38
2.3 Spent coffee grounds.....	39
2.3.1 Energy content.....	43
2.3.2 Lipids	45
2.3.3 Moisture content and dewatering of SCG.....	53
2.4 Oil extraction.....	55
2.4.1 Solvent extraction	55
2.4.2 Supercritical fluid extraction	70
2.4.3 Mechanical expression	72
2.4.4 Defatted SCG	74
2.5 Utilization of SCG lipids for biodiesel production.....	77
2.5.1 Transesterification of SCG lipids	77
2.5.2 Direct transesterification of SCG	85
2.5.3 Biodiesel derived from SCG oil	87

2.6 Conclusions	92
2.7 Research objectives	93
3. Experimental Materials and Methodology.....	95
3.1 Materials.....	95
3.1.1 Coffee samples.....	95
3.1.2 Extraction solvents.....	95
3.2 Methods	101
3.2.1 Thermal drying SCG for moisture removal and water content determination	101
3.2.2 Particle sizing of dry SCG	103
3.2.3 Laboratory scale solvent extraction.....	105
3.2.4 Pilot plant scale solvent extraction	116
3.2.5 Mechanical expression	117
3.2.6 Free fatty acid content determination through titration.....	121
3.2.7 Transesterification process	123
3.2.8 Determination of fatty acid profile.....	127
3.2.9 Determination of gross calorific value.....	128
3.2.10 Ash content determination	130
3.2.11 Combustion experiments	130
4. Characterization of SCG	134
4.1 Characteristics of solid samples and extracted lipids	134
4.2 SCG drying characteristics.....	142
4.3 Conclusions	144
5. Effect of solvent extraction parameters and SCG properties on the efficiency of oil recovery	146
5.1 Soxhlet solvent extraction	146
5.1.1 Effect of process duration and SCG-to-solvent ratio on lipid extraction efficiency	146

5.1.2 Effect of SCG particle diameter and moisture content on lipid extraction efficiency	149
5.1.3 Effect of solvent selection on lipid extraction efficiency	154
5.2. Pilot plant solvent extraction	162
5.3 Conclusions	167
6. Effect of elevated temperature and pressure on the efficiency of oil recovery through solvent extraction.....	169
6.1 Accelerated solvent extraction.....	169
6.1.1 Effect of process temperature on lipid extraction efficiency	171
6.2 Solvent extraction in a closed pressurized vessel.....	175
6.2.1 Effect of pressure on lipid extraction efficiency.....	175
6.2.2 Effect of pressurized solvent extraction duration and number of extraction cycles on lipid extraction efficiency	179
6.3 Conclusions	182
7. Combined mechanical pressing and solvent extraction for water removal and lipid recovery.....	184
7.1 Mechanical pressing for water removal from SCG.....	184
7.2 Mechanical expression of lipids.....	186
7.3 Mechanical pressing as pretreatment prior to solvent extraction.....	188
7.4 Conclusions	192
8. Transesterification of SCG lipids and engine tests.....	194
8.1 Transesterification of SCG lipids.....	194
8.1.1 Acid-catalyzed pretreatment	194
8.1.2 Base-catalyzed transesterification.....	199
8.1.3 Oil and biodiesel properties.....	204
8.2 Combustion experiments.....	209
8.3 Conclusions	230
9. Conclusions and recommendations for further work	232
9.1 Conclusions	232

9.2 Recommendations for future work	235
A. Pressure vessel design.....	237
A.1 Determination of minimum wall thickness requirements.....	237
A.2 O-ring	238
A.3 Threads.....	238
A.4 Catia Drawings	239
B. Mechanical ram press design	241
B.1 Determination of minimum wall thickness requirements.....	241
B.2 O-rings	242
B.2.1 Piston O-rings.....	242
B.2.2 Internal cylinder O-rings	242
B.3 Threads.....	243
B.4 Catia Drawings	244
C. Density calculation.....	247
D. NHE methods and molecular weight of SCG oil fatty acids	249
D.1 NHE transesterification method.....	249
D.2 NHE GC method	250
D.3 Percentage and molecular weight of SCG oil fatty acids.....	251
E. Fuel samples specifications.....	252
F. GC-FID	253
G. Engine specifications.....	260
H. NMR method	261
I. Elemental analysis of oil and biodiesel samples.....	265
J. Viscosity measurement	272
References.....	275

List of Figures

Figure 2.1: Annual production of roasted coffee worldwide (International Coffee Association, 2016).....	28
Figure 2.2: Production of coffee in 2015/16 per country (International Coffee Association, 2016).	29
Figure 2.3: Global consumption of roasted coffee per year (International Coffee Association, 2016).....	30
Figure 2.4: Coffee berry structure and sections (adapted from Bresciani et al. (2014))	32
Figure 2.5: Flow-sheet presenting main coffee processing methods (adapted from Franca and Oliveira (2009))	33
Figure 3.1: Overall schematic of processing methods.	101
Figure 3.2: (a) SCG samples contained in pyrex petri dishes during drying, (b) Exterior of oven model used in drying experiments (adapted from “ http://www.keison.co.uk/nabertherm_tr.shtml ”).....	102
Figure 3.3: Sieves loaded with spent coffee grounds and sieve shaker.....	104
Figure 3.4: Schematic representation of the Soxhlet extractor, (adapted from Anisa Aris and Morad (2014)).	106
Figure 3.5: Solvent extraction (Soxhlet) in a fume cupboard.	107
Figure 3.6: ASE 150 key operating features (adapted from (ThermoFisher, 2011)).	108
Figure 3.7: Schematic showing internal gas and solvent flows within the ASE (adapted from (ThermoFisher, 2011)).....	109
Figure 3.8: Prototype stainless steel vessel for static solvent extraction.....	111
Figure 3.9: Schematic representation of experimental setup.	112
Figure 3.10: Rotary evaporator key operating features (adapted from “ http://www.ika.com/owa/ika/catalog.product_detail?iProduct=10002170 ”).....	113
Figure 3.11: Overall schematic of the pilot plant used in extraction experiments.	116
Figure 3.12: Major components of the ram press.....	118
Figure 3.13: Overall schematic of the ram press.....	119
Figure 3.14: Screw press used for SCG mechanical expression.	120

Figure 3.15: Titration experimental set-up (adapted from “ http://sachiacidbase.weebly.com/titrations.html ”).	122
Figure 3.16: Main parts of GC machine.	127
Figure 3.17: (a) Bomb calorimeter (adapted from “ https://www.laboratory-equipment.com/calorimeters/c1-calorimeter-ika.php ”), (b) cutaway view of the equipment (adapted from “ http://docslide.us/documents/thermochemical-equations-calorimetry-at-the-end-of-this-lesson-you-should.html ”).	129
Figure 3.18: Schematic showing operation of the low volume fuel system (adapted from Hellier et al. (2013)).	131
Figure 4.1: Relationship between moisture content and dried particle diameter of five SCG samples. Error bars show standard deviation (σ) calculated from three experimental repeats.	137
Figure 4.2: Relationship between moisture content and dried particle diameter of three ICG samples. Error bars show standard deviation (σ) calculated from three experimental repeats.	137
Figure 4.3: Relationship between moisture content and oil FFA content of SCG samples. Error bars show standard deviation (σ) calculated from three experimental repeats.	139
Figure 4.4: Relationship between oil content of dry SCG samples and FFA content of the oil. Error bars shown represent standard deviation (σ) calculated from three experimental repeats.	141
Figure 4.5: Moisture removal from ICG1 over time with varying sample thickness (7.5-15 mm) and drying temperature (100-200 °C). The standard deviations (σ) shown were calculated from 3 experimental repeats.	142
Figure 4.6: Moisture removal over time with different SCG samples. The standard deviations (σ) shown were calculated from 3 experimental repeats.	143
Figure 5.1: Oil yields per mass of dry ICG1 weight achieved at different Soxhlet extraction durations (0.5 to 24 hours). Error bars show the standard deviation of the mean calculated by three experimental repeats at each timing setting.	146
Figure 5.2: Correlation of the % w/w FFA content of extracted coffee oil with the duration of solvent extraction (2-24 h). The error bars show the standard	

deviation calculated from three titration measurements with oil samples extracted at different durations.....	147
Figure 5.3: ICG1 oil yield achieved at varying SCG-to-solvent ratios. The error bars show the standard deviation calculated from three experimental repeats at each SCG-to-solvent ratio setting.	148
Figure 5.4: Particle diameter distribution of various coffee samples after complete moisture removal. The error bars shown represent the standard deviation of the mean calculated from 3 sizing repeats with the available sieves.....	149
Figure 5.5: Oil yield of various SCG samples when different particle size fractions were used. The error bars represent the standard deviation (σ) of the mean calculated from three experimental repeats.	151
Figure 5.6: Crude extract yields on a dry weight basis versus the respective moisture content for 4 and 8 hours Soxhlet extractions with hexane. The error bars represent standard deviation (σ) calculated from three experimental repeats at each timing setting.	152
Figure 5.7: Crude extract yields on a dry weight basis versus the respective moisture content for 8 hours Soxhlet extractions with ethanol. Error bars represent standard deviation ($\sigma=0.9$) calculated from three experimental repeats.....	153
Figure 5.8: Crude extract extraction ratio versus the E_T^N polarity parameter of the solvent used. Error bars show the standard deviation ($\sigma=3.2$) calculated from three experimental repeats.	154
Figure 5.9: Crude extract extraction ratios extracted versus solvent boiling point. Error bars show the standard deviation ($\sigma=3.2$) calculated from three experimental repeats.	155
Figure 5.10: % w/w FFA content of crude extract samples extracted with various solvents, versus E_T^N solvent polarity parameter. Error bars show the standard deviation ($\sigma=0.9$) calculated from a total of 40 experiments.....	158
Figure 5.11: Relationship between crude extract FFA content obtained through titration and NMR analysis. The error bars represent the standard deviation of the mean ($\sigma=0.9$) for titration results calculated from a total of 40 experiments.	159

Figure 5.12: Composition of oil samples obtained from Soxhlet extraction using different extraction solvents, using ^1H NMR analysis.	160
Figure 5.13: Oil yields and FFA percentages obtained from pilot plant extractions with isohexane.	162
Figure 6.1: Oil yields obtained through ASE with hexane with varying number of static extraction cycles and static cycle duration. The standard deviations (σ) were calculated from three experimental repeats.	170
Figure 6.2: Oil extraction ratios obtained using ASE at various temperatures with different solvents. The standard deviations (σ) were calculated from three experimental repeats.	171
Figure 6.3: Composition of oils obtained from ASE extractions with hexane and ethanol at elevated temperatures, using ^1H NMR spectra.	173
Figure 6.4: Oil extraction ratio obtained against applied pressure at extraction temperatures of 25, 45 and 65 °C. The error bars show the standard deviation (σ) of the mean calculated from 3 experimental repeats at each temperature setting.	175
Figure 6.5: Oil extraction ratios obtained against duration of static extraction at 75 bar and 45 °C. Error bars stand for the standard deviation ($\sigma=0.4$) that was calculated by three experimental repeats.	179
Figure 6.6: Oil extraction ratios obtained from multiple static extraction cycles and washing stages. The standard deviations of the mean that are shown were calculated by sets of three experimental repeats.	181
Figure 7.1: Percentage of moisture removed from wet SCG versus applied pressure at various conditions of temperature and pressing duration. The standard deviation (σ) was 1.0 as calculated from 3 experimental repeats.	184
Figure 7.2: Percentage of moisture removed from wet SCG versus pressing duration at ambient temperature and different pressures. The standard deviation (σ) was 1.0 as calculated from 3 experimental repeats.	185
Figure 7.3: Oil extraction ratios obtained through ASE with SCG pressed at various pressures and thermally dried. Error bars represent standard deviation ($\sigma=0.6$) that was calculated from three experimental repeats.	189
Figure 7.4: Crude extract extraction ratios obtained through ASE with hexane and ethanol against the moisture content of the SCG sample. The standard deviations were calculated from three experimental repeats.	190

Figure 8.1: FFA content of ICG2 oil versus duration of acid-catalyzed esterification at a constant catalyst-to-FFA weight percentage of 3.2 % w/w. The standard deviation of each point was found to be 0.3 as calculated from three experimental repeats and a total of 27 titration measurements. 196

Figure 8.2: FFA content of ICG2 oil versus duration of acid-catalyzed esterification at a constant catalyst-to-FFA weight percentage of 6.4 % w/w. The standard deviation of each point was found to be 0.3 as calculated from three experimental repeats and a total of 27 titration measurements. 196

Figure 8.3: Base-catalyzed transesterification reaction yields against catalyst-to-pretreated oil weight percentage. The standard deviation (σ) was found to be 0.5 as calculated by a total of 9 experimental repeats. 200

Figure 8.4: Base-catalyzed transesterification reaction yield against methanol-to-pretreated oil molar ratio. The error bars represent standard deviation ($\sigma=0.5$) that was calculated from three experimental repeats. 202

Figure 8.5: (a) In-cylinder pressure of ICG2 oil, reference diesel and 100 % v/v ICG2, soya and rapeseed FAMES, (b) 20 % v/v FAME and fossil diesel blends, (c) 7 % v/v FAME and fossil diesel blends at constant injection timing. 211

Figure 8.6: (a) In-cylinder pressure of ICG2 oil, reference diesel and 100 % v/v ICG2, soya and rapeseed FAMES, (b) 20 % v/v FAME and fossil diesel blends, (c) 7 % v/v FAME and fossil diesel blends at constant ignition timing. 212

Figure 8.7: (a) Heat release rate of ICG2 oil, reference diesel and 100 % v/v ICG2, soya and rapeseed FAMES, (b) 20 % v/v FAME and fossil diesel blends, (c) 7 % v/v FAME and fossil diesel blends at constant injection timing. 214

Figure 8.8: (a) Heat release rate of ICG2 oil, reference diesel and 100 % v/v ICG2, soya and rapeseed FAMES, (b) 20 % v/v FAME and fossil diesel blends, (c) 7 % v/v FAME and fossil diesel blends at constant ignition timing. 215

Figure 8.9: Ignition delay against biodiesel content at conditions of constant injection timing. The error bars shown represent standard deviation ($\sigma=0.16$) calculated by 6 experimental repeats with reference diesel. 217

Figure 8.10: Ignition delay against biodiesel content at conditions of constant ignition timing. The error bars shown represent standard deviation ($\sigma=0.18$) calculated by 6 experimental repeats with reference diesel.	217
Figure 8.11: Peak heat release rate against biodiesel content at constant injection timing. The error bars shown represent standard deviation ($\sigma=2.9$) calculated by 6 experimental repeats with reference diesel.	219
Figure 8.12: Peak heat release rate against biodiesel content at constant ignition timing. The error bars shown represent standard deviation ($\sigma=5.6$) calculated by 6 experimental repeats with reference diesel.	219
Figure 8.13: Exhaust gas NO _x emissions of fuel samples and reference fossil diesel against biodiesel content at constant injection timing. The error bars shown represent standard deviation ($\sigma=46.7$) calculated by 6 experimental repeats with reference diesel.	221
Figure 8.14: Exhaust gas NO _x emissions of fuel samples and reference fossil diesel against biodiesel content at constant ignition timing. The error bars shown represent standard deviation ($\sigma=40.2$) calculated by 6 experimental repeats with reference diesel.	221
Figure 8.15: CO emissions against biodiesel content at constant injection timing. The error bars shown represent standard deviation ($\sigma=7.3$) calculated by 6 experimental repeats with reference diesel.	223
Figure 8.16: CO emissions against biodiesel content at constant ignition timing. The error bars shown represent standard deviation ($\sigma=10.1$) calculated by 6 experimental repeats with reference diesel.	224
Figure 8.17: THC emissions against biodiesel content at constant injection timing. The error bars shown represent standard deviation ($\sigma=7.6$) calculated by 6 experimental repeats with reference diesel.	224
Figure 8.18: THC emissions against biodiesel content at constant ignition timing. The error bars shown represent standard deviation ($\sigma=9.5$) calculated by 6 experimental repeats with reference diesel.	225
Figure 8.19: (a) Particulate emissions of ICG2 oil, reference diesel and 100 % v/v ICG2, soya and rapeseed FAMES, (b) 20 % v/v FAME and fossil diesel blends, (c) 7 % v/v FAME and fossil diesel blends at constant injection timing.	226

Figure 8.20: (a) Particulate emissions of ICG2 oil, reference diesel and 100 % v/v ICG2, soya and rapeseed FAMES, (b) 20 % v/v FAME and fossil diesel blends, (c) 7 % v/v FAME and fossil diesel blends at constant ignition timing.	227
Figure 8.21: Total particulate mass emitted against biodiesel content at constant injection timing. The error bars shown represent standard deviation ($\sigma=0.002$) calculated by 6 experimental repeats with reference diesel.	229
Figure 8.22: Total particulate mass emitted against biodiesel content at constant ignition timing. The error bars shown represent standard deviation ($\sigma=0.006$) calculated by 6 experimental repeats with reference diesel.	229
Figure A.1: Internal cylinder drawing.....	239
Figure A.2: External cylinder drawing.	240
Figure B.1: External cylinder drawing.	244
Figure B.2: Internal cylinder drawing.....	244
Figure B.3: Piston drawing.	245
Figure B.4: Upper cap drawing.	245
Figure B.5: Supporting plate drawing.....	246
Figure B.6: Handle drawing.....	246
Figure C.1: ICG2 oil density determination.	247
Figure C.2: ICG2 pretreated oil density determination (conditions of acid-catalyzed pretreatment can be found in Table 8.1 - Trial 5).....	247
Figure C.3: ICG2 biodiesel density determination.....	248
Figure F.1: Supelco 37 Component FAME Mixture on SP-2380 Column. ...	254
Figure F.2: GC-FID chromatogram obtained with 37 FAME component mixture.	255
Figure F.3: GC-FID chromatogram obtained with ICG2 biodiesel ((Table 8.2 – trial 6).	255
Figure F.4: GC-FID chromatogram obtained with soya biodiesel.....	256
Figure F.5: GC-FID chromatogram obtained with soya biodiesel.....	256
Figure H.1: Example ^1H NMR spectrum highlighting some main spectral peaks and their assignments. Spectrum shown is of the oil extracted from SCG using ASE with hexane solvent at 125 °C. (a) $-\text{CH}_3$, (b) $-(\text{CH}_2)_n-$, (c) $-\text{OCO}-\text{CH}_2-\text{CH}_2-$, (d) $\text{CH}_2-\text{CH}=\text{CH}$, (e) $-\text{OCO}-\text{CH}_2-$, (f) $=\text{HC}-\text{CH}_2-\text{CH}=\text{}$, (g) $\text{R}'\text{OCH}_2-\text{CH}(\text{OR}')-$	

CH₂OR", (h) R'OCH₂-CH(OR')-CH₂OR", (i) -CH=CH-, (j) residual solvent
CHCl₃..... 262

List of Tables

Table 2.1: Chemical composition of green and roasted coffee beans (adapted from Farah (2012)).	36
Table 2.2: Characterization of dry SCG.	41
Table 2.3: HHVs of dried SCG and SCG oil.	44
Table 2.4: Dry weight oil yields extracted from other researchers.	45
Table 2.5: Fatty acid composition of SCG oils.	48
Table 2.6: Characterization of SCG oil.	52
Table 2.7: Soxhlet extraction oil yields on a dry weight basis reported in other studies when hexane was the solvent used.	58
Table 2.8: Characterization of defatted SCG.	75
Table 2.9: Properties of SCG biodiesel.	88
Table 3.1: Chemical formulas and properties of the solvents used in the experimental part of this thesis.	99
Table 4.1: Characteristics of solid samples and extracted lipids. The standard deviation of the mean is shown as calculated from three experimental repeats.	135
Table 5.1: Comparison between the yields achieved from the present study and other researchers.	157
Table 5.2: Fatty acid profile of examined ICG1 oil samples and selected vegetable oils.	165
Table 6.1: Average % w/w FFA content and HHV of oil samples extracted after 20 minutes at varying pressure conditions and a constant temperature of 65 °C. The standard deviations calculated by three experimental repeats were 0.7 % w/w for FFAs and 0.43 MJ/kg for HHVs.	178
Table 7.1: Fatty acid composition of expressed RDCB oil.	187
Table 8.1: Acid-catalyzed esterification experimental conditions.	195
Table 8.2: Base-catalyzed transesterification experimental conditions.	200
Table 8.3: Elemental composition of SCG oil and biodiesel.	204
Table 8.4: Fatty acid profile and properties of SCG, soya and rapeseed biodiesel. The standard deviations in the case of Acid value and HHV were calculated from three experimental repeats.	207

Table 8.5: Injection timings in constant ignition timing experiments.	210
Table A.1: Pressure vessel specifications.	237
Table A.2: O-ring specifications.	238
Table A.3: Thread specifications.	238
Table B.1: Ram press specifications.	241
Table B.2: Piston O-ring specifications.	242
Table B.3: Internal cylinder O-ring specifications.	242
Table B.4: Threads specifications.	243
Table D.1: NHE gas chromatography settings.	250
Table D.2: Fatty acid profile of ICG1 oil and molecular weight of individual fatty acids.	251
Table E.1: Properties of reference fossil diesel and biodiesel samples.	252
Table F.1: Composition of Supelco 37 Component FAME mix.	253
Table F.2: ICG2 biodiesel (Table 8.2 - trial 6).	257
Table F.3: ICG2 biodiesel (Table 8.2 - trial 7).	258
Table F.4: ICG2 biodiesel (Table 8.2 - trial 8).	258
Table F.5: Soya biodiesel.	259
Table F.6: Rapeseed biodiesel.	259
Table G.1: Research engine specifications.	260
Table H.1: Composition of oils obtained from Soxhlet extraction using different extraction solvents, using ¹ H NMR spectra. Estimations were made of the apparent molar ratios of the components (using adjusted peak integral values), and derived estimates of mass concentration.	264
Table J.1: Viscosity measurement of raw ICG2 oil.	273
Table J.2: Viscosity measurement of ICG2 biodiesel.	273

Nomenclature

ASE – Accelerated solvent extraction

AV – Acid value

CAD – Crank angle degrees

DAG – Diglyceride

DAQ – Data acquisition system

FAAE – Fatty acid alkyl ester

FAME – Fatty acid methyl ester

FFA – Free fatty acid

FID – Flame ionization detector

FRCG – Fresh retail coffee ground

GC – Gas chromatography

HHV – Higher heating value

HRR – Heat release rate

ICG – Instant coffee grounds

IMEP – Indicated mean effective pressure

KV – Kinematic viscosity

MAE – Microwave-assisted extraction

MAG - Monoglyceride

MW – Molecular weight

NHE – New Holland Extraction Ltd.

NMR – Nuclear magnetic resonance

PID – Proportional integral derivative

PHRR – Peak heat release rate

PUFA – Polyunsaturated fatty acid

RCG – Retail coffee grounds

RDCB – Roasted defective coffee beans

SCG – Spent coffee grounds

SFA – Saturated fatty acid

SFE – Supercritical fluid extraction

SOC – Start of combustion

SOI – Start of injection

TAG - Triglyceride

TDC – Top dead centre

THC – Total hydrocarbon

UAE – Ultrasound-assisted extraction

UFA – Unsaturated fatty acid

1. Introduction

Fossil fuels continue to account for the majority of global energy consumption, constituting 86 % of the total energy consumed in 2016, while petroleum oil remains the world's dominant fuel, making up approximately a third of all the energy consumed worldwide (BP, 2017). The transport sector, which is responsible for 27 % of current energy use (REN21, 2017), is the largest consumer of refined petroleum oil, and 95 % of all fuel used globally for transportation purposes in 2015 came from oil products (U.S. Energy Information Administration, 2017).

The continuous use of fossil fuels in combustion related activities is responsible for the increasing concentration of greenhouse gases in the atmosphere (IEA, 2017), and emissions of carbon dioxide (CO₂) resulting from the oxidation of carbon in fuels upon combustion rose at an average rate of 1.6 % per year between 2005 and 2015 (BP, 2017). The prolonged over-dependency on fossil fuels has caused an increase of the carbon dioxide concentration in the atmosphere by 40 % since the mid-1800s due to anthropogenic activities (IEA, 2017), while they are also associated with price fluctuations and reliance on imported products (Canakci and Sanli, 2008; Pinzi et al., 2009).

Fossil fuels are expected to continue dominating the energy sector for the next 30 years at least, while transport is considered as the most problematic sector to wean from petroleum products (REN21, 2017). The diversity of transport energy demands is such that electrification cannot be effective in sectors like heavy duty vehicles, aviation and marine transport, and consequently sustainable biofuels will play a crucial role in their decarbonisation (Energy and Climate Change committee, 2017). For example, heavy duty vehicles represent only 1.5 % of road vehicles, however, they are responsible for ~20 % of the United Kingdom's CO₂ emissions (Energy and Climate Change committee, 2017). The United Kingdom is obligated to produce 15 % of its total energy consumption from renewable sources, including 10 % of its transport fuel requirements, by 2020; currently only 8.31 % of all energy used

and 4.23 % of transport fuel is by renewable energy sources (Energy and Climate Change committee, 2017).

Therefore, the use of renewable and sustainable liquid biofuels is a matter of critical importance in order to reduce the emissions of greenhouse gases and avoid harmful climate change, while simultaneously addressing the continuous increase of energy demand (BP, 2017; Demirbas, 2011; REN21, 2017). Renewable biofuels such as biodiesel and bioethanol, which currently represent 3 % of transport fuels in the United Kingdom, are produced from sugar, starch, plant oils and various waste sources, and their combustion emits no net fossil carbon as the greenhouse gases released are equal to those absorbed during production, however, they are responsible for emissions related to collateral processes such as drying and transport, which are low relative to fossil fuel combustion (Alajmi et al., 2017; Energy and Climate Change committee, 2017). Furthermore, biofuels are biodegradable and offer advantages which include portability, availability, reduced dependency on expensive or unreliable imports, while they can also contribute to industrial development and improved trade balances (Alajmi et al., 2017; REN21, 2017).

Biodiesel is a renewable liquid fuel consisting of alkyl monoesters of fatty acids, and has been widely accepted by the transport sector as it is compatible with current diesel engine technology and existing distribution networks, and offers advantages over petroleum diesel such as negligible aromatic and sulfur content, inherent lubricity and higher flash point (Canakci and Gerpen, 2001; Canakci and Sanli, 2008; Demirbas, 2009; Kwon et al., 2013). In addition, biodiesel is a potentially carbon neutral fuel with emissions of SO₂, SO₃, unburnt hydrocarbons and particulate matter lower than that of conventional diesel according to several studies (Al-Hamamre et al., 2012; Canakci and Sanli, 2008; Knothe et al., 2005; Kwon et al., 2013; Ma and Hanna, 1999).

Nevertheless, the high cost of biodiesel production from biomass sources, such as vegetable and animal oils, has restricted its further commercialization as a sustainable fuel, as it cannot compete economically with conventional

fossil diesel (Al-Hamamre et al., 2012; Kwon et al., 2013; Moser, 2009). In particular, the feedstock used for biodiesel production accounts for approximately 60 % up to 95 % of the total fuel cost (Al-Hamamre et al., 2012; Alajmi et al., 2017; Canakci and Sanli, 2008; Leung et al., 2010; Ma and Hanna, 1999; Zhang et al., 2003). Furthermore, there is a high economic and indirect environmental cost of utilizing edible oils for fuels, as they have high energy and land requirements during cultivation, compete with food resources and are subject to potential future depletion (Al-Hamamre et al., 2012; Canakci and Sanli, 2008; Gui et al., 2008; Haile, 2014; Kwon et al., 2013).

Moreover, assigning land to energy rather than food production raises social issues by local populations and necessitates agricultural expansion elsewhere at a significant carbon cost (indirect land-use change) (Energy and Climate Change committee, 2017; REN21, 2017). In order to avoid extensive indirect land-use change, the European Union has set a limit of 7 % on the proportion of transport biofuels produced from food crops (Energy and Climate Change committee, 2017).

Therefore, if food grade lipids could be replaced by non-edible oils, such as waste cooking oils, inedible animal fats or other agro-industrial or municipal waste residues that contain suitable lipids, for example coffee industry residues, this would significantly reduce biodiesel costs and potentially make it a sustainable substitute to diesel (Al-Hamamre et al., 2012; Canakci and Sanli, 2008; Kwon et al., 2013; Zhang et al., 2003). Biofuels such as those made from waste sources are known as 'advanced biofuels', and do not directly compete for agricultural land, thus resulting in lower indirect land-use change and greenhouse gas emissions (Energy and Climate Change committee, 2017).

SCG are the main residues of the coffee beverage industry and they represent a massive waste stream that poses a significant disposal challenge due to the presence of toxic compounds like caffeine, polyphenols and tannins that may result in environmental pollution when SCG are disposed to landfill (Mussatto et al., 2011a; Silva et al., 1998; Vardon et al., 2013). However, SCG also contain lipids, approximately 11-20 % w/w on a dry weight basis, that can be

potentially used as a feedstock for production of sustainable and cost-effective biodiesel without the need for cultivating energy crops and/or converting food to fuel (Al-Hamamre et al., 2012; Deligiannis et al., 2011; Jenkins et al., 2014; Kondamudi et al., 2008; Pichai and Krit, 2015). In addition, the defatted SCG can be utilized as a further source of biomass energy in the form of fuel pellets, or as feedstock for bioethanol production (Berhe et al., 2013; Kondamudi et al., 2008; Kwon et al., 2013).

Nevertheless, feedstock properties such as the high moisture content of the SCG and the relatively high FFA content of the extracted lipids (Caetano et al., 2012; Gómez-De La Cruz et al., 2015), can impact on the efficiency of oil extraction and biodiesel production, incurring a significant energy cost, potentially reducing the possible environmental benefits of utilizing this waste material as a biodiesel feedstock. Such issues render the valorization of SCG as a biodiesel feedstock a difficult challenge, with the process of oil extraction restricted to date to laboratory scale methods. Therefore, the investigations presented in this work, which include a comprehensive feedstock characterization and cover all of the processing steps required to produce biodiesel from SCG, were conducted in the hope that the knowledge and insight gained will improve the understanding of the processes and contribute to their future industrialization.

1.1 Thesis structure

The present report is divided in four main sections including Literature review (Chapter 2), Experimental materials and methodology (Chapter 3), Results and discussion (Chapters 4, 5, 6, 7 and 8) and finally Conclusions and Recommendations for further work (Chapter 9), followed by Appendices and References. The literature review provides a detailed overview of the current knowledge in the field of SCG lipid recovery and valorization, while the Experimental materials and methodology chapter presents the different coffee samples used and describes the methods applied in the experimental part of this study.

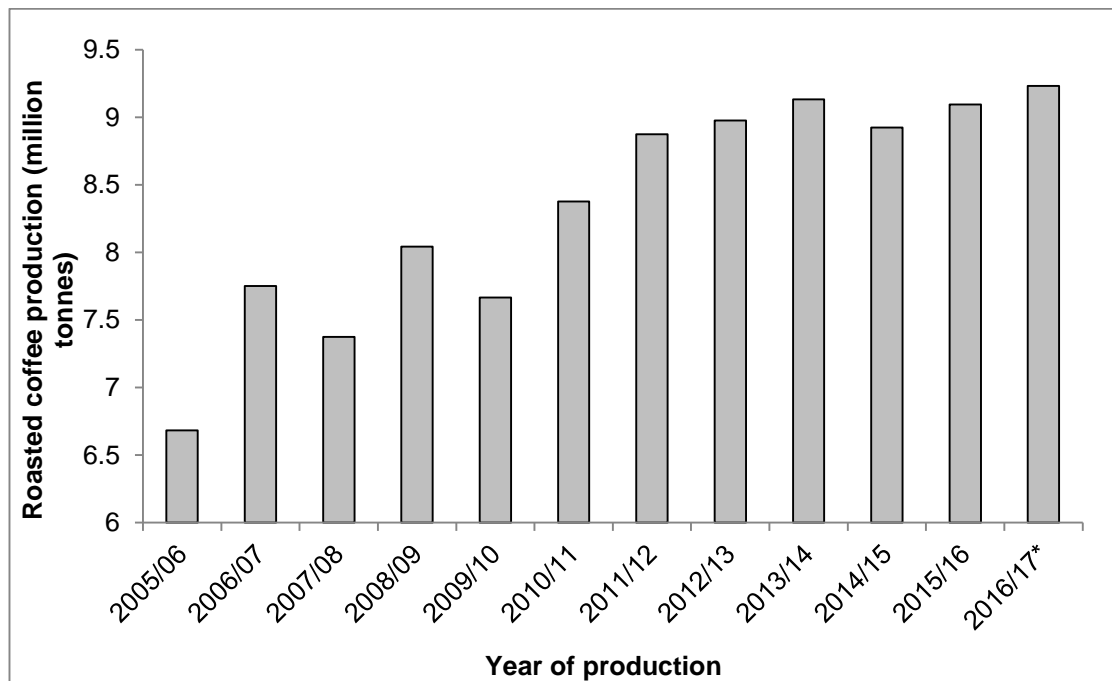
In Chapters 4 to 8, the obtained results are presented and discussed so as to interpret the significance of experimental findings, determine trends and

compare with those reported in previous studies. These are related to the main research objectives listed in Section 2.7. Finally, in Chapter 9 key findings and conclusions are highlighted and new areas for future research recommended, while additional information regarding the experimental methodology can be found in the Appendices A-J.

2. Literature review

2.1 Availability of coffee

Coffee is an agricultural crop that is cultivated in about 80 countries and is the most widely consumed beverage worldwide, while it is also the second largest traded commodity after petroleum oil (Campos-Vega et al., 2015; Farah, 2012; Murthy and Madhava Naidu, 2012). According to the International Coffee Association (2016), 9.1 million tonnes of roasted coffee were produced worldwide between October 2015 and September 2016 with a 1.8 % increase in global coffee production compared to 2014/15. Figure 2.1 shows the annual global production of coffee since 2005/6.



*: estimate.

Figure 2.1: Annual production of roasted coffee worldwide (International Coffee Association, 2016).

It can be seen in Figure 2.1 that the annual production of coffee has increased by 26.5 % since 2005/6, while the worldwide production between October 2016 and September 2017 is expected to be 9.2 million tonnes, an increase of 1.5 % relative to the year 2015/16 (International Coffee Association, 2016).

Figure 2.2 shows the percentage contribution by country to worldwide coffee production in the year 2015/16.

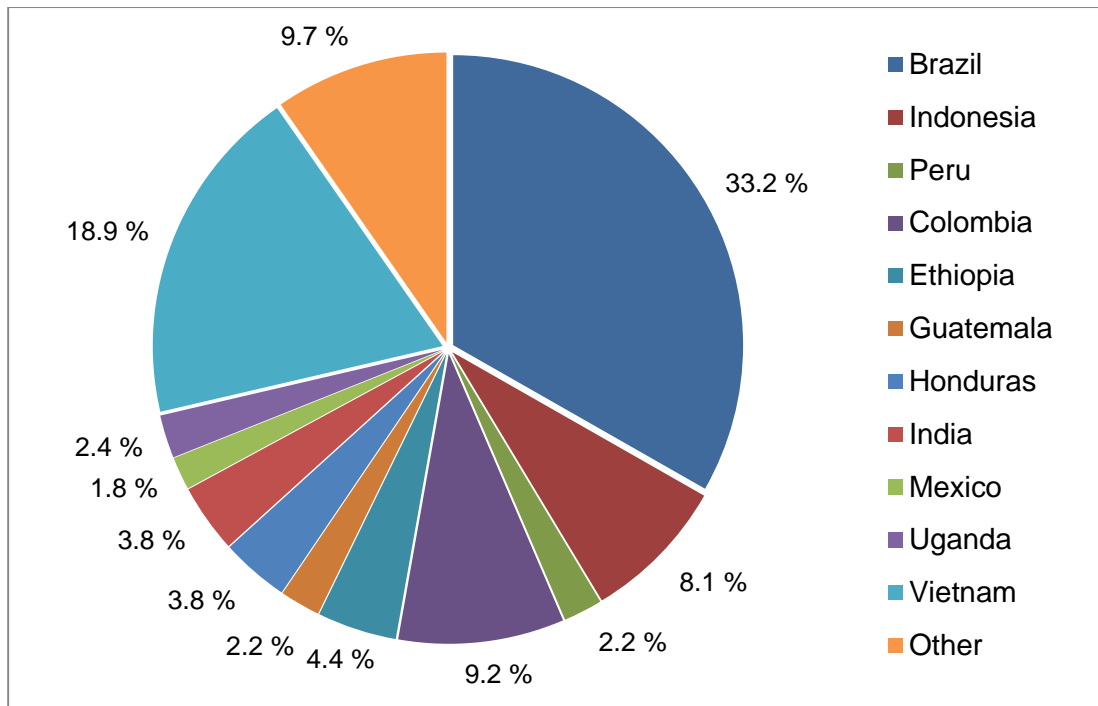


Figure 2.2: Production of coffee in 2015/16 per country (International Coffee Association, 2016).

Figure 2.2 shows that Brazil accounted for the largest part of the global coffee production in 2015/16 producing 33.2 % of the total, followed by Vietnam and Indonesia which produced 18.9 % and 9.7 % respectively (International Coffee Association, 2016).

There are approximately 80 species that have been identified to belong in the genus *Coffea* (Murthy and Madhava Naidu, 2012), however, only two types of beans are economically significant and are cultivated for commercial use: *Coffea Arabica* and *Coffea canephora*, which are most commonly known Arabica and Robusta respectively (Zuorro and Lavecchia, 2012). Arabica is considered to be a coffee of superior quality due to the milder and more flavourful taste developed during roasting of the beans (Bertrand et al., 2003), and represents 70-75 % of the total worldwide production (Jenkins et al., 2014; Zuorro and Lavecchia, 2012). Robusta beans contain approximately twice the amount of caffeine compared to Arabica beans (Clarke and

Vitzthum, 2008; Jenkins et al., 2014), with their caffeine content being greater than 2.5 % on a dry weight basis, while that of Arabica beans is approximately 1.5 % w/w (Brando, 2004), and are mostly used for the production of soluble coffee extracts such as instant coffee (Zuorro and Lavecchia, 2012).

Total worldwide production of Arabica coffee in 2015/16 accounted for ~5.3 million tonnes, while Robusta coffee accounted for 3.8 million tonnes (International Coffee Association, 2016). The production of Arabica coffee is estimated to increase in 2016/17 by 10.2 % relative to 2015/16, whereas Robusta coffee output is expected to decrease by 10.6 % (International Coffee Association, 2016). The bulk of the coffee produced is processed and sold for human consumption, usually as blends of the two coffee varieties in order to control the strength of the coffee flavor and adjust the caffeine content (Jenkins et al., 2014). Figure 2.3 shows the worldwide consumption of roasted coffee per year since 2012/13.

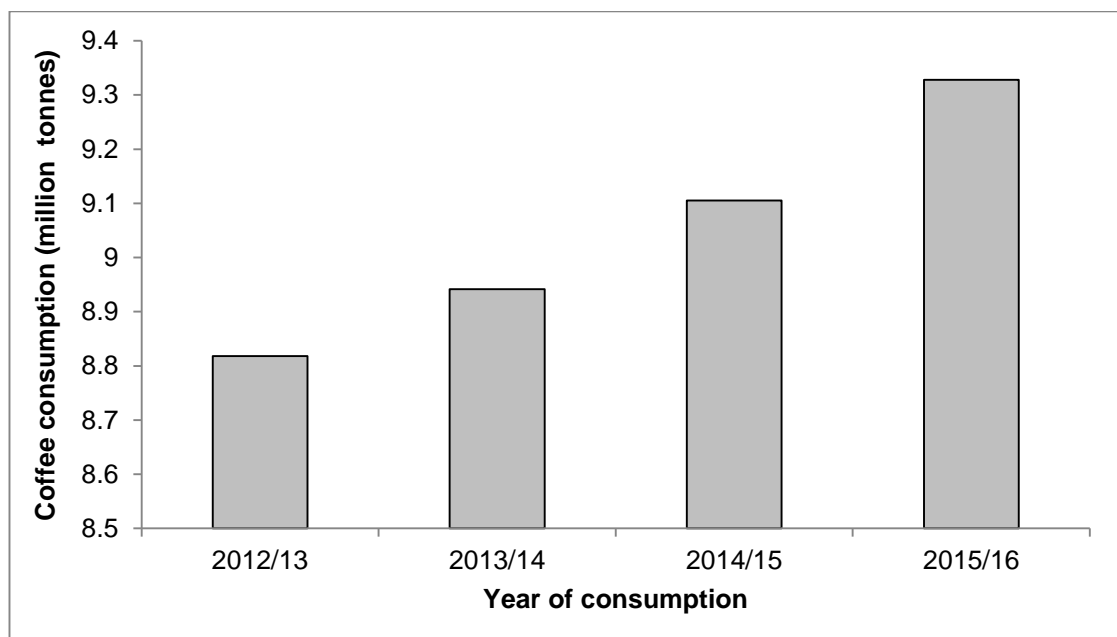


Figure 2.3: Global consumption of roasted coffee per year (International Coffee Association, 2016).

It can be seen in Figure 2.3 that the worldwide consumption of coffee between October 2015 and September 2016 was 9.32 million tonnes, a quantity that is higher than the global production during this period of time (Figure 2.1), with the deficit covered by stocks accumulated in previous years (International

Coffee Association, 2016). Furthermore, the global consumption of coffee has increased significantly since 2012/13, with an average annual growth rate of 1.9 % (International Coffee Association, 2016). The coffee consumption during the calendar year 2015/16 in the European Union was 2.5 million tonnes, while 0.22 million tonnes of coffee were consumed in the United Kingdom, an amount that corresponds to approximately 3.3 kg of coffee per capita (International Coffee Association, 2016).

2.2 Processing of coffee beans within the beverage industry

The coffee processing industry comprises a wide range of intermediate products, starting from the harvested coffee berries, then to green beans and finally to the consumable beverage (Franca and Oliveira, 2008). The solid residues generated during the processing of coffee can be divided into those formed in producing countries (coffee pulp, parchment and green defective beans), and those mostly produced in consuming countries after the coffee roasting and brewing procedure, which are commonly known as silver skin and SCG respectively (Murthy and Madhava Naidu, 2012).

2.2.1 Production of green coffee

Processing of raw coffee berries takes place at the coffee producing sites and aims to remove all the covering layers that surround the bean, lower the water content from ~65 % w/w initially to about 11-13 % w/w, and obtain green coffee beans according to market requirements (Brando, 2004; Clarke, 1985). During the processing of coffee berries into green beans more than 50 % of the fruit mass is discarded (Cruz et al., 2012; Toschi et al., 2014). Figure 2.4 shows the internal structure of a coffee berry and its different sections.

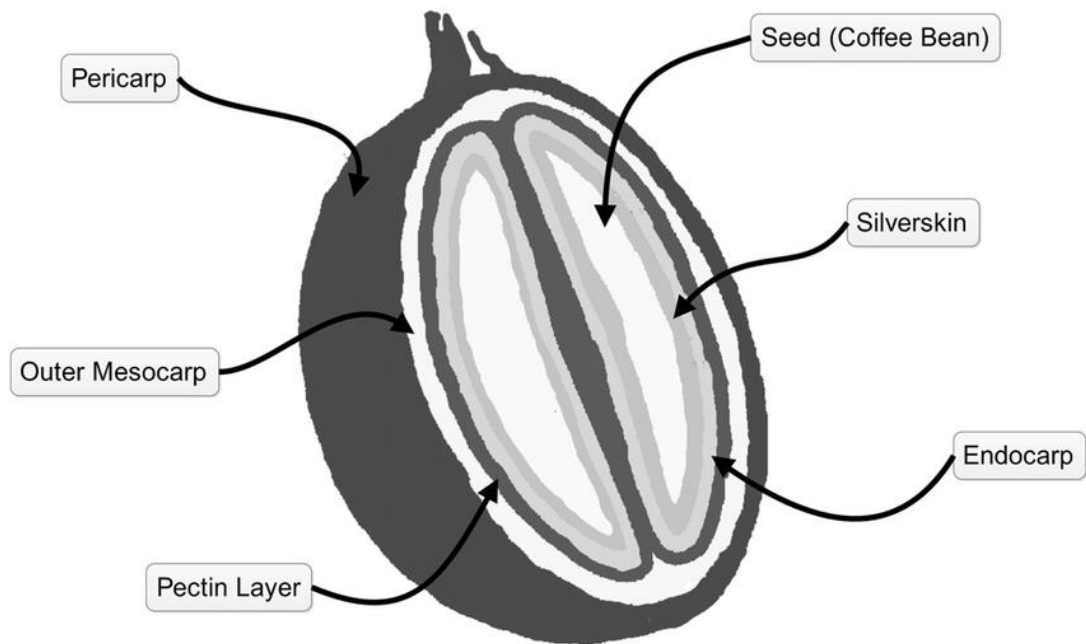


Figure 2.4: Coffee berry structure and sections (adapted from Bresciani et al. (2014))

Raw coffee processing begins immediately after harvesting and three different methods are used for pulp (pericarp and mesocarp – Figure 2.4) extraction to produce green coffee beans depending on the coffee species and producing country (Brando, 2004; Farah, 2012; Vincent, 1987).

In the dry processing method, which is used for almost all Robusta coffees worldwide and for 80 % of Brazilian and Ethiopian Arabicas, the whole berry is dried together by exposure to sun or air dryers and the pulp and parchment (endocarp –Figure 2.4) are mechanically removed afterwards (Brando, 2004; Farah, 2012). During the wet processing method, which is used in some producing countries for a small percentage of Robustas and for the remaining Arabicas, the pulp is removed mechanically and the remaining mucilage (part of the mesocarp – Figure 2.4) that sticks to the parchment is removed by fermentation prior to washing, polishing, sun-drying or air-drying and hulling of the parchment to yield green coffee beans (Brando, 2004; Farah, 2012; Murthy and Madhava Naidu, 2012). Figure 2.5 describes in schematic form the two major methods employed during the processing of the freshly harvested coffee berries to produce green coffee beans, along with the by-products that are generated.

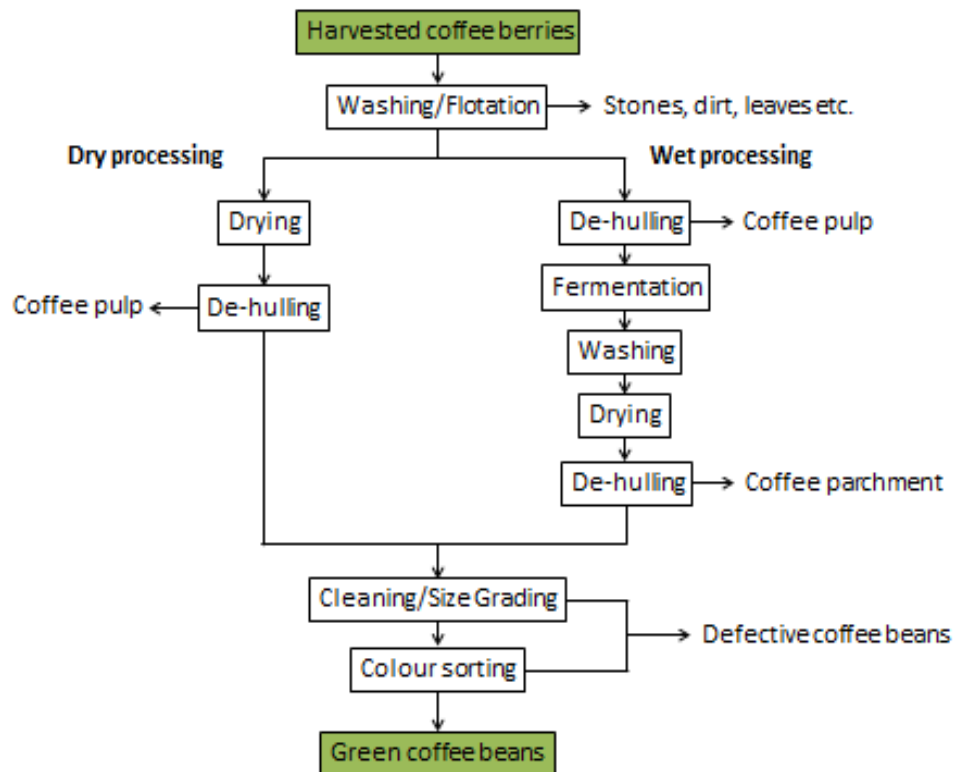


Figure 2.5: Flow-sheet presenting main coffee processing methods (adapted from Franca and Oliveira (2009))

The most recent semi-dry process, which is mostly used in Brazil and combines aspects of both dry and wet processing, involves pulp removal without removing the mucilage followed by drying, and green coffee beans are obtained by hulling the dry parchment and adhered mucilage (Brando, 2004; Farah, 2012). The green coffee beans produced by any of these methods are mechanically or electronically sized, graded and sorted depending on size, colour and shape to identify and remove defective beans prior to commercialization in the international market (Farah, 2012; Franca et al., 2005; Franca and Oliveira, 2008).

The remaining healthy green coffee beans are suitable for storage, roasting, steam-treatment or decaffeination (Brando, 2004; Farah, 2012). The main compounds of green coffee are carbohydrates, proteins and free amino acids, lipids, minerals, organic acids, ash, caffeine, chlorogenic acid, trigonelline and water (Farah, 2012; Murthy and Madhava Naidu, 2012). Coffee seeds contain lipids stored in the endosperm tissue as an energy reserve for germination

and post-germination growth (Crisafulli et al., 2014), the content of which has been reported to range between 11 and 20 % w/w depending on coffee species and regional origin (Al-Hamamre et al., 2012; Kondamudi et al., 2008). Linoleic and palmitic are the predominant fatty acids found in green coffee oil, with moderate quantities of oleic and stearic acids, low amounts of eicosanoic and linolenic acids and traces of myristic and palmitoleic acids, while the oil also contains 19-25 % w/w of unsaponifiable matter (Oliveira et al., 2008; Speer and Kölling-Speer, 2006).

Defective coffee beans constitute approximately 20 % of total coffee production mass by weight and can be classified as black, sour or brown and immature (Franca et al., 2005; Oliveira et al., 2006). Green defective coffee beans are generally smaller, lighter and less humid (7.9 to 8.7 % w/w moisture) than healthy ones, with lower protein and oil contents, and different amounts of cellulose, lignin and hemicellulose (Farah, 2012; Franca et al., 2005; Franca and Oliveira, 2008; Oliveira et al., 2006). Defective beans have a lipid content ranging between 10 % and 12 % on a dry weight basis and a lipid composition not significantly different than that of oil from healthy beans, however, their lipids contain a higher free fatty acid content and an unsaponifiable content that has been reported to be about 24 % w/w (Franca and Oliveira, 2008; Oliveira et al., 2008). Green defective coffee beans are usually dumped in the producing country's internal market to be roasted along with healthy beans in order to increase the coffee reserves, resulting in consumption of a low-grade roasted coffee (Franca et al., 2005; Franca and Oliveira, 2008), but have been investigated as a raw material for the preparation of activated carbons (Franca and Oliveira, 2009).

The different processing methods of raw coffee along with the time of harvest, local climatic and storage conditions are known to have an impact on the chemical composition of the beans (Dias et al., 2012; Franca et al., 2005; Jenkins et al., 2014; Jham et al., 2001; Selmar et al., 2008). In particular, prolonged duration of storage results in lipid oxidation (Selmar et al., 2008) and increase of the free fatty acid content (Speer and Kölling-Speer, 2006), while the processing method used influences the levels of amino acids (Dias et al., 2012), chlorogenic acids (Duarte et al., 2009), and carbohydrates

(Knopp et al., 2006) present. Differences in the drying processes utilized during processing of the coffee berries into green beans has also been reported to impact on the lipid composition by altering the relative percentages of di- and triglycerides (Jham et al., 2001).

Furthermore, drying of the coffee seeds after harvesting can damage the endocarp tissue, especially when drying is performed at a temperature of 60 °C (Borém et al., 2008). In addition, Joët et al. (2010) reported a significant increase in the dry weight lipid content of green Arabica beans processed through the wet method.

2.2.2 Roasting of green coffee beans

The bulk of green coffee is roasted in order to gain the characteristic coffee aroma and flavor for beverage production (Farah, 2012; Murthy and Madhava Naidu, 2012), while a small amount is subjected to decaffeination prior to roasting (Farah, 2012; Jenkins et al., 2014). Roasting can be separated into three phases: drying during which water is evaporated and aromatic volatile substances are slowly released, pyrolysis at temperatures between 210 °C and 240 °C based on the degree of roasting required, and subsequent cooling by air or water (Farah, 2012; Murthy and Madhava Naidu, 2012).

The pyrolysis process results in significant physical, chemical and structural changes in the beans that include: considerable volume increase, change of color from green to light brown or black, breaking down of proteins and carbohydrates, and transformation of polyphenolic compounds into a complex mixture of melanoidins and other compounds commonly known collectively as Maillard reaction products (Farah, 2012; Murthy and Madhava Naidu, 2012; Mussatto et al., 2011b; Sacchetti et al., 2009). In addition, roasting has been reported to slightly reduce levels of phenolic compounds (Duarte et al., 2005) and tocopherols (Farah, 2012), decrease the chlorogenic acid content by 50 % and increase caffeine by approximately 30 % by mass (Pilipczuk et al., 2015).

The oil content of coffee on a mass basis has been reported to increase during roasting at 210-216 °C due to the beans dry matter loss (Franca and

Oliveira, 2008; Oliveira et al., 2006), while roasting of coffee beans at 216 °C has been found to result in oxidative chemical changes including partial oxidation of polyunsaturated fatty acids present in the coffee oil (Budryn et al., 2012). Martín et al. (2001) and Ratnayake et al. (1993) found that no significant differences could be detected in the fatty acid composition of the oil from green and roasted coffee. In particular, the roasting process only increases the trans fatty acid levels (C18:2ct and C18:2tc) (Speer and Kölling-Speer, 2006). Table 2.1 shows the chemical composition of green and roasted Arabica and Robusta seeds.

Table 2.1: Chemical composition of green and roasted coffee beans (adapted from Farah (2012)).

Component	% dry matter			
	Green Arabica	Green Robusta	Roasted Arabica	Roasted Robusta
Lipids				
<ul style="list-style-type: none"> Coffee oil (triglycerides with unsaponifiables, sterols and tocopherols) Diterpenes 	15-17	7-10	17	11
Carbohydrates	45.1-58.1	54.3-64.4	38.3-40.5	42.3-43.9
Nitrogenous Compounds	12-14.8	13.9-19.2	9.8-11.5	10.6-12.8
Acids and esters	5.5-9.3	7.5-12.7	4.3-4.9	5.9-6.4
Minerals	3-4.2	4.4-4.5	4.5	4.7
Melanoidins	-	-	25	25

It can be seen in Table 2.1 that roasting has a significant effect on the proportions of the major compounds present in coffee grounds. Moreover, coffee roasting at temperatures above 200 °C leads to the loss of water, volatile compounds and organic mass, resulting in the concentration of large amounts of vapors that cause high internal pressure and therefore decrease

the bean density, and is responsible for altering the structure and porosity of the cell walls and forming fine micropores that allow mobilized oil to migrate to the bean surface (Franca et al., 2005; Schenker et al., 2000). The loosening of coffee cell wall structure that occurs during roasting also increases the solubility of the cell wall components, which mainly include arabinogalactans and mannans by means of polysaccharide polymerization (Campos-Vega et al., 2015). The effect of roasting conditions on coffee bean structure can be observed in that higher roasting temperatures led to greater bean volume, pore volume and larger micropores in cell walls relative to beans that have undergone low-temperature roasting (Schenker et al., 2000).

The main by-product of the coffee roasting process in consuming countries is silver skin, also known as husk or chaff, which is the integument of the outer layer of green coffee beans and represents about 4.2 % by mass of the bean (Ballesteros et al., 2014; Borrelli et al., 2004; Murthy and Madhava Naidu, 2012). Coffee silver skin is rich in soluble dietary fiber and has high antioxidant capacity because of the presence of phenolic compounds and melanoidins, thus making it a possible source of such components (Borrelli et al., 2004; Murthy and Madhava Naidu, 2012), while it can also be considered as a substrate for solid-state fermentation (Narita and Inouye, 2014), as combustible biomass (Saenger et al., 2001) or as compost (Narita and Inouye, 2014; Toschi et al., 2014). Furthermore, coffee silver skin contains lipids ranging between 1.9 and 5.2 % on a dry weight basis with a fatty acid composition similar to that of green and roasted coffee beans, while the moisture content varies between 2.6 and 8.2 % w/w depending on storage duration and conditions (Toschi et al., 2014).

In many occasions defective coffee beans are roasted along with healthy ones either due to mistakes in sorting, or intentionally in producing countries like Brazil where defective beans represent about 50 % of the roasted coffee consumed (Franca et al., 2005; Oliveira et al., 2006). Defective coffee beans roast to a lesser degree than healthy beans under the same roasting conditions (Franca et al., 2005; Franca and Oliveira, 2008), and RDCB can be differentiated by non-defective ones only by an evaluation of their volatile profile (Franca and Oliveira, 2009).

According to previous studies RDCB have a slightly lower lipid content than non-defective roasted beans, and which remains relatively stable during roasting and has been reported to range between 9.2 and 10 % w/w (Oliveira et al., 2006). The fatty acid composition of the oil recovered from RDCB was found to be similar to that of green or roasted non-defective beans (Oliveira et al., 2008, 2006). The moisture content of RDCB is as low as zero immediately after roasting, and can increase up to 3 % w/w as the beans tend to absorb water from surrounding air (Franca et al., 2005; Franca and Oliveira, 2008; Oliveira et al., 2006). According to Oliveira et al. (2006) the oil extracted from RDCB can be considered for application in the food and pharmaceutical sectors, while defective coffee beans have been previously investigated as a source of lipids for biodiesel production by Oliveira et al. (2008).

After roasting, the non-defective coffee beans are ground to a size related to the method by which they are to be brewed and marketed as ground roast coffee or used for production of instant coffee (Farah, 2012). Instant coffee production includes treating roasted ground coffee with water heated at 175 °C under conditions of high pressure to maintain water liquid in order to extract soluble compounds, cooling of this soluble material and spray-drying or freeze-drying to reach a moisture level of ~5 % (Farah, 2012; Mussatto et al., 2011b). A quantity of 1 kg of green coffee beans results in the production of about 0.33 to 0.45 kg of instant coffee with a moisture content of 3 % w/w (Acevedo et al., 2013), with approximately 50 % of the worldwide coffee production processed for soluble coffee preparation (Cruz et al., 2012; Murthy and Madhava Naidu, 2012; Pujol et al., 2013). Instant coffee is known to have a relatively high acidity content compared to roasted coffee grounds (Farah, 2012; Romeiro et al., 2012).

2.2.3 Coffee brewing

There are many different brewing methods, including drip-filtering, boiling, percolation and espresso, although all share the same principle of using hot (90-95 °C) or boiling water to extract the essential aromatic oils from the coffee grounds (Farah, 2012; Murthy and Madhava Naidu, 2012), and result in approximately 30 % of the coffee mass being solubilized in water (Jenkins et

al., 2014). The most common method of coffee brewing is by filter, however, the consumption of espresso coffee has increased significantly in the past few decades (Mussatto et al., 2011b). These two brewing methods have been found by Todaka et al. (2016) to result in SCG particles of similar size after brewing, with espresso particles being slightly smaller (100 % w/w < 500 nm) than filter coffee particles (90.3 % w/w < 500 nm). The varying conditions employed in the different brewing methods, such as pressure and temperature, affect the chemical composition and oil content of the coffee (Farah, 2012; Jenkins et al., 2014; Mussatto et al., 2011b).

The high temperatures applied during coffee brewing extract thermolabile compounds like chlorogenic acids, while the hot water removes water soluble components such as polysaccharides, melanoinids and caffeine, and leads to considerably increased moisture content in the SCG that are collected after brewing (Farah, 2012). The majority of the oil remains in the coffee grounds after brewing (Campos-Vega et al., 2015), however, Jenkins et al. (2014) reported that a large portion of unsaponifiable material was removed. Moreover, coffee grounds brewed through the drip-filtering method or treated for brewing of instant coffee have been found to contain significantly more lipids relative to those treated by cafetière, espresso and aero-press machine, potentially due to the higher pressure applied during these methods that result in extraction of lipids (Campos-Vega et al., 2015; Jenkins et al., 2014; Ratnayake et al., 1993). The brewing method applied is also responsible for the diverging concentrations of diterpenes in SCG with boiled and Turkish style coffee extracting the highest amounts (Gross et al., 1997).

2.3 Spent coffee grounds

SCG are the residues produced after the coffee making procedure and can be separated into two categories; those generated during the production of instant coffee and those generated from coffee brewing (Cruz et al., 2012). SCG obtained during treatment of roast and ground beans with hot water to prepare instant coffee account for a worldwide average of 6 million tonnes of waste produced per year (Mussatto et al., 2011a), with about 2 kg of wet SCG obtained for each kg of instant coffee produced (Murthy and Madhava Naidu,

2012). SCG are also generated through the direct brewing of retail roasted coffee in cafeterias, restaurants and houses through drip-filtering or espresso machines, with approximately 50 % of the worldwide roasted coffee production utilized in this way (Cruz et al., 2012). Moreover, several previous studies refer to SCG as the residues obtained by the instant coffee industry alone (Acevedo et al., 2013; Ballesteros et al., 2014; Mussatto et al., 2011a, 2011b).

SCG are solid residues with fine particle size (75-430.5 μm when dried), and high humidity (75-85 %) and acidity with an approximate pH of 4.2-5.7 (Bok et al., 2012; Cruz et al., 2012; Go et al., 2016; Mussatto et al., 2011b; Silva et al., 1998; Somnuk et al., 2017; Todaka et al., 2016). SCG represent a huge amount of waste that poses a significant disposal challenge as discarding it to landfill is problematic due to the high oxygen demand during decomposition of its organic materials, and the toxic character of the material attributable to the presence of compounds such as caffeine, polyphenols and tannins that can result in damage to the environment (Mussatto et al., 2011a, 2011b; Silva et al., 1998; Vardon et al., 2013).

At present, the majority of the SCG generated by the instant coffee industries is collected by specialized agencies that sell it for a variety of purposes since it contains organic compounds of value such as lipids, sugars, proteins and other components in amounts that justify their exploitation (Campos-Vega et al., 2015; Mussatto et al., 2011b; Pujol et al., 2013; Zuorro and Lavecchia, 2012). Currently, SCG are most commonly used as compost, animal feed and substrate for mushroom growth, however, these applications do not exploit the high energy content of SCG (Campos-Vega et al., 2015; Preethu et al., 2007). Table 2.2 shows the chemical composition of SCG on a dry weight basis.

Table 2.2: Characterization of dry SCG.

References	Elemental composition (%)						Lipids (%)	Crude protein (%)	Carbohydrates (%)	Lignin (%)	Sugar (%)	Ash (%)
	C	H	N	O	S	P						
Somnuk et al. (2017)	52.95	6.76	2.10	38.07	0.12	-	14.7	14.39	21.43	-	14.09	1.59
Vardon et al. (2013)	56.1	7.2	2.4	34.0	0.14	0.18	16.2	15.4	-	-	-	1.8
Todaka et al. (2016)	55.86	7.02	2.33	34.79	-	-	21.27	-	-	-	-	2.17
Go et al. (2016)	-	-	-	-	-	-	13.78- 16.51	10.95- 11.03	25.36-34.14	-	-	1.63- 1.73
Pujol et al. (2013)	57.16- 59.77	7.17- 7.57	1.18- 1.32	-	-	-	19.67- 25.41	-	-	19.84- 26.51	22.00- 24.13	-
Acevedo et al. (2013)	-	-	-	-	-	-	26.4	10.32	36.87	-	-	0.47
Caetano et al. (2014)	67.3	-	2.2	-	-	-	6.0	13.7	-	33.6	-	2.2
Tsai et al. (2012)	52.54	6.95	3.46	34.82	0.10	-	-	-	-	39.4	-	0.73

It can be seen in Table 2.2 that dry SCG contain high carbon and oxygen content, low nitrogen and ash content and traces of sulfur and phosphorus. Lignin and carbohydrates were found in similar proportions of 19.8-39.4 % w/w and 21.4-36.8 % w/w respectively, with crude protein and sugar accounting for lower amounts of the total SCG mass. Furthermore, SCG were reported to contain a total 51-55 % w/w of extractives, including lipids, ethanol and water soluble compounds such as polyphenols (1.5-6 % w/w), tannins (0.02-4 % w/w), chlorogenic acid (2.3 % w/w), sterols (0.5-3.1 % w/w) and caffeine (0.02 % w/w) (Murthy and Madhava Naidu, 2012; Pujol et al., 2013). The composition of dry SCG presented in Table 2.2 shows a degree of variation in different studies, possibly attributable to the different origin and species of the samples used, in addition to roasting and brewing methods applied, and the different methods of analysis used in previous studies (Go et al., 2016).

Several alternative approaches to the valorization of SCG have been investigated, and tentatively applied in producing countries (Cruz et al., 2012). These include its utilization as a source of polysaccharide material and sugar (Mussatto et al., 2011a; Pujol et al., 2013), as a source of antioxidant material (Yen et al., 2005), as a precursor for activated carbon production (Kante et al., 2012; Tsai et al., 2012), as a substitute for wood powder (Silva et al., 1998) and as a source of terpenes (Campos-Vega et al., 2015) and phenolic compounds (Zuorro and Lavecchia, 2012).

Previous studies have also examined the utilization of SCG as absorbent for removal of cationic dyes in wastewater treatments (Franca et al., 2009), or for removal of metal ions from waste water (Fiol et al., 2008). Nevertheless, these strategies have not yet been routinely implemented at an industrial scale (Haile, 2014; Mussatto et al., 2011a), while a number of researchers have highlighted the high oil and energy content of SCG (Sections 2.3.1 and 2.3.2), that along with the minimal presence of sulfur (Table 2.2) can potentially make SCG a sustainable feedstock for biofuel production (Al-Hamamre et al., 2012; Caetano et al., 2012; Deligiannis et al., 2011; Gómez-De La Cruz et al., 2015; Jenkins et al., 2014; Kondamudi et al., 2008; Kwon et al., 2013; Rocha et al., 2014; Vardon et al., 2013). For example, Nestle has pledged to reduce

quantities of waste in Europe by 2020 using spent SCG as a source of renewable energy in more than 20 Nescafe factories (Campos-Vega et al., 2015). In particular, SCG have been used for production of biodiesel (Al-Hamamre et al., 2012; Caetano et al., 2014; Deligiannis et al., 2011), bioethanol (Kwon et al., 2013; Murthy and Madhava Naidu, 2012), fuel pellets (Kondamudi et al., 2008; Silva et al., 1998), biochar (Kelkar et al., 2015; Tsai et al., 2012) and bio-oil by pyrolysis (Kelkar et al., 2015).

2.3.1 Energy content

Table 2.3 shows the energy content of SCG and SCG oil measured in previous studies as expressed through higher heating value (HHV). It can be seen in Table 2.3 that SCG have a dry weight energy content ranging between 19.3 and 25.7 MJ/kg in terms of HHV, with an approximate average of 22 MJ/kg, while lipids extracted from SCG have been found to have a HHV between 35.86 and 43.2 MJ/kg.

Table 2.3: HHVs of dried SCG and SCG oil.

References	HHV of SCG (MJ/kg)	HHV of SCG lipids (MJ/kg)
Al-Hamamre et al. (2012)	20.79	35.86-39.00
Haile (2014)	-	38.22
Campos-Vega et al. (2015)	19.61	-
Silva et al. (1998)	24.9	-
Tsai et al. (2012)	23.5	-
Go et al. (2016)	22.83-24.39	-
Bok et al. (2012)	22.74	-
Romeiro et al. (2012)	25.7	-
Zuorro and Lavecchia (2012)	23.72-24.07	-
Vardon et al. (2013)	23.4	-
Berhe et al. (2013)	-	37.88
Abdullah and Bulent Koc (2013)	-	43.2
Caetano et al. (2012)	19.3	36.4
Deligiannis et al. (2011)	21.16	-
Caetano et al. (2014)	19.3	35.4-40.8
Somnuk et al. (2017)	23.1	38.37

From the previous studies presented in Table 2.3, it is apparent that SCG have a HHV greater than most agro-industrial residues and woody biomass (HHV: 19 – 21 MJ/kg) (Bok et al., 2012; Caetano et al., 2014; Vardon et al., 2013; Zuorro and Lavecchia, 2012). This variation in SCG energy content can be possibly attributed to variation in lipid content and overall composition due to the origin, upstream processing and different blends of coffee varieties (Al-Hamamre et al., 2012; Jenkins et al., 2014; Speer and Kölling-Speer, 2006). The high energy content of dry SCG relative to other forms of biomass makes them an attractive bioresource for direct utilization as fuel pellets (Cruz et al., 2012; Kondamudi et al., 2008; Silva et al., 1998), with one possible application their utilization within the coffee industry (Corrêa et al., 2014). However, it has been suggested that the considerable amount of nitrogen found in the grounds

(Table 2.2) may result in high NO_x emission upon combustion (Vardon et al., 2013).

Table 2.3 also shows that SCG lipids have a slightly lower HHV than that of petroleum crude oils (41-48 MJ/kg) but similar to that of other vegetable oils or animal fats (Fassinou, 2012; Haile, 2014), and therefore can be considered an attractive feedstock for biodiesel production (Al-Hamamre et al., 2012; Caetano et al., 2012; Jenkins et al., 2014; Kondamudi et al., 2008; Vardon et al., 2013).

2.3.2 Lipids

The lipid content of SCG on a dry weight basis has been found to range between 6 % w/w and 27.8 % w/w according to previous studies, with most researchers reporting values between 10 % w/w and 18 % w/w (Campos-Vega et al., 2015). Table 2.4 shows the oil yields obtained from unspecified retail, espresso and instant SCG in previous studies.

Table 2.4: Dry weight oil yields extracted from other researchers.

References	SCG residue type	% Oil yield on dry weight basis
(Abdullah and Bulent Koc, 2013; Ahangari and Sargolzaei, 2013; Akgün et al., 2014; Al-Hamamre et al., 2012; Caetano et al., 2014; Deligiannis et al., 2011; Go et al., 2016; Haile, 2014; Jenkins et al., 2014; Kondamudi et al., 2008; Rocha et al., 2014; Vardon et al., 2013)	Retail	6-21.5
(Couto et al., 2009; Cruz et al., 2012; Najdanovic-Visak et al., 2017; Pichai and Krit, 2015; Somnuk et al., 2017)	Espresso	7.5-18.3
(Acevedo et al., 2013; Lago et al., 2001)	Instant	19.9-27.8

Table 2.4 shows that SCG used for production of instant coffee generally contain higher lipid content relative to SCG generated from coffee shops (retail) or espresso machines, something possibly attributable to the different conditions of processing and coffee brewing. Moreover, commercial SCG have been reported to contain more lipids compared to SCG produced in a laboratory environment (Campos-Vega et al., 2015). The wide variation of SCG oil yields obtained in previous studies can likely be attributed to the different blends of coffee varieties used in the samples, the origin of coffee (cultivation, climate, time of picking) and the upstream processing (processing and roasting) (Al-Hamamre et al., 2012; Jenkins et al., 2014; Oliveira et al., 2008). Moreover, it has been seen that the different methods of coffee brewing generally do not significantly affect the lipid content of SCG (Campos-Vega et al., 2015). Yields of SCG oil are also a function of the selected extraction procedure and the conditions applied (Ahangari and Sargolzaei, 2013; Al-Hamamre et al., 2012; Caetano et al., 2012; Campos-Vega et al., 2015; Couto et al., 2009; Pichai and Krit, 2015; Rocha et al., 2014).

Coffee oil is mainly comprised of triglycerides, usually above 80 % w/w of the total, and smaller and varying amounts of diglycerides, monoglycerides and FFAs with the glyceride portion accounting for 80-95 % w/w of the total (Campos-Vega et al., 2015; Jenkins et al., 2014; Pichai and Krit, 2015). The remaining component of coffee oil consists of a relatively large proportion of unsaponifiable compounds, including diterpenes (12.3 % w/w), sterols (1.9 % w/w), tocopherols, phosphatides and waxes (Campos-Vega et al., 2015; Crisafulli et al., 2014; Ratnayake et al., 1993; Speer and Kölling-Speer, 2006). The unsaponifiable component of lipids extracted from SCG was found by Jenkins et al. (2014) to range between 0.1 and 40 % w/w depending on the geographic origin of the coffee beans, likely attributable to differing harvesting and drying procedures.

In addition, coffee oil contains antioxidants which increase the stability of the oil and prevent decomposition (Al-Hamamre et al., 2012). In particular, the nitrogenous brown-colored compounds of coffee (Maillard reaction products) exhibit antioxidant capacity and inhibit lipid peroxidation, while the diterpenes kahweol ($C_{20}H_{26}O_3$) and cafestol ($C_{20}H_{28}O_3$) and phenolic compounds

contained in coffee oil such as vanillic acid, sinapic acid, ferulic acid, *p*-coumaric acid, caffeic acid and chlorogenic acid are also known for their antioxidant activity (Acevedo et al., 2013; Campos-Vega et al., 2015).

FFAs are defined as those that are not linked with a glycerol backbone and they can be found in lipids extracted from SCG at varying concentrations. In general, FFA levels between ~3 % w/w and ~20 % w/w are common in previous studies (Al-Hamamre et al., 2012; Go et al., 2016; Haile, 2014; Kwon et al., 2013; Vardon et al., 2013), however values as low as 0.31-0.4 w/w (Deligiannis et al., 2011; Pichai and Krit, 2015) and as high as 59 % w/w (Caetano et al., 2012) have been reported, suggesting a significant variation in the composition of oil extracted from different sources with different extraction parameters. The FFA content of the oil is a major quality factor, as high amounts of FFA increase oil acidity, kinematic viscosity, susceptibility to oxidation and speed up degradation (Al-Hamamre et al., 2012; Predojević, 2008).

SCG oil contains both saturated and unsaturated fatty acids and is principally composed of linoleic, palmitic, oleic and stearic acids in proportions not unlike those found in other common edible vegetable oils like soybean oil (Abdullah and Bulent Koc, 2013; Ahangari and Sargolzaei, 2013; Haile, 2014; Jenkins et al., 2014). Eicosanoic and linolenic acids are also present in SCG oils, while lauric and myristic acids can be found in certain oils depending on the SCG sample origin, processing and the extraction conditions applied (Campos-Vega et al., 2015). Table 2.5 shows the fatty acid profile of oils extracted with various methods from different types of SCG residues including retail, espresso and instant coffee residues determined in previous studies, with the mass percentage of each fatty acid relative to total oil weight presented.

Table 2.5: Fatty acid composition of SCG oils.

References	C12:0	C14:0	C16:0	C18:0	C18:1	C18:2	C18:3	C:20	SFA	PUFA
Retail SCG										
Jenkins et al. (2014) - SCG from Costa Rica, suspension in heptane	ND	ND	35.4	6.7	6.7	49.9	TR	1.2	43.3	49.9
Jenkins et al. (2014) - SCG from Vietnam, suspension in heptane	ND	ND	41.4	13.5	24.0	22.0	TR	0.00	54.9	22.0
Ahangari and Sargolzaei (2013) – Soxhlet (hexane)	3.54	1.97	43.61	6.58	8.15	32.41	1.30	2.44	58.14	33.71
Ahangari and Sargolzaei (2013) – UAE (hexane)	3.54	2.03	43.41	6.63	8.20	32.39	1.30	2.50	58.11	33.69
Ahangari and Sargolzaei (2013) – MAE (hexane)	3.54	1.96	43.55	6.55	8.27	32.51	1.27	2.35	57.95	33.78
Ahangari and Sargolzaei (2013) – SFE	7.56	2.51	33.72	5.45	6.01	36.12	1.72	6.91	56.15	37.84
Haile (2014) – Soxhlet (hexane)	NM	NM	35.80	8.10	13.9	37.3	NM	3.2	47.1	37.3
Rocha et al. (2014) – UAE (hexane)	NM	NM	35.9	7.5	10.7	40.2	0.4	NM	45.1	43.2
Abdullah and Bulent Koc (2013) – Soxhlet (hexane)	NM	NM	27.8	6.24	6.90	35.2	0.9	2.1	36.14	36.1
Abdullah and Bulent Koc (2013) – UAE*	NM	NM	29.1	6.13	7.28	35.7	0.97	2.38	37.61	36.67
Deligiannis et al. (2011) – Soxhlet (hexane)	NM	NM	34	10.91	7.16	23.27	NM	4.04	48.95	23.27
Vardon et al. (2013) – Soxhlet (hexane)	NM	NM	33.9	7.3	8.3	45	1.5	2.5	43.7	46.5
Akgün et al. (2014) – Soxhlet (hexane)	ND	TR	27.70	7.57	10.03	47.77	1.38	3.41	38.68	49.15

References	C12:0	C14:0	C16:0	C18:0	C18:1	C18:2	C18:3	C:20	SFA	PUFA
Akgün et al. (2014) – Soxhlet (dichloromethane)	ND	TR	25.77	8.25	10.39	47.78	1.36	4.05	38.07	49.14
Akgün et al. (2014) – SFE	ND	TR	26.34	7.63	10.18	48.50	1.40	3.61	37.58	49.9
Espresso SCG										
Couto et al. (2009) – Soxhlet (hexane)	3.57	1.99	43.65	6.49	8.15	32.45	1.31	2.39	58.1	33.76
Couto et al. (2009) – SFE	7.41	2.4	37.08	6.20	8.13	35.22	ND	3.54	56.6	35.22
Cruz et al. (2012) - Soxhlet (petroleum ether)	ND	0.1	32.80	7.10	10.30	44.2	1.50	2.60	42.6	45.7
Instant SCG										
Acevedo et al. (2013) – Soxhlet (hexane)	NM	0.05	32.45	8.35	9.00	45.04	4.12	NM	40.85	49.16
Acevedo et al. (2013) – Suspension in hexane	NM	0.06	30.11	8.46	9.34	45.13	4.46	NM	38.63	49.59
Acevedo et al. (2013) – SFE	NM	ND	35.78	6.25	8.72	46.53	2.02	NM	42.03	48.55
Somnuk et al. (2017) – Suspension in solvent	0.02	0.09	34.44	0.00	7.74	43.12	1.18	2.83	37.38	44.3

ND: not detected, NM: not mentioned, TR: traces, SFA: saturated fatty acids, PUFA: polyunsaturated fatty acids, SFE: Supercritical fluid extraction, UAE: Ultrasound assisted extraction, MAE: Microwave assisted extraction, *: Two-phase solvent extraction enhanced with ultrasonication.

It can be seen in Table 2.5 that differences in the brewing method that generates retail, espresso and instant SCG do not have a systematic effect on the fatty acid profile of the oil, something that has also been reported by Ratnayake et al. (1993) and Jenkins et al. (2014). Another observation is that in some oils linoleic acid is present at the highest concentration of all the detected fatty acids, while in other samples palmitic acid can be found in concentrations greater than linoleic acid. Martín et al. (2001) found that SCG oils can be generally categorized into two classes based on their fatty acid composition: those with low palmitic (<40%) and high linoleic (>40%) acids and reversely, those with high palmitic (>40%) and low linoleic (<40%) acids. According to Martín et al. (2001) and (Budryn et al., 2012) such differences in composition can be most likely attributed to the origin of the coffee sample, and more specifically the climatic conditions during growth of the crop, and the different blends of coffee varieties that may have been used during brewing.

In addition, Jenkins et al. (2014) demonstrated that the majority of coffee oils examined from various SCG samples have similar composition irrespective of the origin and type of bean, however, differences in fatty acid profile can be found as is the case for SCG oils extracted from samples that were cultivated in Vietnam and Costa Rica (Table 2.5).

Furthermore, it can be seen in Table 2.5 that the lipid extraction method used is another factor that can possibly affect the fatty acid composition of SCG oil. In particular, different solvent extraction methods used within the same study were found to yield SCG lipids with somewhat similar fatty acid profiles as was the case with the fatty acid profiles reported by Ahangari and Sargolzaei (2013), Abdullah and Bulent Koc (2013) and Acevedo et al. (2013), while Akgün et al. (2014) demonstrated that the use of different solvents in Soxhlet extraction does not significantly affect the fatty acid profile of the recovered SCG oil (Table 2.5). However, the use of Supercritical fluid extraction (SFE), which is discussed in Section 2.4.2, resulted in SCG oil with varying percentages of the main fatty acids present relative to solvent-extracted SCG oil in two of the previous studies (Ahangari and Sargolzaei, 2013; Couto et al., 2009).

Based on its composition, the oil recovered from SCG is considered an attractive material for use in the food and pharmaceutical industries due to the health benefits and antioxidant activity of the polyphenols present (Acevedo et al., 2013; Oliveira et al., 2006; Ribeiro et al., 2013), while the high presence of palmitic acid in the SCG oil renders it a possible source for soap manufacture (Campos-Vega et al., 2015). Furthermore, SCG oil has potential for use in the cosmetics industry as palmitic acid provides good skin protection as a sun filter (Acevedo et al., 2013)

Various SCG oil properties, like density, kinematic viscosity, saponification value and water and sulfur content, which are important for the potential utilization of the oil either directly as an engine fuel or as a biodiesel feedstock, have been determined in previous studies that extracted oil from SCG and are presented in Table 2.6.

Table 2.6: Characterization of SCG oil.

References	Density at 15 °C (kg/m ³)	Kinematic viscosity at 40 °C (mm ² /s)	Water content % (w/w)	Sulfur content % (dry w/w)	Saponification value (mg _{KOH} /g)
Deligiannis et al. (2011)	933.8	46.96	0.08	0.00045	-
Haile (2014)	917	42.65	0.03	-	167.28
Al-Hamamre et al. (2012)	1180.4-1149 ^a	53.06-238.04	-	0	173.9-222.6
Berhe et al. (2013)	922.8	35.50	0.025	-	-
Vardon et al. (2013)	-	49.64	0.033	-	-
Caetano et al. (2014)	912-914	14.9-43.9	0.092-0.133	-	-
Caetano et al. (2012)	917	22.23	0.2	-	-
Abdullah and Bulent Koc (2013)	890	62.0 ^b	1.78	0.006	-

^a: Density measured at 25 °C, ^b: Kinematic viscosity measured at 20 °C.

It can be seen in Table 2.6 that SCG oil has a high density that ranges between 890 and 1149 kg/m³ in previous studies, with the variations found within the same study attributed to solvent selection and moisture content of SCG (Al-Hamamre et al., 2012; Caetano et al., 2014). Furthermore, the high kinematic viscosity of the oil, which also varies depending on the solvent used and the wetness of the grounds, is an inhibitory factor for direct utilization as engine fuel because it can result in pump blockage and oil ring sticking (Al-Hamamre et al., 2012; Caetano et al., 2012; Haile, 2014). The relatively high viscosity and density of SCG oil render it unsuitable for direct utilization as a fuel as it will polymerize and lead to formation of deposits in the engine (Haile, 2014).

Table 2.6 also shows that SCG oil contains low amounts of water ranging between 0.02-1.78 % w/w, and a near zero sulfur content, while the relatively high saponification value indicates a high degree of oxidation and possible occurrence of hydrolysis reaction (Haile, 2014; Knothe, 2007). Finally, SCG oil is mostly composed of carbon (76.16-81.17 % w/w) and hydrogen (10.9-11.91 % w/w) with small amounts of oxygen (7.25-13 % w/w) and traces of nitrogen (0.13-0.45 % w/w) according to Al-Hamamre et al. (2012), while the variations in the elemental composition can be attributed to the different solvents used for lipid extraction.

2.3.3 Moisture content and dewatering of SCG

SCG normally contain a relatively high moisture content varying from between 50 and 85% w/w depending on the brewing process used (Al-Hamamre et al., 2012; Gómez-De La Cruz et al., 2015), though have also been reported as containing lower levels of moisture of between 18–45% w/w by Deligiannis et al. (2011). The water is present either as unbound excess moisture arising from the brewing process, with SCG used in the production of instant coffee generally retaining higher moisture levels than retail SCG generated from coffee bars, or bound moisture entrapped within the microstructure of the solid particles, levels of which vary with the origin and type of the bean (Al-Hamamre et al., 2012; Gómez-De La Cruz et al., 2015).

The relatively high moisture content of SCG can be a potential disadvantage for the valorization of SCG as a raw material for biofuels, and especially for the recovery of lipids as most extraction methods require a dry feedstock (Corrêa et al., 2014; Gómez-De La Cruz et al., 2015). Furthermore, when SCG are directly utilized as fuel pellets, their moisture content should be reduced to increase calorific value and combustion efficiency of biomass (Gómez-De La Cruz et al., 2015). Thermal drying at temperatures ranging between 50 °C and 105 °C and for durations up to 48 hours has been used for dewatering SCG at laboratory scale prior to lipid recovery and further processing (Al-Hamamre et al., 2012; Caetano et al., 2014; Haile, 2014; Kondamudi et al., 2008; Vardon et al., 2013).

Gómez-De La Cruz et al. (2015) investigated the effect of SCG sample thickness between 5 and 20 mm, drying duration up to 4.2 hours and drying temperature between 100 °C and 250 °C on the efficiency of the drying process through a convective oven, and found that drying time decreases with temperature increase and sample thickness decrease. Corrêa et al. (2014) examined the drying of SCG in a cyclonic dryer at temperatures ranging between 59 °C and 271 °C and found the moisture reduction to be inversely proportionate to the solid mass flow and directly proportionate to the applied temperature.

Mechanical expression is another method that can be used for dewatering a range of biomaterials, either at ambient temperature or combined with thermal drying, for subsequent solvent extraction or direct use as fuel pellets (Berk, 2013; Clayton et al., 2006; Schwartzberg, 1997). Mechanical expression has been previously used for water removal from SCG, as was demonstrated by Schwartzberg (1997), who removed 63 % w/w of the moisture content from SCG by applying 600 bar of pressure by a ram press (ram speed of 500 mm/min) at room temperature. A previous study considering lignite, bio-solids and bagasse investigated mechanical dewatering at temperatures ranging between 20 and 200 °C and pressures from 15 to 240 bar, for a constant duration of 5 minutes, and found that processing conditions of 150 °C and 120 bar removed approximately 55 to 75 % of the water present (Clayton et al., 2006).

2.4 Oil extraction

Oil extraction is one of the most important steps in the valorization of SCG, as the extraction method used has an effect not only on the yield of the obtained oil, but also on its physical and chemical properties (Ahangari and Sargolzaei, 2013; Al-Hamamre et al., 2012). The methods that have been previously investigated for lipid recovery from SCG include different variations of solvent extraction (discussed in Section 2.4.1) and SFE (Section 2.4.2). Solvent (Soxhlet) extraction has also been used for lipid recovery from coffee silver skin (Toschi et al., 2014) and RDCB (Oliveira et al., 2006).

2.4.1 Solvent extraction

The solvent extraction of lipids from SCG is a process of separating a soluble component from the insoluble solid matrix in which it is dispersed with the use of an organic solvent (Berk, 2009; Duroudier, 2016; Johnson and Lusas, 1983; Rao, 2009). This process, also known as leaching, has been previously referred as a solid-liquid extraction to distinguish it from liquid-liquid extraction, in which a liquid organic solvent phase is used to extract a liquid component from another liquid phase, usually aqueous (Berk, 2009; Rao, 2009). The mechanism of solid-liquid extraction is based on the preferential dissolution of the solute, which in the case of oil extraction from oilseeds is already to liquid state, from the solid matrix in the liquid solvent (T. Toledo, 1993).

The process initially involves the penetration of solvent in the solid, followed by dissolution and transport of the solutes from the interior of solid particles to the solid-solvent interface (Berk, 2009; Rao, 2009). Subsequently the solutes are dispersed in the bulk of the solvent by means of diffusion and agitation (Berk, 2009). Solid-liquid extraction is a mass-transfer process, the rate of which determines the duration required to achieve equilibrium between phases (T. Toledo, 1993). The mass transfer rate depends on the length of the diffusion path that the solute must cross within the solvent-saturated solid and is therefore affected by the particle size (Berk, 2009; T. Toledo, 1993). However, very small particles will impede percolation of solvent through the solid matrix and increase the probability of fines being extracted along with the desired solute (T. Toledo, 1993). The rate of mass transfer is also affected by

the surface area and porosity of the solid, the viscosity and diffusivity of the solvent into the solvent matrix, the temperature of extraction and the degree of agitation which might be employed to improve diffusivity (Berk, 2009; Rao, 2009), and this has been previously described by Equation 2.1:

$$\frac{dM}{dt} = k A (C_s - C) \quad (\text{Equation 2.1})$$

Where M is mass transferred in time t, C_s is the saturated concentration of solute in the solvent, C is concentration of solute dissolved in the solvent at any time t, A is the available area of contact and k is a mass transfer coefficient (Rao, 2009).

The highest possible solute concentration in the solvent is the saturation concentration and therefore, the solvent to solid ratio must be high enough to ensure that the resulting solution will be below the saturation concentration of the solute when the equilibrium is reached (T. Toledo, 1993). Equilibrium is achieved when the solute concentration is equal in both the solid and the solvent phase, and consequently multiple extraction stages with fresh or recycled solvent are required in order to obtain a concentrated extract (Berk, 2009). Consequently, a high solubility of the solute in the solvent will reduce the number of stages needed to reach a desired degree of solute removal (Berk, 2009; T. Toledo, 1993).

Regarding the molecular processes involved in the solvent extraction of oil, the non-polar oil molecules are initially desorbed from their site in the oil-bearing material in an endothermic reaction and diffused through the organic part of the matrix to reach the matrix-solvent interface (Freeman et al., 2011; Johnson and Lusas, 1983; Mustafa and Turner, 2011). Thereafter, oil molecules diffuse into the solvent phase and energy is required to dissociate the solvent molecules so as they can accommodate them, with polar solvents requiring more energy than non-polar due to stronger intermolecular forces (Johnson and Lusas, 1983; Mustafa and Turner, 2011). Finally, oil and solvent molecules interact in an exothermic process, where the released energy is higher when polar solvents are used (Johnson and Lusas, 1983). In general, oil molecules dissolve in a solvent when the intermolecular forces of attraction between oil molecules and solvent molecules can be overcome by the

intermolecular forces of the oil-solvent solution (Reichardt and Welton, 2010a).

Based on the strength of the interactions between oil and oil-bearing matrix the extraction process can be separated into two stages, the initial and brief solubility-controlled phase in which the oil-matrix interactions are quite weak, and the longer desorption-controlled phase that follows where there are stronger interactions between oil and matrix or long diffusion paths inside the sample matrix (Mustafa and Turner, 2011).

There are a number of studies that have investigated the recovery of lipids from SCG through solvent extraction, with the majority of them using a Soxhlet method with dry SCG (Acevedo et al., 2013; Al-Hamamre et al., 2012; Berhe et al., 2013; Caetano et al., 2014, 2012; Cruz et al., 2012; Deligiannis et al., 2011; Haile, 2014; Kondamudi et al., 2008; Kwon et al., 2013; Lago et al., 2001; Vardon et al., 2013).

Soxhlet solvent extraction has been the baseline method used in most studies, and in most cases when other methods are investigated, the extraction ratios obtained are expressed relative to the yield obtained through a Soxhlet method using hexane as the solvent (Abdullah and Bulent Koc, 2013; Ahangari and Sargolzaei, 2013). Soxhlet solvent extraction involves the solubilisation of the oil present in SCG by a liquid organic solvent and its separation from the solvent-wetted grounds through numerous cycles of evaporation and condensation of the solvent (Harwood et al., 1998; Johnson and Lusas, 1983). Hexane is regarded as the most effective solvent in studies which have considered a range of solvents (Al-Hamamre et al., 2012; Kondamudi et al., 2008). Table 2.7 shows the oil yields obtained from SCG by Soxhlet solvent extraction with hexane in previous studies, along with information about the oil FFA content, SCG-to-solvent ratio and process duration where these were disclosed.

Table 2.7: Soxhlet extraction oil yields on a dry weight basis reported in other studies when hexane was the solvent used.

References	(%) w/w Oil yield on dry weight basis	(%) w/w FFA content	Process duration (h)	SCG-to-solvent ratio (w/v)
Deligiannis et al. (2011)	15	0.31	-	-
Kondamudi et al. (2008)	13.4	-	1	1:3
Al-Hamamre et al. (2012)	11.2-15.3	3.65	0.25-0.5	1:4.2
Caetano et al. (2012)	16	59*	2.5-9.5	1:20
Ahangari and Sargolzaei (2013)	16.7	-	6	1:15
Haile (2014)	15.6	4.9*	4-8	-
Acevedo et al. (2013)	26.4	-	5	1:125
Berhe et al. (2013)	19.73	7.4	6	-
Vardon et al. (2013)	16.2	5.6	8	-
Abdullah and Bulent Koc (2013)	13	-	8	1:15
Go et al. (2016)	13.78-16.51	-	8	-
Couto et al. (2009)	18.3	-	-	-

*: FFA content calculated in oil extracted with 50:50 v/v mixture of hexane and isopropanol.

A direct comparison of the results presented in Table 2.7 is challenging due to the different SCG types used, which would likely have differing absolute oil contents and varying compositions, along with the various conditions of duration and SCG-to-solvent ratios employed. Nevertheless, it can be seen in Table 2.7 that most researchers have used Soxhlet durations of about 6 to 8 hours, while there seems to be no systematic effect of duration or SCG-to-solvent ratio on the FFA content of the extracted SCG oil.

Variations of solvent extraction have also been used for oil extraction from SCG, including Microwave-assisted extraction (MAE), Ultrasound-assisted extraction (UAE) and suspension of SCG in a solvent. MAE has been used by

Ahangari and Sargolzaei (2013), who irradiated dry retail SCG suspended in solvent for 10 minutes and obtained extraction ratios ranging between 77.25 and 82.3 % w/w of the total available oil calculated through Soxhlet (Table 2.7), with higher irradiation power leading to higher extraction ratios. UAE of a SCG-solvent suspension at ambient conditions was also examined in the same study with an extraction ratio of ~83 % w/w of the available oil after 45 minutes (Ahangari and Sargolzaei, 2013). The oil extracted with both of these methods had a similar oil composition with oil extracted through Soxhlet in the same study (Table 2.5).

UAE has also been investigated by Rocha et al. (2014) for lipid extraction from dry retail SCG suspended in hexane, with a maximum yield of 12 % w/w obtained, while the fatty acid profile of the extracted oil is presented in Table 2.5. Abdullah and Bulent Koc (2013) examined oil removal from wet SCG using two-phase solvent extraction (methanol and hexane) enhanced with ultrasonication at room temperature and extracted 98 % w/w of the available oil in 30 minutes (Table 2.7). The fatty acid profile of the oil obtained through by UAE was almost identical to that of oil extracted through Soxhlet (Table 2.5). On the contrary, Caetano et al. (2014) reported that the use of ultrasound in Soxhlet extraction did not improve the extraction efficiency from SCG.

Another variation of solvent extraction is the suspension of SCG in a solvent, which has been investigated by Jenkins et al. (2014), Pichai and Krit (2015), Somnuk et al. (2017), Najdanovic-Visak et al. (2017) and Acevedo et al. (2013). Oil yields between 7 and 14.75 % w/w were obtained when retail (Jenkins et al., 2014), and espresso SCG were used (Najdanovic-Visak et al., 2017; Pichai and Krit, 2015; Somnuk et al., 2017), while suspension of instant SCG in hexane for 5 hours resulted in an oil yield of 11.2 % w/w (Acevedo et al., 2013), significantly lower than the yield achieved by Soxhlet method at the same duration (26.4 % w/w – Table 2.7). However, it should be noted that a much higher SCG-to-solvent ratio of 1:4 w/v was used in this case relative to that used in Soxhlet extraction (1:125 w/v - Table 2.7) (Acevedo et al., 2013), and this along with the non-recirculating operation might have been responsible for the low oil yield. The fatty acid profile of the oil obtained by the

SCG-solvent suspension was not significantly different than that of Soxhlet extracted oil (Table 2.5).

Generally, based on the results obtained by studies that have examined multiple methods, Soxhlet is the most effective in removing lipids, while insignificant variations in the oil fatty acid composition and FFA content have been observed when different variations of solvent extraction were used relative to that obtained by Soxhlet extraction (Acevedo et al., 2013; Ahangari and Sargolzaei, 2013). However, the duration of MAE and UAE in both of these studies was significantly shorter than Soxhlet extraction duration, with the relatively high extraction ratios obtained suggesting an increased extracting efficiency when microwave power or ultrasonication is combined with solvent extraction.

In addition, Accelerated solvent extraction (ASE), also known as pressurized fluid extraction, is a solvent extraction method that has been utilized for extraction of lipids from oilseeds such as rapeseed (Matthäus and Brühl, 2001), soybean (D. Luthria et al., 2004; Matthäus and Brühl, 2001), pistachio kernels (Sheibani and Ghaziaskar, 2008), sunflower seeds (Matthäus and Brühl, 2001), corn kernels (Moreau et al., 2003), oats (Moreau et al., 2003) and rice bran (Jalilvand et al., 2013). ASE operates at elevated temperature and pressure conditions either with static extraction cycles, or with continuous flow of the selected liquid organic solvent (Camel, 2001; Carabias-Martínez et al., 2005; Kaufmann and Christen, 2002; D. Luthria et al., 2004), and is investigated in this study for lipid extraction from SCG.

Due to the difficulty of comparing results of oil extraction from SCG in previous studies, and especially those that used Soxhlet method at a variety of durations and SCG-to-solvent ratios, the influence of each of the various solvent extraction processing parameters will be discussed independently from others in the following Sections (2.4.1.1-2.4.1.7).

2.4.1.1 Effect of process duration

The effect of solvent extraction duration has been partly addressed by Al-Hamamre et al. (2012) using a Soxhlet process for extraction from SCG for short durations of between 15 and 30 min, but without revealing a clear

correlation between oil yield and extraction time. Pichai and Krit (2015) also investigated the effect of extraction duration by suspending SCG in hexane for durations up to 39.8 minutes with obtained yields ranging between 12.66 % w/w and 14.63 % w/w at a constant SCG-to-solvent ratio of 1:15 w/w, and revealing a small beneficial effect of prolonged duration on lipid extraction efficiency. Furthermore, Go et al. (2016) extracted lipids from SCG through the Soxhlet method and found that 2 hours of extraction were sufficient, with prolongation of duration to 8 hours resulting in insignificant oil yield increase. Finally, Abdullah and Bulent Koc (2013) found that prolongation of the two-phase UAE duration from 5 to 30 minutes resulted in the extraction of an additional 80 % w/w of lipids. Information regarding any possible effect of duration on the composition of the SCG extracted oil was not provided in any of the aforementioned studies.

Solvent extraction at varying durations was also performed in the studies of Somnuk et al. (2017) and Caetano et al. (2012), however, different solvents were used for extraction at different durations, thus complicating the evaluation of the duration effect on the process. Nevertheless, the highest oil yield in the study of Caetano et al. (2012) was achieved during the longer lasting extraction of 9.5 hours with octane.

Picard et al. (1984) who investigated the solvent extraction of lipids from fresh roasted Robusta grounds, found that with increasing extraction time from 6 to 8 hours the oil yield increased from 11.4 to 11.6 % w/w, and then slightly decreased at longer durations of 10 and 12 hours to 11.0 and 10.9 % w/w respectively. The effect of extraction duration on the oil yield obtained from other oilseeds such as soybean, sunflower and cotton by Soxhlet solvent extraction has been previously investigated, with durations between 3.5 and 5 hours found to be optimal as shorter durations reduced oil yields, while further increase in extraction duration did not further increase obtained yields (Kerbala University, 2010; Lawson et al., 2010). Another study examining the Soxhlet extraction of oil from jatropha seeds concluded that most of the oil was extracted after 6 hours, although a slightly higher oil yield was achieved after 8 hours (Sayyar et al., 2009).

Previous studies have also investigated the effect of process duration on ASE extraction of lipids with varying results. For example, Jalilvand et al. (2013) and Sheibani and Ghaziaskar (2008) performed extraction of rice bran oil and pistachio oil through ASE for durations ranging between 5 and 30 minutes and reported no significant change in the extraction yield. In addition, Yao and Schaich (2015) investigated lipid removal from dry pet food through ASE (40 °C, 103 bar) at static extraction durations of 5, 10 and 20 minutes and found a prolonged process duration to be counterproductive for extraction efficiency.

2.4.1.2 Effect of SCG-to-solvent ratio

The ratio of dry SCG-to-solvent has a significant impact on the oil yield obtained from SCG, with Pichai and Krit (2015) investigating SCG-to-hexane mass ratios between 1:5.1 and 1:24.9 and reporting a correlation between decreasing SCG-to-solvent ratio and improved oil yield. This observation was explained by enhanced diffusion and flow of oil through the pores and surface of SCG due to increased solvent quantity (Pichai and Krit, 2015). In addition, Najdanovic-Visak et al. (2017) also examined the effect of SCG-to-hexane ratio in a SCG and solvent suspension at 60 °C, and found that a decrease in SCG-to-solvent ratio from 1:8 w/v to 1:15 w/v resulted in improved yield, with further decrease to 1:25 w/v leading to insignificant oil yield increase. A similar relationship of SCG-to-solvent ratio and lipid extracting efficiency was found in UAE trials with SCG performed by Rocha et al. (2014) and Abdullah and Bulent Koc (2013) who tested SCG-to-hexane ratios between 1:2-1:4 w/v and 1:1-1:2 w/v respectively and found the lowest of the examined ratios to result in the highest oil recovery.

The effect of seed to solvent ratio on extraction efficiency of oil has also been investigated with other oilseeds such as soybean, sunflower, cottonseed and jatropha seeds with contrasting results (Bulent Koc and Fereidouni, 2011; Kerbala University, 2010; Sayyar et al., 2009). The effect of soybean seed to hexane ratio on lipid extraction efficiency was investigated by Bulent Koc and Fereidouni (2011) through ultrasound assisted Soxhlet extraction, with a correlation between increasing seed to solvent ratio from 1:10 to 1:2 w/v and increasing oil yield observed. Similar observations have been made when extracting lipids from soybean,

sunflower and cottonseed at seed to solvent ratios of 1:1 w/v, 1:5 w/v and 1:10 w/v (Kerbala University, 2010).

However, Sayyar et al. (2009) found that the efficiency of the lipid extraction from jatropha seeds increased when the seed-to-solvent ratio was decreased from 1:4 to 1:6 w/v and a marginal increase in oil yield was achieved with a ratio of 1:7 w/v. It was theorized that this increase in oil yield with a low solid-to-solvent ratio up to a limit could be attributable to the decrease in the concentration gradient between solid and liquid phase which favors mass transfer, in agreement with Pichai and Krit (2015) when investigating lipid extraction from SCG (Sayyar et al., 2009).

2.4.1.3 Effect of SCG particle size

With regards to the impact of SCG particle size on the obtained oil yield, Go et al. (2016) performed Soxhlet extraction with two SCG samples of average particle sizes of 430.5 ± 32.3 and 374.7 ± 8.3 μm , and obtained oil yields of 16.51 ± 0.73 % w/w and 13.78 ± 0.43 % w/w respectively. However, the difference in oil recovery could be potentially attributed to the different origin of the SCG samples. Furthermore, pretreatment methods that affect particle size like milling and extrusion have been reported in one occasion to have no effect on the oil yield obtained from SCG with ethanol (Campos-Vega et al., 2015).

On the contrary, previous studies investigating lipid extraction from other oilseeds (e.g. soybean) have highlighted the need for size reduction by grinding prior to solvent extraction in order to increase surface area of oil-bearing particles and facilitate oil removal (Akoh, 2005; Varzakas and Tzia, 2015). For example, Folstar et al. (1976) used sieves of 0.12 mm up to 0.85 mm to size green Arabica coffee grounds and observed a slight decrease in the oil yield as the particle size increased.

Studies on lipid extraction from other oilseeds have most commonly investigated the effect of seed flake thickness on the solvent extraction efficiency, and this has been found to linearly correlate with average particle size, with a particle size of 0.22 mm corresponding to a flake thickness of 0.18 mm (Lawson et al., 2010). The formation of flakes includes the heating of

dehulled or cracked oilseed at high temperatures to soften prior rolling them into flakes. Soybean seed flakes of thicknesses between 0.2 and 0.3 mm were reported to result in higher oil extraction rates, while a decrease in flake thickness from 5 to 0.5 mm resulted in yield increases in the case of oil extraction from soybean, cottonseed and sunflower seed (Akoh, 2005; Kerbala University, 2010; Lajara, 1990; Lawson et al., 2010; Varzakas and Tzia, 2015). It was generally suggested that small and thin flakes offer good solvent permeability and oil diffusion, but poor percolation of solvent, while large thick seed flakes possess inverse properties due to surface area decrease, with a balance between these two limiting conditions resulting in optimum oil yields (Akoh, 2005; Kerbala University, 2010; Lajara, 1990; Lawson et al., 2010; Varzakas and Tzia, 2015).

Finally, Sayyar et al. (2009) investigated the extraction of lipids from jatropha seeds with various particles sizes and found that an intermediate particle size (0.5–0.75 mm) resulted in the highest oil yields, with lower oil recoveries being reported in the case of larger and smaller particles. The reduction in oil yield observed when jatropha seed particles smaller than 0.5 mm were used, with only 40 % of oil being extracted relative to the size range of 0.5–0.75 mm, was attributed to agglomeration of fine particles that reduced the surface area available for solvent flow (Sayyar et al., 2009).

2.4.1.4 Effect of SCG moisture content

The effect of SCG moisture content on the efficiency of lipid extraction with hexane through Soxhlet has been investigated by Caetano et al. (2014), with a moisture presence of 65.7 % w/w significantly hindering the oil recovery process, and leading to oil with higher density and viscosity values relative to lipids extracted from dry SCG samples. Najdanovic-Visak et al. (2017) suspended SCG of moisture contents between 0 and 50 % w/w in hexane at a temperature of 60 °C for 60 minutes and reported a substantial decrease of oil extraction ratio (up to 70 % w/w) with moisture increase, attributing this trend to reduced solubility of lipids in the hydrophobic solvent used. However, Abdullah and Bulent Koc (2013) performed a successful lipid extraction from SCG with a moisture content of 67 % w/w by a two-step UAE method and

found no significant effect of SCG moisture presence on the extracted oil composition (Table 2.5), except for a higher oil water content (Table 2.6).

In previous studies examining the extraction of lipids from other oilseeds, an intermediate moisture content of 9–11 % w/w resulted in peak oil yields, with higher levels of moisture found to interfere with the solvent penetration and oil diffusion, especially when hexane was the solvent used as it is highly insoluble in water (Akoh, 2005; Kerbala University, 2010; Lajara, 1990; Lawson et al., 2010). Lower feedstock moisture contents were observed to result in lower yields due to the reduced solubility of phosphatides in the absence of water (Lajara, 1990). On the contrary, a previous study that investigated the Soxhlet solvent extraction of oil with ethanol from partially dried flax seeds with moisture content up to 12 % w/w reported a decrease in oil yield with increasing moisture content (Ali and Watson, 2014).

Furthermore, Jalilvand et al. (2013) investigated the dynamic (i.e. continuous solvent flow) pressurized fluid extraction of oil from rice bran with a moisture content of 10.2 % w/w with hexane and achieved a 100 % extraction ratio at a temperature of 77 °C, however, the elevated temperature and pressure under which this process took place may have been responsible for the efficiency of the extraction.

2.4.1.5 Effect of solvent pressure

Most solvent extraction methods operate at conditions of atmospheric pressure, with the exception of MAE which can achieve pressures above the ambient in closed vessels (Veggi et al., 2013), and ASE, in which a high-pressure pump increases the extraction pressure (ThermoFisher, 2011).

In MAE the importance of pressure on process efficiency is considered to be relatively low compared to that of microwave power and temperature (Kaufmann and Christen, 2002; Veggi et al., 2013). Ahangari and Sargolzaei (2013) investigated the extraction of oil from SCG through MAE by irradiating the SCG and solvent suspension at power levels of 200 W and 800 W, without specifying though the pressure achieved.

The effect of pressure on the process efficiency has been evaluated in the case of ASE extraction of oil from pistachio kernels and rice bran. The effect of pressure (10 to 150 bar) on the extraction of pistachio oil with hexane at 60 °C was found to be negligible (Sheibani and Ghaziaskar, 2008). However, Jalilvand et al. (2013) investigated dynamic ASE extraction of rice bran oil with hexane at a temperature range of 40 °C to 80 °C and at pressures ranging between 20 and 140 bar, and found that the oil yield increased significantly with increasing pressure up to 75 bar, with a further increase decreasing oil yield.

Other studies investigating the extraction of various compounds through ASE have also considered the effect of pressure. For example, these include the extraction of taxanes from the bark of *Taxus cuspidata* at 150 °C, where an increase of pressure from 10 to 202.7 bar did not change the obtained yields (Kawamura et al., 1999). Similarly in the extraction of essential oils from herbal plants (Carabias-Martínez et al., 2005), and polyaromatic hydrocarbons from soils and polymer samples (Giergielewicz-Mozajska et al., 2001), no effect of pressure was observed.

However, in other ASE studies an increase of pressure led to improved recoveries: the extraction of pesticides from moisturized soils at a temperature range of 100-150 °C where pressure increase from 34.4 to 103.4 bar was found to be beneficial (Camel, 2001), extraction of steroids from plant material at temperatures ranging between 40 and 100 °C where recovery slightly improved when the pressure was increased from 100 to 250 bar (Kaufmann et al., 2001), extraction of polyaromatic hydrocarbons from silica at 100 °C where the pressure ranged from 34.4 to 172.4 bar and higher pressures resulted in improved recoveries (Richter et al., 1996). Moreover, pressurized fluid extraction of essential oil from *Lavandula angustifolia* with ethanol at temperatures ranging between 60 and 100 °C showed that a pressure increase from 10 to 36 bar increased the oil yield, with a further increase up to 50 bar having a negligible effect on the process efficiency (Kamali et al., 2014).

Generally, increase of pressure favors the penetration of the solvent into the matrix pores and enhances solubility and desorption kinetics, thus resulting in increased extraction efficiency (Camel, 2001; Kaufmann et al., 2001; Kaufmann and Christen, 2002; Matthäus and Brühl, 2001; Mustafa and Turner, 2011; Richter et al., 1996). However, the increase in extraction pressure is also likely to result in increase of the viscosity and surface tension of the solvent (Mezger, 2006; Rusanov and Prokhorov, 1996). According to previous studies, the effect of pressure is of minor importance in ASE and its main advantage is that it enables solvents to remain liquid at temperatures above their boiling point (Camel, 2001; Carabias-Martínez et al., 2005; Kaufmann and Christen, 2002; Mustafa and Turner, 2011), although, Luthria et al. (2004) and Richter et al. (1996) have suggested that a system pressure above the threshold required to maintain the solvents in liquid state (~100 bar), provides rapid filling and flushing of the extraction cells used.

2.4.1.6 Effect of extraction temperature

The effect of process temperature on the solvent extraction of oil from SCG has been examined in the study of Rocha et al. (2014) through UAE at temperatures between 20 °C and 60 °C, with the highest yield achieved at the highest temperature, while Najdanovic-Visak et al. (2017) also found a beneficial effect of increasing temperature within the same range in oil extraction through suspension of SCG in hexane. In the Soxhlet method, the extraction temperature depends on the boiling point of the solvent used, and therefore temperature cannot be considered as an independent process parameter, however, it is a significant factor in the ASE method (Camel, 2001; Luthria et al., 2004).

Previous studies that investigated the effect of extraction temperature (40 °C to 100 °C) on the accelerated solvent extraction of lipids from sources including rice bran (Jalilvand et al., 2013), pistachio seed (Sheibani and Ghaziaskar, 2008) and corn kernels and oats (Moreau et al., 2003), observed that increase of extraction temperature resulted in improved oil yield. Increase of the extraction temperature decreases the strength of solvent intermolecular forces and thus its viscosity, allowing better penetration into the matrix particles, and decreases surface tension allowing the solvent to better coat the

feedstock and therefore increase rates of lipids extraction (Camel, 2001; Kaufmann and Christen, 2002; Richter et al., 1996). A decrease in surface tension also leads to easier formation of cavities, and lipid molecules are more quickly dissolved in the solvent (Richter et al., 1996).

Generally, an increase in temperature improves the solubility of lipids, as high temperature can disrupt the cohesive and adhesive interactions between oil molecules and oil-matrix molecules respectively, thus facilitating mass transfer and increasing the diffusion rate of the lipids (Johnson and Lusas, 1983; Richter et al., 1996; Yao and Schaich, 2015). However, high extraction temperatures (100-200 °C) may decrease the selectivity of the process and result in the extraction of bound lipids, impurities and cell wall components like arabinogalactans and mannans (Campos-Vega et al., 2015; Quinn, 1988; Zuorro and Lavecchia, 2012)

2.4.1.7 Effect of solvent composition

The selection of solvent is an important process parameter in the solvent extraction of lipids from SCG as it impacts on the yield and composition of the obtained oil, and has been investigated in previous studies with varying results (Al-Hamamre et al., 2012; Caetano et al., 2012; Kondamudi et al., 2008). Caetano et al. (2012) performed Soxhlet extractions from SCG with hexane, heptane, octane, ethanol, isopropanol and mixtures of hexane and isopropanol ranging from 50:50 v/v to 80:20 v/v, and found that the greatest oil yield was obtained with octane (26.5 % w/w) and the lowest with hexane and ethanol (16 % w/w). However, the duration of these extractions varied with each solvent without being specified, and the high yield obtained with octane can possibly be attributed to the high process temperature (close to the boiling point of octane, 126 °C). In addition, Haile (2014) found that a 50:50 v/v mixture of hexane and isopropanol removed more lipids relative to hexane and diethyl ether, possibly due to the increased solubility of SCG polar compounds in isopropanol.

Al-Hamamre et al. (2012) used pentane, hexane, toluene, chloroform, acetone, isopropanol and ethanol in Soxhlet extractions from SCG and found that hexane removed the highest amount of lipids (15.28 % w/w) and

chloroform the lowest (8.6 % w/w), while the polar solvents used generally resulted in lower oil yields compared to the non-polar, and in addition resulted in the extraction of a black gummy material. It was suggested that this material might be composed of proteins, carbohydrates and other compounds produced by complexes of fatty acids and carbohydrate breakdown components that can possibly inhibit the extraction process (Al-Hamamre et al., 2012). Somnuk et al. (2017) suspended SCG in hexane, ethanol and methanol, with hexane found to be the most effective and methanol the least effective solvent in terms of lipids extraction with yields of 14.7 % w/w and 7.5 % w/w respectively. Akgün et al. (2014) found hexane more efficient in extracting lipids from SCG relative to dichloromethane during Soxhlet experiments.

Kondamudi et al. (2008) found that use of dichloromethane in Soxhlet resulted in a slightly higher oil yield than hexane and diethyl ether. A possible explanation for this is the drying process, which was carried out at a temperature of 50 °C and may potentially have led to incomplete moisture removal. Therefore the slightly polar character of dichloromethane could have been responsible for the oil yield increase relative to that obtained with hexane, as polar solvents can improve the extraction rate from wet samples by extracting polar compounds (e.g. phosphatides) (Johnson and Lusas, 1983). For example, Moreau et al. (2003) examined the ASE extraction of oil from corn kernels with a moisture content of 14-16 % w/w using hexane, dichloromethane, isopropanol and ethanol and observed a correlation between increasing solvent polarity and higher oil yield.

Generally, non-polar solvents are better suited to oil extraction than polar ones, because the absence of strong polar charges allows easier penetration of the solvent into the low polar matrix of SCG (Al-Hamamre et al., 2012; Pujol et al., 2013). Polar solvents like alcohols are known to extract higher amounts of FFAs and undesired products such as proteins, carbohydrates, Maillard reaction products, phosphatides and other compounds (Al-Hamamre et al., 2012; Johnson and Lusas, 1983; Kondamudi et al., 2008).

Increased presence of FFAs in oil extracted with polar solvents relative to that recovered with non-polar ones was observed in the studies of Al-Hamamre et al. (2012), Kondamudi et al. (2008), Akgün et al. (2014) and Somnuk et al. (2017). Furthermore, according to Somnuk et al. (2017) extraction with ethanol and methanol led to oil with different proportions of mono-, di- and triglycerides relative to hexane, while Akgün et al. (2014) reported similar fatty acid profiles of oils extracted with hexane and dichloromethane (Table 2.5).

Moreover, the solvent selection does not appear to significantly affect the HHV of the extracted oil, with the exception of oil recovered with chloroform or propanol which resulted in SCG oil of somewhat lower HHV. The selection of extraction solvent has been observed to slightly affect the density but results in considerable differences of the kinematic viscosity of the oil, although without any systematic effect of solvent polarity (Al-Hamamre et al., 2012; Caetano et al., 2014). In conclusion, solvent selection impacts on the average chain length of fatty acids and the number of ester bonds present in the oil as expressed by the saponification (173.9-222.6 mg_{KOH}/g) and ester value respectively (166.6-213.5 mg_{KOH}/g), while it also slightly affects the oil elemental composition (Al-Hamamre et al., 2012).

With regards to the economic aspects of solvent selection, extraction with high boiling point solvents requires high amounts of energy if a reflux method is used, while utilization of low boiling point solvents may result in significant losses during extraction (Al-Hamamre et al., 2012). In large scale facilities safety aspects should also be considered for solvent selection, as well as availability and price (Johnson and Lusas, 1983).

2.4.2 Supercritical fluid extraction

SFE is an extraction method where a supercritical fluid, most often CO₂, is used for recovery of lipids or other compounds of interest, and which has been previously used for lipid removal from dry SCG, with obtained extraction ratios of the available oil ranging from 82.6 to 98.1 % w/w relative to Soxhlet oil yield (Acevedo et al., 2013; Ahangari and Sargolzaei, 2013; Akgün et al., 2014; Couto et al., 2009). In addition, CO₂ can be coupled with co-solvents such as ethanol or methanol that modify the conditions of the process and the

extraction yield. When CO₂ is used without a co-solvent the process takes place at conditions above the critical temperature (31.85 °C) and critical pressure (78 bar) of the fluid (Ahangari and Sargolzaei, 2013). The most important parameters in SFE extraction of lipids are pressure and temperature of the fluid and type and percentage of the co-solvent (Ahangari and Sargolzaei, 2013).

Couto et al. (2009) extracted oil from SCG in the pressure range of 150 to 300 bar at temperatures ranging between 39.85 °C and 59.85 °C and found that extraction yield increased with pressure increase at constant temperature. This is in agreement with the studies performed by Ahangari and Sargolzaei (2013) and Akgün et al. (2014) who conducted SFE experiments with SCG at similar temperatures (32.85-66.85°C) and at pressures ranging between 200 - 300 bar and 116 - 284 bar respectively. These observations, which are similar to those found during SFE of lipids from food residues (Reverchon and De Marco, 2006), can be attributed to the increased density of CO₂ at high pressures which results in increased capacity for solubilisation of lipids (Ahangari and Sargolzaei, 2013; Akgün et al., 2014; Couto et al., 2009).

However, the effect of temperature is more complex as an increase of temperature decreases the density of the supercritical fluid (and therefore its extraction efficiency), but also increases the solubility of the lipids (Couto et al., 2009). Varying effects of SFE temperature have been reported in previous studies, with Ahangari and Sargolzaei (2013) reporting oil yield decrease with increasing temperature, while Couto et al. (2009) observed increased oil yield with increasing temperature when the process was performed at pressures of 250 and 300 bar, but a reverse effect at 200 bar. The solubility of the lipids has been reported to be independent of the SFE temperature at pressures higher than 300 bar (Akgün et al., 2014; de Azevedo et al., 2008).

Regarding the influence of the use of a co-solvent, previous studies that investigated the SFE extraction of lipids from SCG agree that the addition of a co-solvent improves the oil yield and speeds up the extraction process, probably due to increase in the solvent density (Ahangari and Sargolzaei, 2013; Couto et al., 2009). In addition, Ahangari and Sargolzaei (2013)

compared water, ethanol and hexane as SFE co-solvents and found hexane to be the most effective in terms of oil recovery followed by ethanol and water, while a positive effect of increased co-solvent volume was observed on the oil yield.

Moreover, according to Couto et al. (2009) and Ahangari and Sargolzaei (2013), the fatty acid composition of the oil extracted by SFE was found to contain considerably different amounts of the main fatty acids typically found in SCG oil compared to oils extracted through solvent extraction, while the fatty acid profile of the SFE recovered oil was also significantly different depending on the extraction conditions. On the contrary, Akgün et al. (2014) and Acevedo et al. (2013) recovered SCG oil samples with similar fatty acid profiles by Soxhlet and SFE extraction (Table 2.5).

2.4.3 Mechanical expression

Mechanical expression of lipids is a method that has not been investigated before for lipid recovery from SCG, but is commonly used for oil removal from other oilseeds such as soybean (Bargale et al., 1999; Kemper, 2005), palm fruit (Kemper, 2005), rapeseed (Willems et al., 2008b), sesame seed (Willems et al., 2008b) flax seed (Ali and Watson, 2014; Willems et al., 2008b), rubber seed (Santoso et al., 2014) and almond seed (Adesina and And Bankole, 2013). Mechanical pressing has been previously used for oil recovery from ground RDCB by Oliveira et al. (2006), although the obtained yield and pressing conditions were not specified. The main factors that influence the mechanical expression of oil are applied pressure, heating temperature, moisture content, pressing duration and particle size (Sorin-Stefan et al., 2013).

Mechanical pressing of oilseeds is usually combined with thermal drying for better results, and a temperature of about 90 -100 °C facilitates lipid removal by decreasing the oil viscosity, destroying mould and rupturing the cell structure (Ali and Watson, 2014; Sorin-Stefan et al., 2013; Willems et al., 2008b), while materials that undergo mechanical expression are partially dried prior to the pressing procedure (Ali and Watson, 2014; Bargale et al., 1999; Khan and Hanna, 1983; Willems et al., 2008b). Ali and Watson (2014)

investigated the oil expression from flax seeds of water content between 4 and 12 % w/w with a screw press, and found that the yield increased with increasing moisture within the range investigated (Ali and Watson, 2014). (Willems et al., 2008b) investigated the expression of oil from sesame seeds with a hydraulic press at feedstock moisture contents of between 0 % and 5.5 % w/w and found that the highest yield was obtained at a moisture level of 2.1 % w/w.

Generally, an increase in the mechanical pressure applied leads to an oil yield increase in mechanical expression from oilseeds at pressures ranging from 100 to 700 bar (Santoso et al., 2014; Willems et al., 2008b), with pressures greater than 450 bar having shown an improvement in the oil yield up to 15 % w/w (oil/oil) relative to presses operating at lower pressures (Willems et al., 2008b). Furthermore, Santoso et al. (2014) who examined the hydraulic expression of oil from rubber seed at pressures between 80 and 120 bar, found a correlation between increasing duration of pressing (30 to 90 minutes) and higher oil yield, while in the case of pressing sesame seeds the yield increased for the first ten minutes of pressing and remained approximately constant thereafter (Willems et al., 2008b). Regarding the effect of particle size on the oil yield, Adesina and And Bankole (2013) found similar oil yields when pressing fine (< 0.5 mm) and coarse (> 0.5 mm) almond seeds, with pressing of the fine sample resulting in slightly improved lipid recovery. However, according to Adeeko and Ajibola (1990) the rate of oil expression from groundnuts increased when more coarse grounds (between 2.36 mm and 4.75 mm) were used compared to fine grounds (< 2.36 mm).

Mechanical oil expression is generally considered to be relatively inefficient when compared with other extraction methods, leaving a significant portion of the available oil in the pressed cake (Ali and Watson, 2014; Kemper, 2005; Sorin-Stefan et al., 2013). In particular, mechanical expression can reduce the oil in an oil-bearing material to between 5 and 10 % by weight, while solvent extraction typically reduces the oil to less than 1% w/w (Bargale et al., 1999; Kemper, 2005). However, mechanical expression results in oil free of dissolved chemicals and undesired non-lipid compounds that are co-extracted from cell walls during solvent extraction (Khan and Hanna, 1983; Sorin-Stefan

et al., 2013; Willems et al., 2008b), while it can also be employed as a pretreatment step prior to solvent extraction, resulting in improved oil recoveries due to cell distortion and partial oil removal from the feedstock caused by applied pressure (Johnson and Lusas, 1983; Kemper, 2005).

Regarding the effect of mechanical pressing on the composition of the oil, Oliveira et al. (2006) reported that the fatty acid profile of expressed RDCB oil had no significant differences with solvent extracted RDCB oil. However, the unsaponifiable content of the expressed oil was found to be 12.8 % w/w, while oil recovered by solvent extraction had a significantly lower amount of unsaponifiables of 9.2 % w/w and it was theorized that this difference can be attributed to the reduced selectivity of mechanical expression (Oliveira et al., 2006). Finally, Knowles and Watkinson (2014) found that mechanical expression of oil from borage, blackcurrant and primrose seed resulted in considerably lower FFA content relative to oil obtained from the same feedstock by solvent extraction, and attributed it to thermal degradation that may occur during solvent extraction and preferential extraction of FFAs during solvent extraction.

2.4.4 Defatted SCG

Defatted SCG are the solid residues obtained after the oil extraction process, with a particle size slightly smaller than SCG before oil extraction ranging between 216.2 and 314 μm according to Go et al. (2016) and Somnuk et al. (2017). Their elemental composition and characteristics are presented in Table 2.8, where all the values are expressed as dry weight percentages, except for HHV which is expressed in MJ/kg.

Table 2.8: Characterization of defatted SCG.

References	Elemental composition (%)						Crude protein (%)	Carbohydrates (%)	Lignin (%)	Sugars (%)	Ash (%)	HHV (MJ/kg)
	C	H	N	O	S	P						
Vardon et al. (2013)	51.8	6.3	2.8	38.8	0.17	0.17	18.2	-	-	-	2.4	20.1
Go et al. (2016)	-	-	-	-	-	-	11.97-13.20	25.70-37.32	-	-	1.86 - 2.07	20.03-20.27
Caetano et al. (2014)	69.5	-	2.0	-	-	-	12.3	-	32.5	-	2.0	19.0
Deligiannis et al. (2011)	52.02	6.31	0.49	-	-	-	-	-	-	-	4.2	21.16
Somnuk et al. (2017)	48.34	6.17	2.39	43.01	0.09	-	14.80	20.44	-	12.93	1.86	20.40
Todaka et al. (2016)	49.90	6.19	2.53	41.38	-	-	-	-	-	-	2.47	20.85
Al-Hamamre et al. (2012)	-	-	-	-	-	-	-	-	-	-	-	17.73-19.57

The values shown in Table 2.8, when compared with the composition of dry SCG (Table 2.2), suggest that there is no significant difference in protein and ash content before and after oil extraction from SCG. Furthermore, Caetano et al. (2014) found that the solvent extraction of lipids contributes to lignin solubilization due to swelling of lignin molecules and breakdown of polymer chains, while a comparison with Table 2.2 shows a reduced presence of sugars in SCG after lipid extraction. The differences in the composition of defatted SCG between the various studies can be attributed to the different original composition of SCG that is a function of type, origin, blend and processing of the samples, along with the varying characterization methods used (Caetano et al., 2014; Go et al., 2016).

In addition, defatted SCG generally contain higher oxygen and lower carbon content than SCG due to the extraction of lipids, which explains the lower HHVs of the defatted SCG samples (Caetano et al., 2014; Vardon et al., 2013). The differences in HHV of defatted SCG observed in the study of Al-Hamamre et al. (2012) occurred due to the different solvents used for lipid extraction. The energy content of defatted SCG is similar to that of woody biomass (19-21 MJ/kg) and therefore is suitable for direct combustion or thermochemical conversion, with the near zero sulfur content being beneficial for bio-oil production, although, the presence of nitrogen can result in high NO_x emissions upon combustion (Vardon et al., 2013). Furthermore, nitrogen can be recovered for use as fertilizer, whereas, the protein present in the defatted SCG can be used as a nutritious animal feed (Berhe et al., 2013; Somnuk et al., 2017; Vardon et al., 2013). The ash that occurs from burning of defatted SCG may also be considered a potential ingredient for fertilizers due to the presence of phosphorus, calcium and magnesium (Silva et al., 1998; Somnuk et al., 2017).

Previous studies have used defatted SCG, or proposed them as suitable for utilization as fuel pellets (Berhe et al., 2013; Haile, 2014; Kondamudi et al., 2008), compost (Berhe et al., 2013; Deligiannis et al., 2011), or sugar source (Go et al., 2016), while the potential valorization of defatted SCG as a feedstock for bio-oil (Vardon et al., 2013), bio-char (Vardon et al., 2013), and

bioethanol (Berhe et al., 2013; Kwon et al., 2013; Rocha et al., 2014) has also been investigated.

2.5 Utilization of SCG lipids for biodiesel production

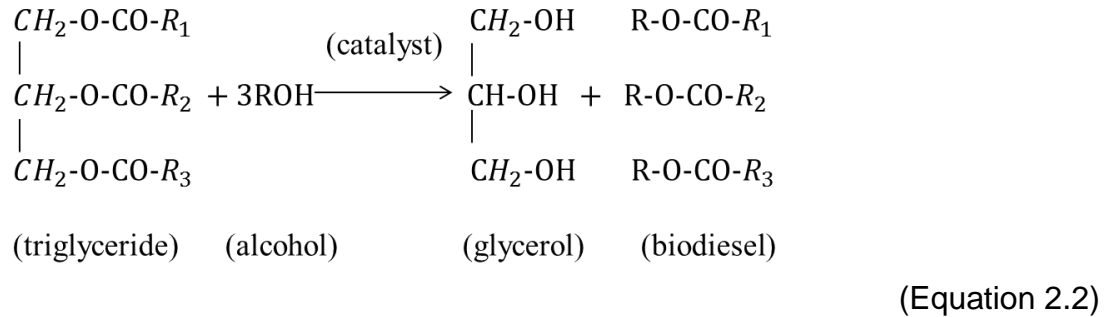
Lipids found in SCG have been suggested to be a very promising feedstock for the potential production of cheap and high-quality biodiesel (Al-Hamamre et al., 2012; Kondamudi et al., 2008). The glycerides and FFAs present in the SCG oil can be transesterified with short chain monohydric alcohols, such as ethanol or methanol, in the presence of a catalyst at elevated temperature, to yield fatty acid alkyl esters (FAAE), which are commonly referred to as biodiesel (Al-Hamamre et al., 2012; Kwon et al., 2013). The lipids extracted from SCG have been previously used for biodiesel production through transesterification in several studies (Al-Hamamre et al., 2012; Berhe et al., 2013; Caetano et al., 2014, 2012; Deligiannis et al., 2011; Haile, 2014; Jenkins et al., 2014; Kondamudi et al., 2008; Kwon et al., 2013; Vardon et al., 2013). Transesterification of oil extracted from SCG has also been investigated with the use of lipases as catalysts (Ferrario et al., 2013; Swanepoel et al., 2016).

In addition, previous studies have examined the potential of direct, or *in-situ*, transesterification of wet or dried SCG in order to obtain biodiesel without the need for a separate lipid extraction step (Calixto et al., 2011; Liu et al., 2017; Najdanovic-Visak et al., 2017; Park et al., 2016; Tuntiwattanapun et al., 2017).

2.5.1 Transesterification of SCG lipids

Transesterification of triglycerides is a stepwise process which includes three distinct steps: First, one alcohol molecule reacts with a triglyceride molecule yielding one fatty acid alkyl ester (FAAE) and one diglyceride molecule, which subsequently reacts with alcohol to liberate another FAAE molecule and produce a monoglyceride. Finally, the monoglyceride molecule undergoes alcoholysis to generate FAAE and glycerol. Each triglyceride molecule that goes through complete conversion reacts with three alcohol molecules in the presence of a basic or acidic catalyst and generates three moles of biodiesel and one mole of glycerol (Caetano et al., 2014; Leung et al., 2010; Moser,

2009). The chemical reaction that takes place during transesterification is presented in Equation 2.2 where R₁, R₂ and R₃ are fatty acids (Leung et al., 2010):



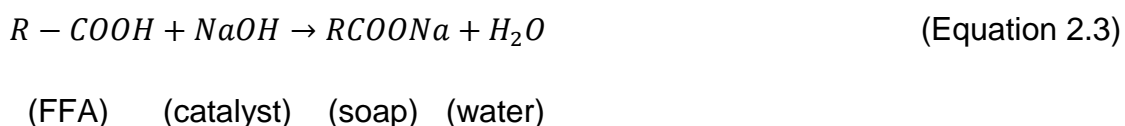
Transesterification is a reversible procedure, however, the rates of the reverse reaction are negligible, principally because glycerol is not miscible in biodiesel, especially when the alcohol moiety is from methanol (Moser, 2009).

Generally, methanol is the preferred alcohol because of its low cost, while it has also been reported to be advantageous compared to other alcohols because it reacts quickly with triglycerides and easily dissolves base catalysts (Leung et al., 2010; Ma and Hanna, 1999). An alcohol to triglyceride molar ratio higher than the stoichiometric, and therefore an excess of alcohol, can result in higher conversion into esters in shorter duration, while it also prevents quick jellification of glycerol, however, there is an optimal ratio that is associated with FFA content and type of catalyst, after which any further increase will not improve the reaction yield (Leung et al., 2010; Vyas et al., 2011). The concentration of catalyst also affects the efficiency of the transesterification process, with increase of catalyst amount leading to improved reaction yield until an optimal value, with further increase of its amount leading to a slight yield decrease because of soap formation (Eevera et al., 2009; Leung et al., 2010).

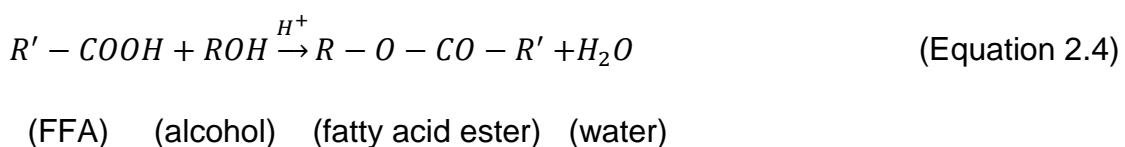
Regarding the effect of reaction time on the conversion yield, initially the reaction is slow due to mixing and dispersion of alcohol into the oil, although the rate of reaction subsequently increases to reach a maximum yield at a duration of ~90 minutes, with further prolongation having little positive effect on process efficiency but possibly leading to lower conversion yields (Eevera et al., 2009; Leung et al., 2010). Another significant parameter is reaction

temperature which should be below the boiling point of the alcohol when the process takes place at ambient pressure, with temperature increase reducing oil viscosity and generally resulting in higher reaction yields at shorter durations, until the optimum temperature is reached after which the yield may decrease due to acceleration of the saponification reaction of triglycerides (Eevera et al., 2009; Leung et al., 2010; Leung and Guo, 2006). In general, optimal temperatures of transesterification process have been found to range between 50 °C and 60 °C (Freedman et al., 1984; Leung et al., 2010; Leung and Guo, 2006; Ma and Hanna, 1999).

The conversion level of vegetable oils, including SCG oil, to biodiesel is strongly dependent on the quality of the feedstock (Al-Hamamre et al., 2012; Caetano et al., 2012; Deligiannis et al., 2011). A FFA content above 1-1.5 % w/w of the oil inhibits alkaline transesterification by forming stable soap emulsions that impede separation of FAAEs from glycerol (Al-Hamamre et al., 2012; Caetano et al., 2012; Deligiannis et al., 2011). Furthermore, soaps bind with the alkali catalyst and consequently higher quantities of catalyst are required (Leung et al., 2010). The saponification reaction of FFAs with a basic catalyst, in this case NaOH, is presented in Equation 2.3 (Leung et al., 2010):

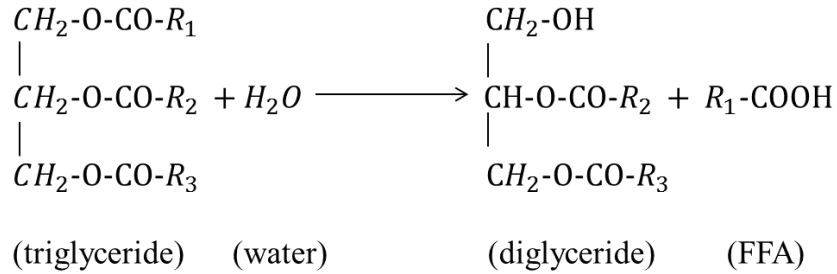


Nevertheless, FFAs can react with an alcohol and convert into alkyl esters by an acid-catalyzed process as per Equation 2.4 (Leung et al., 2010):



In addition, an increased kinematic viscosity of the oil, which strongly depends on the presence of FFAs, increases the power consumption when mixing the reactants in the transesterification process and leads to lower biodiesel yield (Al-Hamamre et al., 2012; Meher et al., 2006). Regarding the water content of the oil, a value below 0.3-0.5 % is desirable when the oil is considered for biodiesel production as water can hydrolyze the triglycerides to diglycerides

and increase the quantity of FFAs in the oil (Caetano et al., 2012; Deligiannis et al., 2011; Leung et al., 2010), with the hydrolysis reaction shown in Equation 2.5 (Leung et al., 2010):



(Equation 2.5)

In order to minimize water presence in the SCG oil, previous researchers have applied thermal heating at 100 °C to remove water traces (Kondamudi et al., 2008).

There are three main methods that have been applied in previous studies for the transesterification of SCG lipids into biodiesel mainly depending on the FFA content of the oil, and include the base-catalyzed (Al-Hamamre et al., 2012; Caetano et al., 2014; Deligiannis et al., 2011; Kondamudi et al., 2008), the acid-catalyzed (Jenkins et al., 2014; Kwon et al., 2013; Rocha et al., 2014), and the two-step process consisting of an initial acid-catalyzed esterification of FFAs followed by base-catalyzed transesterification (Berhe et al., 2013; Caetano et al., 2014, 2012; Haile, 2014; Vardon et al., 2013). Regardless of the transesterification method followed, the resulting FFAEs were separated by glycerol, residual alcohol, catalyst and soap by means of gravitational separation in a funnel and/or rotary evaporation and washing with warm and acidified deionized water, followed by drying to remove residing water and filtration to remove solid traces (Berhe et al., 2013; Haile, 2014; Vardon et al., 2013). The biodiesel yields obtained in previous studies were estimated after the separation and purification of the obtained FFAEs and are expressed relative to initial oil weight.

2.5.1.1 Single base-catalyzed transesterification

Several studies have suggested that a single step alkali-catalyzed transesterification can be successfully conducted when the FFA content of the

oil is less than 1-1.5 % w/w (Al-Hamamre et al., 2012; Berchmans and Hirata, 2008; Caetano et al., 2012; Canakci and Gerpen, 2001; Kumar Tiwari et al., 2007), while other studies decrease this limit to a FFA content of 0.5 % w/w (Zhang et al., 2003), however, oil samples with higher FFA levels have been transesterified by this method in some previous studies (Al-Hamamre et al., 2012; Caetano et al., 2014). A base-catalyzed transesterification of SCG oil with FFA contents ranging between 0.31 and 3.65 % w/w was performed by Al-Hamamre et al. (2012), Caetano et al. (2014) and Deligiannis et al. (2011), while Kondamudi et al. (2008) converted the FFAs into soap by mixing the oil with a basic solution and purifying it by centrifugation before proceeding to base-catalyzed transesterification.

In previous studies, SCG oil was esterified by anhydrous methanol in the presence of sodium or potassium hydroxide at temperatures ranging between 60 °C and 85 °C for reaction durations between 1 and 4 hours, with the quantity of methanol and catalyst used expressed in different ways and therefore making comparison difficult (Al-Hamamre et al., 2012; Caetano et al., 2014; Deligiannis et al., 2011; Kondamudi et al., 2008). Deligiannis et al. (2011) used a 9:1 molar ratio of methanol to oil with 1 % w/w of NaOH as catalyst at a temperature of 65 °C to achieve a conversion rate of 92 % w/w in 1 hour from SCG oil with a negligible FFA content of 0.31 % w/w, while Kondamudi et al. (2008) achieved 100 % conversion of FFA-free oil to biodiesel by mixing it with 40 % v/v methanol and 1.5 % w/w of KOH for 2 hours at a temperature of 70 °C. Caetano et al. (2014) performed a base-catalyzed reaction of oil with FFA content of 2.8 % w/w by adding 40 % w/w methanol with previously dissolved 1.4 % w/w NaOH and achieved a fatty acid methyl ester (FAME) yield of 86 % w/w in a 3 hour reaction at 60 °C.

Al-Hamamre et al. (2012) transesterified oil with FFA content of 3.65 % w/w by mixing it with a methanol-2.5 % KOH solution at FFA to methanol-KOH molar ratios of 1:5 and 1:9, and observed improved oil conversion to FAMEs with longer reaction time (1 to 4 hours) and lower FFA/methanol-KOH ratio, while increase in reaction temperature (65 °C to 85 °C) reduced the reaction time. The reaction yields achieved in this study ranged between 55.5 % w/w and 85.5 % w/w, with the highest yield obtained after 4 hours of reaction at 65 °C

with a FFA/methanol-KOH ratio of 1:9 (Al-Hamamre et al., 2012). Generally, a molar ratio of alcohol to triglycerides of 6:1 is sufficient for a successful conversion of oil into biodiesel through the base-catalyzed transesterification, while a NaOH concentration of approximately 1.5 % w/w has been reported as the optimal in terms of reaction yield (Caetano et al., 2014; Eevera et al., 2009; Leung et al., 2010).

2.5.1.2 Single acid-catalyzed transesterification

Previous studies that extracted oil from SCG with FFA contents of 8.34 to 20 % w/w have performed a single step acid-catalyzed transesterification process to produce FAMES, since the high FFA content of the oil rendered it unsuitable for the base-catalyzed process (Kwon et al., 2013; Rocha et al., 2014). Acid catalyzed transesterification has been used either as the sole processing method (Jenkins et al., 2014; Kwon et al., 2013), or after saponification and acid hydrolysis of the oil (Rocha et al., 2014). Kwon et al. (2013) performed transesterification with methanol and ethanol in the presence of sulfuric acid for 48 hours with oil containing 20 % w/w FFAs and achieved a biodiesel yield of 97.5 % w/w. The reaction with ethanol required higher temperatures and alcohol weight ratios compared to transesterification with methanol (Kwon et al., 2013). Jenkins et al. (2014) obtained a yield of 99 % w/w of the glyceride portion of the oil by adding 10 g oil in excess of methanol (~50 ml) in the presence of sulfuric acid (10 % w/w of the oil) and refluxing the mixture for 24 hours, although without specifying the initial FFA content of the sample.

Rocha et al. (2014), utilizing SCG oil with a FFA content of 8.34 % w/w, initially performed saponification with an alcoholic solution of KOH in an ultrasonic bath followed by acid hydrolysis. Thereafter, ultrasound-assisted acid esterification with a methanol to fatty acid molar ratio of 9:1 at the presence of H₂SO₄ (3.5 %) was performed for 60 minutes at a temperature of 60 °C, resulting in FAME yield of 97 % (Rocha et al., 2014). This work demonstrated the positive effect of ultrasound on the efficiency of the acid-catalyzed process by completing the transesterification of the oil in a fraction of the time required in other studies (Jenkins et al., 2014; Kwon et al., 2013; Rocha et al., 2014).

In general, the acid-catalyzed transesterification process when used as the sole treatment of SCG oil to produce FAMES leads to high conversion yields, however, has the disadvantage of requiring relatively long reaction duration and high methanol to oil molar ratios (Jenkins et al., 2014; Kwon et al., 2013; Leung et al., 2010). Moreover, the utilization of an acid catalyst has been reported by Jenkins et al. (2014) to result in formation of dark blue-green non-saponifiable precipitates from substances like terpenes, sterols and organic acids.

2.5.1.3 Two-step transesterification

SCG lipids with high FFA contents that inhibit direct base-catalyzed transesterification can also be treated by a two-step process that includes an acid-catalyzed esterification step prior to the base-catalyzed process, and has been described as the most efficient procedure for conversion of high acidity samples into biodiesel in previous studies that extracted SCG lipids with FFA levels between 3.65 and 59.5 % w/w (Al-Hamamre et al., 2012; Berhe et al., 2013; Caetano et al., 2014, 2012; Haile, 2014; Vardon et al., 2013). Compared to saponification of FFAs prior to further processing to produce biodiesel, acid-catalyzed pretreatment makes good use of them as they are converted into FAMES (Leung et al., 2010).

In the pretreatment acid-catalyzed step, methanol and sulfuric or hydrochloric acid have been utilized to convert the FFAs present in SCG oil to esters and reduce their levels below the limit that is suitable for alkali-catalyzed transesterification in one or several successive esterification steps (Al-Hamamre et al., 2012; Caetano et al., 2014, 2012; Haile, 2014; Vardon et al., 2013). Thereafter, the pre-treated oil was allowed to settle and subsequently separated from unreacted methanol and water prior to transesterification with methanol at the presence of potassium or sodium hydroxide, or sodium methoxide (Al-Hamamre et al., 2012; Berhe et al., 2013; Haile, 2014; Vardon et al., 2013).

Previous studies have utilized a range of conditions during two-step transesterification. Haile (2014) mixed the oil (4.9 % w/w FFA content) three consecutive times with methanol at a molar ratio of alcohol to FFA of 20:1 in

the presence of HCl (10 % w/w of total fatty acid content) for 90 minutes at a temperature of 54 °C to achieve a FFA level of 0.5 % w/w, before proceeding to the alkaline reaction at the same duration and temperature conditions, with a methanol to oil molar ratio of 9:1 and 1 % w/w of KOH achieving a FAME yield of 82 % w/w. Berhe et al. (2013) achieved a FAME yield of 73.4 % w/w from SCG oil (7.36 % w/w initial FFA content) by performing both stages of two-step transesterification at a higher temperature (60 °C) and longer duration (120 minutes) but at the same methanol and catalyst ratios as Haile (2014), although H₂SO₄ and NaOH were substituted for HCl and KOH, and the FFA content of the oil after pretreatment was 0.9 % w/w.

Vardon et al. (2013) treated SCG lipids (5.66 % w/w initial FFA content) with 35 % v/v methanol and 1 % v/v sulfuric acid at reflux for 4 hours, and subsequently mixed the acid-pretreated oil with methanol (6:1 methanol molar ratio) and 0.5 % w/w sodium methoxide (CH₃ONa) relative to lipid weight in a reflux condenser for 1 hour to obtain a FAME yield of 96 % w/w. Caetano et al. (2012) extracted SCG lipids with 59.5 % w/w FFA content and performed three successive esterifications with 40 % w/w methanol and 1 % w/v H₂SO₄ for 2 hours at 60 °C, followed by an alkali-catalyzed reaction with 40 % w/w methanol and previously dissolved 1 % w/w NaOH at the same conditions of duration and temperature to obtain a relatively low conversion yield of 60.5 % w/w, suggesting that despite the three esterification steps the FFA content was still sufficiently high to lead to soap formation and hinder the reaction.

Al-Hamamre et al. (2012) initially converted FFAs to esters by mixing oil (3.65 % w/w FFA content) with 20 % v/v methanol and 0.1 % v/v sulfuric acid for 4 hours and transesterified the pre-treated oil with methanol (6:1 molar ratio to oil) and 1.5 % KOH for 6 hours at 60 °C to achieve a conversion rate of 99 %. A comparison between single alkali catalyzed transesterification (Section 2.5.1.1) and two-step transesterification performed with lipids of the same FFA content (3.65 % w/w) was performed in this study with the two-step process resulting in a higher FAME yield, while the amount of catalyst required in the second step was lower relative to single alkaline transesterification due to reduction of the FFA content (Al-Hamamre et al., 2012).

Generally, previous studies that have investigated the two-step transesterification of vegetable oils have suggested that an increase in the amount of catalyst used in the acid-catalyzed pretreatment step decreases the FFA content of the oil (Canakci and Gerpen, 2001), with a 5 % w/w of sulfuric acid relative to FFA weight working well within the FFA range of 15-35 % w/w (Chai et al., 2014). Moreover, a molar ratio of methanol to FFA of 19.8:1 to 20:1 has been found to be optimal for acid-catalyzed pretreatment of oil samples with FFA content ranging between 15 and 25 % w/w (Caetano et al., 2014; Chai et al., 2014; Haile, 2014). In conclusion, the two-step transesterification process has been shown to successfully convert the majority of oil with high FFA content into FAME in a fraction of the time that would be required in a single acid-catalyzed process (Canakci and Gerpen, 2001).

2.5.2 Direct transesterification of SCG

A different approach for the production of biodiesel directly from dried or wet SCG has been adopted in previous studies that treated the grounds with methanol and catalyst to obtain FAMES (Calixto et al., 2011; Liu et al., 2017; Najdanovic-Visak et al., 2017; Park et al., 2016; Tuntiwattanapun et al., 2017).

Najdanovic-Visak et al. (2017) added dry SCG to a mixture of methanol and sodium hydroxide at a temperature of 60 °C and achieved a maximum FAME yield of 96 % w/w of the available oil. In a study performed by Liu et al. (2017), SCG were first impregnated with sulfuric acid due to the relatively high FFA content of SCG oil, and then mixed with deionized water for homogeneous coating before thermal drying and transesterification with methanol at temperatures between 60 and 80 °C, obtaining a maximum reaction yield of 98.6 % w/w.

Tuntiwattanapun et al. (2017) dried and washed SCG with methanol to reduce the FFA content, then dried again and suspended the SCG in methanol in the presence of NaOH for 3 hours, at temperatures ranging between 30 and 60 °C, and converted >80 % w/w of the oil into FAMES. In all cases, filtration was used to separate the liquid phase from the meal and

residual methanol was removed by rotary evaporation, while FAMEs were separated from glycerol by liquid-liquid extraction with hexane followed by evaporation of hexane (Liu et al., 2017; Najdanovic-Visak et al., 2017; Tuntiwattanapun et al., 2017).

In general, previous studies have shown that an increase of reaction temperature up to 70 °C resulted in an increase in FAME yield, and also eliminated the negative effect of using coarse SCG (>0.42 mm) (Liu et al., 2017; Tuntiwattanapun et al., 2017). Furthermore, increased base catalyst concentration and methanol to oil molar ratio have been reported to improve the conversion yield until an optimum point, with further increase favouring the backward reaction (Najdanovic-Visak et al., 2017), while a sulfuric acid concentration increase up to 20 % enhanced the process efficiency, with the selection of an acidic catalyst however increasing the duration up to 12 hours (Liu et al., 2017).

Calixto et al. (2011) investigated the direct transesterification of dried SCG with supercritical methanol, pure or with CO₂ at pressures ranging between 100 and 300 bar, and temperatures of 200 °C to 330 °C without using a catalyst and obtained a FAME yield of 84.9 % which increased to 93.4 % when CO₂ was added, with temperature and pressure increase having a beneficial effect on the reaction yield. Finally, Park et al. (2016) used methanol, chloroform and acid catalysts for direct transesterification of SCG with moisture content up to 80 % w/w at temperatures ranging between 75 °C and 125 °C, and found an optimum temperature of 95 °C and the most effective catalysts to be sulfuric and hydrochloric acid. Interestingly, the utilization of a different acid catalyst was found to result in FAMEs with significantly varying fatty acid composition (Park et al., 2016). In addition, a SCG moisture content up to 20 % w/w did not inhibit the process, but a higher moisture content of 80 % w/w impeded the process resulting in a reaction yield of about 40 % w/w (Park et al., 2016).

In conclusion, direct transesterification of SCG has been found to be a successful alternative method for production of FAMEs compared to solvent extraction and subsequent lipid transesterification, with high conversion yields

and comparable biodiesel quality (Liu et al., 2017). However, it requires relatively high methanol to oil molar ratios, and the moisture content of the samples should be significantly decreased prior to the reaction to reduce the alcohol requirement and improve the FAME yield obtained (Leung et al., 2010; Najdanovic-Visak et al., 2017; Park et al., 2016).

2.5.3 Biodiesel derived from SCG oil

Several studies have investigated the properties of SCG biodiesel and its suitability as a potential alternative fuel to fossil diesel (Berhe et al., 2013; Caetano et al., 2012; Deligiannis et al., 2011; Haile, 2014; Jenkins et al., 2014; Liu et al., 2017; Tuntiwiwattanapun et al., 2017; Vardon et al., 2013). Generally, the FA profile of SCG biodiesel is identical to the fatty acid profile of its source oil (Rocha et al., 2014), and primarily comprises of palmitic and linoleic acid, with lower concentrations of oleic, stearic and eicosanoic acid and traces of other fatty acids (Table 2.5). In addition, the fatty acid composition of SCG biodiesel is similar to that of biodiesel produced from soybean and corn (Rocha et al., 2014). Table 2.9 shows SCG biodiesel properties measured in previous studies, either as pure FAMES or blended with diesel at volume ratios of 5% and 20 % biodiesel. Table 2.9 also shows the generally applicable diesel quality requirements for use in diesel engines according to European standard EN 14214 (BSI Standard, 2014).

Table 2.9: Properties of SCG biodiesel.

References	Density at 15 °C (kg/m ³)	Kinematic viscosity at 40 °C (mm ² /s)	HHV (MJ/kg)	Acid value (mg _{KOH} /g)	Water content (ppm)	Sulfur content (ppm)	Cloud point (°C)	Pour point (°C)	Oxidation stability at 110 °C (h)
Deligiannis et al. (2011)	894.3	5.61	39.49	0.36	255.6	4.5	13	-	7.9
Haile (2014)	880	5.4	39.6	0.7	-	-	13	-	-
Berhe et al. (2013)	891.5	5.26	38.4	0.78	-	-	14	-	-
Caetano et al. (2012)	911	12.88	-	2.14	-	-	-	-	-
Kondamudi et al. (2008)	-	5.84	-	0.35	-	8	11	2	3.05
Tuntiwiwattanapun et al. (2017)	-	3.81-4.33	-	1.40-5.10	204-247	-	12.8-13	9.5-10.3	4.9-8.8
Jenkins et al. (2014)	841-927	3.5-5.5	-	-	-	-	-	-1 -16	-
Vardon et al. (2013) - B100	892	5.19	39.6	0.11	632	35.9	13.1	13	0.2
Vardon et al. (2013) - B20	856.4	2.75	43.9	0.16	124	14.1	-4.7	-11.7	5.2
Vardon et al. (2013) - B5	850.1	2.40	44.8	0.17	43	9.4	-13.2	-22.7	13.2
EN 14214	860-900	3.5-5	-	<0.5	<500	10	-	-	>8

It can be seen in Table 2.9 that the acid value of SCG biodiesel samples obtained ranges between 0.36 and 5.10 mg_{KOH}/g, with a value above the standard limit of 0.5 mg_{KOH}/g being an indication of incomplete reaction due to high oil FFA content that possibly resulted in soap formation and hindered the transesterification process, as was the case in the study of Caetano et al. (2012), and/or an inefficient neutralization procedure (Caetano et al., 2014; Tuntiwiwattanapun et al., 2017). Biodiesel with an acid value above 0.5 mg_{KOH}/g can potentially cause corrosion in diesel engines and fuel sediment leading to filter plugging (Tuntiwiwattanapun et al., 2017), while a high FAME acid value is also related to high kinematic viscosity (Al-Hamamre et al., 2012). The acid value of SCG biodiesel was reduced by Caetano et al. (2014) by ensuring low oil FFA content prior to transesterification, and by reducing the amount of acidic catalyst used for neutralization of the base catalyst in the study of Tuntiwiwattanapun et al. (2017).

The kinematic viscosity of pure SCG biodiesel, which affects the fuel flow through the fuel supply system and the atomization upon injection (Jenkins et al., 2014), was found to range between 3.81 and 12.88 mm²/s in previous studies (Table 2.9), with viscosities above the specification limit of 5 mm²/s possibly attributable to incomplete reaction and inefficient purification steps that left glycerol in the ester phase (Deligiannis et al., 2011), along with a large percentage of saturated methyl esters. Jenkins et al. (2014) reported a variation of biodiesel viscosity between 3.5 and 5.5 mm²/s depending on regional origin, bean type and brewing method. In particular, differences in the brewing process impact on the viscosity by removing different compounds prior to oil extraction and esterification (Jenkins et al., 2014). It has been suggested that the viscosity of SCG biodiesel can be decreased by refining of lipids prior to transesterification, decreasing the acid value of the fuel and/or by mixing it with conventional diesel (Caetano et al., 2014; Vardon et al., 2013).

Most of the previous studies obtained biodiesel with a density that was within the specification limits (Table 2.9), a significant result as fuel density is important for diesel fuel injection systems which operate on a volume metering system (Deligiannis et al., 2011; Jenkins et al., 2014), while the relatively high

biodiesel density measured by Caetano et al. (2012) may be a consequence of an incomplete transesterification reaction. Furthermore, the variation in densities of FAMEs obtained from SCG and fresh coffee lipids of different origins and bean types, but similar fatty acid profile, reported by Jenkins et al. (2014), suggests that fuel properties such as density and viscosity also depend on other lipid-soluble compounds present in the SCG biodiesel. However, no input of the brewing process on the resultant FAME density was found by Jenkins et al. (2014).

Table 2.9 shows that most of the previous studies obtained SCG FAMEs with low water presence that was below the standard acceptable limit (Table 2.9). In the study of Vardon et al. (2013) the high water content can possibly be attributed to extensive water washing, while biodiesel contaminated with water is undesirable as can result in engine corrosion (Deligiannis et al., 2011), and degradation in biodiesel quality during storage (Tuntiwiwattanapun et al., 2017).

The cloud point of SCG biodiesel is a cold flow property that indicates the temperature at which the fuel becomes cloudy by the formation of solids upon cooling, while pour point is the temperature at which the fuel ceases to flow, and both depend on the degree of FAME unsaturation, with a high concentration of unsaturated esters leading to low cloud and pour point (Knothe, 2008, 2005; Ramos et al., 2009). It can be seen in Table 2.9 that SCG biodiesel generally has a high cloud point that makes it unsuitable for use in cold climates (Tuntiwiwattanapun et al., 2017). The pour point of SCG-derived biodiesel was found to be lower than the cloud point (Table 2.9), while Jenkins et al. (2014) reported pour point values between -1 and 16 °C for biodiesel obtained from SCG and fresh coffee samples, with SCG derived biodiesel generally having lower pour points relative to FAMEs produced from fresh coffee samples.

Oxidation stability indicates the resistance of a fuel to oxidation during extended storage (Knothe, 2005; Tuntiwiwattanapun et al., 2017), with biodiesel being significantly more prone to oxidation relative to fossil diesel (Deligiannis et al., 2011). Biodiesel produced from coffee oil generally has

better oxidative stability relative to biodiesel derived from other sources because of the presence of endogenous antioxidants (Al-Hamamre et al., 2012; Deligiannis et al., 2011), however, such natural antioxidants can be lost during transesterification resulting in a relatively poor oxidative stability of biodiesel (Vardon et al., 2013).

Oxidation rates of biodiesel mainly depend on its fatty acid composition, with monounsaturated fatty acids, such as oleic acid that can be found in relative high proportions in SCG FAMES (Table 2.5), having higher oxidative stability than less saturated molecules without any adverse effect on fuel cold properties (Pinzi et al., 2009).

According to results obtained from previous studies shown in Table 2.9, SCG biodiesel has low sulfur content, similar to the lipid source (Table 2.6), which can result in low emissions of sulfur oxides and particulate matter upon combustion in diesel engines (Al-Hamamre et al., 2012; Canakci and Sanli, 2008; Deligiannis et al., 2011; Ma and Hanna, 1999). Increased presence of sulfur in SCG biodiesel, as was the case with the study of Vardon et al. (2013), can possibly be attributed to sulfuric acid or magnesium sulfate traces in the fuel as they were used as acid-pretreatment catalyst and biodiesel drying agent respectively.

The HHV of SCG biodiesel determined in previous studies (Table 2.9), was found to be comparable to biodiesel derived from soybean oil (39.9 MJ/kg) and other plant lipid-derived biodiesels (Vardon et al., 2013). The small difference in the HHV of SCG biodiesel samples reported in previous studies can be likely attributed to the different fatty acid profile of the samples, as the quantity of energy depends on the chain length and degree of unsaturation, with increased presence of unsaturated fatty acids lowering the energy content due to lower energy release upon breakdown of one double bond relative to breakdown of two single bonds (Sadrameli et al., 2008).

Another important parameter for the quality of biodiesel that is not presented in Table 2.9 is cetane number which is an indicator of fuel ignition quality in diesel engines and is related to the ignition delay time, with shorter ignition delay time translated into higher cetane number (Knothe, 2005; Pinzi et al.,

2009). The cetane number of a SCG biodiesel was determined by Vardon et al. (2013) who found it to be 60.1 for neat FAMEs, with blended samples of B20 and B5 having cetane numbers of 51.9 and 50.5 respectively, while the minimum required cetane limit is 51 (BSI Standard, 2014).

2.6 Conclusions

SCG is an abundant waste material which contains lipids in amounts that justify its potential use as biodiesel feedstock. Differences in the oil content and composition are attributable to the origin, type and processing of the beans prior to coffee brewing (e.g. roasting, treatment for instant coffee production). The moisture content of SCG mainly depends on the brewing method, and thermal drying has been the most common method for dewatering of SCG prior to lipid extraction. Solvent extraction and SFE are the methods that have been previously investigated for oil recovery from SCG, with SFE resulting in slightly lower oil yields, and in some cases varying fatty acid profile of SCG oil, relative to that recovered through Soxhlet solvent extraction.

In solvent extraction, there is a correlation between increasing oil yield and decreasing SCG-to-solvent ratio, while high SCG moisture contents were generally found to inhibit the lipid extraction process. A beneficial effect of increasing temperature on the extraction efficiency has also been found for temperatures below the boiling point of the solvent, while the solvent used for SCG oil extraction impacts on the yield and composition of the obtained oil, with polar solvents generally extracting oil with higher FFA content relative to that recovered with non-polar ones. SCG oil can be successfully converted into biodiesel through transesterification in the presence of a catalyst, with a two-step transesterification process being the most efficient method for treatment of SCG lipids with a high FFA content, while biodiesel properties vary depending on the respective properties of the oil source and the efficiency of the transesterification process.

Based on the existing knowledge, it can be concluded that there are significant differences between SCG samples originating from different sources, while the efficiency of extraction and the quality of the recovered oil

depend on the extraction process and the feedstock properties. The effect of solvent extraction parameters such as process duration, solvent selection, SCG moisture content and particle size on the efficiency of the oil recovery from SCG have not been investigated in depth in previous studies, while the impacts of elevated temperature (above the boiling point of the solvent) and pressure during extraction have not been previously examined. Furthermore, the use of mechanical expression as a method of oil removal from SCG has not been previously tested, whereas its use as a technique of moisture removal from SCG has been scarcely researched. Following extraction, it is apparent that there is a significant impact of the level of FFAs present in SCG oil on the transesterification process, while the combustion and emission characteristics of SCG oil and SCG derived biodiesel have not been previously investigated.

There is therefore a need for a more comprehensive characterization of the feedstock, and especially of SCG originating from the instant coffee industry. In addition, an increased understanding of the impact of oil extraction and transesterification parameters and feedstock properties on yield and quality of oil and derived biodiesel, is required in order to improve the valorization of SCG as a biodiesel feedstock. In the same context, the performance of SCG biodiesel as a fuel for modern diesel engines is equally important for the future industrialization of biodiesel production from this waste material.

2.7 Research objectives

The overall purpose of this thesis is to investigate in depth the various processing stages required to produce biodiesel from SCG, with a particular focus on the lipid recovery step, so as to determine the effect of various feedstock physical properties and process parameters on the efficiency of the procedure. The present chapter describes the specific objectives of this research which are:

1. To provide a comprehensive feedstock characterization in terms of physical properties such as SCG moisture, lipid and energy content, particle size and FFA content, and identify differences in the physical properties of samples subjected to varying processing methods within the coffee beverage industry.

2. To determine the impact of solvent extraction parameters on the yield and quality of SCG lipids in different laboratory and pilot plant scale solvent extraction methods. These parameters include the:

- Effect of solvent type and quantity.
- Effect of process duration.
- Effect of SCG moisture content and particle size.
- Effect of pressure and temperature.

3. To investigate the use of mechanical pressing as a means of moisture removal and lipid expression from SCG and roasted defective coffee beans (RDCB), and determine the effect of applied pressure, temperature and duration on the efficiency of the process and compare the properties of expressed lipids with those of solvent extracted ones.

4. To undertake the transesterification of SCG solvent-extracted lipids with high FFA content, and investigate the combustion and emissions characteristics of the resultant biodiesel in a light-duty diesel engine.

3. Experimental Materials and Methodology

3.1 Materials

3.1.1 Coffee samples

Several coffee samples were used in this study including roasted coffee grounds that had not been used for coffee brewing, SCG and RDCB. SCG samples from both industrial and retail sources were utilized and the majority of those were provided by Bio-bean Ltd., while SCG from local coffee shops were also used. Information regarding the origin and upstream processing of the SCG samples used was not available, however, it was known that the industrial samples had been utilized for instant coffee production, while the retail samples had mostly been used in espresso machines.

The instant SCG samples provided by Bio-bean Ltd. were named according to their source as Nestle, Pure Mondelez and Mixed Chaff/Mondelez coffee. Two Nestle SCG batches were provided with slightly different oil and moisture content and will be referred to throughout this thesis as ICG1 and ICG2, while Pure Mondelez and Mixed Chaff/Mondelez will be referred to throughout as ICG3 and ICG4, where ICG stands for instant coffee grounds. A retail SCG sample collected from Netrail coffee shops was provided by Bio-bean Ltd. and will be referred to as RCG1, while two more retail samples were collected from local coffee shops and will be referred to as RCG2 and RCG3, where RCG stands for retail coffee grounds.

All of the wet SCG samples were stored in a refrigerator so as to avoid formation of mould, as water governs fermentation and mould growth during storage (Reh et al., 2006). The fresh (pre-brewing) coffee ground sample was provided from the same coffee shop as RCG2 and will be referred to as FRCG (fresh retail coffee grounds). RDCB were provided by Bio-bean Ltd. and were obtained from the same source as ICG1 and ICG2.

3.1.2 Extraction solvents

A wide range of solvents was used in this study to examine solvent property effects on the SCG lipid extraction efficiency. The solvents selected for

investigation through the Soxhlet method were the alkanes: pentane, hexane and heptane, the alcohols: ethanol, propanol, butanol, pentanol and hexanol, dichloromethane, which is an organochloride, and the aromatic hydrocarbon toluene. The solvents used in the ASE experiments were hexane and its structural isomer iso-hexane, heptane, octane and ethanol. Hexane and iso-hexane were the solvents used in the pressurized vessel and pilot plant extractions respectively.

Solvent polarity can be interpreted as the sum of all molecular properties responsible for interactions between solvent and solute molecules (Reichardt and Welton, 2010b). The polarity of a solvent can be characterized by its dielectric constant, a temperature and pressure dependent dimensionless property that represents its ability to reduce the electric force between two charges separated in space and orient its dipoles (Perry et al., 1997; Reichardt and Welton, 2010b). Regarding the relationship between dielectric constant and temperature at conditions of atmospheric pressure, the dielectric constant of a non-polar solvent will generally decrease as temperature increases, for example Bolotnikov and Neruchev (2004) reported that the dielectric constant of hexane linearly decreased from 1.89 at 15 °C to 1.83 at 60 °C, affected by density decrease. In addition, temperature increase affects the dielectric constant of polar solvents because of the heat-induced change of dipole orientation, with the dielectric constant of most of polar liquids decreasing with temperature increase, except for acetic and butyric acids (Hanai et al., 1961). The dielectric constant of a solvent at constant temperature has been reported to slightly increase with pressure increase due to increased density, while an added increase has been observed in polar liquids because of increased interactions between neighboring molecules (Skinner et al., 1968).

As a measure of polarity a higher dielectric constant is correlated with higher polarity and solvents with a dielectric constant higher than 15 are considered to be polar, while solvents with dielectric constants between 5 and 15 are borderline (Brown et al., 2008; Iwunze, 2009; Reichardt and Welton, 2010b). However, the use of dielectric constant of a solvent as a quantitative measure of polarity is not ideal as this approach neglects the interactions between

solvent molecules and specific solute/solvent interactions such as hydrogen bonding (Reichardt and Welton, 2010b).

Another property, complementary to dielectric constant, that has been used for characterization of solvent polarity is permanent dipole moment, which is expressed in Debyes (D) and measures the separation of partial positive and negative charges within the same molecule and is a measurement of the polarity of a chemical bond (Baumgarten, 1989). The orientation of dipolar solvent molecules around a solute molecule in the absence of specific solvent/solute interactions is determined by dipole moment, and values of dipole moment are lowest for hydrocarbons but higher in the case of solvents containing dipolar groups such as $C^+ - O^-$ and $C^+ - Cl^-$ (Baumgarten, 1989; Reichardt and Welton, 2010b).

Similar to dielectric constant, the dipole moment is temperature and pressure dependent. The dipole moment of most dipolar solvents tends to decrease with increase in temperature at conditions of atmospheric pressure due to weakened polarization by the collapse of hydrogen bonds (Ahmad and Rehana, 1980; Kang et al., 2011), while a pressure increase results in dipole moment increase, because of the strengthening effect of increasing pressure on the polarization of solvent molecules (Ahmad and Rehana, 1980; Kang et al., 2011).

An individual quantification of solvent polarity by means of dipole moment is inadequate as the charge distribution of a solvent molecule may not only be given by its dipole moment but also by higher multipole moments (Reichardt and Welton, 2010b). The inefficiency of the aforementioned properties to represent the polarity of a solvent has led to the development of empirical polarity parameters based on known solvent-sensitive reference processes (Reichardt and Welton, 2010c). Such polarity parameters reflect all the intermolecular forces acting in solution and constitute a more comprehensive, but not universal, measure of solvent polarity than single physical properties (Reichardt and Welton, 2010c).

The use of spectroscopic parameters of solvent polarity derived from solvent-sensitive standard compounds absorbing radiation in spectral ranges has

been proposed by Reichardt and Welton (2010c), with the most comprehensive polarity parameter (E_T^N) derived from the UV-Vis charge-transfer absorption band of the negatively solvatochromic pyridinium *N*-phenolate dyes measured at 25 °C and atmospheric pressure conditions for various solvents. Solvents can be classified according to their E_T^N value (ranging between 0.0 and 1.0, where the upper limit corresponds to water) in non-polar aprotic solvents with E_T^N between 0.0 and 0.3, polar aprotic solvents with E_T^N between 0.3 and 0.5 and protic solvents with E_T^N values higher than 0.5, which tend to be polar (Reichardt and Welton, 2010b). Protic solvents are considered those containing a hydrogen atom bound to an oxygen or nitrogen atom and therefore include alcohols.

Table 3.1 shows the different solvents used in this study, along with their chemical formula, molecular weight, boiling point, dielectric constant, dipole moment and the empirical polarity parameter E_T^N . The solvents are presented in Table 3.1 an increasing order of E_T^N .

Table 3.1: Chemical formulas and properties of the solvents used in the experimental part of this thesis.

Solvent	Chemical Formula	Molecular weight (g/mol)	Boiling point (°C)	Dielectric constant at 25 °C	Dipole Moment at 25 °C (D)	Polarity parameter E_T^N at 25 °C (all values obtained from [1])
Pentane	C ₅ H ₁₂	72	36.1 [1]	1.82 [4]	0 [7]	0.009
Hexane	C ₆ H ₁₄	86	68.7 [1]	1.88 [1]	0 [7]	0.009
Iso-hexane	C ₆ H ₁₄	86	60 [2]	1.89 [5]	0.02 [8]	-
Heptane	C ₇ H ₁₆	100	98.5 [1]	1.91 [4]	0 [7]	0.012
Octane	C ₈ H ₁₈	114	126 [1]	1.946 [6]	0 [9]	0.012
Toluene	C ₇ H ₈	92	110.6 [1]	2.38 [1]	0.4 [7]	0.099
Dichloromethane	CH ₂ Cl ₂	85	39.6 [1]	8.93 [1]	1.57 [10]	0.309
Hexanol	C ₆ H ₁₄ O	102	158 [3]	13.33 [4]	1.75 [11]	0.559
Pentanol	C ₅ H ₁₂ O	88	138 [1]	13.9 [1]	1.91 [11]	0.568
Butanol	C ₄ H ₁₀ O	74	117.1 [1]	17.51 [1]	1.74 [12]	0.586
Propanol	C ₃ H ₈ O	60	97.2 [1]	20.45 [1]	1.55 [13]	0.617
Ethanol	C ₂ H ₆ O	46	78.3 [1]	24.55 [1]	1.72 [12]	0.654

[1]: (Reichardt and Welton, 2010d), [2]:(Chang et al., 2010), [3]: (Athankar et al., 2016), [4]: (Sastry and Valand, 1998), [5]: (Johnson and Lusas, 1983), [6]: (Scholte and de Vos, 2010), [7]: (Smallwood, 1996), [8]: (Barratt, 1995), [9]: (<http://www.stenutz.eu/chem/solv6.php?name=octane>), [10]: (Nhu et al., 1989), [11]: (Pieruccini and Saija, 2004), [12]: (Ghanadzadeh et al., 2005), [13]: (Agarwal and Singh, 2016).

It can be seen in Table 3.1 that all of the hydrocarbons are non-polar, while all of the alcohols are polar with the exception of hexanol, which is considered to be mostly non-polar because of the dominance of the long non-polar hydrocarbon chain over the polar -OH moiety, but with some polar properties due to its high dipole moment, while pentanol is slightly polar (Tayar et al., 1991). Dichloromethane is a slightly polar aprotic solvent that solvates positively charged species via its negative dipole.

The utilization of both polar and non-polar solvents allowed for the evaluation of the effect of solvent polarity on the oil extraction efficiency, while the range in solvent boiling point resulted in different process temperatures, useful in understanding the effect of temperature on lipids recovery. Furthermore, the use of solvents of homologous series (alkanes, alcohols) with increasing carbon chain lengths allowed for the determination of the effect of solvent molecular weight on lipid extraction efficiency.

3.2 Methods

The present chapter describes the experimental approach and various techniques used in this thesis. Figure 3.1 shows in schematic form the various steps of processing to which the SCG were subjected during the experiments presented.

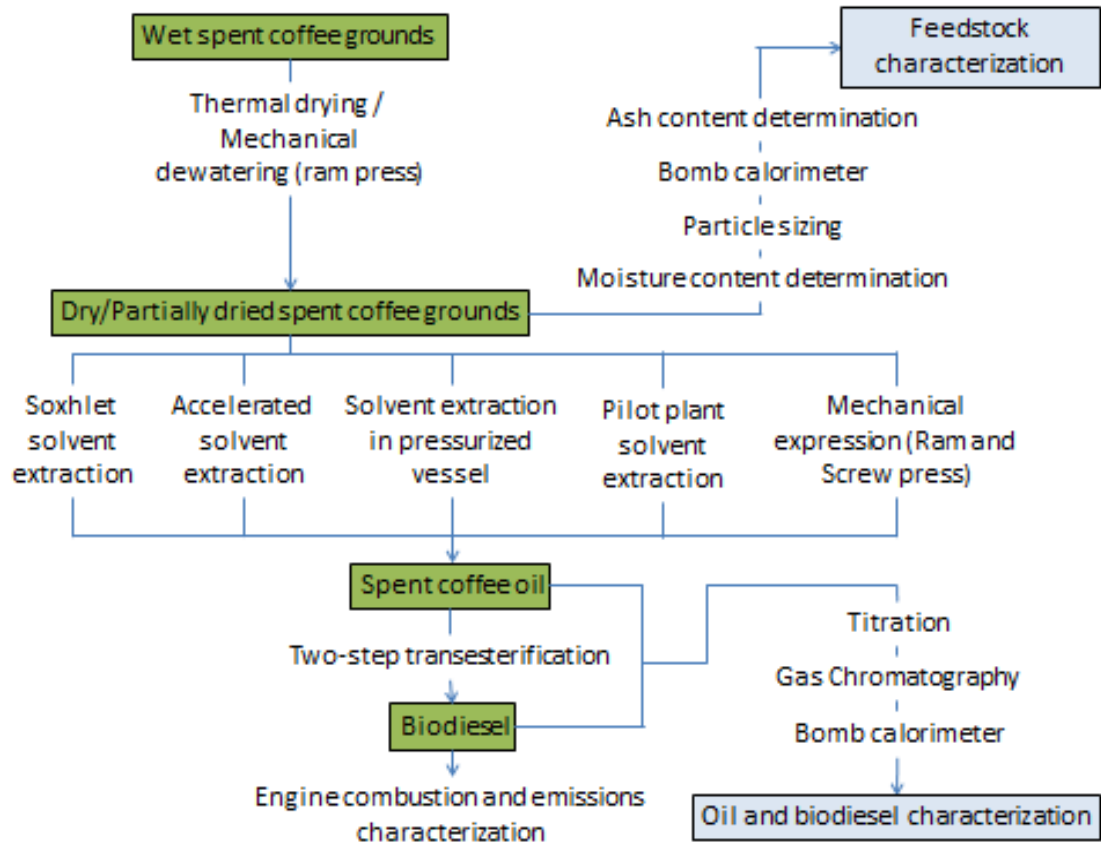


Figure 3.1: Overall schematic of processing methods.

It can be seen in Figure 3.1 that various approaches of dewatering and solvent extraction were undertaken and the following Sections describe in detail the individual processes.

3.2.1 Thermal drying SCG for moisture removal and water content determination

Throughout this work, the term moisture content refers to the mass of liquid component of the wet spent coffee ground (SCG) samples that could be removed thermally or mechanically, and is not intended as an absolute measure of the presence of water. Moisture content determination and complete, or partial, moisture removal for subsequent oil extraction was

accomplished through thermal drying in an electrically heated oven (Nabertherm, model TR 60, Germany) with forced air circulation and a power output of 2.3 kW. SCG were contained in petri dishes made of Pyrex™ borosilicate glass able to withstand high temperatures without any grinding or further size reduction of the grounds performed prior to drying. Three petri dishes of different sizes were used in the experiments loaded with quantities of wet SCG ranging between 60 g and 100 g. The thickness of wet SCG samples was measured with a Forge Steel Vernier caliper with accuracy of ± 0.02 mm. Figure 3.2 shows the oven used and two petri dishes loaded with SCG during drying.



Figure 3.2: (a) SCG samples contained in pyrex petri dishes during drying, (b) Exterior of oven model used in drying experiments (adapted from “http://www.keison.co.uk/nabertherm_tr.shtml”).

Oven temperatures of 100 °C and 200 °C were used and the weight of the petri dishes was measured before and after the addition of wet SCG by placing them on an analytical balance (Kern ABS 320-4N) with a reproducibility of ± 0.2 mg. Similarly with the study conducted by Gómez-De La Cruz et al. (2015) who investigated the drying of SCG, any loss of volatiles due to thermal drying was not considered to be appreciable when the temperature applied was equal to or lower than 200 °C. The oven and balance were situated in a laboratory room with temperature of 23 ± 2 °C and relative humidity of ~40%.

For determination of the total moisture content of the various SCG samples, oven drying was performed with wet samples of 100 g and a thickness of 12.5

mm until there was no change in the measured weight between subsequent measurement intervals. The combined weight of the coffee grounds and petri dish was weighed at intervals of 30 minutes during the drying process, with the petri dishes briefly removed from the oven. Equation 3.1 gives the moisture content value on a weight basis:

$$\% M = \frac{W_0 - W_t}{W_0} \times 100 \quad (\text{Equation 3.1})$$

Where M, W_0 and W_t are the moisture content on a mass basis, initial sample weight and sample weight after drying respectively.

Where required, partially wet SCG samples were obtained by drying 100 g of a sample of 12.5 mm thickness at 100 °C for a shorter duration than that previously determined as required for complete moisture removal, with the drying time necessary to reach desired water content predicted based on previously experimentally determined moisture removal rates for specific coffee masses, sample type and drying conditions. Equation 3.2 yields the moisture content of the sample after the partial drying process:

$$\% M = \frac{W_t - W_{exp}}{W_0} \times 100 \quad (\text{Equation 3.2})$$

Where M, W_t , W_{exp} , W_0 are the moisture content, weight of the sample after drying, expected weight of sample if complete drying were performed, and initial weight of the sample respectively. Equation 3.3 defines the value of W_{exp} :

$$W_{exp} = W_0 - (W_0 \times M_{average} \%) \quad (\text{Equation 3.3})$$

Where $M_{average}$ is the average experimentally determined moisture content of a specific sample of coffee grounds.

3.2.2 Particle sizing of dry SCG

Particle sizing of various SCG samples was undertaken using laboratory test sieves with pore sizes of 1700µm, 850 µm, 500 µm, 425 µm, 355 µm, 300 µm, 150 µm, 89 µm and 75µm and an appropriate vibratory sieve shaker (Retsch AS 200 basic) that was operated at a speed of 40 rpm for 10 minutes. The

maximum number of sieves which could be used simultaneously was less than the number required to achieve the desired resolution in particle diameter, and this necessitated that the sieves should be separated into two groups of 4 and 5 sieves. Figure 3.3 shows the test sieves and sieve shaker used for the experiments.



Figure 3.3: Sieves loaded with spent coffee grounds and sieve shaker.

All of the sieves were weighed over a Sartorius M-prove AY123 balance with repeatability of ± 0.003 g before and after the shaking process in order to calculate the mass of particles that was retained in each. Sieves of pore sizes smaller than $75 \mu\text{m}$ were not required, as no coffee was found to pass through this sieve, as verified by measuring the weight of the sieve bottom pan before and after the procedure. Equation 3.4 gives the percentage of SCG particles of a specific diameter range on a mass per mass basis:

$$\% P = \frac{W_{s2} - W_{s1}}{W_{total}} \times 100 \quad (\text{Equation 3.4})$$

Where P, W_{s1} , W_{s2} and W_{total} are the percentage of certain size particles, initial weight of sieve, weight of sieve after shaking and total weight of coffee used respectively. An average particle diameter for each coffee sample used was also determined as per Equation 3.5.

$$D = \frac{\sum_{i=1}^n \left[\frac{(S \times P)}{100} \right]}{n} \quad (\text{Equation 3.5})$$

Where D, S, P and n are the average particle diameter size, sieve pore size, percentage of particles that remain in a specific sieve and number of test sieves used respectively.

3.2.3 Laboratory scale solvent extraction

Solid-liquid solvent extraction was used for the extraction of lipids from SCG; three experimental methods, two established and one prototype, were used and are explained in Sections 3.2.3.1, 3.2.3.2 and 3.2.3.3. The method followed for subsequent separation of solvent and extracted oil is described in Section 3.2.3.4 and the calculation of oil yield in Section 3.2.3.5.

3.2.3.1 Soxhlet extraction

In this method, lipids are extracted from the oil bearing material semi-continuously with an organic solvent, based on the differing solubility of these compounds. The Soxhlet extractor glassware is a commonly employed apparatus for the extraction of lipids from solid materials and consists of a percolator which allows the circulation of the solvent, a thimble that contains the oleaginous solid material and a siphon mechanism (Harwood et al., 1998). Figure 3.4 shows the Soxhlet glassware parts in a typical set up.

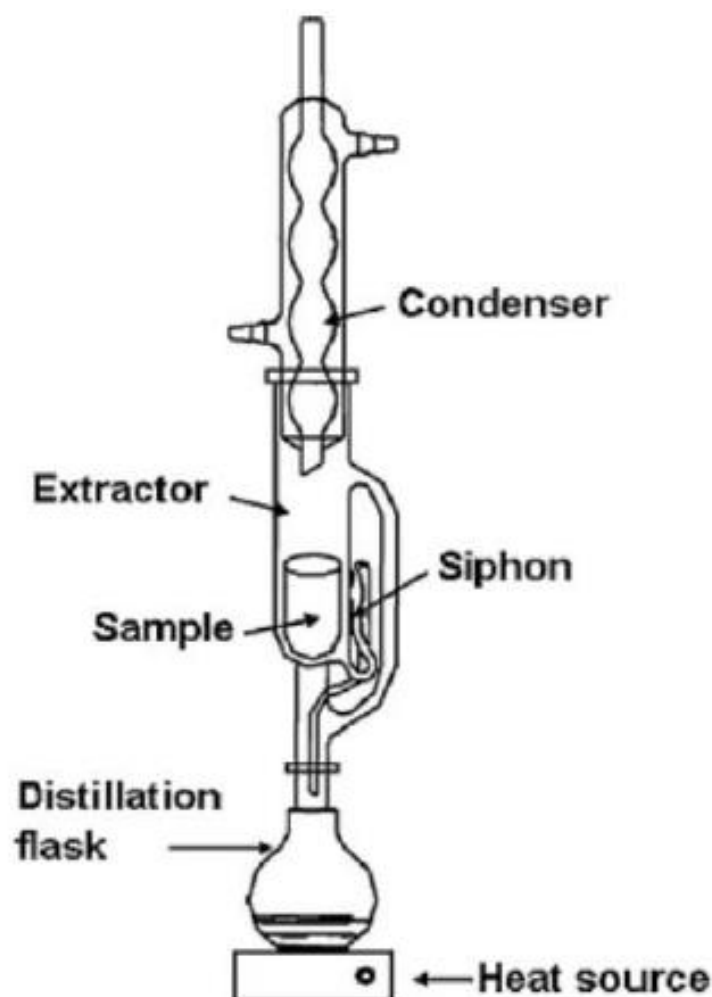


Figure 3.4: Schematic representation of the Soxhlet extractor, (adapted from Anisa Aris and Morad (2014)).

The solvent (heated to reflux) evaporates and moves up into the condenser where it condenses and drips into the extraction chamber containing the sample, dissolving a fraction of the lipid. When the solvent surrounding the thimble surpasses a certain level, an automatic siphon is initiated that carries the solvent and extracted oil to the boiling flask. This cycle, which starts when the first solvent droplet is recycled back into the thimble, can be repeated many times and on each occasion a fraction of the desired compound is extracted.

Oil extraction from dry or partially dry SCG with various solvents was undertaken at atmospheric pressure conditions through the Soxhlet method for durations ranging between 0.5 and 24 hours. A 250 ml Aldrich® Soxhlet apparatus was used in conjunction with a Whatman high purity glass

microfiber thimble of 30 mm diameter and 100 mm height. For each extraction, ~22.5 grams of SCG were loaded in the thimble that was then placed in the main chamber of the Soxhlet extractor. The extractor was placed on top of a distillation flask (250 ml capacity) containing quantities between 100 ml and 200 ml of the selected solvent so as to provide various SCG-to-solvent ratios. Finally a water chilled condenser was placed atop the extractor and the distillation flask was heated by a heating mantle (Electrothermal EM1000CE, 1000ML 230). Figure 3.5 shows the Soxhlet glassware and heating mantle used for oil extraction.

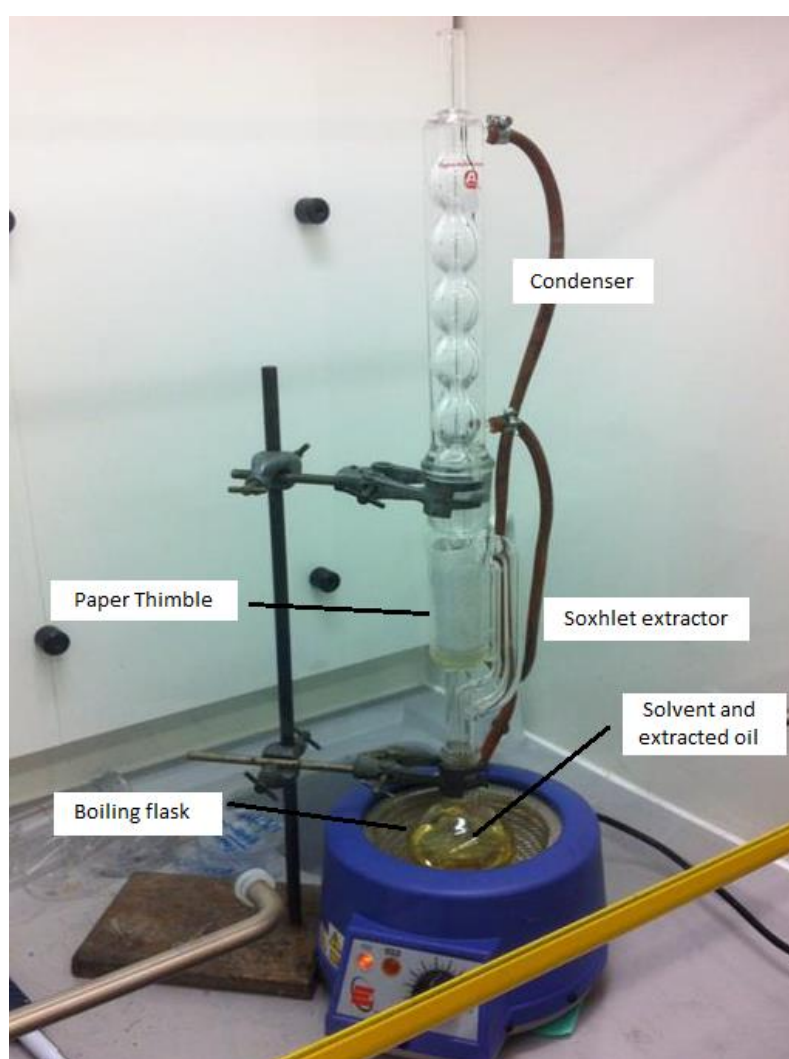


Figure 3.5: Solvent extraction (Soxhlet) in a fume cupboard.

Soxhlet extraction was the method used to determine the oil content of the various dried samples at the baseline conditions of 8 hours (a duration experimentally found to be the most effective) and 1:9 w/v SCG-to-solvent

ratio, while hexane was chosen as the baseline solvent based on previous studies which considered different solvents and found hexane to be amongst the most effective in extracting oils from SCG (Al-Hamamre et al., 2012; Berhe et al., 2013; Couto et al., 2009; Haile, 2014; Kondamudi et al., 2008).

3.2.3.2 Accelerated solvent extraction

Solvent extraction experiments at conditions of elevated temperature and pressure were performed in an ASE 150 (Thermo Fisher Scientific, Dionex). ASE, also known as pressurized fluid extraction, is an extraction method that combines elevated temperature and pressure with liquid organic solvents. ASE is a form of liquid solvent extraction that shares the same principles of the Soxhlet method, however, in ASE the solvents are used near their supercritical region and have better extraction and mass transfer properties compared to techniques that operate at atmospheric pressure, thus leading to relatively fast extractions (20-25 minutes) (Camel, 2001). Figure 3.6 illustrates the main operating features of the ASE 150.

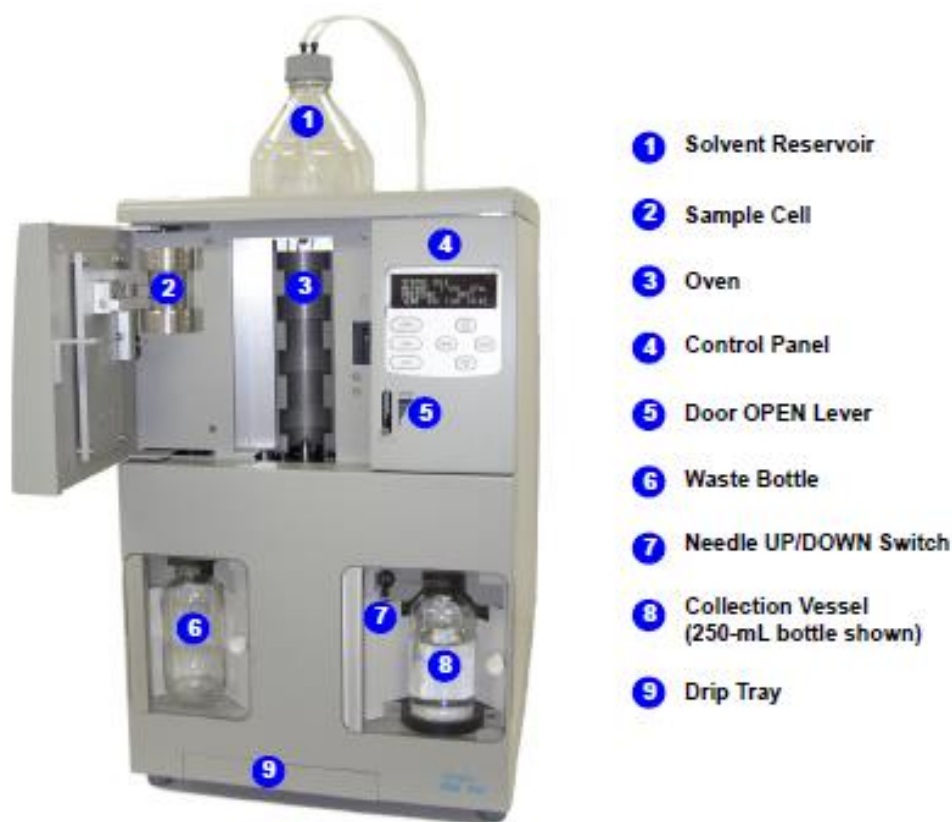


Figure 3.6: ASE 150 key operating features (adapted from (ThermoFisher, 2011)).

The high pressure applied inside the extraction cell (70-140 bar) increases the solvent boiling point of the solvent and allows it to remain in liquid state at elevated temperatures (100-200 °C) (Camel, 2001). However, the ASE unit only allows the extraction temperature to be selected, with the pressure automatically determined and not selectable by the user. Figure 3.7 shows the internal flows of N₂ and solvent, and the major components of an ASE apparatus.

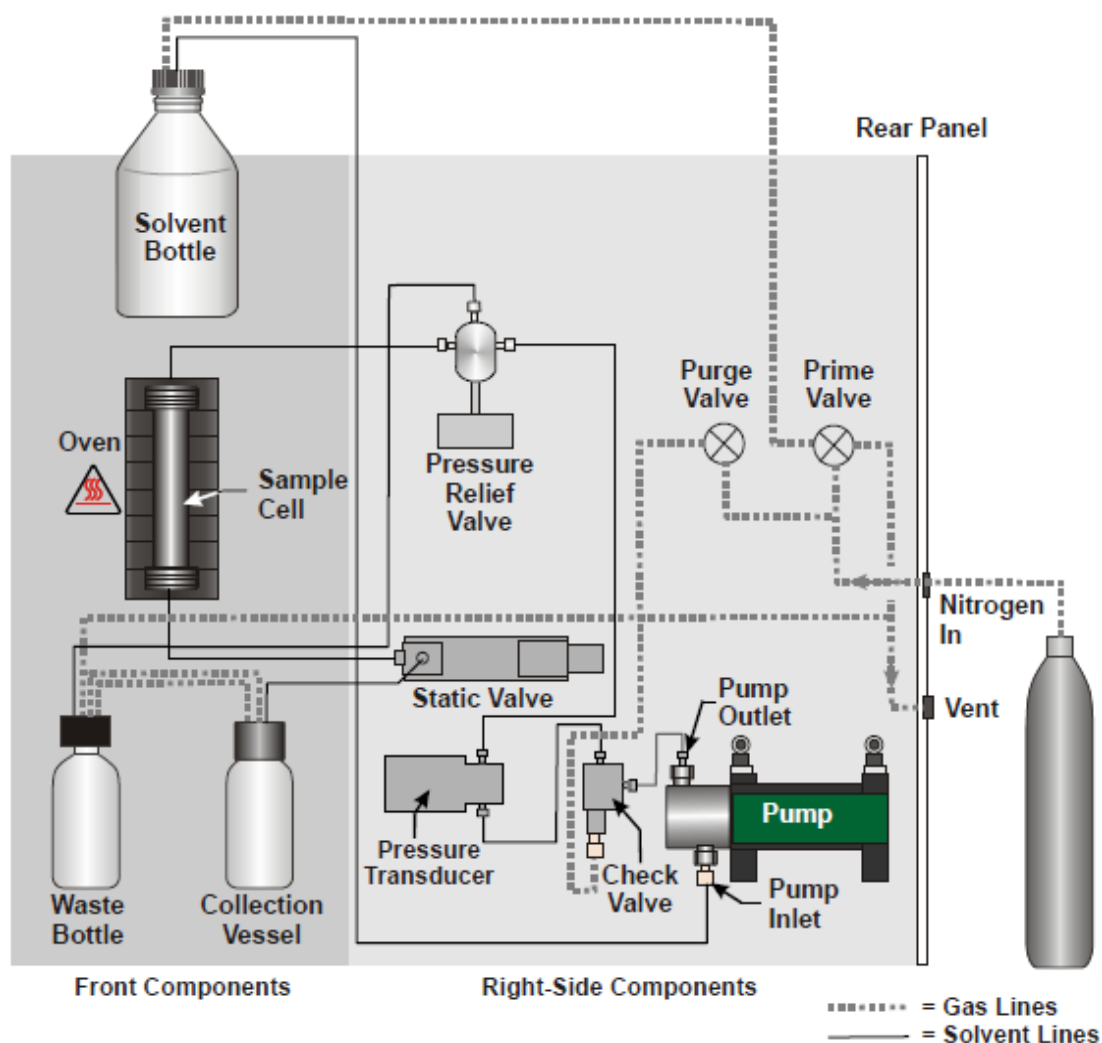


Figure 3.7: Schematic showing internal gas and solvent flows within the ASE (adapted from (ThermoFisher, 2011)).

Solvent extraction with the ASE requires several successive steps. Initially, a stainless steel extraction cell (of either 10 ml or 66 ml capacity) containing the sample, and capped with two filtration end fittings, was loaded into the oven,

which had been preheated to the desired extraction temperature. The small extraction cell (10 ml) accommodated approximately 3.5 g of SCG, while ~23 g could be placed in the larger one (66 ml). The cells were then filled with solvent and pressurized by a high-pressure pump (70 ml/min), using a supply of nitrogen (BOC, oxygen-free) at 10 bar output.

Static extraction conditions were then maintained for a fixed duration, without continuous flow of solvent, followed by pressure release and rinsing of the extracted lipids and “used” solvent into the collection vial through a Dionex™ glass fiber filter inserted at the bottom of the extraction cell. The cell was then refilled by solvent and the second extraction cycle commenced. A maximum of 5 static cycles could be performed per extraction. The SCG-to-solvent ratio was automatically determined by the instrument and ranged from 1:5.8 to 1:6.6 w/v. Following completion of the final static cycle, the cell was purged with compressed nitrogen gas to remove the residual solvent, extracted lipids and final solvent volume.

3.2.3.3 Solvent extraction in a closed pressure vessel

A cylindrical stainless steel vessel with an internal volume of 200 ml was used for the static solvent extraction experiments that investigated the effect of pressure on the recovery of lipids from dry SCG. The pressure chamber, designed on Catia V5 software and manufactured within the UCL Mechanical Engineering workshop, consisted of two parts, a lower removable cylinder with external threads and an upper cylinder with internal threads. Nitrogen at a variety of pressures was supplied to the upper cylinder by a ¼ ″ stainless steel pipe, the gas pressure was measured with a pressure transducer (Gems Sensor, IP67, accuracy: ±1 bar) and temperature monitored by an RS Pro K type stainless steel thermocouple. The pressure and temperature read were recorded by a custom PC data acquisition program (National Instruments Labview) so as to allow the constant observation of the experimental conditions inside the vessel. Figure 3.8 shows the two parts of the pressure vessel along with the sensors and connection to the gas supply pipe.

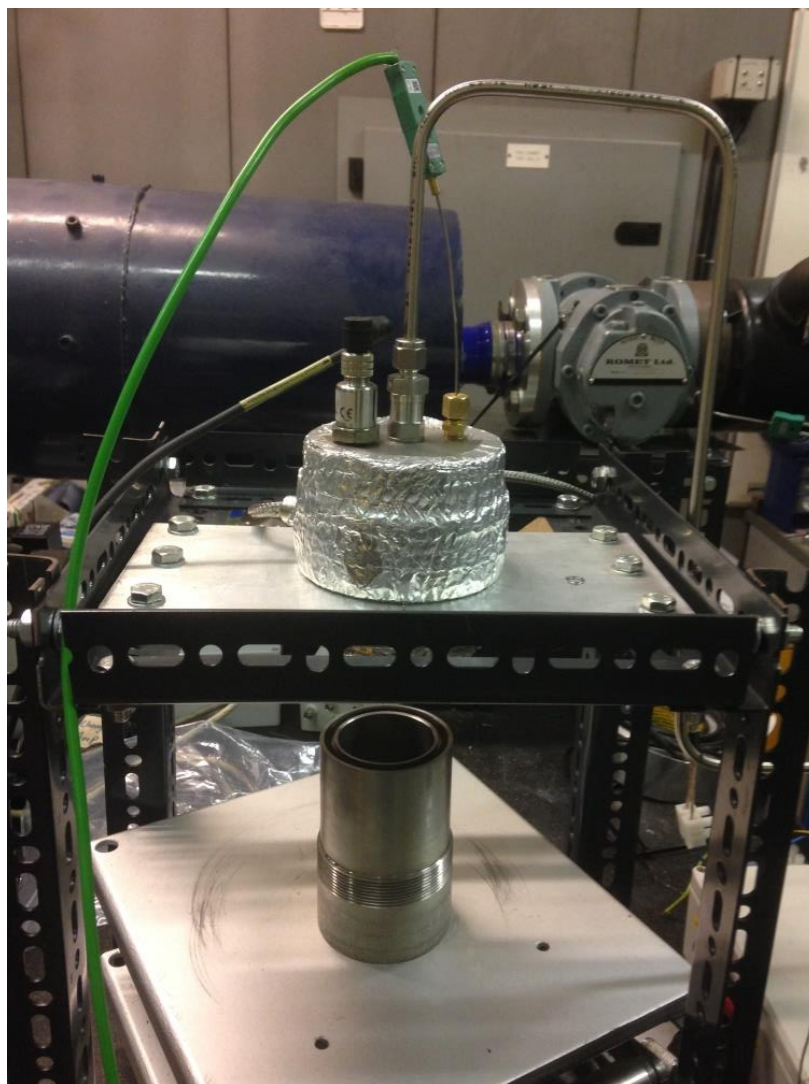


Figure 3.8: Prototype stainless steel vessel for static solvent extraction.

The vessel was pressurized by compressed nitrogen gas supplied through a stainless steel pipe connecting the vessel with a N₂ bottle (BOC, 230 bar capacity). Temperatures above the ambient could be reached by a 550 Watt Mica band heater connected to, and regulated by, a proportional integral derivative (PID) box with the temperature being measured by a second thermocouple placed between the band heater and the vessel external wall. The band heater was attached to the upper cylinder, which was then covered by insulation tape to decrease any loss of heat to the surroundings. The pressure could be manually selected to a desired value by an appropriate pressure regulator (BOC HP S/S High Pressure Nitrogen Regulator 200 bar) fitted on the N₂ bottle, while the vessel was designed to withstand pressure up to 200 bar and temperature up to 200 °C. The Catia V5 drawings along with

the equations used for the dimension calculations can be found in Appendix A. Figure 3.9 shows the major components of the experimental setup in schematic form.

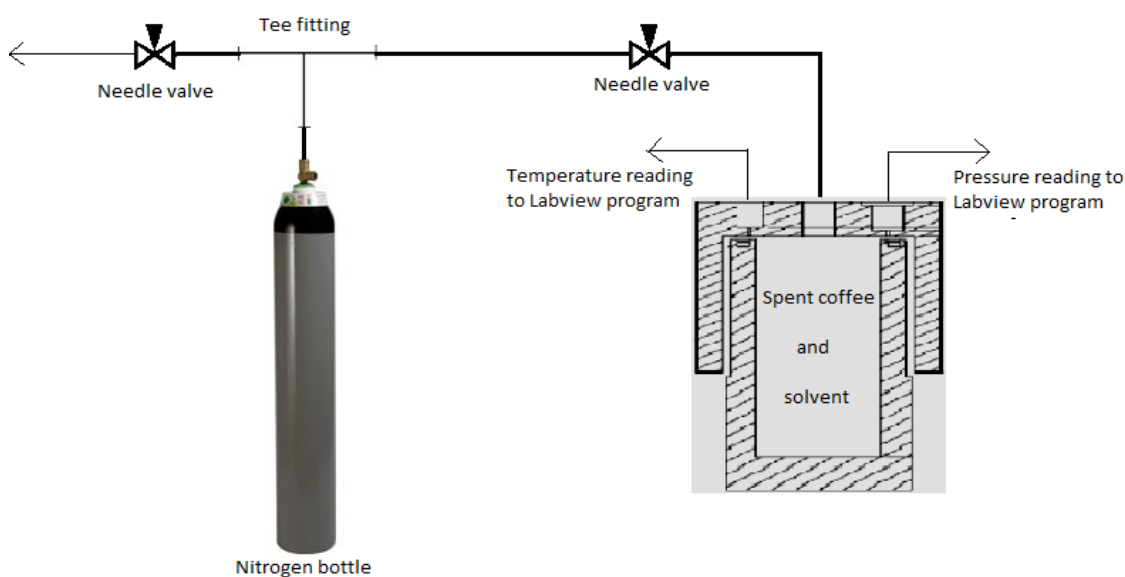


Figure 3.9: Schematic representation of experimental setup.

At the beginning of each experiment, the process needle valve (4A-V4LR-SS, ¼ in) in the gas supply line and close to the vessel (Figure 3.9) was kept closed and was opened only after a pressure of ~10 bar was selected on the pressure regulator so as to avoid any solvent vapours travelling in the pipe. The needle valve close to the nitrogen bottle (Figure 3.9) was kept closed during the test and only opened at the end of the experiment in order to depressurize the vessel. After depressurization, the solvent and SCG mixture was passed through a funnel equipped with a mesh of 0.1 mm aperture and filtrated through a cellulose filter paper with pore size of 20 µm so as to separate the oil and solvent mixture from the spent coffee grounds.

3.2.3.4 Solvent separation

Following a solvent extraction, the extracted oil remained dissolved in the solvent solution and further processing was required to recover it. In most instances, initial separation of extracted compounds, for example lipids, was achieved with a rotary evaporator, which rapidly fractionates and removes excess solvent by applying heat to a rotating round bottomed flask at a reduced pressure. This is achieved through the use of a vacuum pump and

allows solvents to boil at temperatures lower than their boiling point at atmospheric pressure. Furthermore, the rotation of the vessel at approximately 130 rpm maximizes the surface area of the liquid, spreading it over the entire inner surface of the rotating flask and providing agitation, increasing the rate of solvent evaporation, while bumping and foaming are greatly reduced (Williamson, 2003). The rotary evaporator removed the solvent plus any other compounds of similar boiling point, and was therefore useful for lipids recovery since triglycerides typically have much higher boiling points than solvents used for extraction. Figure 3.10 shows the major components of the rotary evaporator used.



Figure 3.10: Rotary evaporator key operating features (adapted from “http://www.ika.com/owa/ika/catalog.product_detail?iProduct=10002170”).

The rotary evaporator used (IKA RV 8) consisted of a heated fluid bath of distilled water (1), a vacuum pump (IKA MVP 10 basic), a 500ml round flask containing the oil-solvent solution (2), vapour duct and clamp to secure the round flask, a rotor (3), a spiral condenser (4), a collecting flask (5) below the condenser to catch the distilling solvent and a lifting mechanism that allowed precise positioning of the glassware in the water bath. The specific model used included digital control of temperature and rotational speed. The duration of the process depended on the initial volume of solvent used in various extraction methods and the solvent used, and varied between 10 and 30 minutes.

The maximum removal of solvent is indicated by the cessation of liquid dripping from the condenser for a period of 30 seconds. The amount of the solvent recovered through rotary evaporation can be calculated simply by weighting the collecting flask before and after the procedure or measuring its volume by transferring the liquid in a volumetric cylinder. The recovered solvent can be reused in subsequent extractions, however, this was not the case for the experiments undertaken in this thesis. The oil sample that remained in the 500 ml round flask was transferred to 16 ml borosilicate glass vials through an appropriate funnel and subjected to a further processing so as to ensure complete removal of any remaining solvent traces. This was accomplished either by nitrogen assisted evaporation or through oven drying.

Nitrogen assisted evaporation was conducted by directing a nitrogen gas stream onto the oil sample surface through a capillary nozzle, while the flow rate was controlled by the gas bottle pressure regulator (BOC Series 8500). Pure dry nitrogen from a pressurized bottle (BOC, 230 bar capacity) was used as it is a non-reactive gas and the gas flow was gradually increased to ~2 bar. The vials were placed in a heated water bath (Fisherbrand 60301) set at 45 °C so as to ensure that the oil sample was maintained in a liquid state. Nitrogen assisted evaporation experiments were performed for 5.5 hours, a duration that was found in preliminary tests to be sufficient for complete solvent removal by measuring the sample weight at regular intervals on a balance (Sartorius M-prove AY123).

An alternative method of thermal drying was also used to remove any remaining solvent after rotary evaporation. This was performed in the same oven used for the SCG moisture removal experiments and the selected temperature was 10 degrees higher than the boiling point of the solvent used. Again, the drying duration was estimated by regularly measuring the weight of the sample until no mass difference was observed between subsequent measurements. In general, 5 hours of drying were sufficient for the removal of the solvent traces.

3.2.3.5 Oil yield calculation

The oil yields achieved from the extraction processes were calculated after the end of the solvent separation procedures as per Equation 3.6.

$$\% \text{ oil yield} = \frac{W_1}{W_2} \times 100 \quad (\text{Equation 3.6})$$

Where W_1 is the weight of the extracted oil and W_2 is the weight of the dry SCG sample. An alternative approach to find the collected oil quantity indirectly and verify the result obtained from Equation 3.6 was to measure the weight loss of the dry SCG sample. Equation 3.7 shows the equation used to calculate oil yield by this method:

$$\% \text{ oil yield} = \frac{W_{\text{initial}} - W_{\text{final}}}{W_{\text{initial}}} \times 100 \quad (\text{Equation 3.7})$$

Where W_{initial} and W_{final} are the initial and final dry weights of the coffee sample in the extraction thimble respectively. The extraction ratio obtained relative to total available oil was calculated based on Equation 3.8:

$$\% \text{ oil extraction ratio} = \frac{\% (w/w) \text{ oil recovered} \cdot 100}{\% (w/w) \text{ oil content}} \quad (\text{Equation 3.8})$$

Where the % (w/w) oil content corresponds to the average hexane-extracted oil yield of the specific SCG batch used in each case, as calculated from 3 experimental repeats through Soxhlet at the conditions specified in Section 3.2.3.1.

3.2.4 Pilot plant scale solvent extraction

Large scale solvent extraction experiments were conducted at New Holland Extraction Ltd. (NHE) in a pilot plant scale batch counterflow solvent extractor of capacity of 8 kg of SCG per batch. The extractor consisted of 6 compartments containing a conveyor belt and was heated to 60 °C through a water pipe running beneath the compartments. Figure 3.11 shows the flow diagram of the NHE pilot plant belt extractor.

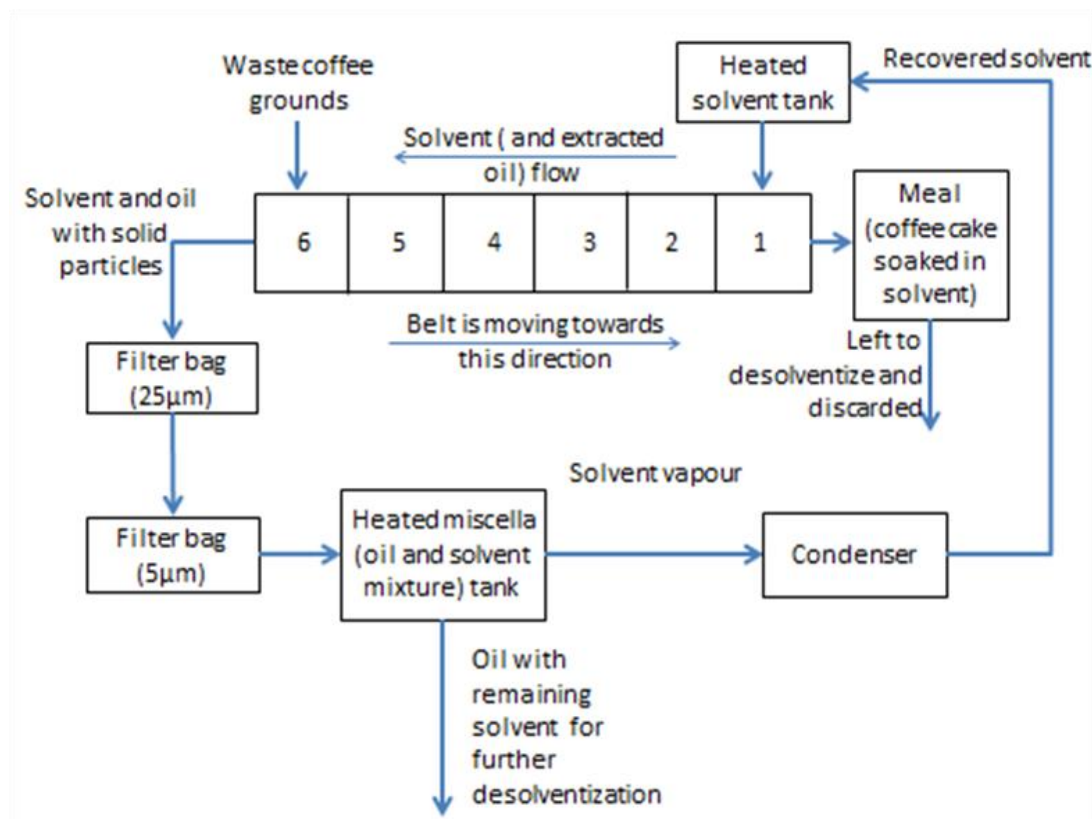


Figure 3.11: Overall schematic of the pilot plant used in extraction experiments.

SCG were added to compartment 6 (Figure 3.11), while iso-hexane was added to compartment 1 at a flow rate of 380 ml/min, resulting in countercurrent contact of feedstock and solvent. The process was performed at a slightly negative vacuum so as to reduce the boiling point of the solvent. Extraction experiments with this plant of durations of 1 and 2 hours were conducted with SCG samples containing moisture contents of 5 and 10 % w/w.

Subsequent to leaving compartment 6 (Figure 3.11), the meal (SCG soaked in solvent) and the miscella (oil and solvent mixture) were collected in separate tanks. The oil and solvent mixture was filtered to remove any solid particles twice through bag filters with pore sizes of 25 μm and 5 μm before reaching the collection tank. This tank was subsequently heated and the resulting solvent vapour was conveyed to a condenser for recovery. The resulting oil, with remaining solvent traces, was subjected to rotary evaporation for further refining of the oil. The oil yield of the process was calculated according to the method described in Section 3.2.3.5.

3.2.5 Mechanical expression

Expression is a process that uses mechanical power to press liquids out of liquid containing particles such as SCG. The feedstock is placed between permeable barriers and mechanical pressure is applied to reduce the volume available and force the liquid out of the solid particles (Sorin-Stefan et al., 2013; Willems et al., 2008a, 2008b). Two mechanical presses with different modes of operation, a batch hydraulic ram press and a continuous screw press (expeller), were used to apply pressure on wet and dry SCG and RDCB. These presses are described in Sections 3.2.5.1 and 3.2.5.2.

3.2.5.1 Ram press

A mechanical ram press was used in experiments which investigated the effect of pressure applied through a hydraulically operated piston on wet and dry SCG and RDCB. The press was designed on Catia V5 software and manufactured by the UCL Mechanical Engineering workshop. The Catia V5 drawings along with the equations used for the dimension calculations of the ram press can be found in Appendix B. The stainless steel cylindrical press had an internal volume of 471.2 ml, when the piston was at its starting position, and was designed to withstand pressure up to 600 bar and temperature up to 200 °C. A ¼ inch internal diameter stainless steel pipe connected the press with a diesel engine that provided the hydraulic fluid (fossil diesel) required to move the piston and pressurize the SCG. This was accomplished by running the engine at a constant speed of 2000 rpm and selecting the desired pressure at the engine common rail, from which diesel

was directed to the hydraulic press at pressures ranging from 150 up to 550 bar with a deviation of ± 1 bar. Figure 3.12 shows the main parts of the hydraulic press.

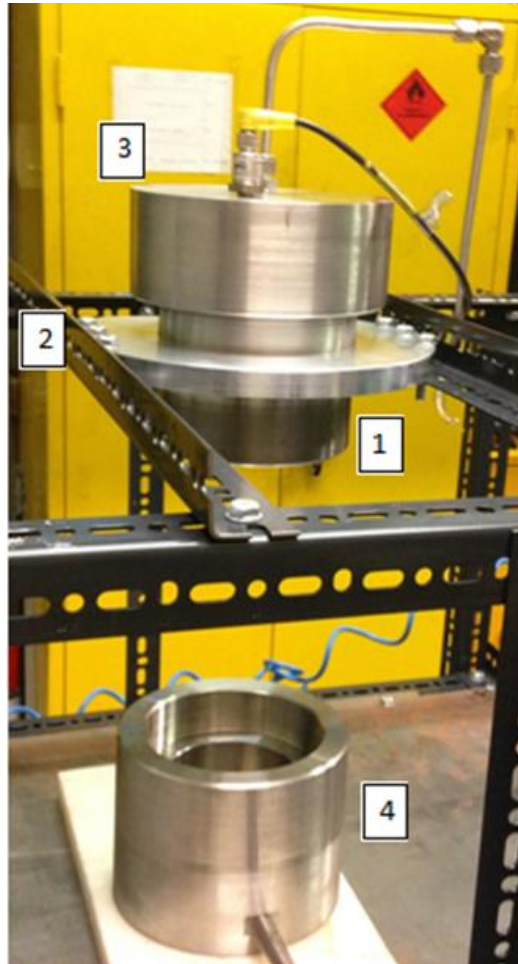


Figure 3.12: Major components of the ram press.

The press consisted of 5 parts (Figure 3.12) including a piston, a cylinder (1) that was secured in a clamp (2) in which the piston could move, a removable upper cap (3) with two threaded holes, one for connection to the diesel supply pipe and one for housing of a pressure transducer (Gems Sensor, IP67, 0.25 % accuracy) from which pressure measurements were constantly read by a custom PC DAQ software (NI Labview), and a removable cylinder (4) that could host a perforated supporting plate on which the SCG were placed on top of a mesh of 0.1 mm aperture. Some experiments were conducted at a temperature above ambient where the heat was applied by a 1000 Watt 2-piece Mica insulated band heater controlled by a PID box. The temperature

was measured by a RS Pro K type stainless steel thermocouple. Figure 3.13 shows a schematic of the ram press set up.

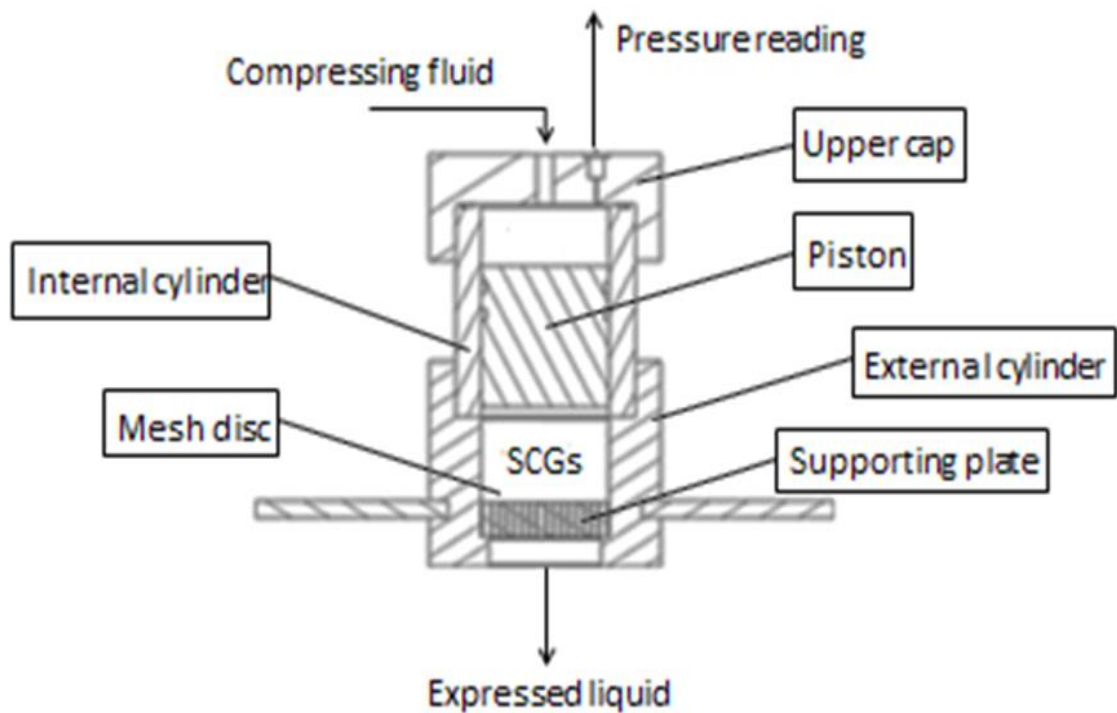


Figure 3.13: Overall schematic of the ram press.

After the end of each experiment, the cylinder containing the SCG was removed and a lab jack was used to push the piston to its starting position and consequently drive the excess diesel to the fuel tank of the engine. Any water or oil removed from SCG and RDCB was collected in a petri dish, and in the case of wet SCG, the pressed cake was subjected to prolonged drying at 100 °C in the oven so as to determine by mass difference the amount of moisture remaining within the grounds. The percentage of moisture removed after each experiment with wet SCG was calculated as per Equation 3.9.

$$\% \text{ Percentage of moisture removed} = \frac{W_{\text{initial}} - W_{\text{press}}}{W_{\text{water}}} \times 100 \quad (\text{Equation 3.9})$$

Where W_{initial} is the original samples mass, W_{press} is the mass of the SCG sample after pressing and W_{water} the total water mass contained in the sample as calculated by the mass difference between the initial and final (after drying) sample. In the case of lipids expression, the oil yields were calculated as per Equation 3.6.

3.2.5.2 Screw press

In mechanical screw pressing, oil is squeezed out of the raw material due to the axial pressure applied to it. This pressure is generated by volumetric compression along the horizontal screw barrel, and is transferred by a worm shaft rotating inside a pressing cylinder (Singh and Bargale, 2000). The worm conveyor shaft increases in diameter towards the discharge end, while the worm flights come closer together so as to steadily increase the pressure on the seed as the volume decreases (Knowles and Watkinson, 2014). The barrel is slotted along its length in order to allow the increasing internal pressure to expel firstly air and then the oil. This pressing procedure aims to apply maximum pressure to a thin cross section of the oil containing material, therefore extracting as much oil as possible (Singh and Bargale, 2000). Figure 3.14 shows the screw press at the tolling manufacturer's site (NHE) used for oil expression in this study.



Figure 3.14: Screw press used for SCG mechanical expression.

The screw press shown in Figure 3.14 had a capacity of approximately 30 kg/hour and was used for expressing lipids from partially dried SCG (5 % w/w and 10 % w/w moisture content) and RDCB. The raw material was fed into the press hopper and the press was pre-heated at 100 °C before starting with a shaft speed of 12 rpm that was later increased up to 30 rpm, while various gap settings and nozzle sizes were used so as to achieve better oil release. Any derived oil was concentrated in a trough beneath the screw and filtered to remove any fine seed debris, while the pressed raw material was discarded. Equation 3.6 was used for calculation of the obtained oil yield.

3.2.6 Free fatty acid content determination through titration

The acid value and FFA content of the SCG oil samples extracted with various solvents were determined through the method of acid-base titration with phenolphthalein as the indicator. The acid value of the oil sample is a measure of acidity, and indirect measure of the amount of free acids, that represents the mass (in mg) of potassium hydroxide required to neutralize the free acid in 1 g of the substance (Nielsen, 2014).

During titration an accurately measured amount of a basic solution of known concentration, KOH (0.1 M) in this study, is slowly added to a solution of unknown acid concentration, the SCG oil, until the equivalence or endpoint is reached. The equivalence point is reached when the number of acid moles in the oil is equal with the number of base moles that have been added and the reactants have stopped reacting. The pH of the solution changes dramatically at the equivalence point and when an indicator that changes color near the equivalence point is chosen, a dramatic color change occurs. Phenolphthalein is an acid-base indicator that changes from colorless in an acid solution to pink in a basic solution with the pH range of the color change located between 8.2 and 10, while the pH at the turning point, when there are equal amounts of acid and base moles and the color change is most noticeable, is 9.4 (<http://www.chemguide.co.uk/physical/acidbaseeqia/indicators.html>). Figure 3.15 shows the major components of a titration experiment.

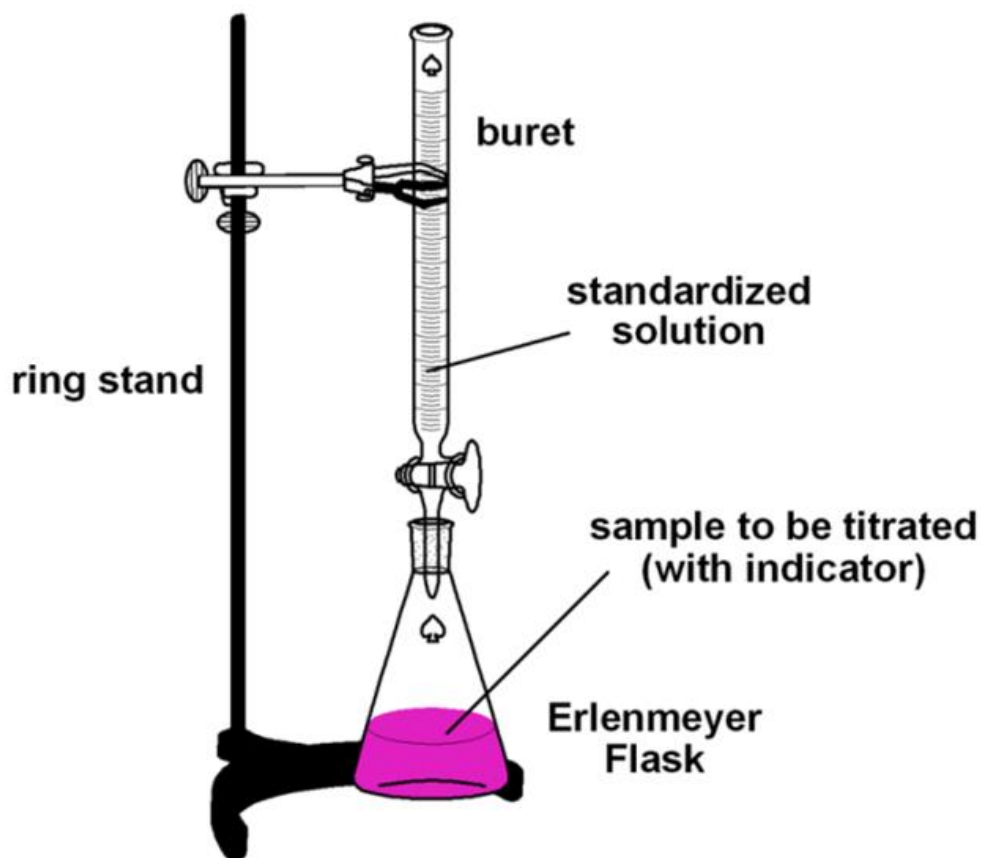


Figure 3.15: Titration experimental set-up (adapted from [“http://sachiacidbase.weebly.com/titrations.html”](http://sachiacidbase.weebly.com/titrations.html))

For each experiment, 50 ml of ethanol and 0.5 ml of phenolphthalein were placed in a 250 ml conical flask located on a magnetic hotplate stirrer (Fisherbrand™ ARE) with temperature selected at 45 °C and stirring at 200 rpm. Ethanol was neutralized with potassium hydroxide released dropwise from a burette until the appearance of pink color before adding about 0.5 g of sample. Thereafter, the titration with aqueous KOH was carried out until the appearance of the first permanent pink color of the same intensity as before adding the sample. In order to consider the titration complete, the color should persist for 10 s. Certain oil samples, especially those extracted with alcohols, had a dark color which impeded the observation of the color change and a pH meter (Hannah, HI991001) with accuracy of ± 0.02 was used to detect the equivalence point. The acid value of the oil sample can be calculated through Equation 3.10 (Nielsen, 2014):

$$AV = \frac{V_{KOH} N_{KOH} 56.1}{W_{Oil}} \quad (\text{Equation 3.10})$$

Where V_{KOH} is the volume of potassium hydroxide required for the titration in ml, N_{KOH} is the molarity of potassium hydroxide and 56.1 its molecular weight (MW) in g/mol. W_{Oil} stands for the weight (g) of the oil sample. The weight to weight FFA ratio (as oleic acid) can be found by Equation 3.11 (Nielsen, 2014):

$$\% FFA = AV \times 0.503 \quad (\text{Equation 3.11})$$

3.2.7 Transesterification process

SCG lipids extracted from an instant coffee ground sample (ICG2) through the New Holland Extractions Ltd. pilot plant (Section 3.2.4) were used in all transesterification experiments, and the FFA content of the oil was found to be 29.91 ± 0.51 % w/w according to the method described in Section 3.2.6. A two-step transesterification process was selected as the most appropriate for the conversion of oil to FAMES based on previous studies that investigated biodiesel synthesis from SCG oils with high FFA content (Al-Hamamre et al., 2012; Caetano et al., 2012; Haile, 2014; Vardon et al., 2013). In this method, the FFAs were initially converted to esters with methanol in an acid-catalyzed pretreatment step, and thereafter, when the FFA content of the oil had been reduced to a suitable level, a base-catalyzed transesterification step was conducted. Methanol was used in both steps and was preferred over ethanol as it is the smallest molecular weight alcohol, and can potentially increase the reaction speed (Leung and Guo, 2006; Ma and Hanna, 1999). Prior to esterification, the ICG2 oil samples were subjected to heating at 100 °C for 5 hours in an oven to remove any residual water traces.

3.2.7.1 Acid-catalyzed pretreatment

In the first part of the transesterification process, ICG2 coffee oil which had been previously homogenized by preheating at 55 °C in a water bath (Fisherbrand 60301) for 30 minutes, and methanol were mixed in the presence of sulfuric acid in a 250 ml conical glass flask located on a magnetic hotplate stirrer (Fisherbrand ARE) at temperatures of 50 °C and 60 °C. Methanol and oil are immiscible and therefore the stirring speed was kept

constant at 600 rpm so as to ensure efficient mixing, as suggested by previous researchers (Caetano et al., 2012; Chai et al., 2014; Haile, 2014). The mixture was stirred for 4 hours after the start of the reaction, a duration that was found to be sufficient in previous studies (Al-Hamamre et al., 2012; Vardon et al., 2013), while the % w/w FFA content of the mixture was measured at 2, 3 and 4 hours through titration (Section 3.2.6).

In order to determine the desired experimental molar ratios of methanol-to-FFA and weight percentages of catalyst to FFA, the density of the oil and the average molecular weight of fatty acids present in the oil had to be measured. The density of methanol is 0.791 g/ml, while its molecular weight is 32.04 g/mol (Sadeghi and Azizpour, 2011), and the density of sulfuric acid is 1.83 g/ml (Shitov et al., 2009).

The density of the oil was calculated by adding quantities of 1 ml into a 10 ml volumetric cylinder, measuring the weight on a precision balance and then drawing a graph of mass against volume. Thereafter, a straight best fit line was drawn and the ICG2 oil density was found from its gradient (Appendix C). The average molecular weight of fatty acids present in the ICG2 oil was calculated based on the fatty acid profile of SCG oil from the same source (ICG1) determined through gas chromatography, where the molecular weights of the individual fatty acids present in the oil were calculated by summing the appropriate number of carbon, hydrogen and oxygen atoms (Appendix D). The transesterification and gas chromatography method used at New Holland Extraction Ltd. to determine the fatty acid profile of the ICG1 oil can be found in Appendix D. The average molecular weight (g/mol) of a single fatty acid in this oil was calculated as per Equation 3.12:

$$\text{Fatty acid average molecular weight} = \frac{\sum f_i}{\sum \left(\frac{f_i}{MW_i}\right)} = 273.54 \quad (\text{Equation 3.12})$$

Where f_i corresponds to the % w/w fraction of each fatty acid in ICG1 oil and MW_i to the molecular weight of an individual fatty acid. The molecular weight of a triglyceride in ICG2 oil was measured by Equation 3.13:

$$\text{Triglyceride average molecular weight} = 3 \times MW_f + 38.049 = 858.68$$

(Equation 3.13)

Where MW_f is the fatty acid average molecular weight calculated by Equation 3.12, and 38.049 the weight of the glycerol backbone (Shrestha and Gerpen, 2010).

Oil samples that had been pre-treated at the aforementioned conditions were left to settle for 24 hours in a separating funnel and the bottom layer was separated from the top layer of unreacted methanol and water with a separation funnel. The resulting sample was then subjected to rotary evaporation (Section 3.2.3.4) to remove any residual methanol and water. Any oil loss relative to the initial samples weight was measured according to Equation 3.14:

$$\% \text{ w/w Oil loss} = \frac{W_{\text{initial}} - W_{\text{pretreated}}}{W_{\text{initial}}} \times 100 \quad (\text{Equation 3.14})$$

Where W_{initial} and $W_{\text{pretreated}}$ correspond to the initial and pre-treated oil respectively.

3.2.7.2 Base-catalyzed transesterification and FAMES purification

In this step of the process, pre-treated oil with FFA content below 1.5 % w/w was mixed with methanol in the presence of potassium hydroxide. All the alkali-catalyzed experiments were conducted in a 250 ml conical flask located on a magnetic hotplate stirrer (Fisherbrand ARE), at a temperature of 60 °C (measured with a thermometer) for 4 hours at varying methanol-to-pretreated oil molar ratios and catalyst-to-pretreated oil weight percentages, while the mixture was constantly stirred at 600 rpm with a magnetic stirrer.

In order to determine the desired experimental methanol-to-oil molar ratios and catalyst to oil weight percentages, the density and molecular weight of oil previously subjected to acid-catalyzed esterification were determined. The density of the pre-treated oil was measured with the method used for the determination of the crude oil density (Appendix C). The molecular weight of the pre-treated oil was calculated based on the assumption that it contained approximately 70 % w/w triglycerides, assuming that the majority of

triglycerides have not yet reacted with methanol to yield FAMEs, ~1.5 % w/w FFAs and ~28.5 % FAMEs due to the esterification process. The average molecular weight of FFAs and triglycerides were previously determined (Equation 3.12, Equation 3.13), while the average MW of FAMEs was found to be 287.54 g/mol by replacing in the FFA molecule the hydrogen atom of the –OH group with a methyl group (-CH₃). Therefore, the average MW of the pre-treated oil was measured as per Equation 3.15.

$$\begin{aligned} \text{Pret – treated oil average MW} &= (0.285 \times MW_f) + (0.7 \times MW_t) + \\ &(0.15 \times MW_{fame}) = 724.05 \end{aligned} \quad (\text{Equation 3.15})$$

Where MW_f, MW_t and MW_{fame} correspond to the molecular weights of FFAs, triglycerides and FAMEs found in the pre-treated oil respectively.

The reaction product was allowed to settle in a separation funnel and after 24 hours the upper biodiesel and unreacted methanol phase was separated from the lower glycerol phase. Unreacted methanol was removed from the FAMEs by rotary evaporation (Section 3.2.3.4) and the resulting ester phase was successively washed with warm (55 °C) distilled water until neutral pH. The pH was measured constantly measured by a Hannah, HI991001 pH meter. The washing process also served as a way to remove residual catalyst, glycerol, methanol and soap from the coffee biodiesel. Thereafter, the FAMEs were subjected to thermal heating at 100 °C for 5 hours and subsequently a further drying step of drying with sodium sulfate to remove residual water was carried out. Finally, a filtration process with cellulose membranes (Whatman, 4-7µm) was performed to remove solid traces. The % w/w FAME reaction yield relative to pre-treated ICG2 oil was calculated according to Equation 3.16.

$$\% \text{ Reaction yield} = \frac{W_{FAME}}{w_{pretreated\ oil}} \times 100 \quad (\text{Equation 3.16})$$

Where W_{FAME} and W_{pretreated oil} represent the mass of biodiesel and pre-treated ICG2 oil respectively.

3.2.8 Determination of fatty acid profile

SCG derived biodiesel was characterized in terms of fatty acid profile by Gas chromatography coupled with a Flame ionization detector (GC-FID), along with soya and rapeseed FAMES obtained from BP for comparison purposes. GC is an analytical technique used to identify the different components of a mixture. The GC system used (Agilent 7890B) is illustrated in Figure 3.16.

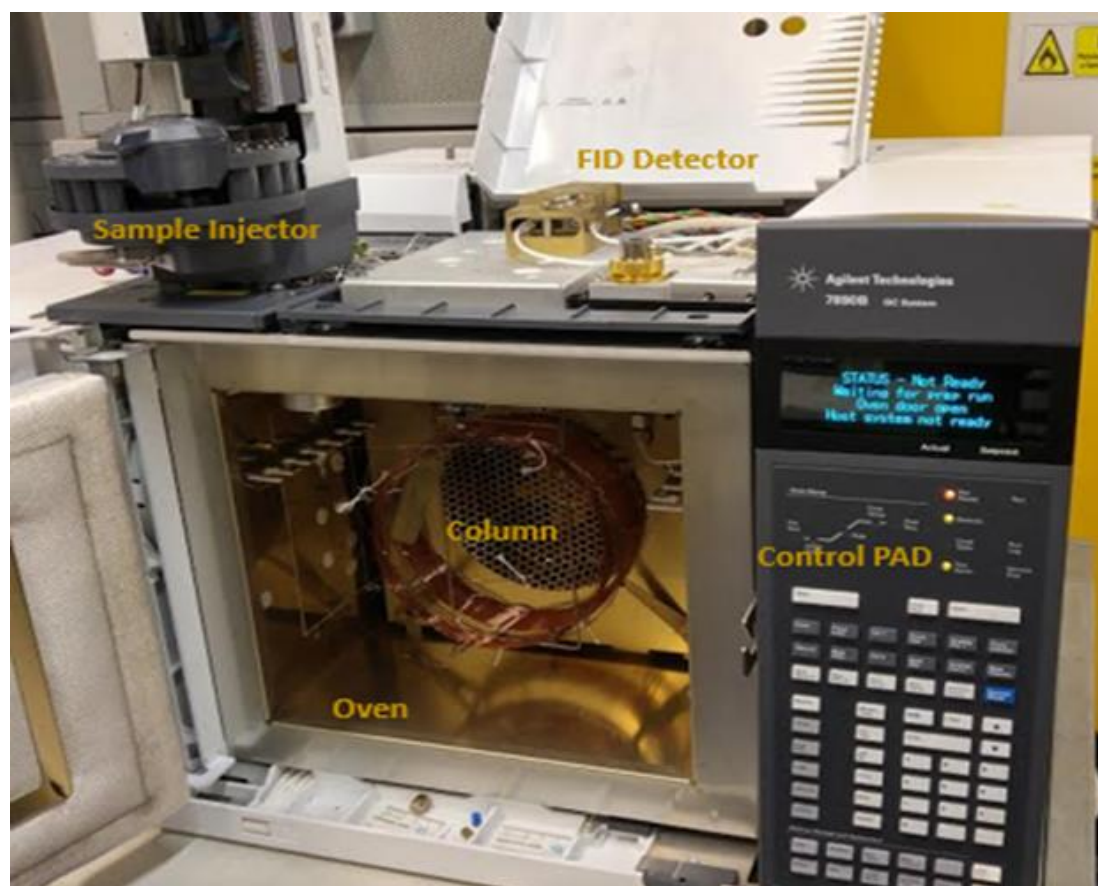


Figure 3.16: Main parts of GC machine.

The Gas Chromatograph was equipped with a Supelco SP-2380 capillary column (30m x 0.25 mm internal diameter, max temperature 275 °C) coated with 90% biscyanopropyl/10% cyanopropylphenyl siloxane stationary phase (0.2 μm film thickness), and a helium mobile phase (flow rate: 20 ml/min) which carried the sample molecules through the heated column. An injection port, maintained at 250 °C, and a FID detector (260 °C) were located at the inlet and outlet of the column respectively. The injection volume for each solution was 1 μl and the split ratio with the carrier gas 50:1. The oven was

programmed initially to maintain a temperature of 50 °C for 2 minutes and then increase the temperature up to 250 °C at a ramp rate of 5 °C per minute.

Prior to experimentation with SCG derived biodiesel samples, a 37-Component FAME mixture (Supelco, CRM47885) was used as a standard in order to create a calibration curve which would help identify the various components in the chromatogram according to retention time. The 37-Component FAME mixture was diluted in dichloromethane at five different concentrations: 625, 1250, 2500, 5000 and 10000 µg/ml so as to create a calibration curve. The FAME samples were diluted in dichloromethane at 5000 µg/ml, however, in order to achieve the desired concentration the density of SCG FAMEs had to be calculated beforehand (Appendix C). The densities of soya and rapeseed FAMEs were known and can be found in Appendix E.

After the GC-FID tests, the various fatty acids present in each sample were determined, based on the retention time of the peaks observed in the obtained chromatogram, and through comparison with the 37-FAME mixture component chromatogram, while the concentration of each was calculated from the peak areas. For each compound of the calibration standard that was found in the biodiesel samples, a calibration curve of concentration against peak area was plotted based on the serial dilutions of the 37-FAME mixture, and a line of best fit of the format $y=ax+b$ (where y is the peak area, x the concentration and a , b are constants) was found (Appendix F). The percentage of a specific fatty acid can be found by Equation 3.17.

$$\% \text{ Component Percentage} = \frac{x}{5000} 100 \quad (\text{Equation 3.17})$$

Where x is the concentration of the fatty acid and the denominator represents the concentration of the sample in µg/ml.

3.2.9 Determination of gross calorific value

The gross calorific value of various solid and liquid samples including dry SCG, defatted SCG, SCG oil samples, SCG derived biodiesel and RDCB was determined by using an IKA® C1 Bomb calorimeter system. The bomb calorimeter was connected to a pure compressed O₂ cylinder (BOC, UN: 1072, 99.5 % purity, 200 bar capacity) which provided oxygen supply at a

pressure of 30 bar through a suitable regulator (BOC, HP1800 Series), and a cooler (IKA® RC 2 basic) that provided water at a temperature of 18–21 °C (“IKA Calorimeter C1, Operating instructions”).

Initially, a precisely measured quantity of the sample (~0.5 g) was placed in an acetobutyrate capsule of known calorific value. The sample containing capsule was then placed in the combustion chamber where it is ignited at an excess of oxygen by means of electrical energy through a cotton thread that is attached to an ignition wire. The cotton thread, which also has a known calorific value, was in direct contact with the sample in a stainless steel crucible. Figure 3.17 shows the equipment used for measurement of calorific value and a cutaway view of a typical bomb calorimeter.

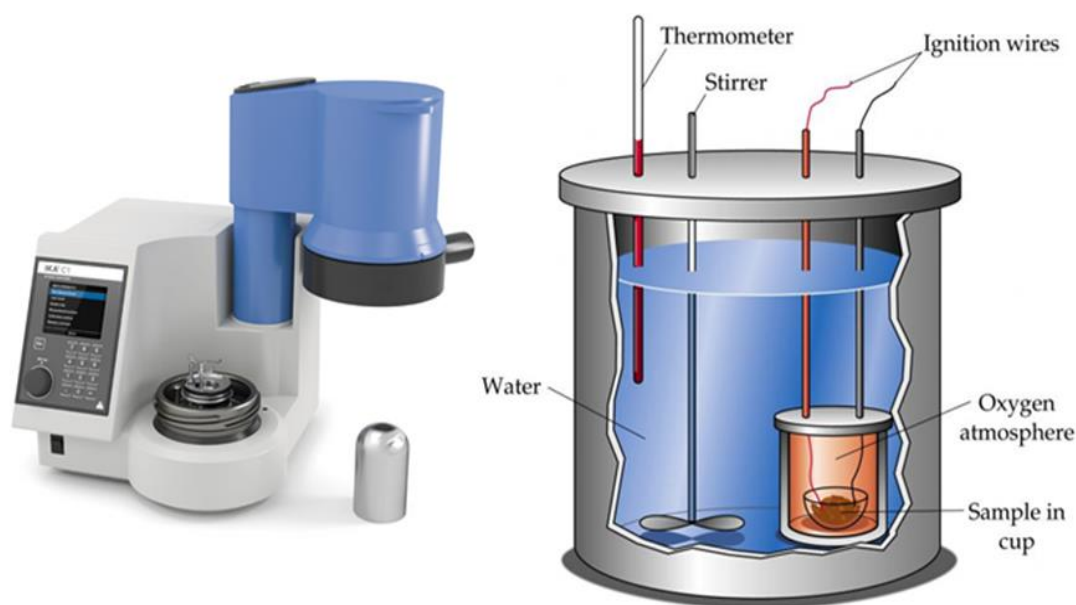


Figure 3.17: (a) Bomb calorimeter (adapted from “<https://www.laboratory-equipment.com/calorimeters/c1-calorimeter-ika.php>”), (b) cutaway view of the equipment (adapted from “<http://docslide.us/documents/thermochemical-equations-calorimetry-at-the-end-of-this-lesson-you-should.html>”).

As the sample burns, it increases the temperature of the surrounding air, which expands through a tube that leads the air out of the bomb calorimeter. The escaping air heats the water that is surrounding the combustion chamber when the system is operating, and the change in the water temperature allows the calculation of the gross calorific value of the sample. The calorific values

of the plastic capsule and the cotton thread were subtracted from the final value of the quotient of the heat liberated and the weight of the oil sample. The gross calorific value of the sample, which includes the heat of vaporization of the newly formed water vapour produced by oxidation of hydrogen in the sample, was calculated according to Equation 3.18.

$$H_g = \frac{W_{water} C \Delta T}{W_{sample}} \quad (\text{Equation 3.18})$$

where H_g is the gross calorific value, W_{water} is the mass of the surrounding water, C the heat capacity of the system, ΔT the temperature increase and W_{sample} the mass of the oil sample (“IKA Calorimeter C1, Operating instructions”).

3.2.10 Ash content determination

The ash content of dry raw and defatted SCG samples of the instant and retail coffee industry (ICG2 and RCG3) was determined by placing 0.5 g of the sample in a previously washed with deionized water and dried crucible, and incinerating it in a muffle furnace (Carbolite) at a temperature of 550 °C for 24 hours, a method similar to those performed by Caetano et al. (2012), Pujol et al. (2013) and Scully et al. (2016). The ash content of each sample was determined gravimetrically as per Equation 3.19.

$$\% \frac{w}{w} \text{ Ash content} = \frac{W_0 - W_f}{W_0} \times 100 \quad (\text{Equation 3.19})$$

Where W_0 is the initial weight of the sample and W_f the sample weight after heating. The experiments were performed in triplicate so as to determine the standard deviation of the mean.

3.2.11 Combustion experiments

3.2.11.1 Engine

All combustion experiments were conducted in a single cylinder, direct injection compression ignition research engine, the specification of which can be found in Appendix G. An ultralow volume fuel system, originally conceived by Schönborn et al. (2007) and later redesigned by Hellier et al. (2012), which allowed comprehensive testing with fuel samples as small as 100 ml was

used. This system uses the engine common rail system as a hydraulic fluid supply to pressurize the sample fuel to the desired injection pressure via two free pistons that separate it from the standard common rail diesel fuel (Hellier et al., 2013; Koivisto et al., 2016). A bypass operated by high pressure needle valves allowed fossil reference diesel from the engine pump circuit to flow at pressure and flush the test fuel circuit and combustion chamber between every test run (Hellier et al., 2013). Figure 3.18 shows a schematic of the system.

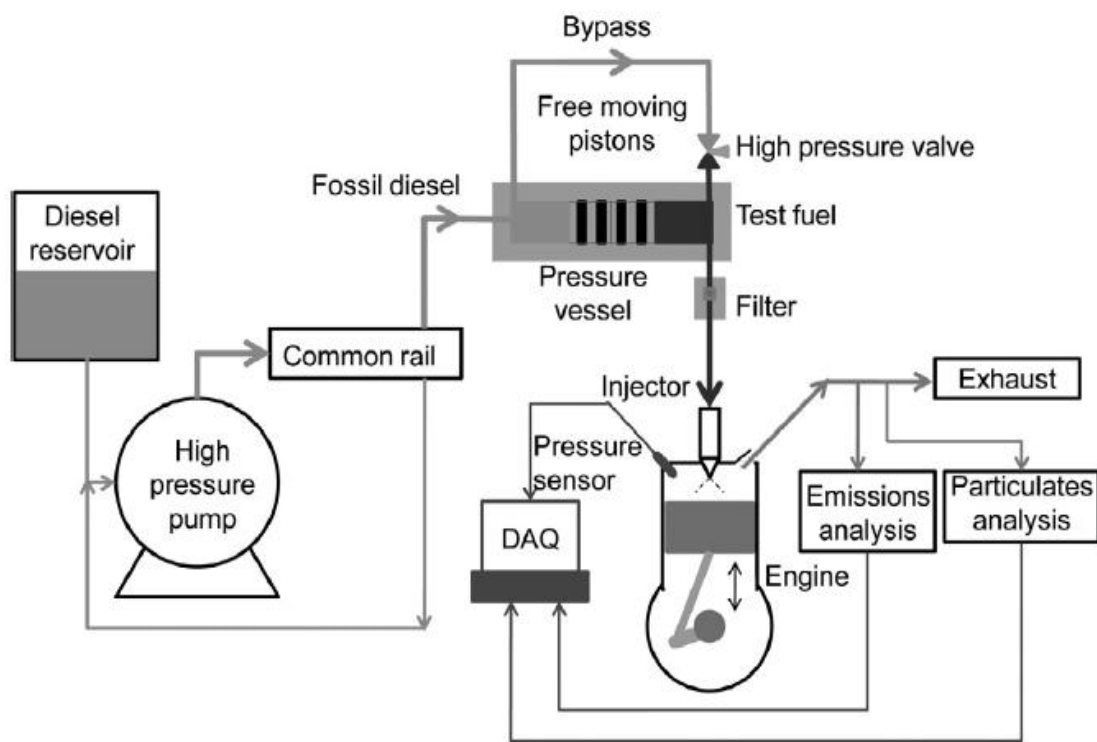


Figure 3.18: Schematic showing operation of the low volume fuel system (adapted from Hellier et al. (2013)).

The in-cylinder gas pressure was continuously measured and logged with a PC data acquisition system (National Instruments) at every 0.2 crank angle degrees (CAD) using a piezoelectric pressure transducer (Kistler 6056AU38) and charge amplifier (Kistler 5011). The in-cylinder gas pressure was pegged each combustion cycle at the bottom dead centre (induction stroke) by a piezoresistive pressure transducer (Druck PTX 7517-3257) located in the engine intake manifold, 160 mm upstream of the intake valves. The data

acquisition system (DAQ) recording the cylinder gas pressure was triggered by a shaft encoder every 0.2 CAD, which was the shaft encoder resolution. The shaft encoder also produced a top dead centre (TDC) signal, which was recorded by the DAQ. For each experiment, several consecutive engine cycles were recorded and an average of these was used in the subsequent heat release rate analysis, which was derived from the measured in-cylinder pressure during post-processing (MATLAB).

3.2.11.2 Fuel samples investigated

The samples tested in the engine include raw ICG2 oil, ICG2 neat biodiesel produced according to the method described in Section 3.2.7, neat soya and rapeseed biodiesel obtained from BP, and blends of the aforementioned biodiesel samples with reference fossil diesel containing 7 % v/v and 20 % v/v FAMES. The aim of the engine experiments was to measure the combustion characteristics and the gaseous and particulate exhaust emissions so as to evaluate the performance of each of the sample fuels.

3.2.11.3 Experimental conditions

All combustion experiments were conducted at engine speed of 1200 rpm and 600 bar injection pressure, with the exception of experiments performed with raw SCG oil, and the injection duration was adjusted for every fuel sample so that the engine indicated mean effective pressure (IMEP) was always constant at 4 bar. Operation of the research engine at a load of 4 bar IMEP represents a common engine load prevailing during passenger vehicle urban driving conditions. The engine speed of 1200 rpm is somewhat below those found in urban driving conditions, as is the injection pressure of 600 bar, and these settings were selected in order to reduce the consumption rate of fuels used in this study, given the laborious process of producing SCG biodiesel.

Each test day was started and ended with a reference diesel fuel test, so as to detect any day to day drift or longer term change in the experimental equipment and instrumentation. The reference diesel tests also provided a measure of the test-to-test repeatability of the exhaust gas emissions. Each of the fuel samples and the reference diesel were tested at two experimental conditions of constant fuel injection timing and constant start of ignition timing.

At constant injection timing the start of injection (SOI) was fixed at 5.0 CAD before TDC, and the start of combustion (SOC) for each fuel sample varied depending on the ignition delay of that fuel. Ignition delay was defined as the time between SOI and SOC, while SOC was defined as the time in CAD (after SOI and before the time of peak heat release rate) at which the minimum value of cumulative heat release occurs (Hellier et al., 2013).

For constant ignition timing, the SOI was varied so that the SOC of all fuels always occurred at TDC. All the experiments were conducted with the test fuels maintained at ambient conditions (~30 °C), except for the raw coffee oil which was heated to 45 °C to avoid solidification. Previous studies have reported that a rise in temperature up to 38 °C caused only a small decrease in the ignition delay that was of low significance (Koivisto et al., 2015a, 2015b). When raw SCG oil was used, the fuel injection pressure was initially increased to 860 bar at constant injection conditions and 940 bar at constant ignition conditions, in order to ignite the sample before decreasing it to measurement conditions (600 bar).

3.2.11.4 Analysis of exhaust gas emissions

For each combustion experiment the engine exhaust gas was sampled unfiltered 180 mm downstream of the exhaust valves and the sample was fed through heated lines (80 °C) to two analyzers. A Horiba MEXA 9100 HEGR was used to determine the dry concentrations of nitrogen oxides (NO_x), carbon monoxide (CO), carbon dioxide, oxygen and total hydrocarbon (THC) emissions and the wet concentration of unburned hydrocarbons. A Cambustion DMS 500 differential mobility spectrometer was used to determine the exhaust particle size distribution from 10 to 1000 nm, total mass and number of particles per unit volume of exhaust gas. The particle density was assumed to be 1.77 g/cm³ (Park et al., 2004).

The following chapters present results obtained from the application of the described experimental methods, while Chapter 4 concentrates on the physical properties of various coffee residues including fresh roasted and spent coffee grounds and roasted defective beans.

4. Characterization of SCG

This chapter presents a characterization of SCG samples originating from different sources, and utilized in the subsequent experimental studies presented in this thesis, and a study of SCG moisture removal by thermal drying.

4.1 Characteristics of solid samples and extracted lipids

The different coffee samples used in this study were characterized in terms of moisture content, average dry particle diameter, oil yield extracted by Soxhlet on dry weight basis and FFA content of extracted oil according to the methods described in Sections 3.2.1, 3.2.2, 3.2.3.1 and 3.2.6 respectively, while the energy content of dry grounds and lipids, and ash content of SCG were determined based on the methods explained in Sections 3.2.9 and 3.2.10 respectively. The results obtained are presented in Table 4.1, which also includes the standard deviations calculated from three experimental repeats. The oil yields were obtained with a SCG-to-hexane ratio of 1:9 w/v after 8 hours of Soxhlet extraction. When extraction ratios obtained from different SCG samples are compared in following Sections, it is the amount of the available oil extracted using hexane (Table 4.1) that is presented in terms of extraction ratio.

Table 4.1: Characteristics of solid samples and extracted lipids. The standard deviation of the mean is shown as calculated from three experimental repeats.

Sample	Moisture content (%) w/w	Average dry particle diameter (mm)	Oil content of dry samples (%) w/w	FFA content (%) w/w	HHV of dry samples (MJ/kg)	HHV of lipids (MJ/kg)	HHV of dry defatted samples (MJ/kg)	Ash content of dry SCG (%) w/w	Ash content of dry defatted SCG (%) w/w
ICG1	57.45 ± 1.04	0.66 ± 0.02	24.26 ± 1.62	24.24 ± 0.84	25.50 ± 0.30	38.94 ± 0.30	20.17 ± 0.69	-	-
ICG2	67.13 ± 1.75	-	25.16 ± 1.09	29.91 ± 2.8	25.86 ± 0.10	39.05 ± 0.15	20.58 ± 0.26	0.73 ± 0.03	1.32 ± 0.04
ICG3	69.9 ± 0.9	1.18 ± 0.06	30.45 ± 0.94	38.3 ± 0.67	-	39.35 ± 0.08	-	-	-
ICG4	63.3 ± 2.4	0.83 ± 0.03	25.84 ± 1.21	31.2 ± 1.37	-	39.24 ± 0.17	-	-	-
RCG1	64.2 ± 0.6	0.76 ± 0.08	14.84 ± 0.85	21.61 ± 0.78	-	38.91 ± 0.09	-	-	-
RCG2	54.7 ± 1.3	0.58 ± 0.03	13.38 ± 0.83	17.23 ± 1.04	-	39.01 ± 0.23	-	-	-
FRCG	3.3 ± 0.4	0.50 ± 0.01	12.33 ± 1.10	16.78 ± 1.32	-	38.93 ± 0.11	-	-	-
RCG3	62.15 ± 1.41	-	14.80 ± 1.36	15.46 ± 0.41	22.37 ± 0.07	38.95 ± 0.34	19.85 ± 0.11	1.02 ± 0.03	1.57 ± 0.03
RDCB	2.66 ± 0.37	-	11.41 ± 0.75	7.82 ± 0.21	21.34 ± 0.18	38.80 ± 0.16	19.60 ± 0.54	-	-

The measured SCG moisture contents presented in Table 4.1 are similar to those reported by Kondamudi et al. (2008) - (50-60% w/w), Haile (2014) - (57.6 % w/w), Gómez-De La Cruz et al. (2015) - (58.5 % w/w) and Abdullah and Bulent Koc (2013) - (67 % w/w) and higher than the moisture content found by Deligiannis et al. (2011) - (18-45 % w/w) and Ahangari and Sargolzaei (2013) - (48 % w/w). This variance in the SCG moisture content results can be likely attributed to the use of different coffee brewing procedures that can significantly increase the moisture content of SCG, along with the initial bound moisture of the coffee samples. However, Table 4.1 does not show a clear difference between industrial and retail SCG samples. In addition, all the samples presented in Table 4.1 have been stored and transported in bulk, except for the retail samples RCG2, RCG3 and the fresh roasted sample FRCG that were obtained from local coffee shops, something that could have potentially affected their moisture content.

The moisture content of the FRCG sample is significantly lower relative to the water residing in other samples, as it has not been used for coffee brewing and therefore has not been treated with water (Table 4.1). The water present in this sample can therefore be attributed to long storage and the hygroscopic nature of coffee grounds (Corrêa et al., 2016). The moisture content of the RDCB was found to be similar to values reported in previous studies (Franca et al., 2005; Franca and Oliveira, 2008; Oliveira et al., 2006). Further experimental results related to the removal of SCG residing moisture through thermal drying are presented in Section 4.2, while moisture removal through mechanical pressing is discussed in Section 7.1.

The average particle diameter of dried industrial samples used in this study ranged between 0.66 and 1.18 mm, while dried RCGs and FRCGs were found to have lower average particle size with diameters of 0.58 to 0.76 mm and 0.50 mm respectively (Table 4.1), with the values calculated as per Equation 3.5. The relatively higher mean particle size of ICGs compared to RCGs can possibly be attributed to particle compaction during the high pressure treatment of roasted grounds with water for instant coffee production. The values presented in Table 4.1 show that there is a correlation between increasing particle diameter and increasing moisture content for both the

instant and retail coffee groups. Figures 4.1 and 4.2 show the relationship between the two variables for all SCG samples of Table 4.1 and for ICG samples respectively, while linear regression lines have been added.

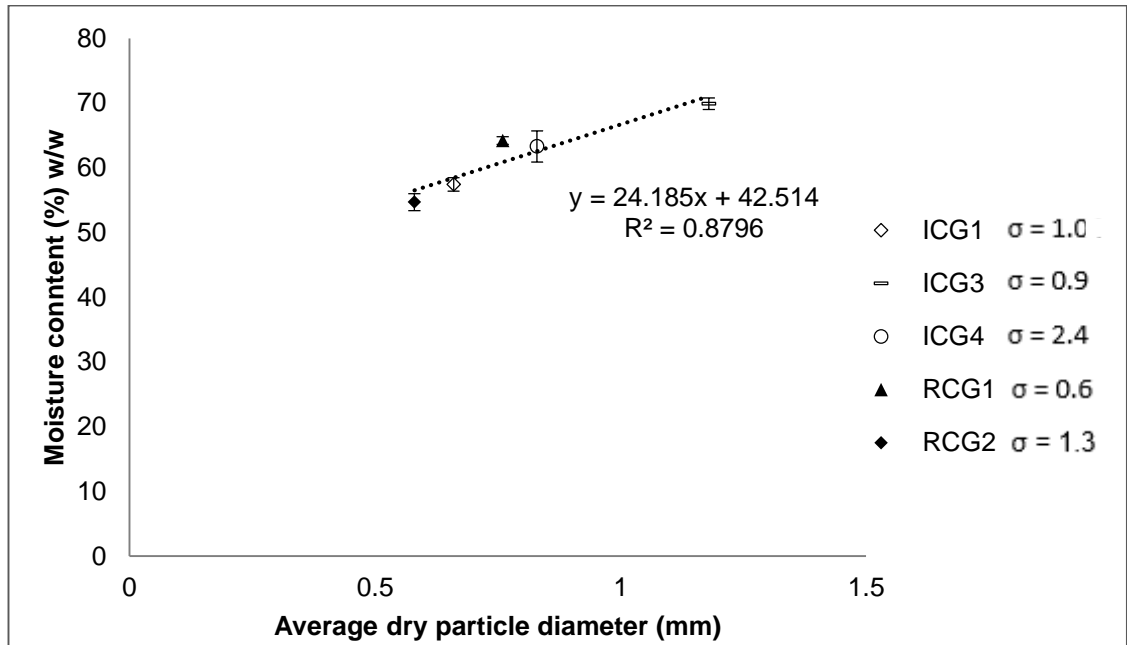


Figure 4.1: Relationship between moisture content and dried particle diameter of five SCG samples. Error bars show standard deviation (σ) calculated from three experimental repeats.

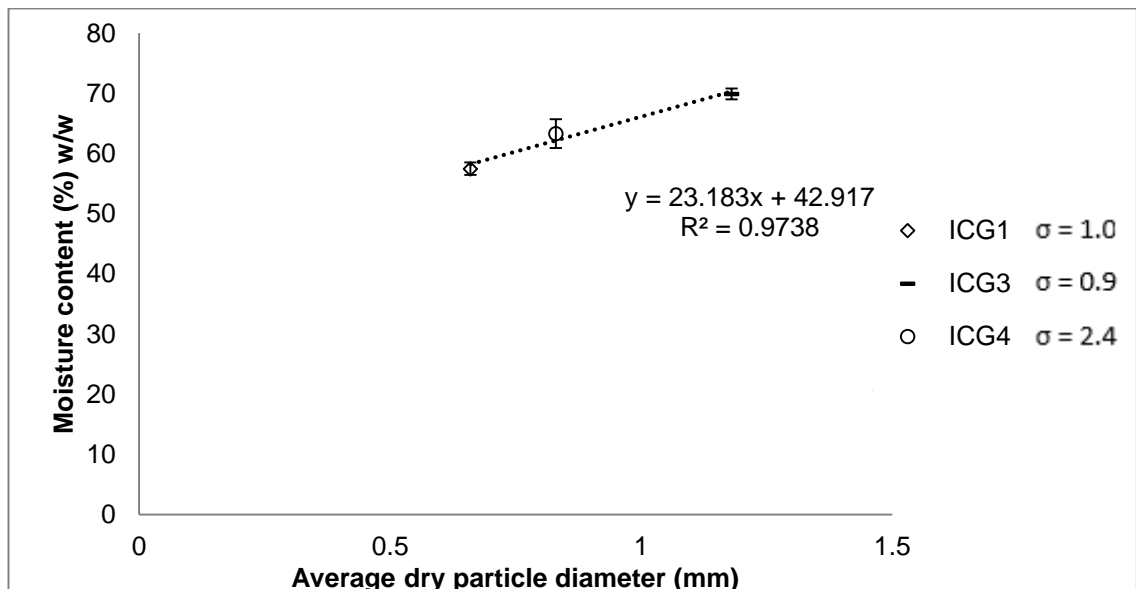


Figure 4.2: Relationship between moisture content and dried particle diameter of three ICG samples. Error bars show standard deviation (σ) calculated from three experimental repeats.

It can be seen in Figure 4.1 that plotting the two variables for five SCG samples revealed a linear relationship with a coefficient of determination (R^2) value of 0.88. The coefficient of determination measures the strength and direction of linear relationship between two variables on a scatterplot. ICG samples presented in Figure 4.2 also showed a linear relationship between moisture content and dried particle diameter with $R^2 = 0.97$. This can likely be attributed to larger interstitial gaps forming between particles of larger diameter that retain more unbound moisture during brewing. The particle size of SCG can also impact on drying rate as it modifies the distance the bound water has to diffuse (Reh et al., 2006).

The average particle diameter of FRCG increased after brewing and the larger size of RCG2 particles can possibly be explained by the compression and compaction of coffee grounds during the brewing process, leading some particles to compact together. The high average particle diameter of certain samples is an indication of a higher proportion of large particles, with a detailed particle size distribution presented in Section 5.1.2.1, while any relationship between particle diameter and oil yield is investigated in Section 5.1.2.2.

Furthermore, Table 4.1 shows that SCG from the instant coffee industry contain a significantly higher quantity of oil relative to the retail SCG examined. This observation is in agreement with the range of oil yields reported from previous studies regarding lipid extraction from instant SCG and retail/espresso SCG which are shown in Table 2.4. The higher lipid content of industrial samples can be possibly attributed to the processing required for production of instant coffee, and in particular the treatment of roasted grounds with water at high temperature (175 °C) and pressure which extracts water-soluble solid compounds and volatiles (Farah, 2012; Mussatto et al., 2011b), and consequently increases the mass portion of oil in the ICGs.

The oil contents of FRCG and RCG2 samples are quite similar suggesting that the coffee brewing procedure used, an Espresso machine, did not remove lipids from the grounds. Other studies have suggested that different brewing methods of roasted fresh coffee could lead to variation in the concentration of

unsaponifiables like diterpenes, which are found in small proportions in the coffee oil (Table 2.1), thus potentially altering the obtained crude oil yield (Al-Hamamre et al., 2012; Gross et al., 1997).

It can also be seen from Table 4.1 that the oil yield extracted from the roasted defective coffee beans (RDCB) was considerably lower than that obtained from SCG samples, but slightly higher than previously reported RDCB lipid yields which ranged between 9.2 and 10 % w/w (Oliveira et al., 2006). RDCB have been previously reported to have lower oil content relative to healthy roasted beans Oliveira et al. (2006).

The FFA content of lipids extracted from dried samples after 8 hours of extraction with hexane and a SCG-to-solvent ratio of 1:9 w/v was found to range between 24.24 and 38.3 % w/w for ICG-extracted lipids, and between 15.45 and 21.61 % w/w for RCG-extracted lipids (Table 4.1). The increased presence of FFAs in ICG oil compared to RCG oil can possibly be attributed to the treatment of grounds with water during instant coffee production that potentially resulted in hydrolysis of triglycerides into diglycerides and FFAs as per Equation 2.5. The relationship between SCG moisture content and oil FFA content of SCG samples presented in Table 4.1 is presented in Figure 4.3 where a linear regression line has been added.

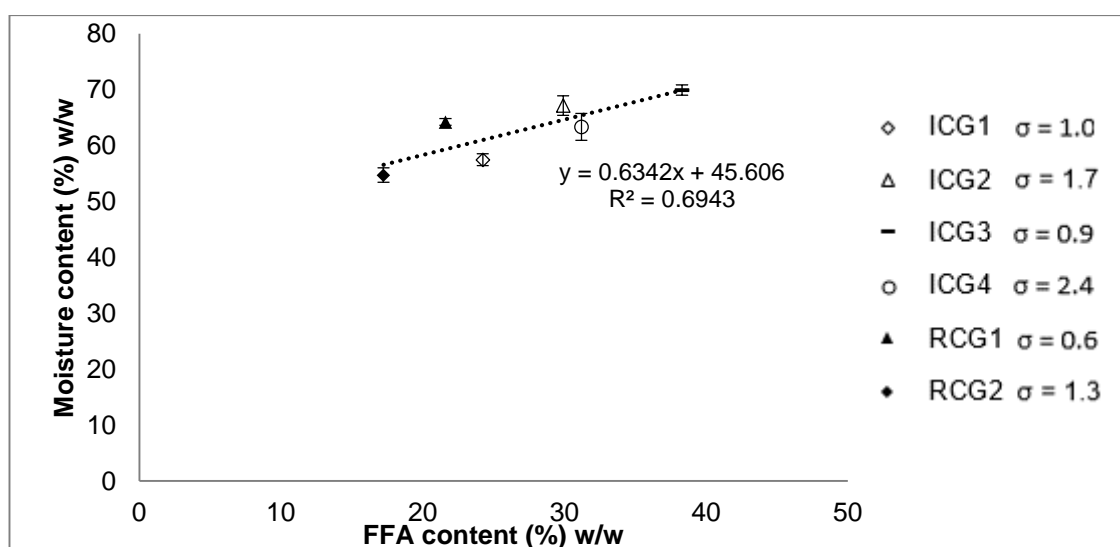


Figure 4.3: Relationship between moisture content and oil FFA content of SCG samples. Error bars show standard deviation (σ) calculated from three experimental repeats.

Figure 4.3 shows that there is a weak correlation between higher SCG moisture content and increased FFA content of the lipids with $R^2=0.69$. Furthermore, the duration of storage of the SGC samples with high residual moisture might have also affected the levels of FFAs in the coffee oil. In particular, Speer and Kölling-Speer (2006) found that prolonged storage of green coffee (up to 18 months), especially at conditions of relatively high temperature (25-40 °C) and moisture (11.8 % w/w) can result in increased concentration of FFAs in the oil.

The measured FFA values, especially those obtained from ICG samples, are relatively high when compared with levels of FFAs found in previous studies, which commonly used retail SCG and found FFA content of the oil ranging from ~3 to ~20 % w/w when hexane was the solvent used for Soxhlet extraction (Al-Hamamre et al., 2012; Berhe et al., 2013; Go et al., 2016; Haile, 2014; Kwon et al., 2013; Vardon et al., 2013), while values as low as 0.31 % w/w and as high as 59 % w/w have been reported by Deligiannis et al. (2011) and Caetano et al. (2012) respectively. Since the same general extraction method and solvent has been used in all these studies with slight differences in process duration and SCG-to-solvent ratio, the high degree of variation further suggests that there is significant effect of upstream processing, brewing method and storage conditions on the FFA levels of coffee oil, along with factors that determine the initial amount of FFAs in green coffee such as origin and coffee species (Franca and Oliveira, 2008).

Table 4.1 also shows that the FFA content of the oil extracted from RDCB was significantly lower than other lipid samples, as RDCB have not been treated with water either for production of instant coffee or for coffee brewing and therefore hydrolysis of triglycerides has not taken place. In addition, the FFA content of oil extracted from FRCGs was found to be slightly lower compared to that obtained from the same sample after brewing process in an Espresso machine (RCG2), a finding which supports the theory that treatment with water, in this case for coffee brewing, increases the FFA content of lipids by hydrolyzing triglycerides as per Equation 2.5.

Finally, Figure 4.4 shows a comparison between the oil content of all SCG samples presented in Table 4.1 and the respective FFA content of the oil extracted from those samples, while a linear regression line has been added.

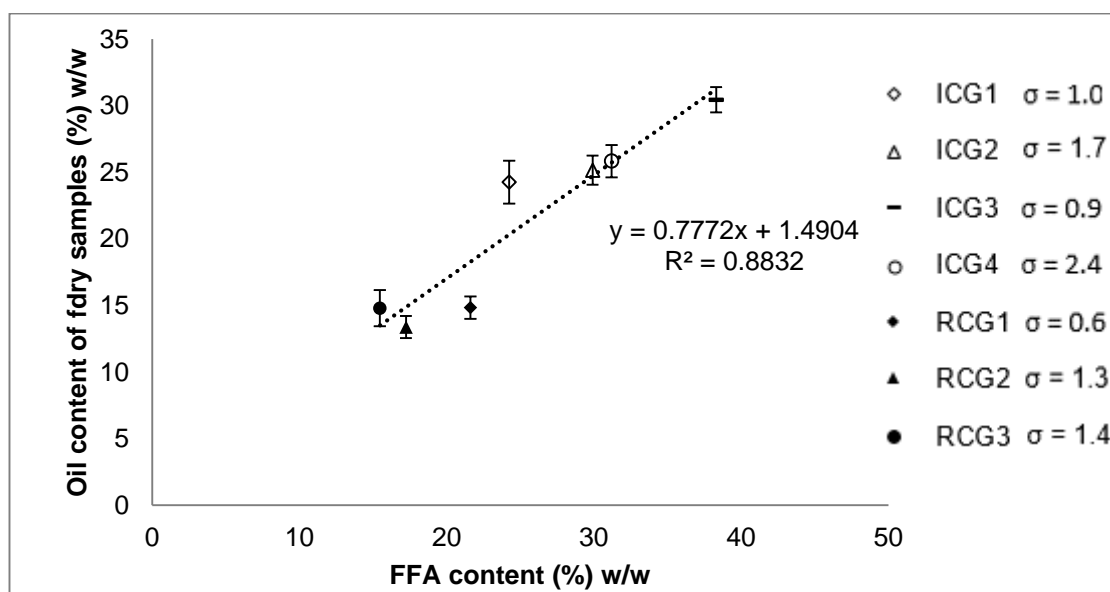


Figure 4.4: Relationship between oil content of dry SCG samples and FFA content of the oil. Error bars shown represent standard deviation (σ) calculated from three experimental repeats.

It can be seen in Figure 4.4 that there is a weak correlation between increasing oil content and higher FFA content, with $R^2=0.88$.

Moreover, Table 4.1 shows the HHVs of the dried ICG samples to be slightly higher than that of dried RCG and RDCB, something that can likely be attributed to the lower lipid content of these samples, while dried defatted SCG grounds were found to have reduced energy contents because of the removal of energy-dense lipids. The HHVs of the extracted lipids were found to be similar for all samples ranging between 38.80 MJ/kg and 39.35 MJ/kg. The HHV values measured for dried SCG, defatted SCG and lipids fall within the range encountered in the literature (Table 2.3, Table 2.8). The variance in the energy content of SCG lipids extracted from different sources can be in part attributed to the different fatty acid profile of the oils and particularly to the varying degree of unsaturation (Moussa et al., 2014).

The ash contents of selected ICG and RCG raw and defatted samples are also presented in Table 4.1, and the values obtained from defatted SCG were higher than those measured prior to the extraction of lipids due to the increase of ash proportion in the grounds caused by the removal of oils. The measured ash content values are similar to those found in previous studies (Table 2.2, Table 2.8).

4.2 SCG drying characteristics

Drying experiments were conducted with ICG1 samples of various thicknesses at temperatures of 100 and 200 °C according to the method described in Section 3.2.1 so as to investigate the effect of sample thickness and drying temperature on the moisture removal efficiency. Figure 4.5 shows the relationship between moisture content and duration of drying with varying ICG1 sample thickness and drying temperature, while the standard deviations shown represent the reproducibility of the obtained results.

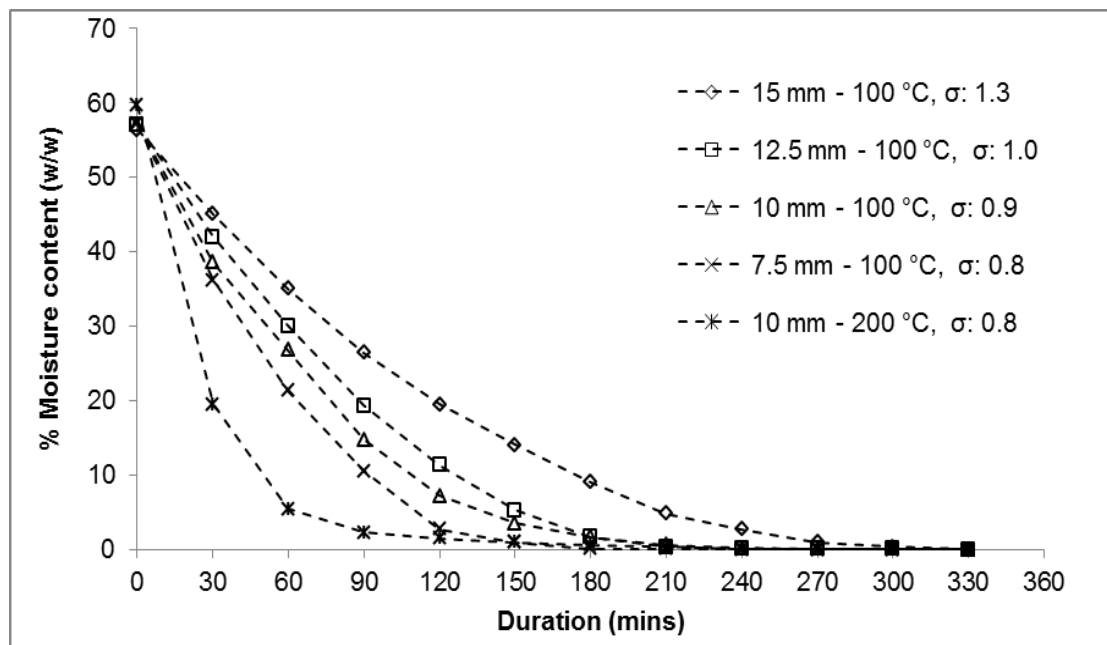


Figure 4.5: Moisture removal from ICG1 over time with varying sample thickness (7.5-15 mm) and drying temperature (100-200 °C). The standard deviations (σ) shown were calculated from 3 experimental repeats.

Figure 4.5 shows that a decrease of the sample thickness led to higher rates of moisture removal and a significant decrease of the time required to remove the bulk of the residing water. Furthermore, drying at 200 °C considerably

accelerated the process of removing water from SCCs relative to a drying temperature of 100 °C, when samples with the same thickness were used. In particular, 90 % of the total moisture present was removed after 60 minutes of drying at 200 °C, while approximately 150 minutes were required for the same level of water reduction at 100 °C.

Therefore, increasing the drying temperature and reducing the sample thickness both decreased the duration required for moisture removal from the SCG, an observation which is in agreement with the study conducted by Gómez-De La Cruz et al. (2015). It is tentatively suggested that the high drying ratios observed during the initial stages of the process can be attributed to removal of unbound moisture, which is present between individual molecules and is therefore easier to be removed, while the subsequent decrease of drying rate that prolonged the drying duration was possibly due to the removal of bound moisture held within the coffee particles.

Figure 4.6 shows the percentage of moisture relative to the initial moisture content over drying time at 100 °C for SCG samples with a constant sample thickness of 10 mm.

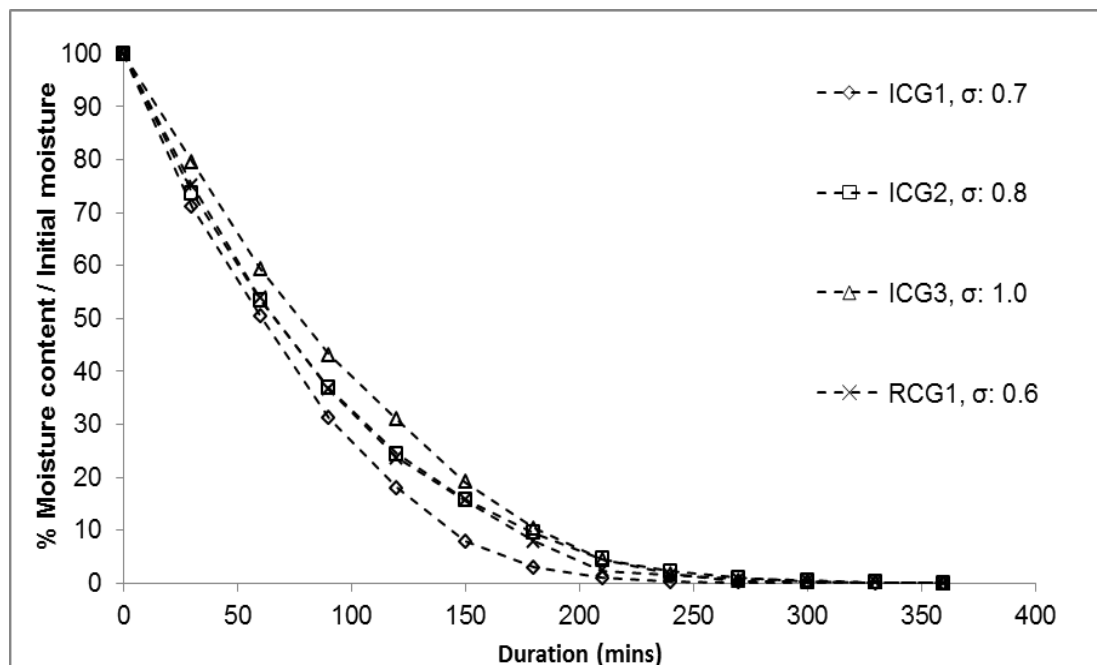


Figure 4.6: Moisture removal over time with different SCG samples. The standard deviations (σ) shown were calculated from 3 experimental repeats.

It can be seen in Figure 4.6 that all samples show similar drying rates, with moisture content approaching zero after 4 h. It is interesting to note that the required drying time for complete water removal is not significantly affected by the different initial moisture contents of the samples or their mean particle size (Table 4.1).

4.3 Conclusions

The oil content of the different RCG samples ranged from 13.4 to 14.8 % w/w, while ICGs contained significantly more oil, between 24.3 and 30.4 % w/w, due to the extraction of water soluble compounds during the processing for production of instant coffee. Coffee grounds from the same source were found to have similar dry weight lipid contents before and after brewing in an espresso machine, however, brewing resulted in an increase of the FFA content of residual oil due to hydrolysis of triglycerides in the presence of water, while the slight increase of the average dry particle diameter and the less homogeneous particle distribution can be possibly attributed to the pressurization of the grounds during brewing in the espresso machine.

The apparent moisture content of various SCG samples was found to range between 54 and 70 % w/w, and a relationship between SCG initial moisture content and dry particle size distribution was observed, with samples containing particles of large average diameter tending to possess higher moisture content. A correlation between higher SCG moisture content and increased levels of FFAs of the corresponding lipids was observed potentially owing to enhanced hydrolysis of triglycerides at higher moisture SCG contents, while FFAs were found to increase as a percentage of the extracted oil as the total oil yield increased. Finally, the duration required for drying of SCG below 2 % w/w was decreased by ~120 minutes when a cake thickness of 10 mm and a drying temperature of 200 °C were selected as opposed to cake thickness of 15 mm and 100 °C drying temperature.

The characterization of various SCG samples in terms of oil, moisture, FFA and energy content and particle size is followed by a study which focuses on the effect of solvent extraction factors on SCG oil yield and quality, while both

laboratory and pilot plant solvent extraction were investigated at conditions of atmospheric pressure.

5. Effect of solvent extraction parameters and SCG properties on the efficiency of oil recovery

This chapter presents the results obtained through Soxhlet and pilot plant scale solvent extractions regarding the impact of extraction duration, SCG-to-solvent ratio, solvent selection, SCG particle size and moisture content on the efficiency of the lipid recovery from SCG.

5.1 Soxhlet solvent extraction

5.1.1 Effect of process duration and SCG-to-solvent ratio on lipid extraction efficiency

This section investigates the effect of solvent extraction parameters including duration, and SCG-to-solvent ratio on the efficiency of lipid recovery from SCG through the Soxhlet method (Section 3.2.3.1). Figure 5.1 shows the oil yields obtained from ICG1 on a dry weight basis with varying Soxhlet duration and a constant dry SCG-to-hexane ratio of 1:9.0 w/v, while a logarithmic best fit line has been added.

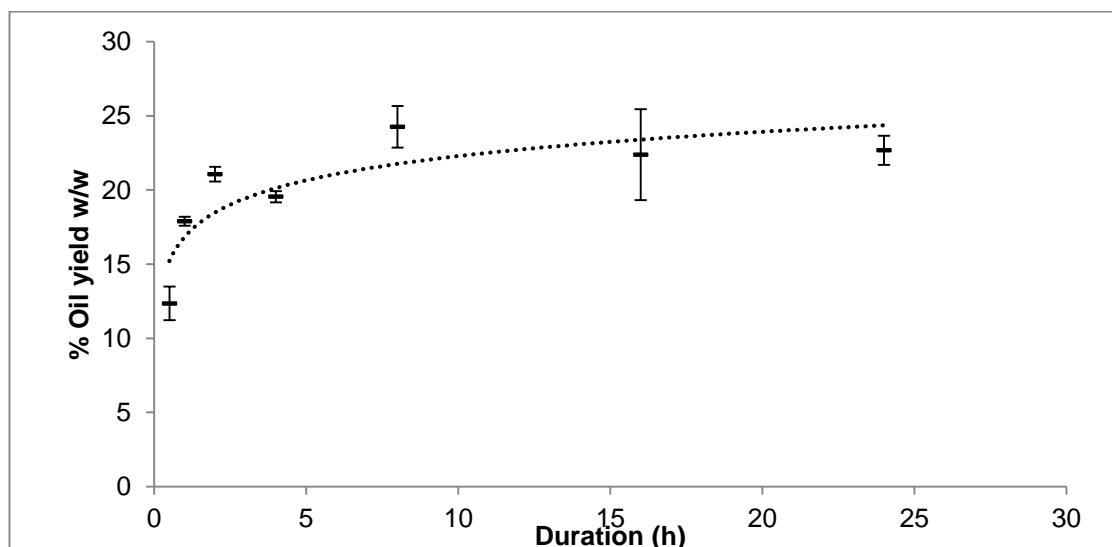


Figure 5.1: Oil yields per mass of dry ICG1 weight achieved at different Soxhlet extraction durations (0.5 to 24 hours). Error bars show the standard deviation of the mean calculated by three experimental repeats at each timing setting.

Figure 5.1 shows that the highest oil yield was achieved at 8 hours of solvent extraction, with a subsequent slight decrease of oil yields obtained at durations greater than 8 h. This is in agreement with Picard et al. (1984) and Sayyar et al. (2009) who investigated oil extraction via Soxhlet from roasted Robusta grounds and jatropha seeds respectively and found a duration of 8 hours to be ideal for oil recovery. Figure 5.1 also shows that the extracted oil yield reduces considerably when the duration of Soxhlet extraction is less than 2 hours. This is likely because the short duration of extraction does not allow sufficient time for the recirculating solvent to extract the total available oil from the SCG, and is in agreement with previous studies investigating the extraction of lipids from other oilseeds through Soxhlet which suggested that durations longer than 3.5 hours result in more efficient extractions (Kerbala University, 2010; Lawson et al., 2010).

Figure 5.2 shows the FFA content of ICG1 oil samples that were obtained at different durations of Soxhlet extraction with hexane at a SCG-to-solvent ratio of 1:9.0 w/v measured according to the method described in Section 3.2.6. A linear regression line has also been added.

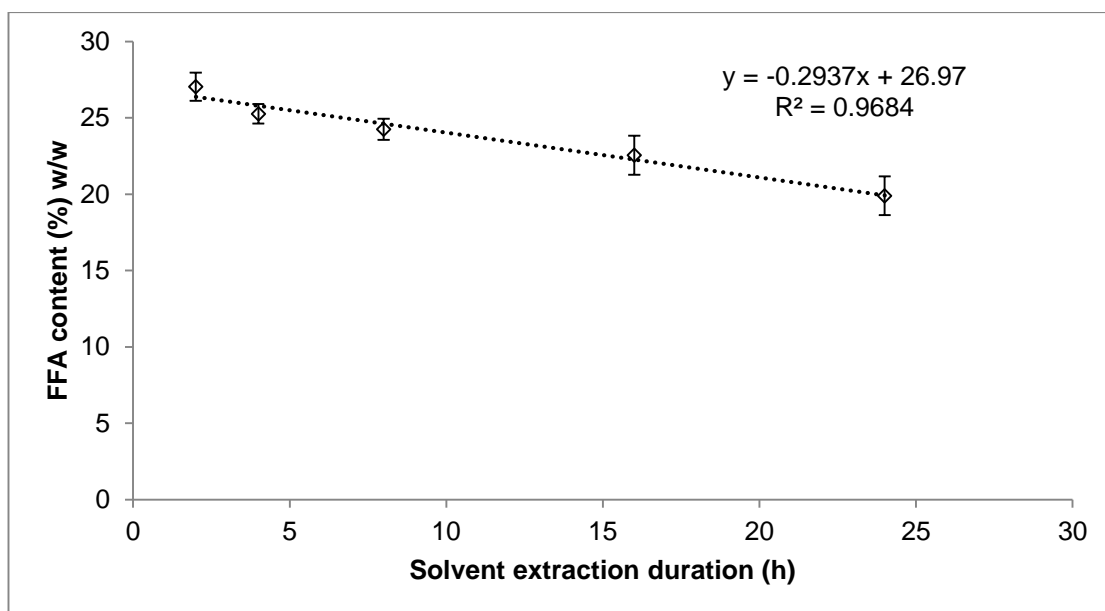


Figure 5.2: Correlation of the % w/w FFA content of extracted coffee oil with the duration of solvent extraction (2-24 h). The error bars show the standard deviation calculated from three titration measurements with oil samples extracted at different durations.

Figure 5.2 shows that the FFA content of the extracted oil decreases with increasing duration of solvent extraction, with a R^2 value of 0.97. It is suggested that FFAs, as smaller molecules than triglycerides or diglycerides may have been preferentially desorbed from the SCG matrix before these larger molecules due to their lower Van der Waals forces, and consequently the fraction of these was higher when the duration of extraction was short. However, as the duration of extraction increased, more triglycerides were recovered and therefore the percentage of FFAs in the collected oil decreased.

The effect of the dry ICG1 to solvent ratio on the oil yield was examined at a constant Soxhlet duration of 8 hours with hexane. Figure 5.3 shows the relationship between SCG-to-hexane ratio and obtained ICG1 oil yield, while a logarithmic best fit line has been added.

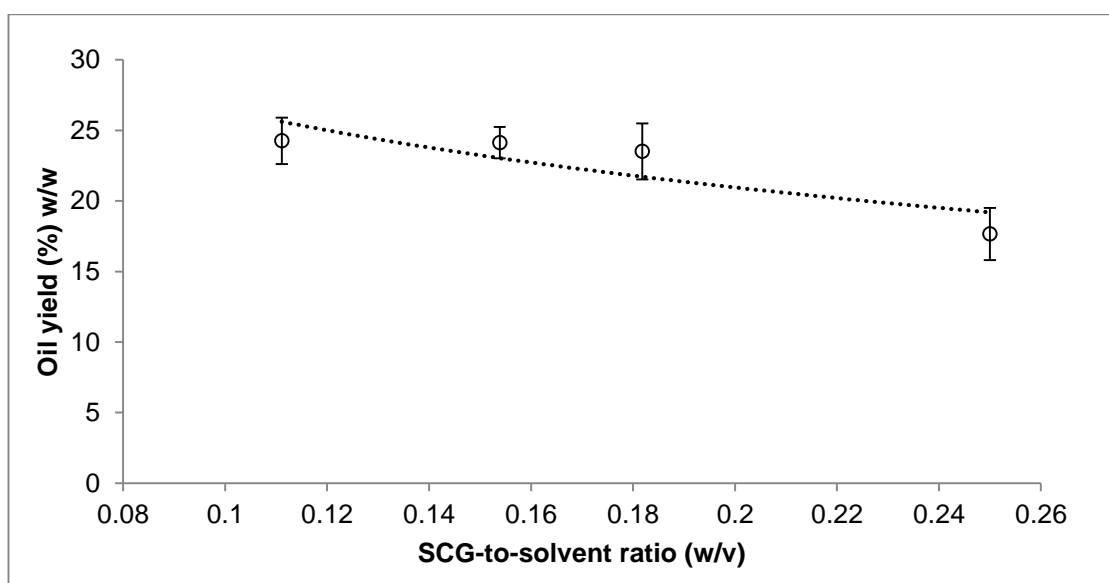


Figure 5.3: ICG1 oil yield achieved at varying SCG-to-solvent ratios. The error bars show the standard deviation calculated from three experimental repeats at each SCG-to-solvent ratio setting.

It can be seen in Figure 5.3 that the variation of the SCG-to-solvent ratio, which ranged between 1:9.0 and 1:4.0 w/v, or 0.11 and 0.25 w/v as shown in the figure, caused a change in the obtained oil yield between approximately 24.6 % w/w and 17.6 % w/w, with a tendency for higher yield at the lower SCG-to-solvent ratios. The same relationship between decreasing seed to

solvent ratio and increasing oil yield was observed by Pichai and Krit (2015) and Sayyar et al. (2009) during oil extraction from SCG and jatropha seeds respectively. The slight difference in oil yield obtained at the three lower SCG-to-solvent ratios suggests that oil extraction from dry SCG can be successfully performed with a ratio of 1:5.5 w/v (or 0.18), with further increase of solvent quantity used only resulting in slightly improved lipid yields. The decrease of obtained oil yield with increase of SCG-to-solvent ratio above 1:5.5 w/v can be attributed to saturation of the solvent.

5.1.2 Effect of SCG particle diameter and moisture content on lipid extraction efficiency

5.1.2.1 Particle size determination

The coffee particles diameter distribution of SCG and FRCGs was calculated through the use of various test sieves as described in Section 3.2.2. Figure 5.4 shows the dry particle diameter distribution of various coffee samples.

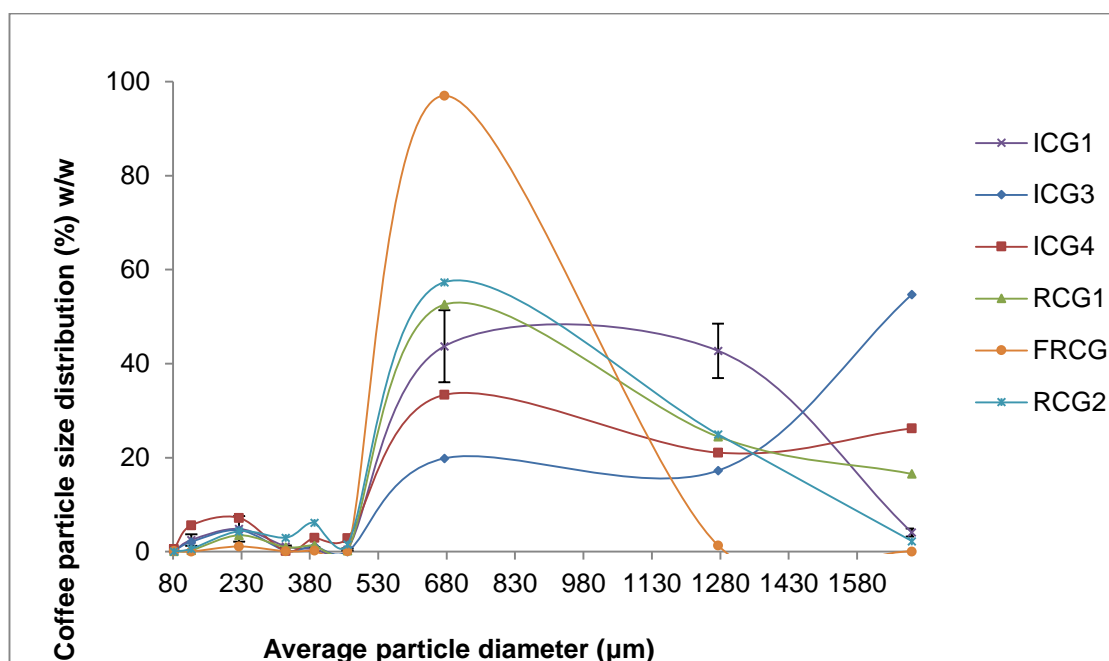


Figure 5.4: Particle diameter distribution of various coffee samples after complete moisture removal. The error bars shown represent the standard deviation of the mean calculated from 3 sizing repeats with the available sieves.

Figure 5.4 shows that the different coffee samples exhibit significant variation in particle diameter distribution; this can possibly be attributed to the grinding process of the roasted grounds, along with the different methods that they may have been subjected to during upstream processing and/or brewing. Most of the SCG samples have a particle diameter less than 1700 μm and more than 500 μm , while ICG3 has the largest fraction of particles (57.41 % w/w) of diameter greater than 1700 μm .

Figure 5.4 also shows that 97 % w/w of the FRCG sample has a particle diameter between 500 μm and 850 μm , and is therefore the most homogeneous in terms of particle size distribution of all the coffee samples. This low variance of particle diameter in FRCG can be likely attributed to the coffee machine grinder that reduces the roasted coffee beans to a predetermined size depending on the method by which they are to be brewed. The particle size distribution of the same coffee grounds following brewing with hot water (RCG2) is significantly different, with 57 % w/w of the grounds now within a size of 500-850 μm , while 27 % w/w had a diameter greater than 850 μm and 15.5 % w/w a diameter less than 500 μm . These findings suggest that brewing process in an Espresso machine results in compression of some coffee particles into larger particle blocs, while fragmenting and reducing the size of others.

5.1.2.2 Effect of SCG particle diameter on solvent extraction efficiency

Various size fractions of dry ICG1, ICG3, ICG4 and RCG1 samples were used at a fixed SCG-to-hexane ratio of 1:9.0 w/v, and extraction duration of 8 h. Each of the SCG samples was split into fractions of the following particle diameter: <0.5 mm, 0.5 mm < d < 0.85 mm and d > 1.7 mm. Figure 5.5 presents the oil yield achieved from different particle size fractions of each SCG sample.

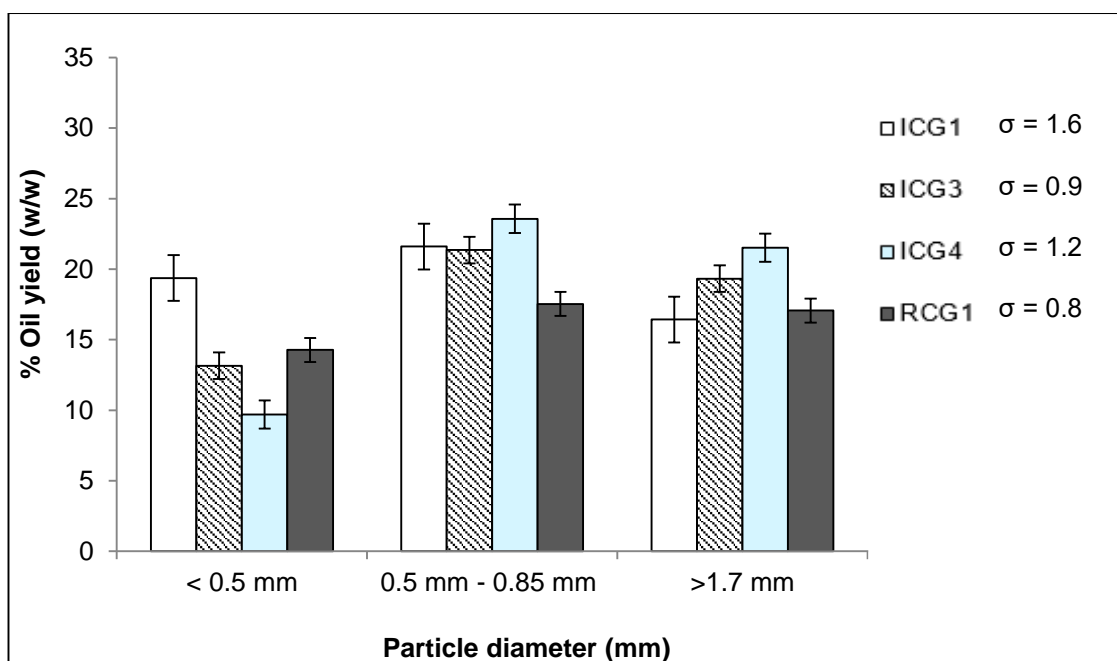


Figure 5.5: Oil yield of various SCG samples when different particle size fractions were used. The error bars represent the standard deviation (σ) of the mean calculated from three experimental repeats.

Figure 5.5 shows that an intermediate particle diameter between 0.5 and 0.85 mm led to higher oil recoveries from all the SCG samples. This is in agreement with (Sayyar et al., 2009) who achieved the highest oil recoveries from jatropha seeds with particle size meal between 0.5 and 0.75 mm. With the exception of ICG1, solvent extraction from SCG particles of diameter larger than 1.7 mm resulted in higher oil recoveries relative to trials with SCG particles of diameter smaller than 0.5 mm, something that can possibly be attributed to the compaction and agglomeration of the fine particles that result in reduction of the surface area. This is in contrast with previous studies on the solvent extraction of lipids from oilseeds which suggested that a small seed particle size of 0.2–0.3 mm is beneficial for the extraction efficiency of the process (Akoh, 2005; Folstar et al., 1976; Kerbala University, 2010; Lajara, 1990; Lawson et al., 2010; Varzakas and Tzia, 2015). Nevertheless, for all SCG samples, except RCG1, higher oil yields were obtained without sizing (the average particle diameter of the different SCG samples can be found in Table 4.1), suggesting that a mix of different size particles facilitates the solvent and oil flow, therefore leading to higher oil recoveries.

5.1.2.3 Effect of SCG moisture content on solvent extraction efficiency

The effect of various ICG1 moisture levels on the crude extract yield was examined with hexane at a SCG-to-solvent ratio of 1:9.0 w/v, while three repeats were performed for every experiment. Figure 5.6 shows the relationship found between moisture content and achieved yield on a dry weight basis, while the various moisture content levels of the samples were achieved with thermal drying based on the method described in Section 3.2.1.

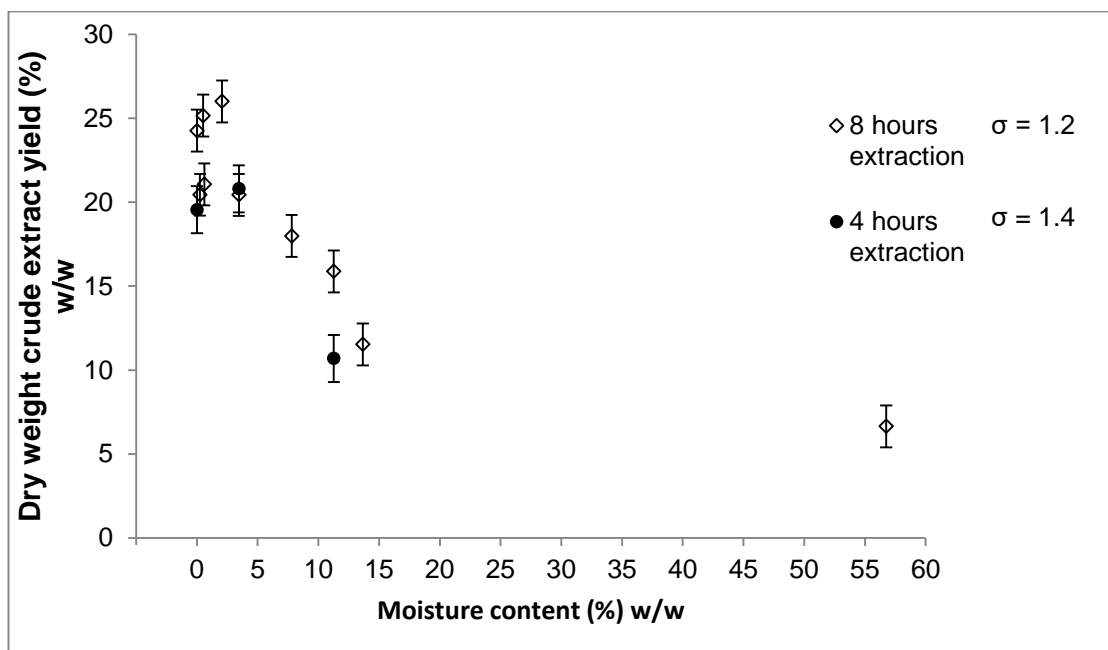


Figure 5.6: Crude extract yields on a dry weight basis versus the respective moisture content for 4 and 8 hours Soxhlet extractions with hexane. The error bars represent standard deviation (σ) calculated from three experimental repeats at each timing setting.

Figure 5.6 shows that a moisture content of approximately 2 % w/w did not affect the solvent extraction process negatively and was actually beneficial as it resulted in a slightly higher crude extract yield relative to those obtained from SCG samples with lower moisture contents. Moisture contents greater than 2 % w/w resulted in lower crude extract yields, however a SCG sample with a moisture level of roughly 3.5 % w/w yielded ~20 % w/w at both the durations of 4 and 8 hours, which is not a significant drop from the peak yield of ~25 % w/w.

The obtained results are consistent with previous studies that reported SCG oil yield decrease with increasing moisture presence when hexane was the solvent used (Caetano et al., 2014; Najdanovic-Visak et al., 2017). However, studies considering other oilseeds including soybeans found optimum oilseed moisture contents for solvent extraction between 9-11 % w/w, highlighting the differences in extraction characteristics between SCG and other feedstocks (KerbalaUniversity, 2010; Lajara, 1990; Lawson et al., 2010).

The effect of moisture on the extraction of crude extracts from SCG was also investigated with ethanol at a SCG-to-solvent ratio of 1:9.0 w/v for a constant duration of 8 hours. Figure 5.7 shows the dry weight crude extract yield extracted from ICG1 through Soxhlet with ethanol against the moisture content of the sample.

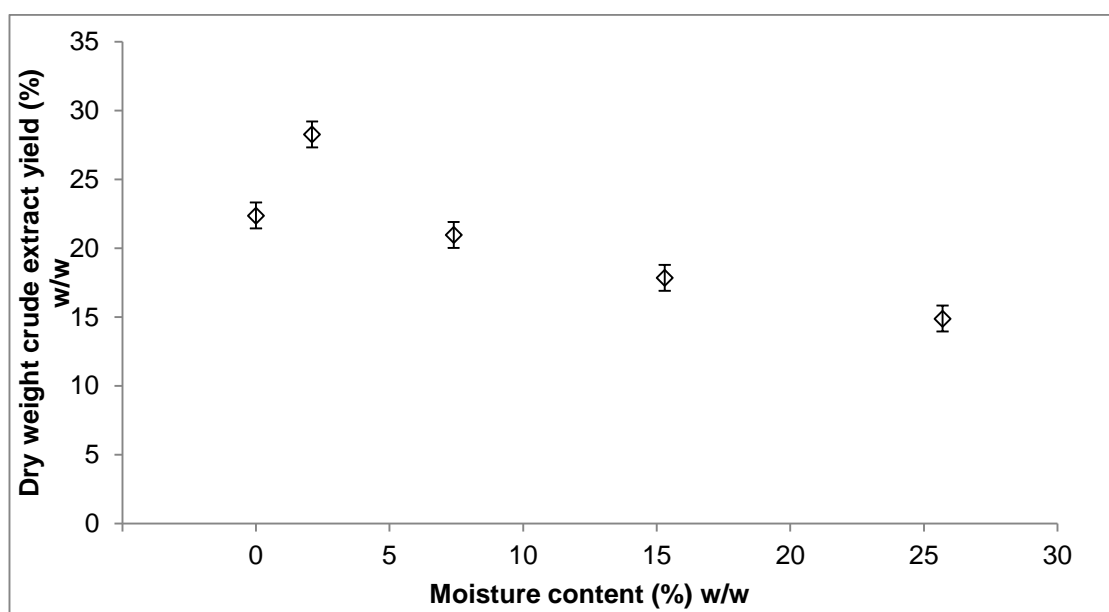


Figure 5.7: Crude extract yields on a dry weight basis versus the respective moisture content for 8 hours Soxhlet extractions with ethanol. Error bars represent standard deviation ($\sigma=0.9$) calculated from three experimental repeats.

Figure 5.7 shows that a moisture content of ~2 % w/w was beneficial for extraction with ethanol, similar to experiments performed with hexane (Figure 5.6), while the relatively high crude extract yield (28.3 % w/w) obtained at this moisture content can be potentially attributed to enhanced extraction of polar

compounds (Johnson and Lusas, 1983). Increase of moisture content above this limit resulted in decreased yields, however, a comparison with the yields presented in Figure 5.6 indicates that ethanol was less sensitive to the presence of water relative to hydrophobic hexane which is insoluble in water. In general, the presence of water in the feedstock is known to seal the micropores which contain the lipids and therefore prevent their extraction by not allowing contact with the solvent, while it is also responsible for emulsion formation (Matthäus and Brühl, 2001; Richter et al., 1996).

5.1.3 Effect of solvent selection on lipid extraction efficiency

The effect of solvent selection on the efficiency of Soxhlet extraction of crude extracts from dry SCG was investigated and all the experiments were performed with the ICG1 sample except for the heptane trials, where the RCG3 sample was used. Figure 5.8 shows the crude extract extraction ratio obtained against the polarity of the solvent used, expressed by its E_T^N polarity parameter measured at 25 °C (Table 3.1), while Figure 5.9 shows the extraction ratios achieved with different solvents versus the solvent boiling point.

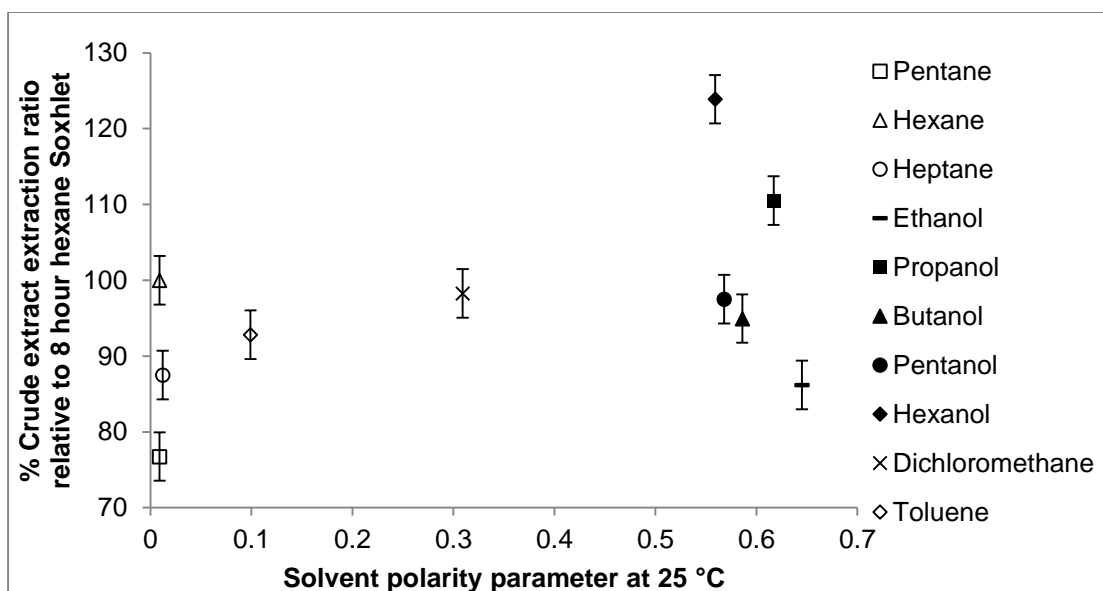


Figure 5.8: Crude extract extraction ratio versus the E_T^N polarity parameter of the solvent used. Error bars show the standard deviation ($\sigma=3.2$) calculated from three experimental repeats.

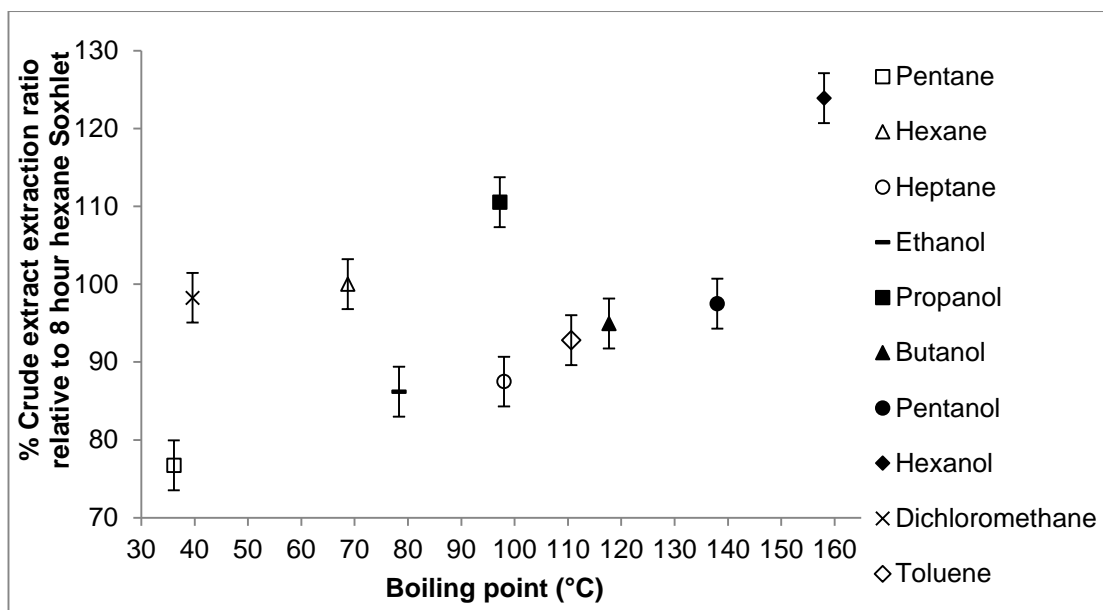


Figure 5.9: Crude extract extraction ratios extracted versus solvent boiling point. Error bars show the standard deviation ($\sigma=3.2$) calculated from three experimental repeats.

Figure 5.8 shows that the extraction ratios obtained with non-polar solvents range from 76.7 to 123.8 % w/w relative to 8 hour Soxhlet oil yield with hexane, with pentane extracting the lowest crude extract quantity and hexanol the highest. The polar alcohols resulted in extraction ratios between 86.18 and 110.52 % w/w with ethanol achieving the lowest extraction ratio and propanol the highest. A weak trend of decreasing extraction ratio with increasing E_T^N polarity parameter of alcohols, and therefore increasing solvent polarity, can be observed in Figure 5.8, especially if propanol is excluded.

Figure 5.9 shows that the highest crude extract extraction ratio was achieved with the solvent of highest boiling point (hexanol), and the lowest with the lowest boiling point solvent (pentane). This suggests that there might be a weak relationship between increasing solvent boiling point and higher extraction ratio. High temperatures (100-200 °C) are known to cause the loosening of the coffee cell wall structure and increase the solubility of components like arabinogalactans and mannans (Campos-Vega et al., 2015; Quinn, 1988). Therefore, it is suggested that the high extraction temperature achieved with solvents like hexanol may have decreased the selectivity of the process, and resulted in the extraction of polar molecules such as cell wall

components and bound lipids (Campos-Vega et al., 2015; Zuurro and Lavecchia, 2012).

It is interesting to note that with regards to any possible effect of the solvent molecular weight on the extraction ratio, while the highest extraction ratio was obtained by hexanol, the solvent of highest molecular weight (Table 3.1), no clear relationship between molecular weight and solvent extraction efficiency was found within the range investigated, and any effects would be secondary to polarity. This suggests that the penetration of the solvent molecules into the SCG was not limited by the solvent molecular weight and hence molecule size. This can be likely attributed to the high temperatures used in upstream coffee processing (drying after harvesting and roasting) that deform the structure of cell walls and change porosity, thus leading to the formation of large micropores and resulting in loss of selective permeability (Aguilera and Stanley, 1999; Borém et al., 2008; Quinn, 1988). Such conditions also cause the fusion of oil bodies that migrate to the bean surface (Aguilera and Stanley, 1999; Borém et al., 2008; Schenker et al., 2000). The influence of molecular weight therefore appears to be indirect through its relation with the boiling point which dictates the temperature of Soxhlet extraction. It is likely therefore, that other physical properties that increase with molecular mass, such as surface tension and dynamic viscosity are also secondary in importance to the extraction.

Other studies have also examined the effect of different solvents on oil extraction efficiency through Soxhlet extraction, and these are shown in Table 5.1 along with the average crude extract yields achieved in this study. Only results from solvents that have also been used in the present research are shown, and actual oil yields from all studies are presented instead of extraction ratios for comparison purposes. The SCG-to-solvent ratios used by Al-Hamamre et al. (2012), Caetano et al. (2012) and Kondamudi et al. (2008) were 1:3 w/v, 1:20 w/v and 1:4.2 w/v respectively.

Table 5.1: Comparison between the yields achieved from the present study and other researchers.

Solvent	ICG1	RCG3	(Al-Hamamre et al., 2012)	(Kondamudi et al., 2008)	(Caetano et al., 2012)
Non-polar					
Pentane	18.61	-	15.18	-	-
Hexane	24.26	14.80	15.28	13.4	16
Heptane	-	13.14	-	-	18
Toluene	22.51	-	14.32	-	-
Polar					
Dichloromethane	23.83	-	-	15.2	-
Ethanol	20.90	-	12.92	-	16

In general, Table 5.1 shows that previous studies reported oil yields of a magnitude similar to RCG3, a fact that can likely be attributed to the source of coffee samples. Al-Hamamre et al. (2012) similarly to the present study achieved one of the lowest yields with ethanol and attributed it to the formation of complex formations between fatty acids and carbohydrate breakdown components that inhibit the extraction process. Kondamudi et al. (2008) found that use of dichloromethane resulted in a slightly higher crude oil yield than hexane with a possible explanation being the drying process, which was carried out at a temperature of 50 °C and may potentially have led to incomplete moisture removal. Therefore the slightly polar character of dichloromethane may have been responsible for the slight yield increase relative to that obtained with hexane, as polar solvents can improve the extraction rate from wet samples (Johnson and Lusas, 1983). Caetano et al. (2012) achieved a higher oil yield with heptane compared to hexane and ethanol extractions, however, extractions with the various solvents were conducted for different and not specified durations.

The FFA content of the crude extract samples obtained through Soxhlet solvent extraction with different solvents was determined according to the

method described in Section 3.2.6. Figure 5.10 shows the weight percentage of each sample that corresponds to FFAs, against the polarity of the solvent used, as expressed through its E_T^N polarity parameter measured at 25 °C (Table 3.1), while a linear line of best fit has also been added. All the samples were extracted from the ICG1 sample.

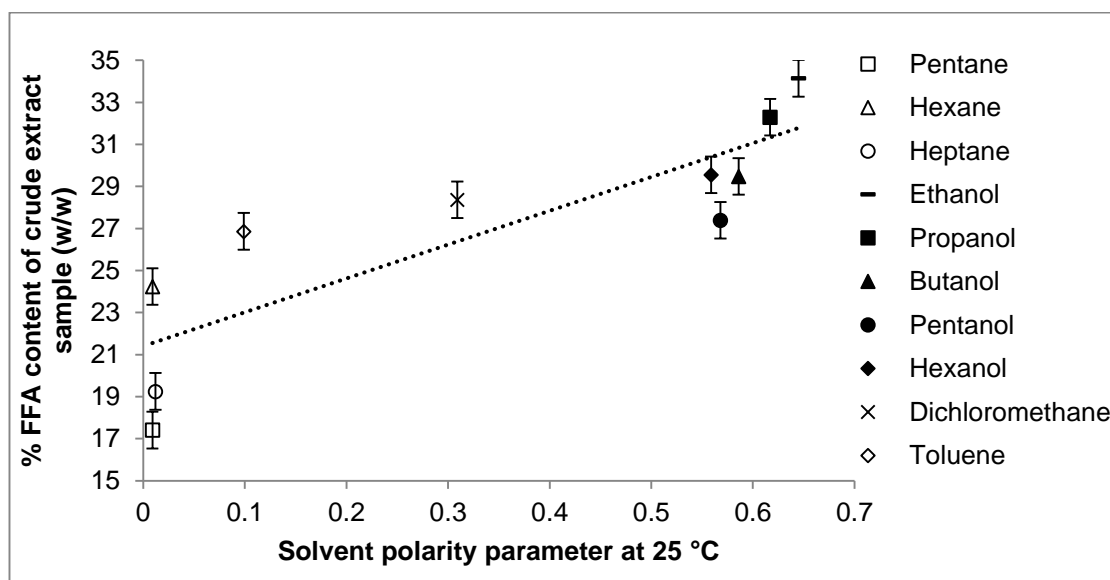


Figure 5.10: % w/w FFA content of crude extract samples extracted with various solvents, versus E_T^N solvent polarity parameter. Error bars show the standard deviation ($\sigma=0.9$) calculated from a total of 40 experiments.

Notwithstanding the fact that polarity is subject to temperature change (Ahmad and Rehana, 1980; Bolotnikov and Neruchev, 2004; Kang et al., 2011), it is apparent in Figure 5.10 that there is a trend of increasing FFA content of the recovered crude extract with increasing E_T^N solvent polarity parameter, and thus solvent polarity. This is in agreement with previous studies which suggest that polar solvents tend to extract higher amounts of FFAs (Al-Hamamre et al., 2012; Johnson and Lusas, 1983; Kondamudi et al., 2008). Other compounds of acidic character, such as phosphatidic acid and carbohydrate derived acids, may have been extracted due to the high polarity of some solvents (Harwood et al., 1998; Mercier et al., 1980).

Furthermore, the high temperature applied when solvents with high boiling points were used may have resulted in thermal degradation of lipids, possibly an effect of temperature enhanced triglyceride hydrolysis with any residual

bound water held within the grounds after drying (Fernando and Hewavitharana, 1990), thus leading to formation of FFAs. Therefore, the strong acidic character of some samples can be possibly attributed to a synergistic effect of polarity and extraction temperature that resulted in preferential extraction of FFAs when polar solvents were used.

Figure 5.11 shows the linear relationship between the crude extract % FFA content measured through titration and that estimated through Nuclear magnetic resonance (NMR) spectroscopy as described in Appendix H, for various solvents.

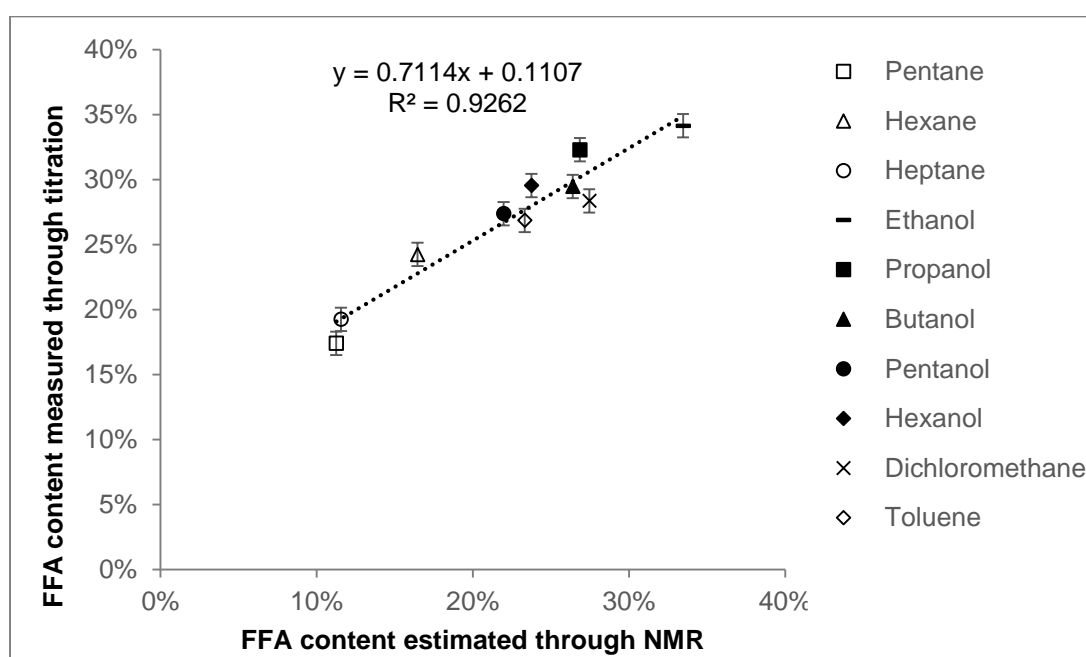


Figure 5.11: Relationship between crude extract FFA content obtained through titration and NMR analysis. The error bars represent the standard deviation of the mean ($\sigma=0.9$) for titration results calculated from a total of 40 experiments.

Figure 5.11 shows that notwithstanding sources of error in both methods, comparison of the results obtained by NMR to the conventional titrimetric method suggests that both methods yield comparable results, while the two result sets have a strong linear relationship ($R^2=0.92$). Nevertheless, the NMR method appears to give a systematically lower estimation of FFA content.

The composition of the crude extract samples obtained with different solvents through Soxhlet was also determined with the NMR method (Appendix H), and Figure 5.12 shows the estimated percentage of the oil structural compounds by mass.

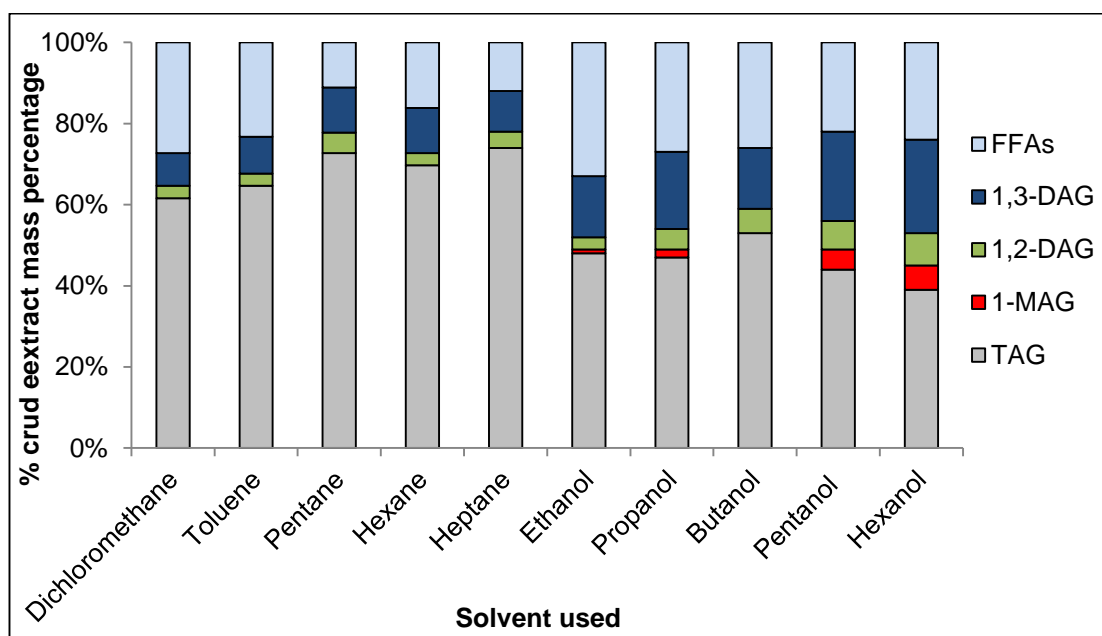


Figure 5.12: Composition of oil samples obtained from Soxhlet extraction using different extraction solvents, using ^1H NMR analysis.

It can be seen in Figure 5.12 that triglycerides and FFAs were the main components of each sample, and that the proportions of these varied significantly between samples extracted with different solvents. The comparative level of mono- and diglycerides also varied significantly, with higher levels of these generally present in the crude extracts obtained with the longer chained alcohols (Figure 5.12). In addition, the NMR analysis showed an unidentified peak that was apparent only in the spectra of the samples obtained from Soxhlet extraction using propanol, butanol, pentanol and hexanol. A two-dimensional COSY NMR experiment was carried out on the propanol sample, and the peak was seen to be coupled to $-\text{OCO}-\text{CH}_2-$ (Appendix H), therefore, it is tentatively suggested that this peak could arise from alkyl esters present in the sample. Alkyl esters could have been produced by esterification of FFA or glycerides during the extraction process by reaction with the alcohol solvents.

This observation could also account for the higher levels of mono- and diglycerides present in the crude extracts obtained with these solvents. The unidentified peak was not observed in samples arising from ethanol, and had a smaller relative area for the short-chained alcohols. The potential presence of esters in some of the SCG crude extract samples is supported by previous studies which investigated direct transesterification of SCG oil, where extraction and transesterification were undertaken simultaneously (Calixto et al., 2011; Liu et al., 2017; Tuntiwattapanun et al., 2017).

Therefore, the high temperatures applied during solvent extraction from SCG with higher alcohols and the prolonged process duration (8 hours) might have created suitable conditions for a single-step biodiesel production despite the absence of a catalyst, thus resulting in partial oil esterification and formation of esters. Alternatively, the result could simply indicate that the higher alcohols extract relatively higher levels of mono- and diglycerides.

The obtained results show that selection of solvent used for extraction could have direct implications for the intended use of the crude extracts, depending on whether greater proportions of glycerides or FFAs are desirable. If the intention is to produce biodiesel, then a high temperature extraction with a long chain alcohol is a potential route to one step extraction and transesterification, however, elevated temperatures and polar alcohols may result in a higher FFA content, which is undesirable for a final biodiesel product. Furthermore, the ester alcohol moiety chain length can have implications for diesel engine combustion and emission characteristics (Hellier et al., 2012).

Finally, the HHVs of crude extracts extracted with ethanol and that of the corresponding defatted SCG was measured according to the method described in Section 3.2.9 in order to compare with the values measured after Soxhlet extraction with hexane at the same conditions (Table 4.1). ICG1 crude extracts extracted with ethanol had a HHV of 38.23 ± 0.21 MJ/kg, which is slightly lower than the HHV of hexane extracted lipids, potentially due to higher content of non-glyceride compounds present in the ethanol-extracted oil sample. The HHV value of the defatted ethanol-treated SCG was found to

be 20.45 ± 0.24 , which is slightly higher than that of hexane-treated defatted SCG, suggesting that the strong polar character of ethanol has hindered the diffusion of the non-polar SCG lipids leaving part of the available lipids within the grounds.

5.2. Pilot plant solvent extraction

Solvent extraction experiments at pilot plant scale were undertaken at New Holland Extraction Ltd. according to the method described in Section 3.2.4, where the only variables that could be modified were the duration of the process and the moisture content of the SCG.

As completely dry samples of the required mass were not available, two ICG1 samples with moisture contents of 5 % w/w and 10 % w/w and one RCG1 sample with moisture content of 5 % w/w were utilized. Figure 5.13 shows the oil yields obtained with the various SCG samples at extraction durations of 1 and 2 hours on a dry weight basis, with the values shown corresponding to the % mass percentage of FFAs in each of the recovered oil samples.

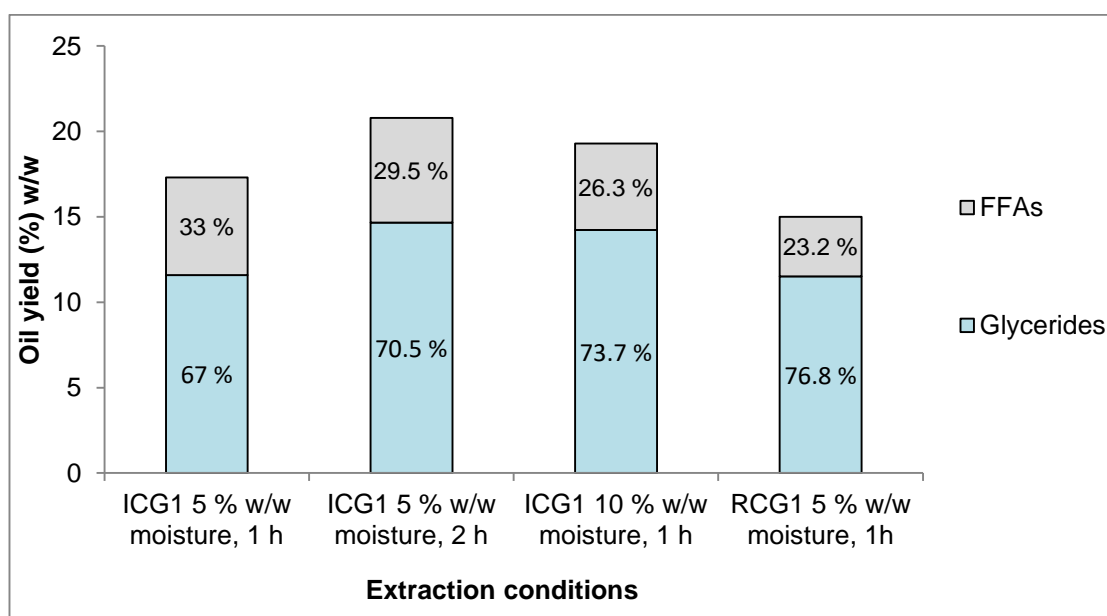


Figure 5.13: Oil yields and FFA percentages obtained from pilot plant extractions with isohexane.

It can be seen in Figure 5.13 that at extraction durations of 1 and 2 hours with 5% w/w moisture content, ICG1 oil yields of 17.3 and 20.8 % w/w were

obtained respectively. These oil yields are directly comparable with those achieved at the same durations with the Soxhlet method (17.9 % w/w and 21.06 % w/w) and dry ICG1 samples (Figure 5.1), and support the finding that increasing duration (below 8 h) increases extracted oil yields. Pilot plant extraction with partially dried RCG1 for 1 hour achieved an oil yield of 15.0 % w/w, which is slightly higher than that obtained through 8 hours Soxhlet (Table 4.1).

The oil yield achieved from an ICG1 sample with 10 % w/w moisture after 1 hours of extraction was 19.3 % w/w and this suggests that an intermediate portion of moisture in the feedstock does not hinder the pilot plant scale extraction process. The presence of water might in fact be responsible for the extraction of additional water soluble compounds such as proteins, phosphatides and carbohydrates, increasing the overall extraction yield (Lajara, 1990; D. L. Luthria et al., 2004), as was possibly also the case with the partially dried RCG1 sample. This is in contrast with results obtained through Soxhlet extraction when samples of various moisture contents were used and suggests that the pilot plant is less sensitive to the presence of water, potentially due to the countercurrent contact of SCG and solvent. In general, considering the oil content of ICG1 and RCG1 samples obtained at laboratory scale (Table 4.1), the results of pilot plant scale extraction process showed the laboratory scale Soxhlet experiments to be representative of industrial scale processes that could be utilized for extraction of lipids from SCG.

Regarding the FFA content of the extracted ICG1 lipids, it can be seen in Figure 5.13 that an increase of pilot plant extraction duration resulted in recovered ICG1 oil with a lower quantity of FFAs. Extraction with ICG1 sample of 10 % w/w moisture for 1 hour yielded oil with FFA content of 26.3 % w/w, a value lower than that of lipids extracted from samples with 5 % w/w moisture, which could possibly be explained by the increased extraction of water soluble compounds that potentially resulted in a slight reduction of the mass portion of FFAs in the oil. The FFA content of the RCG1 lipids was found to be 23.2 % w/w, slightly higher than that of RCG1 oil extracted through Soxhlet (Table 4.1), potentially due to the short pilot plant extraction duration.

The determination of the fatty acid profile of the SCG oil samples extracted at the pilot plant was carried out onsite according to the method described in Appendix D. Table 5.2 shows the % fatty acid composition of the oil samples by mass, along with that of soybean and palm oil, two major biodiesel feedstocks (Kondamudi et al., 2008), for comparison purposes.

Table 5.2: Fatty acid profile of examined ICG1 oil samples and selected vegetable oils.

Sample	C16:0	C18:0	C18:1	C18:2	C18:3	C20:0	SFA	UFA	PUFA
ICG1, 5 % w/w moisture, 1 h	32.4	8.1	10.2	41.7	1.1	3.8	45.4	53.9	42.9
ICG1, 5 % w/w moisture, 2 h	34.6	8.1	9.3	40.7	1	4	47.8	52.2	41.8
ICG1, 10 % w/w moisture, 1 h	32.4	7.5	10.1	43.1	0.9	3.1	44.1	55.3	44.1
RCG1, 5 % w/w moisture, 1 h	32.7	7.1	9.1	44.9	1.3	2.7	43.5	56.5	46.2
Palm oil [1]	44	4	40	10	NM	NM	48	50	10
Soybean oil [2]	9	4	28	49.5	NM	NM	13	77.5	49.5

[1]: (Gunstone, 1996), [2]: ("<http://www.chempro.in/fattyacid.htm>"), NM: not mentioned, SFA: saturated fatty acids, UFA: unsaturated fatty acids, PUFA: polyunsaturated fatty acids.

Table 5.2 shows that in all of the examined SCG oil samples linoleic (C18:2), palmitic (C16:0), oleic (C18:1), stearic (C18:0), eicosanoic (C20:0) and linolenic (C18:3) were the fatty acids with the highest weight percentages in a decreasing order of magnitude, while other fatty acids that are not disclosed in the table were found in considerably lower amounts (<0.5). Oil extracted from 5 and 10 % w/w ICG1 samples consisted of both saturated (44.1–47.8 % w/w) and unsaturated fatty acids (52.2–55.3 % w/w), with the portion of polyunsaturated fatty acids ranging from 41.8 to 44.1 % w/w. The bulk of the extracted ICG1 oils (92.4–93.1 %) comprised of linoleic, palmitic, oleic and stearic acid, followed by small amounts of eicosanoic and linolenic acid. The absence of significant differences in the fatty acid profiles of the three examined ICG1 oil samples suggests that the moisture content of SCG and the duration of solvent extraction did not have an important effect on the extracted oil composition. Furthermore, the oil extracted from RCG1 was found to have a similar fatty acid profile with ICG1 lipids.

The determined fatty acid compositions are in good agreement with SCG oil fatty acid profiles reported in previous studies (Table 2.5). In particular, SCG oil obtained by Haile (2014), which has a very similar fatty acid profile to oil extracted from ICG1, resulted in biodiesel that was found to be within the standard limits (EN 14214) for parameters including density, kinematic viscosity, iodine value, acid value and flash point.

It can also be seen from Table 5.2 that coffee derived oil shares the major fatty acids in somewhat similar percentages with soybean oil and has an almost identical saturated to unsaturated fatty acid ratio with palm oil. The suitability of an oil as a biodiesel feedstock is highly dependent on the fatty acid profile (Knothe et al., 2005), and the relatively high percentage of oleic acid in the coffee oil (9.3–10.2 % w/w in oil extracted from ICG1 - Table 5.2) is potentially beneficial for biodiesel production, as the relatively long alkyl chain length with only one double bond results in high oxidative stability and a low melting point (Pinzi et al., 2009).

On the contrary, the high level of polyunsaturated fatty acids in the obtained coffee oil is a potential disadvantage for biodiesel production as it is closely

related to the oxidation rate and the degradation tendency of the fuel (Knothe, 2008; Pinzi et al., 2009; Ramos et al., 2009). In addition, higher degrees of alkyl moiety unsaturation have been implicated in higher engine exhaust NO_x emissions, however, this has found to be secondary to properties such as fuel cetane number (Hellier and Ladommatos, 2015). The influence of the fatty acid profile of SCG oil and derived biodiesel on combustion and emission characteristics is discussed in depth in Section 8.2.

5.3 Conclusions

An extraction duration of 8 hours was found to result in the highest oil yields in Soxhlet extraction, with durations shorter than 2 hours resulting in considerably reduced oil yields and suggesting that this duration is not sufficient for complete extraction, while a correlation between increasing duration of extraction and decreasing FFA content of recovered oil was observed. Regarding the effect of SCG-to-solvent ratio on extraction efficiency, a decrease from 1:4.0 w/v to 1:9.0 w/v resulted in increased SCG oil yield, with solvent saturation being responsible for the lower oil yield obtained at a SCG-to-solvent ratio of 1:4.0 w/v. Soxhlet extraction experiments with coffee samples of discrete particle diameters found a mix of particles of different diameters to lead to higher oil yield, possibly because a mix of particles of different sizes offers an increased surface area without impeding solvent percolation.

Furthermore, Soxhlet experiments with partially dried SCG showed that minimal moisture content resulted in slight crude extract yield increase relative to completely dry SCG when hexane and ethanol were the solvents used, potentially due to enhanced recovery of polar compounds in the presence of water, however, further increase of moisture inhibited the extraction with both solvents. Nevertheless, ethanol showed a reduced sensitivity to high moisture presence compared to hexane because of its polar character. A relationship between increasing solvent boiling point and higher extraction ratio was observed in Soxhlet experiments with various solvents, suggesting that higher extraction temperature reduced the process selectivity, however, no systematic impact of solvent molecular weight could be observed. A weak

trend of decreasing extraction ratio with increasing alcohol polarity was found, possibly because of the non-polar character of SCG lipids.

The FFA content of crude extracts obtained with various solvents increased with increasing solvent polarity, while the comparative levels of mono- and diglycerides also varied significantly with higher concentrations found in samples extracted with long-chained alcohols, potentially due to esterification reactions occurring simultaneously with lipid extraction. The HHV of crude extracts extracted with ethanol was found to be slightly lower than that of hexane-extracted oil, while the higher HHVs of defatted SCG treated with ethanol suggested an incomplete extraction of oil.

Pilot plant extractions revealed that an increase of process duration from 1 to 2 hours resulted in increased recovery of lipids and reduced levels of FFAs, in agreement with Soxhlet experiments. Increase of the SCG moisture content from 5 % w/w to 10 % w/w resulted in slightly improved oil yield and lower concentration of FFAs in the oil, probably due to the extraction of water-soluble compounds along with extracted lipids, revealing a reduced sensitivity of pilot plant solvent extraction to water presence relative to Soxhlet extraction. Determination of the fatty acid profile of obtained lipids showed that varying durations of extraction and moisture contents of the examined SCG did not affect the composition of the recovered lipids. The similarity of the fatty acid profile of the extracted lipids to that of other vegetable oils commonly used as biodiesel feedstocks suggested that the obtained oil was suitable for biodiesel production.

Following the determination of the impact of various solvent extraction parameters on SCG oil yield and quality through experiments performed at conditions of atmospheric pressure, Chapter 6 concentrates on the effect of elevated temperature and pressure on the oil yield obtained from SCG and its composition.

6. Effect of elevated temperature and pressure on the efficiency of oil recovery through solvent extraction

This chapter presents the results obtained through ASE and pressurized vessel experiments regarding the impact of extraction temperature and pressure on the efficiency of lipid recovery from SCG.

6.1 Accelerated solvent extraction

The oil yields recovered at elevated temperatures through ASE were obtained according to the method described in Section 3.2.3.2 that includes three static cycles of 5 minutes duration during which the sample is in contact with the solvent, and are expressed on a dry weight basis. Preliminary experiments were performed with the ASE in order to determine the optimum static cycle duration as well as the ideal number of static cycles in terms of oil extraction efficiency from dry SCG at a constant temperature of 125 °C. The maximum static extraction cycle duration that could be selected was 10 minutes, while a maximum of 5 static cycles could be performed per extraction. The oil yields obtained from the ICG2 sample with hexane at different conditions are presented in Figure 6.1, while each point represents a separate experiment.

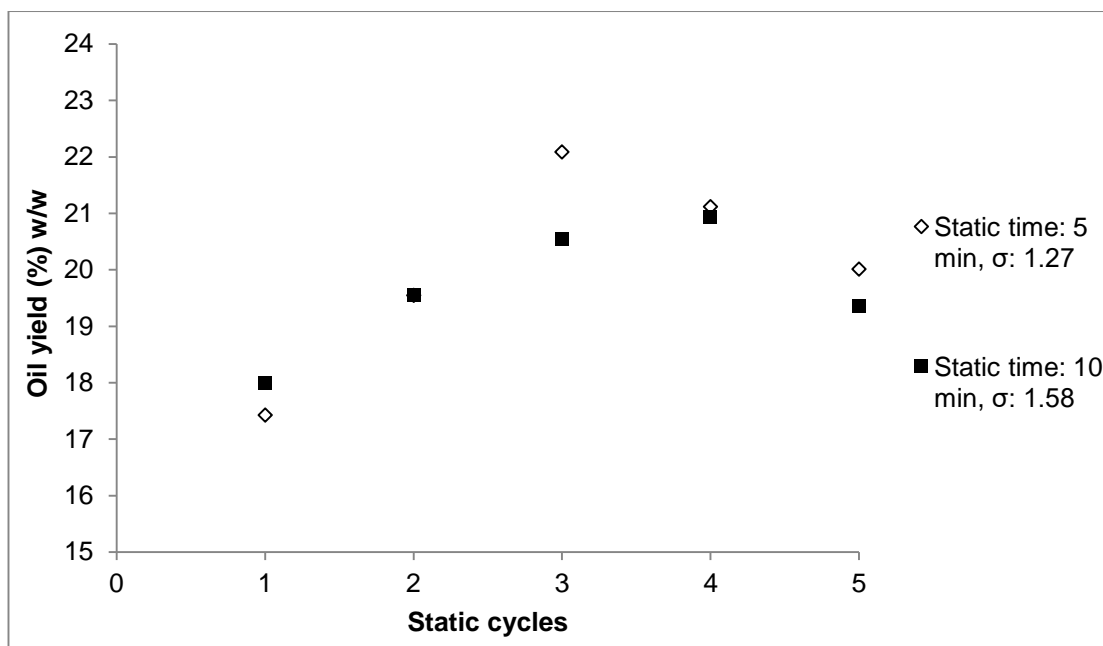


Figure 6.1: Oil yields obtained through ASE with hexane with varying number of static extraction cycles and static cycle duration. The standard deviations (σ) were calculated from three experimental repeats.

Figure 6.1 shows that addition of static extraction cycles initially resulted in improved oil yields for both of the examined cycle durations, however, an optimum number of cycles that led to maximum oil recovery was observed, which varied depending on cycle duration. Further increase of the number of static cycles above this optimum was found to result in slightly lower oil yields. The initial increase of the oil yield with additional extraction cycles can be explained by the introduction of fresh solvent and insufficient process duration, however, the subsequent slight oil yield decrease can likely be attributed to thermal degradation of lipid components due to prolonged exposure to conditions of high temperature and pressure in the extraction cell (Campos-Vega et al., 2015; Novaes et al., 2015). The obtained results did not show any clear correlation between the static cycle duration and the lipid extraction efficiency. The optimum conditions of 3 static cycles with cycle duration of 5 minutes were used for subsequent ASE experiments.

6.1.1 Effect of process temperature on lipid extraction efficiency

The polar ethanol and the non-polar solvents of the homologous series of alkanes were used (hexane and its branched-chain isomer iso-hexane, heptane and octane) in ASE to investigate the effect of temperature on the lipid extraction efficiency from SCG. Several SCG samples were used due to supply issues and therefore the obtained oil extraction ratios relative to oil yield extracted through the Soxhlet method with hexane are presented (Table 4.1). Figure 6.2 shows the average oil extraction ratios obtained at temperatures ranging from 60 °C to 200 °C when different solvents were used.

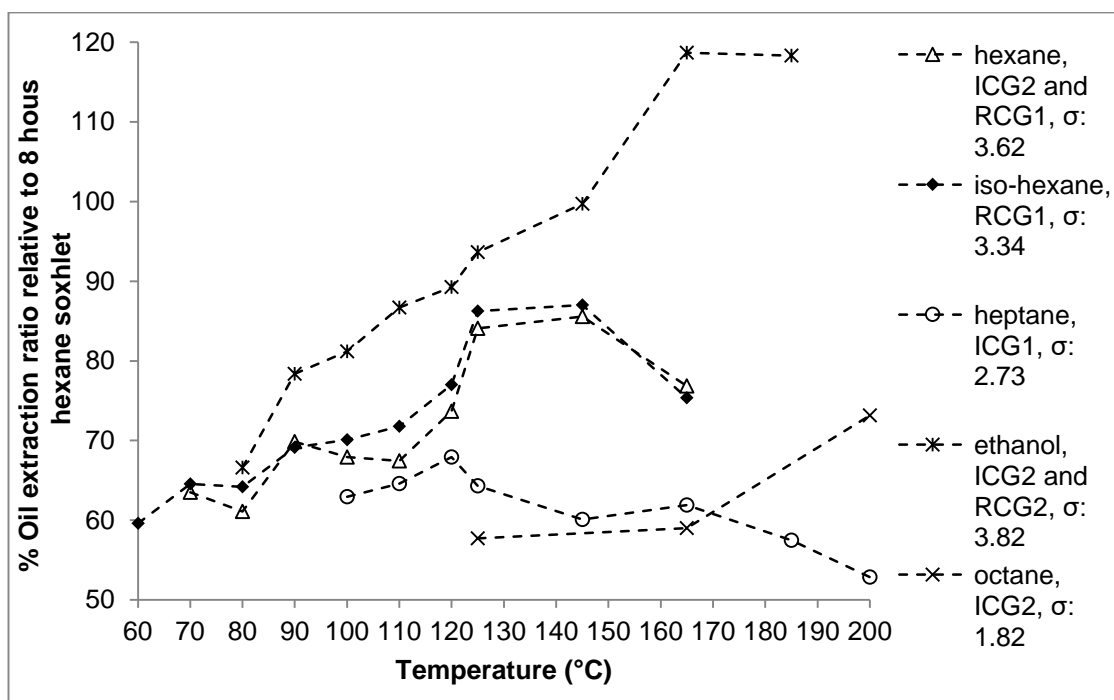


Figure 6.2: Oil extraction ratios obtained using ASE at various temperatures with different solvents. The standard deviations (σ) were calculated from three experimental repeats.

It can be seen in Figure 6.2, that when the extraction was performed with hexane at a temperature close to its boiling point (70 °C), an average oil extraction ratio of 63.5 % w/w relative to 8 hour Soxhlet extraction with hexane was recovered. As the extraction temperature was increased, the oil extraction ratio obtained increased up to a maximum of ~85.5 % w/w at 145 °C, while a further temperature increase led to a slight decrease in oil extraction ratio. Iso-

hexane resulted in oil extraction ratios very similar to those obtained with hexane (maximum of 87 % w/w at 145 °C), something that can be attributed to the almost identical solvent properties (Table 3.1).

When the extraction was conducted with heptane at a temperature close to its boiling point (100 °C), an oil extraction ratio of ~63 % w/w was achieved. An increase in temperature resulted in a slight oil extraction ratio increase, with a maximum of 68 % w/w obtained at 120 °C, but further temperature increase led to lower oil extraction ratios. Octane extracted 57.7 % w/w of the available oil at 125 °C, which slightly increased at 165 °C and reached a maximum at 200 °C (73.1 % w/w). Experiments with octane at higher temperatures were not performed due to equipment limitations, so it is not known if an eventual decrease in oil extraction ratio with increasing temperature would have been observed, as was the case with other solvents (Figure 6.2).

Figure 6.2 suggests that there is an optimum temperature that promotes rapid lipid diffusion rates and results in high oil recoveries. However, the relatively high oil extraction ratios obtained at high temperatures (100-200 °C) may also have occurred due to the extraction of bound lipids and impurities from the solid matrix and ruptured cell walls respectively (Quinn, 1988; Zuorro and Lavecchia, 2012). The slight decrease of oil extraction ratio observed in most cases after a certain temperature is possibly related to reduced stability and degradation of lipid components (Campos-Vega et al., 2015; Novaes et al., 2015). This tendency of increasing extraction efficiency until a critical temperature and subsequent decrease has also been observed in microwave assisted extraction of flavonoids from plant sources (Routray and Orsat, 2012).

Figure 6.2 also shows that when ethanol was used at a temperature similar to its boiling point (80 °C), an average oil extraction ratio of 66.5 % w/w was obtained. The oil extraction ratios increased as the temperature of the ASE process increased up to a maximum of 118.7 % w/w at a temperature of 165 °C, while further temperature increase did not significantly affect the extraction efficiency of the process. The high oil extraction ratio obtained can possibly be attributed to the polar character of ethanol, which potentially resulted in the

extraction of compounds other than triglycerides (e.g. phosphatides, proteins, carbohydrates) (Al-Hamamre et al., 2012; Johnson and Lusas, 1983; Kondamudi et al., 2008), and to the concurrent high extraction temperature that reduced the selectivity of the process.

A comparison of the oil recoveries achieved with the same solvents through Soxhlet and ASE at a temperature close to their boiling point (Figure 5.9 and Figure 6.2), showed that in all cases a higher amount of oil was achieved through Soxhlet due to longer duration and lower SCG-to-solvent ratio.

The composition of selected lipid samples extracted with hexane and ethanol at elevated temperatures was determined by ^1H NMR spectroscopic analysis according to the method described in Appendix H, and the obtained results are presented in Figure 6.3.

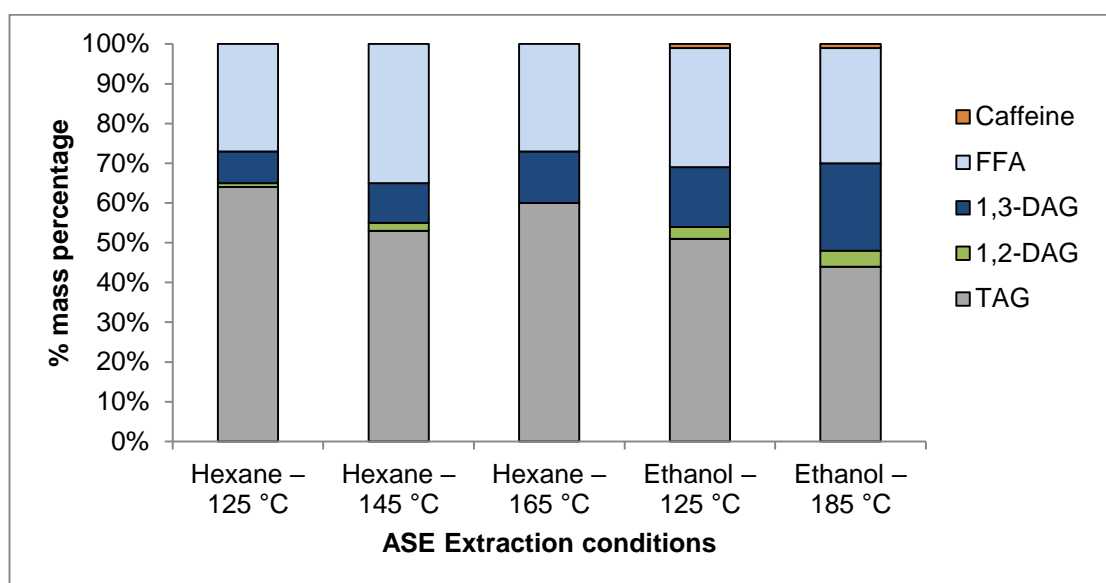


Figure 6.3: Composition of oils obtained from ASE extractions with hexane and ethanol at elevated temperatures, using ^1H NMR spectra.

It can be seen in Figure 6.3 that the main components present in lipid samples extracted through ASE were triglycerides, FFAs and 1,3-diglycerides in a decreasing order of magnitudes, while 1,2-diglycerides were also found in small amounts in most of the examined samples. There is no clear correlation between increasing extraction temperature and FFA content in oil samples extracted either with hexane or with ethanol, however, higher extraction

temperatures resulted in lower concentration of triglycerides and higher quantities of 1,2- and 1,3-diglycerides in both of the examined sample sets. The higher concentration of FFAs in the oil samples extracted with both samples relative to lipids obtained through Soxhlet extraction (Figure 5.12) can be attributed to preferential recovery of FFAs in the short ASE extraction duration, something that has been also observed in Figure 5.2.

An interesting observation from Figure 6.3 is that of the SCG oil extracted with ethanol at temperatures of 125 °C and 185 °C, the spectra of which were unique in that the presence of caffeine was indicated by four identifying singlet peaks. It is suggested that the high temperature of the ASE extraction coupled with the use of the polar ethanol extracted residual caffeine contained in the SCG; the caffeine peaks were not present in the spectra of oil obtained from the lower temperature Soxhlet extraction using ethanol or any other alcohol, nor in the spectra of oil obtained by ASE with hexane at temperatures of 125 °C, 145 °C and 165 °C. The presence of the caffeine could have implications for the properties of the oil and its derivatives (for example as a carrier of molecular nitrogen), and therefore potentially impacts on the suitability of ethanol as an extraction solvent under high temperature conditions.

Regarding the impact of extraction temperature on the energy content of the obtained lipids, the HHV of ICG2 oil samples extracted with ethanol at temperatures of 125 °C, 145 °C, 165 °C and 185 °C was determined according to the method described in Section 3.2.9. The increase of extraction temperature within the examined range was found to have little effect on the HHV of the lipids, with the obtained values ranging between 38.53 MJ/kg and 38.84 MJ/kg, and there was no systematic impact of extraction temperature on the oil HHV. The obtained HHV values were slightly lower than the HHV of ICG2 oil extracted through Soxhlet with hexane (Table 4.1), something possibly attributable to the extraction of undesired compounds of lower energy content due to high process temperature and solvent polarity that resulted in decreased HHVs.

The effect of SCG moisture on ASE extraction efficiency was investigated with samples that had been previously subjected to mechanical pressing for water removal, and the results obtained are presented in Section 7.3

6.2 Solvent extraction in a closed pressurized vessel

6.2.1 Effect of pressure on lipid extraction efficiency

Solvent extraction experiments at conditions of elevated pressure were performed in a closed bespoke pressurized vessel with dried RCG3 according to the method described in Section 3.2.3.3. Figure 6.4 shows the oil extraction ratios achieved from 20 minutes of static pressurized solvent extraction at different conditions of temperature and pressure. The SCG-to-solvent ratio was kept constant at 1:6 w/v, while the pressurized static extraction was preceded by a pre-heating period of 20 minutes. The oil extraction ratios that are shown in Figure 6.4 are expressed relative to the average hexane extracted Soxhlet yield (Table 4.1).

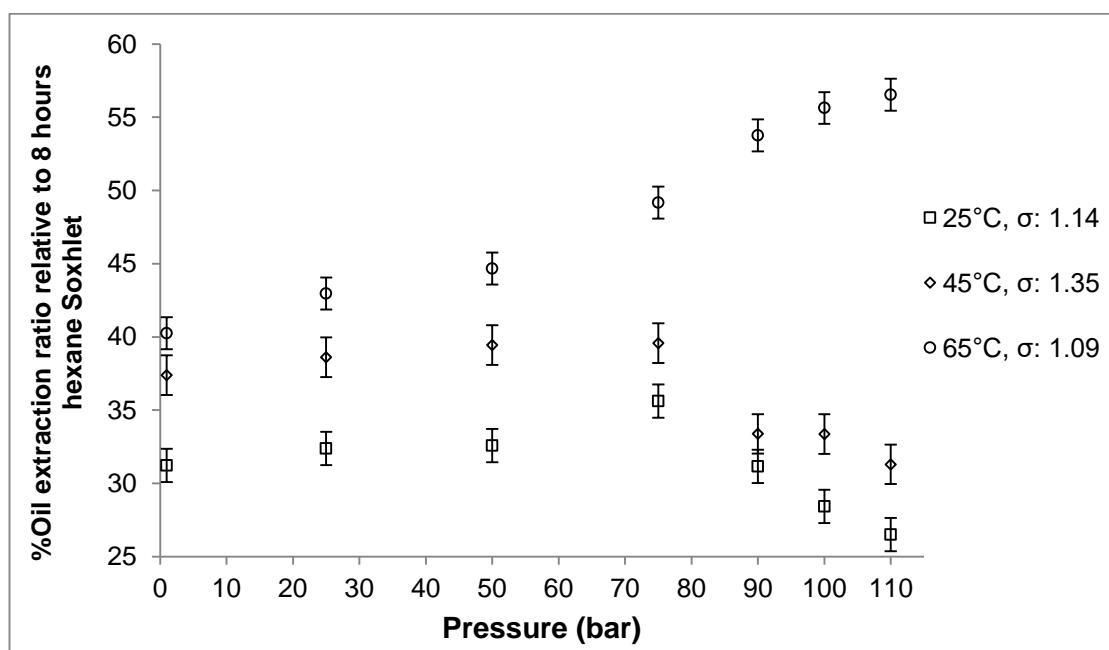


Figure 6.4: Oil extraction ratio obtained against applied pressure at extraction temperatures of 25, 45 and 65 °C. The error bars show the standard deviation (σ) of the mean calculated from 3 experimental repeats at each temperature setting.

It can be seen in Figure 6.4 that when the static extraction was performed at conditions of ambient pressure and temperature (approximately 25 °C), ~31 % w/w of the available oil was extracted. As the applied pressure was gradually increased, while temperature remained ambient, the oil extraction ratio increased to reach a maximum of 35.6 % w/w at 75 bar. Further increase of pressure resulted in a decrease of the obtained oil extraction ratio with the lowest extraction ratio of 26.5 % w/w achieved at the highest applied pressure (110 bar). An almost identical trend, but with consistently higher oil extraction ratios, was observed when the experimental temperature was raised to 45 °C. Similarly to the experiments conducted at room temperature, the oil extraction ratio slightly increased with pressure to reach a maximum of 39.5 % w/w at 75 bar, with a further pressure increase leading to lower oil extraction ratios with a minimum of 31.3 % w/w obtained at 110 bar.

When the temperature of the extraction was increased to 65 °C, a temperature close to the boiling point of hexane, the oil extraction ratio achieved at atmospheric pressure was 40.2 % w/w. Experiments at higher pressures showed that the obtained oil extraction ratio increased linearly with pressure increase ($R^2=0.96$), and the highest extraction ratio (56.5 % w/w) was extracted at the highest applied pressure of 110 bar. This is contrary to experiments performed at 25 °C and 45 °C respectively, where any increase in extraction pressure above 75 bar actually reduced oil extraction ratios (Figure 6.4). However, it can be seen that the gradient of this increasing trend decreased at the highest pressures tested, with only a 0.9 % w/w increase in extraction ratio when the extraction pressure was increased from 100 to 110 bar.

The results presented in Figure 6.4 suggest that when solvent extraction of lipids from SCG was performed at temperatures significantly lower than the boiling point of the solvent used, pressures applied above atmospheric and up to 75 bar result in a slight oil extraction ratio increase, although further increase inhibited oil extraction and led to considerably lower extraction ratios. The beneficial effect of pressure increase up to 75 bar in the efficiency of the process can be possibly attributed to improved penetration of solvent into the pores of the feedstock, and the enhanced lipid solubility, mass transfer and

desorption kinetics caused by the increase in pressure (Camel, 2001; Kaufmann et al., 2001; Kaufmann and Christen, 2002; Matthäus and Brühl, 2001; Mustafa and Turner, 2011; Richter et al., 1996). In addition, high extraction pressure tackles problems related to air bubbles found within the matrix that impede the solvent from reaching the oil (Mustafa and Turner, 2011).

However, high pressure is known to increase the surface tension and viscosity of the solvent, with increased surface tension impeding the penetration of the solvent into the matrix of the oilseed and consequently reducing the rate of lipid extraction (Johnson and Lusas, 1983). Viscosity is a measure of internal molecular friction, and as oil removal through solvent extraction is in part governed by capillary flow through a solid matrix, high solvent viscosities can hinder flow and lead to lower extraction rates (Johnson and Lusas, 1983). The reduction in extraction ratio obtained at pressures greater than 75 bar (Figure 6.4) suggests that the inhibition of extraction caused by an increase in solvent surface tension and viscosity becomes more important in determining the overall lipid extraction rate at temperature conditions of 25-45 °C.

The absence of any decrease in obtained extraction ratios at extraction pressure up to 110 bar when conducted at a temperature of 65 °C (Figure 6.4), suggests that any negative effects of increased solvent surface tension and viscosity were countered by improved lipid solubility and diffusion rate due to increased temperature (Johnson and Lusas, 1983; Richter et al., 1996). The positive effects of elevated temperature appear to overcome the negative impact of high pressure on surface tension and viscosity observed at lower temperatures, and, synergistically with the aforementioned beneficial effects of pressure, result in improved oil extraction ratios.

Previous studies have reported that the influence of applied pressure on oil yield is small, or even negligible, when compared to that of temperature (Camel, 2001; Mustafa and Turner, 2011), however, the obtained results suggest that pressure is also a significant factor when the extraction is performed at 75 bar and above. This is in agreement with previous studies which reported that pressure impacts on the efficiency of the extraction process

(Giergielewicz-Mozajska et al., 2001; Jalilvand et al., 2013; Kamali et al., 2014; Kaufmann et al., 2001), while similar results were reported from the pressurized solvent extraction of rice bran oil (Jalilvand et al., 2013).

The FFA content of samples extracted with varying pressure at 65 °C was examined according to the method described in Section 3.2.6 so as to determine any effect of pressure on the concentration of FFAs in the obtained lipids, while the HHV of selected oil samples was measured according to the method described in Section 3.2.9. Table 6.1 shows the average FFA and HHV content of samples extracted at pressure conditions ranging between ambient and 100 bar.

Table 6.1: Average % w/w FFA content and HHV of oil samples extracted after 20 minutes at varying pressure conditions and a constant temperature of 65 °C. The standard deviations calculated by three experimental repeats were 0.7 % w/w for FFAs and 0.43 MJ/kg for HHVs.

Extraction Pressure (bar)	FFA content (%) w/w	HHV (MJ/kg)
1.013 (ambient)	18.7	38.93
25	17.5	38.82
50	19.2	39.12
75	18.1	39.03
100	18.9	38.91

It can be seen in Table 6.1 that extraction pressure has a limited effect on the FFA content of the recovered lipids, with FFA levels ranging between 17.51 % w/w and 19.22 % w/w, while no clear correlation was found between applied pressure and FFA concentration. The FFA content of all the examined samples was higher than that of RCG3 lipids recovered through 8 hours Soxhlet extraction (15.46 ± 0.41 % w/w, Table 4.1), verifying in this way the observation that prolonged solvent extraction duration can be associated with reduced presence of FFAs (Figure 5.2).

Furthermore, the measured HHVs of the lipid samples showed a small degree of variation and were similar to the HHV of Soxhlet extracted RCG3 oil (38.95 ± 0.34 MJ/kg, Table 4.1), suggesting that extraction pressure does not significantly affect the energy content of recovered lipids.

6.2.2 Effect of pressurized solvent extraction duration and number of extraction cycles on lipid extraction efficiency

The effect of process duration on the efficiency of oil recovery through pressurized static solvent extraction in the pressure vessel was investigated with durations ranging between 5 and 60 minutes. Figure 6.5 shows the oil extraction ratios obtained from RCG2 with hexane at 45 °C and 75 bar, against extraction duration.

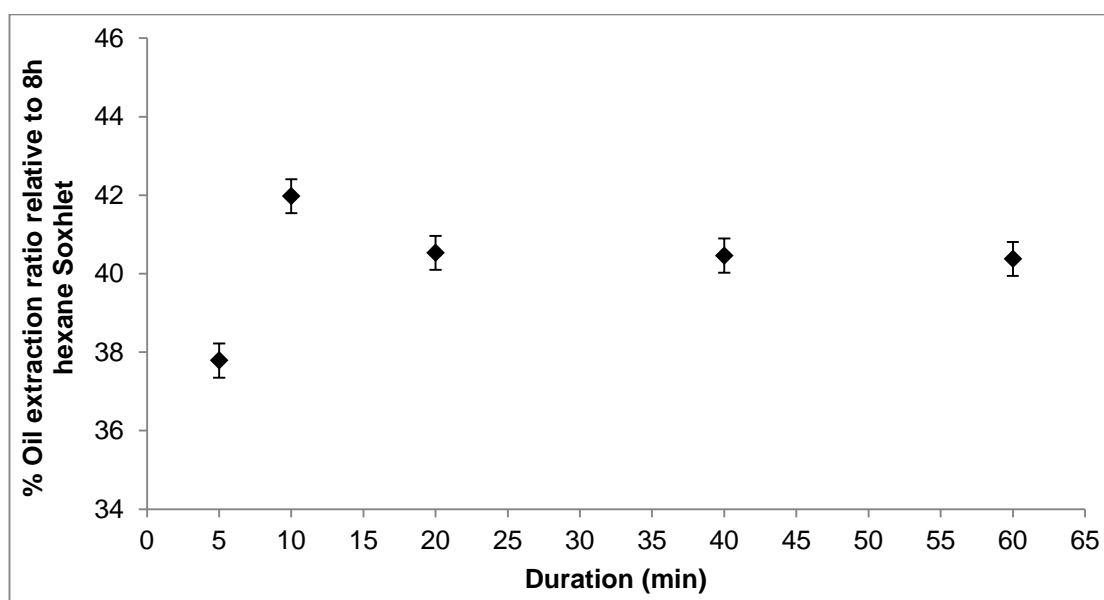


Figure 6.5: Oil extraction ratios obtained against duration of static extraction at 75 bar and 45 °C. Error bars stand for the standard deviation ($\sigma=0.4$) that was calculated by three experimental repeats.

It can be seen in Figure 6.5 that as the duration of the extraction increased from 5 to 10 minutes the obtained oil extraction ratio increased from ~38 % w/w to ~42 % w/w, while a further increase of the extraction duration to 20 minutes resulted in slight decrease of the oil extraction ratio (40.5 % w/w). The initial increase in extraction ratio as the duration increased to 10 minutes, suggests that an extraction duration of 5 minutes did not allow sufficient time

for the extraction of the available oil. Thereafter, and as the process duration increased to 40 and then 60 minutes, the obtained oil extraction ratio did not change significantly, suggesting that the extraction of the oil from SCG was accomplished during the first 10 minutes of the process under these temperature and pressure conditions. The slight decrease of the oil extraction ratio when the duration of the process increased above 10 minutes can be possibly attributed to compression of the sample matrix under extended pressure and/or increased binding of lipids to protein (Yao and Schaich, 2015).

The obtained results are in good agreement with previous studies that investigated pressurized solvent extraction of lipids from various sources such as rice bran (Jalilvand et al., 2013) pistachio kernels (Sheibani and Ghaziaskar, 2008) and dry pet food (Yao and Schaich, 2015) through ASE, and found that a prolongation of static cycle extraction duration from 5 up to 30 minutes could be either insignificant, or even counterproductive, in terms of oil extraction efficiency.

The effect of the number of extraction cycles, with or without washing of the feedstock in between static extraction cycles, on the lipid extraction ratio achieved from SCG was also examined. The introduction of a second static extraction cycle of 20 minutes, with the same SCG sample but with fresh solvent at the same pressure and temperature conditions of 75 bar and 45 °C, resulted in an average oil extraction ratio of 61.84 ± 1.16 % w/w. This extraction ratio was significantly improved relative to 39.57 ± 0.35 % w/w, which was the extraction ratio achieved from a single static cycle at the aforementioned conditions. This finding led to further experimentation with the number of static cycles at the same conditions of temperature (45 °C), pressure (75 bar), pressurized extraction time (20 minutes) and SCG-to-solvent ratio (1:6 w/v or 120 ml of hexane), with washing stages of 1 minute with 120 ml of hexane following each static cycle. The average oil extraction ratios obtained from this set of experiments relative to 8 hours Soxhlet extraction with hexane (Table 4.1) are presented in Figure 6.6.

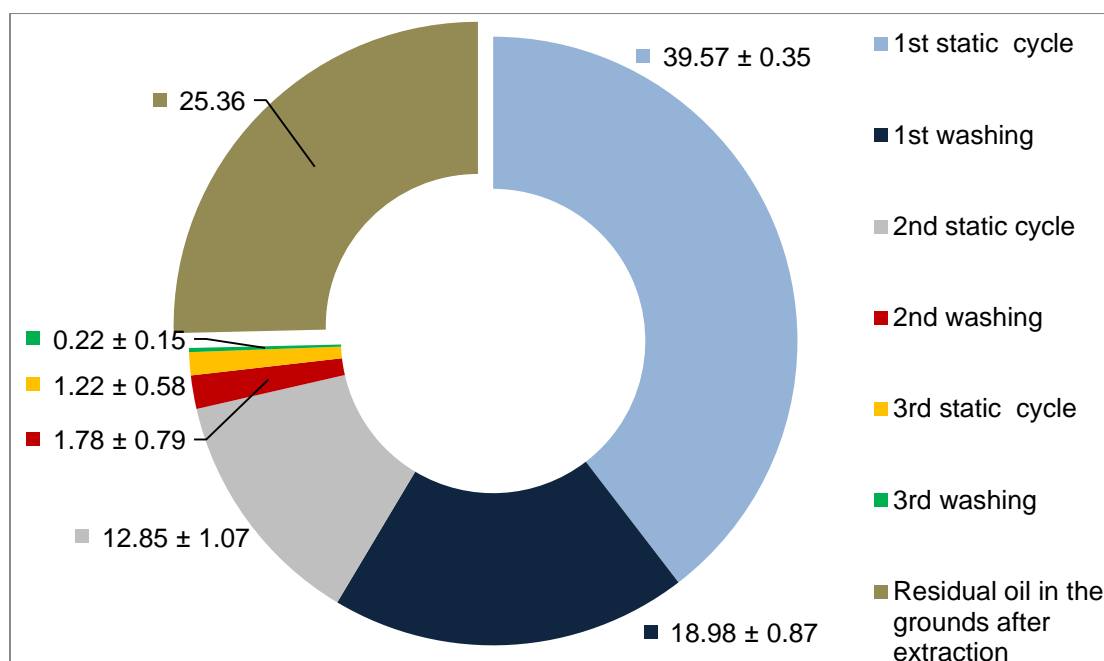


Figure 6.6: Oil extraction ratios obtained from multiple static extraction cycles and washing stages. The standard deviations of the mean that are shown were calculated by sets of three experimental repeats.

Figure 6.6 shows that the introduction of a washing stage after the 1st extraction cycle removed a further 18.98 % w/w of the available oil, a significant amount of lipids when compared to the oil extraction ratio of the 1st static cycle. This oil recovery can be possibly attributed to limited volume or saturation of the solvent used in the 1st static cycle, with the introduction of fresh solvent rapidly removing more oil. The 2nd static extraction cycle resulted in the recovery of an additional 12.85 % w/w of the available oil, while the following washing stage achieved an extraction ratio of 1.78 % w/w. These results suggest that the utilization of fresh solvent along with the extended total duration of the extraction allows recovery of lipids from the desorption-controlled phase, where the interactions between oil and sample matrix are stronger (Mustafa and Turner, 2011).

The addition of a 3rd static cycle followed by another washing stage removed a small further amount of oil and revealed the limit of the extraction efficiency of the process. The cumulative oil extraction ratio was 74.64 % w/w, a very significant amount of the total available oil, especially when considering the relatively low extraction temperature of 45 °C and the total experimental

duration of 63 minutes. Previous studies have also reported that several short consecutive static extraction cycles enhance the extraction efficiency of the process more than a longer single static cycle (Ramos et al., 2002; Yao and Schaich, 2015).

6.3 Conclusions

Experimentation with the number of ASE static cycles revealed an optimum setting (3 cycles), while longer duration of ASE trials at elevated temperature was found to be counterproductive in terms of obtained oil extraction ratio, potentially due to degradation of lipids after prolonged exposure to conditions of high temperature and pressure. Increase of extraction temperature in ASE resulted in higher oil extraction ratios increases for polar solvents than for non-polar ones, possibly attributed to enhanced extraction of polar compounds in conjunction with the reduced process selectivity at high temperatures.

Solvent selection and process temperature had a significant impact on the proportions of di- and triglycerides and FFAs present in the extracted oil, with increasing temperature leading to lower concentration of triglycerides and higher levels of 1,2- and 1,3-diglycerides, while there was no systematic effect of temperature on the FFA content of the recovered lipids. Extraction with ethanol at elevated temperatures (125 and 185 °C) extracted small amounts of caffeine from the SCG, potentially due to high extraction temperature and the polar character of solvent.

A process pressure of up to 75 bar improved the oil extraction ratio obtained through pressurized solvent extraction regardless of the process temperature, however, extraction above 75 bar at temperatures significantly below the boiling point of the solvent resulted in a decrease in oil extraction ratio due to increase of the solvent's surface tension and viscosity at high pressures, while an extraction temperature close to the solvent boiling point led to a linear increase in oil extraction ratio with increasing pressure, as temperature increase countered the negative effect of high pressure. Increase of pressurized static solvent extraction duration from 5 to 10 minutes resulted in improved oil extraction efficiency, while further increase of duration led to a slight decrease of the oil extraction ratio, possibly due to reduced lipid stability.

The introduction of fresh solvent after a single pressurized static extraction, either through a rapid washing stage or via a subsequent extraction cycle, improved significantly the oil recovery suggesting that the initial volume of solvent had become saturated with SCG oil, while relatively short consecutive extraction cycles with fresh solvent were found to be more efficient than a single long cycle in terms of oil extraction ratio. Finally, there was no systematic effect of extraction temperature and pressure on the HHV of SCG lipid samples recovered by ASE and closed pressurized vessel extractions, while the extraction pressure was found to have little effect on the FFA content of the recovered lipids.

The following chapter concentrates on the utilization of mechanical pressing as a method of moisture removal and oil expression from coffee residues, while the effect of mechanical pre-pressing on the efficiency of subsequent solvent extraction is also investigated.

7. Combined mechanical pressing and solvent extraction for water removal and lipid recovery

The hydraulic ram press and the screw press described in Sections 3.2.5.1 and 3.2.5.2 respectively were used for pressing wet and dry SCG samples from the ICG1 batch and RDCB in order to investigate the potential use of mechanical pressing for water removal and lipid expression, along with its use as a pre-treatment prior to solvent extraction.

7.1 Mechanical pressing for water removal from SCG

Wet ICG1 samples were subjected to mechanical pressing in the ram press (Section 3.2.5.1) for durations ranging from 5 up to 30 minutes and for pressures between 150 and 550 bar in order to investigate the efficiency of pressing as a way of SCG dewatering. Pressing experiments were performed at ambient (~25 °C) and elevated temperature (100 °C). Figures 7.1 and 7.2 show the percentage of moisture removed from wet ICG1 samples relative to initial moisture content (Table 4.1), against applied pressure and pressing duration respectively.

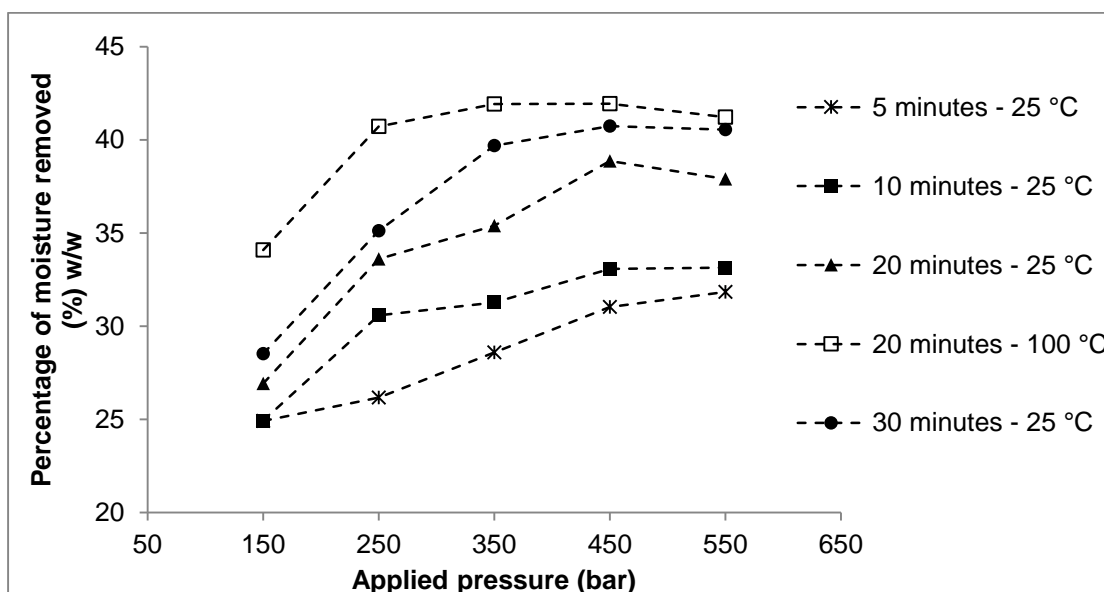


Figure 7.1: Percentage of moisture removed from wet SCG versus applied pressure at various conditions of temperature and pressing duration. The standard deviation (σ) was 1.0 as calculated from 3 experimental repeats.

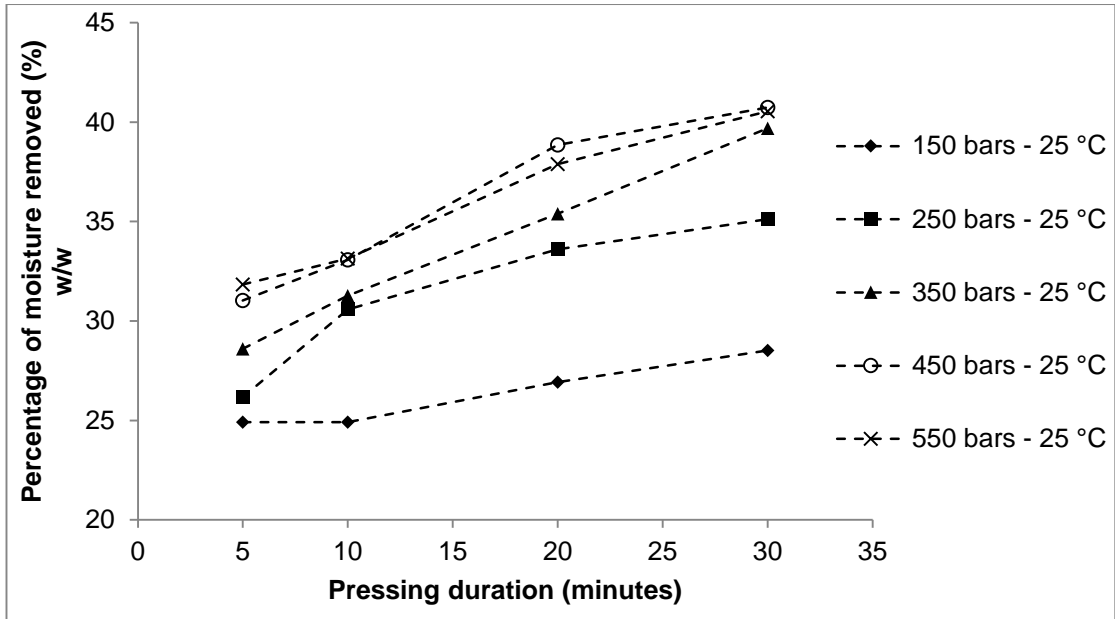


Figure 7.2: Percentage of moisture removed from wet SCG versus pressing duration at ambient temperature and different pressures. The standard deviation (σ) was 1.0 as calculated from 3 experimental repeats.

It can be seen in Figure 7.1 that up to 450 bar there is a relation between increasing pressure and higher percentage of moisture removed from wet SCG. Moreover, the duration of the pressing experiment had an important effect on the moisture removing efficiency of the process, with longer durations resulting in the removal of significantly higher percentages of moisture, with R^2 values ranging between 0.88 and 0.99 (Figure 7.2). The highest percentage of moisture removed at ambient temperature was 40.7 % w/w of the initial water content (57.45 % w/w – Table 4.1) and was achieved after 30 minutes of pressing at 450 bar. The results shown in Figures 7.1 and 7.2 suggest that when the duration of the extraction is longer than 5 minutes, an increase of pressure above 450 bar does not improve the moisture removing efficiency of the process. It is also interesting to note that at all pressures, increasing the pressing duration from 5 minutes to 30 minutes only results in a doubling of the level of moisture content removed.

When the pressing was conducted at an elevated temperature of approximately 100 °C, 41.9 % w/w of the initial moisture was the highest portion of water removed after 20 minutes of pressing at 450 bar. This percentage is slightly higher than that removed at ambient temperature and

similar conditions (38.8 % w/w). Relative to tests conducted for 20 minutes at ambient temperature, heating of the press to 100 °C reduced the influence of pressure, with an increase in pressure above 250 bar resulting in the removal of only a further ~2 % w/w (Figure 7.1). Based on the insensitivity to further pressure increases at elevated temperatures, and high initial rates of moisture removal at all conditions, it is suggested that a considerable fraction of the initial SCG water content is present as unbound excess moisture between individual particles that is easier to remove compared to bound moisture (held within individual particles). Mechanical pressing with the hydraulic ram press was also used as a pretreatment for moisture reduction of wet SCG prior to solvent extraction by ASE and these results are discussed in Section 7.3.

7.2 Mechanical expression of lipids

The hydraulic ram press was also used to expel lipids from dry SCG and SCG with a moisture content of ~5 % w/w. Pressing experiments of 30 minutes duration were conducted at pressures ranging from 150 to 550 bar and at both ambient and elevated temperature of ~100 °C, while at the beginning of each experiment the pressure was gradually increased to the desired pressure at a rate of approximately 50 bar/minute so as to avoid fine particles from blocking the outlet of oil capillaries. Nevertheless, the amount of oil expressed on all occasions was negligible, rendering the trials unsuccessful. This can possibly be attributed to the relatively high dynamic viscosity of waste coffee oil (50.989 mPa s at 40 °C, 8.716 at 100 °C) (Al-Hamamre et al., 2012), the thick cell walls of SCG (2.5 µm thick) that resist rupture (Schwartzberg, 1997), and the densely packed formation of the SCG that potentially resulted in clogging of oil capillary channels between the grounds.

RDCB were also pressed at ambient temperature in the hydraulic ram press for 60 minutes with the pressure applied increased from 350 to 550 bar at intervals of 20 minutes. Oil removal was negligible during the first 40 minutes at pressures between 150 and 350 bar but increased during the last phase of the experiment when a maximum pressure of 550 bar was applied. The amount of lipids expressed corresponded to an actual oil yield of 2.47 % w/w or 21.6 % w/w relative to the average Soxhlet yield achieved with RDCB. While the application of sheer pressure was not efficient in expressing lipids

from RDCB relative to Soxhlet extraction, it is suggested that a small portion of oil could be expressed from the RDCB sample because of the larger size of the beans relative to ICG1 grounds, that led to a loose sample formation when compared to the SCG tested, allowing for the formation of oil capillary channels.

The screw press described in Section 3.2.5.2 was also used for expressing lipids from partially dried ICG1 with moisture contents of 5 and 10 % w/w and from RDCB at a temperature of 100 °C. Similar to the ram press trials, oil release from the SCG was not achieved, rendering these trials unsuccessful. However, lipids were expressed from RDCB with the screw press and a crude oil yield of ~9 % w/w, or 78.8 % w/w relative to the average RDCB Soxhlet yield was obtained. A significant amount of fine particles was expressed along with the coffee oil, and, despite the filtering process, particles of diameter less than 25 µm remained in the oil sample.

The fatty acid profile of the expressed RDCB oil was determined onsite at NHE according to the method described in Appendix D and is shown in Table 7.1.

Table 7.1: Fatty acid composition of expressed RDCB oil.

Fatty acid	% weight percentage
C16:0	32.7
C18:0	7.1
C18:1	8.5
C18:2	44.9
C18:3	1.3
C20:0	2.7
Other	2.8

It can be seen in Table 7.1 that expressed RDCB oil mainly consists of linoleic, palmitic, oleic and stearic acid in proportions similar to those found in ICG1 oil extracted by the pilot plant with iso-hexane (Table 5.2). RDCB and ICG1 grounds were collected from the same industrial source and the similar

fatty acid profile of their lipids suggests that defective and healthy roasted beans, from which the ICG1 sample derived, contain oil of very similar fatty acid composition, in agreement with the findings of Oliveira et al. (2006). Furthermore, it suggests that the treatment of ICG1 to produce instant coffee does not significantly alter the fatty acid profile of the residual oil, while the similar composition of solvent-extracted ICG1 oil and expressed RDCB oil shows that these methods of lipid recovery do not significantly affect the fatty acid profile of the oil, an observation that is in agreement with a study performed by Ali and Watson (2014) with flax seeds.

The FFA content of the expressed RDCB oil was determined according to the method described in Section 3.2.6 and was found to be 4.42 ± 0.31 % w/w, a value which is of similar magnitude to that measured by Oliveira et al. (2006) who reported a FFA content of 4.97 % w/w for expressed RDCB oil. This value is lower than that of RDCB oil extracted through solvent extraction (7.82 ± 0.21 % w/w – Table 4.1) and it is tentatively suggested that mechanical expression extracts RDCB oil predominantly as triglycerides, while solvent extraction appears to preferentially extract FFAs from the feedstock. This observation is also supported by the findings of previous studies that reported mechanical expression to result in oil with lower levels of FFAs relative to lipids recovered through solvent extraction (Knowles and Watkinson, 2014; Willems et al., 2008b).

7.3 Mechanical pressing as pretreatment prior to solvent extraction

In this section the use of mechanical pressing, either as the sole pretreatment of SCG or followed by thermal drying, prior to solvent extraction through the ASE is investigated in order to evaluate its effect on lipid recovery efficiency. Wet ICG2 samples were subjected to pressing for 20 minutes at pressures ranging from 150 to 550 bar in the ram press, followed by thermal drying at 100 °C for 5 hours in an oven to completely remove moisture prior to solvent extraction through ASE. These experiments were conducted so as to investigate any possible effect of SCG pre-pressing on the efficiency of the subsequent solvent extraction, independent of the effect of moisture present.

Hexane was the solvent used and all ASE extractions took place at a temperature of 125 °C. Figure 7.3 shows the obtained oil extraction ratios relative to the average ICG2 oil yield achieved through Soxhlet extraction (Table 4.1) when samples subjected to pressing at different pressures were used.

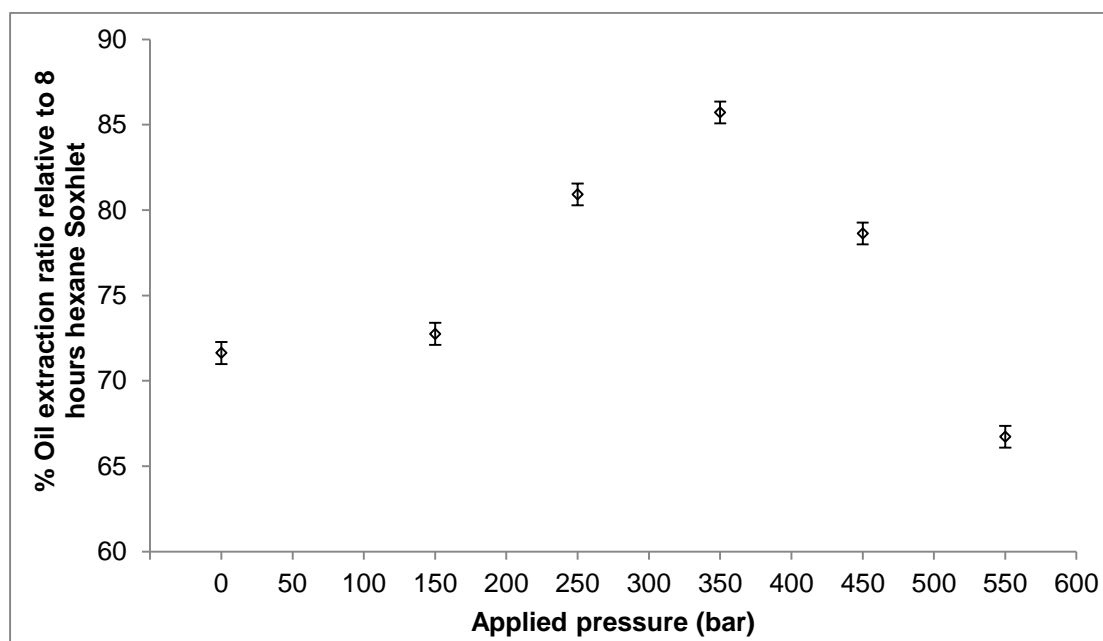


Figure 7.3: Oil extraction ratios obtained through ASE with SCG pressed at various pressures and thermally dried. Error bars represent standard deviation ($\sigma=0.6$) that was calculated from three experimental repeats.

Figure 7.3 shows that when ASE extraction is performed with a sample that has not undergone pressing, the average oil extraction ratio removed is 71.6 % w/w. The amount of oil extracted slightly increased when the sample had been pressed at 150 bar and then significantly improved when samples pressed at 250 and 350 bar were used, with oil extraction ratios of 80.9 and 85.7 % w/w obtained respectively. It can also be seen in Figure 7.3 that relative to pressing at 350 bar, pressing at 450 and 550 bar resulted in a decrease in the percentage of available oil extracted, with an extraction ratio of 66.7 % w/w achieved from the ICG2 samples pressed at 550 bar.

The apparent trend of increasing extraction efficiency with pre-pressing at pressures up to 350 bar can likely be explained by distortion of the cells due to the mechanical pressing, which also leads to the formation of a porous cake

with structural integrity that increases the efficiency of solvent extraction (Johnson and Lusas, 1983; Kemper, 2005). However, it is suggested that pressing at 450 and 550 bar has an inhibitory effect on the efficiency of the subsequent extraction, possibly attributable to the packed formation of the grounds caused by pressing which results in clogging of the oil capillary channels.

Furthermore, SCG which had been partially dried by mechanical pressing were used in ASE experiments with hexane and ethanol, in order to investigate the combined effect of prior mechanical pressing and SCG moisture content on the efficiency of solvent extraction by ASE. Wet ICG2 samples were subjected to pressing in the hydraulic ram press for 20 minutes at pressures of 150, 350 and 550 bar, and at ambient temperature, and resulted in samples with moisture contents of 49.50, 44.72 and 42.07 % w/w respectively. Figure 7.4 shows the crude extract extraction ratio obtained through ASE with hexane and ethanol at 125 °C against the moisture content of the samples, while the extraction ratios obtained when thermally dried and wet SCG were used are also presented for comparison purposes.

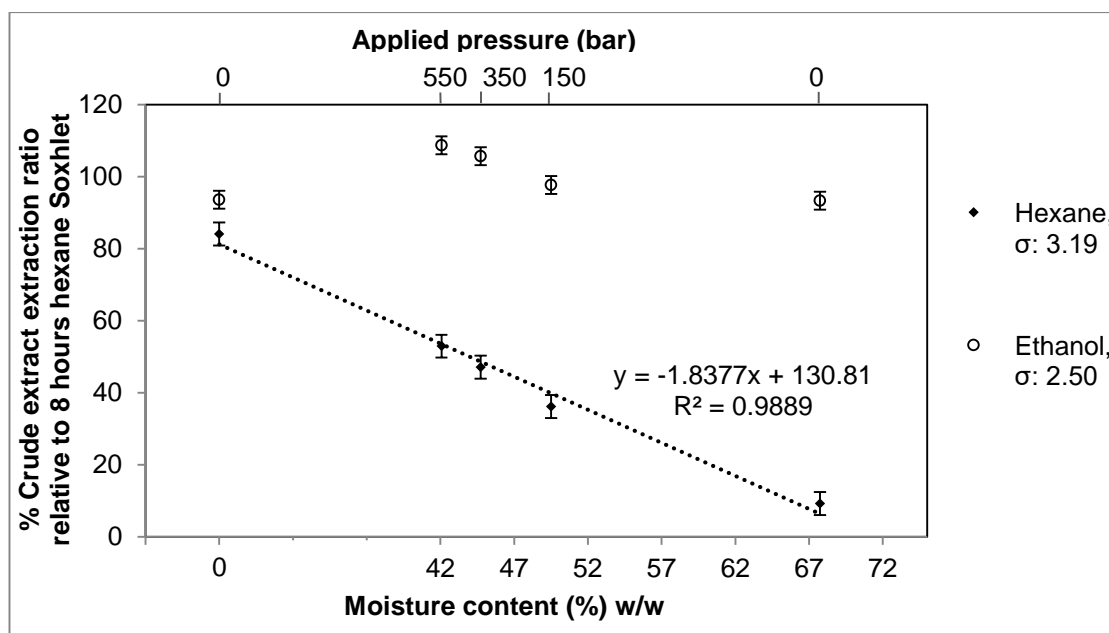


Figure 7.4: Crude extract extraction ratios obtained through ASE with hexane and ethanol against the moisture content of the SCG sample. The standard deviations were calculated from three experimental repeats.

Figure 7.4 shows that there is a correlation between increasing moisture content of the sample and decreasing extraction ratio when hexane was the solvent used ($R^2=0.98$). Hexane achieved extraction ratios of 9.23 and 52.92 % w/w relative to 8 hour Soxhlet extracted oil with hexane when samples with 67.73 % and 42.07 % w/w moisture content were tested respectively. On the contrary, the crude extract extraction ratio obtained with ethanol increased when a sample with a moisture content of 42.07 % w/w was used, and then slightly reduced when the moisture content of the samples tested further increased. Ethanol was found to be considerably more efficient than hexane in removing crude extracts at all moisture contents, resulting in extraction ratios ranging between 93.29 and 108.67 % w/w when samples with moisture contents of 67.73 and 42.07 % w/w were tested respectively. It is interesting to note that an almost identical extraction ratio was obtained from dried and wet SCG when ethanol was used at these conditions (Figure 7.4).

These results suggest that the moisture content of the SCG sample is a serious inhibitory factor for the extracting efficiency of the non-polar hexane, an observation that coincides with the results of Soxhlet extraction with hexane from partially wet SCG (Figure 5.6), but does not significantly impede the process of crude extracts recovery when ethanol is the solvent used. Generally, as water content increases, alcohol solvents become more polar and the solubility of lipids decreases, while solubility of other compounds like phosphatides, sugars and pigments increases, suggesting that the extraction of compounds other than triglycerides might be responsible for the high extraction ratios in the case of ethanol (Johnson and Lusas, 1983). Furthermore, the high extraction efficiency of ethanol with ASE at high moisture contents relative to Soxhlet (Figure 5.7), can be possibly attributed to operation at high temperatures that improves the solubility of oil in the ethanol-water mixture, the diffusion rate of the lipids and the mass transfer properties of the solvent (Camel, 2001; Johnson and Lusas, 1983; Richter et al., 1996). In addition, the heated and vaporized moisture generates internal pressure which ruptures the matrix cells and facilitates oil release (Veggi et al., 2013).

It is suggested therefore that thermal drying of wet SCG may not be necessary prior to solvent extraction at conditions of elevated temperature

when ethanol is the solvent used. Mechanical pressing can be used to remove part of the residing moisture so as to achieve slightly improved extraction ratios with ethanol. The non-polar hexane extracted lower amounts of crude extracts when partially dried SCG were used, and the effect of moisture content appeared to be more important than that of pre-pressing at different pressures, as pressing at 550 bar led to the highest extraction ratio (Figure 7.4), in contrast with SCG samples that had been pressed and subsequently dried in an oven, where it slightly inhibited the process of extraction after complete drying (Figure 7.3).

7.4 Conclusions

Significant moisture removal from SCG was achieved with a ram press (up to 42 % w/w of the total water present), and a correlation between increasing pressure from 150 to 450 bar and higher percentage of moisture removed was observed, with further pressure increase being insignificant or resulting in reduced water removal, possibly because of particle compaction. Longer durations of pressing resulted in the removal of significantly higher moisture percentages, while moisture reduction through pressing was improved at pressures of up to 350 bar and below at an elevated temperature of 100 °C.

Mechanical expression of lipids from SCG was unsuccessful, potentially due to the densely packed formation of the grounds and the high dynamic viscosity of the oil, however, expression of oil was achieved when whole RDCB were pressed, with a screw press being more effective than a ram hydraulic press. The FA profile of oil obtained from RDCB and ICG1 through pressing and solvent extraction with hexane respectively was almost identical, however, hexane extracted oil was found to have a considerably higher FFA content relative to oil expressed from RDCB, potentially because of preferential extraction of FFAs in solvent extraction.

The effect of mechanical pressing as a pretreatment method of wet SCG prior to drying and solvent extraction of lipids from dried SCG was beneficial until a maximum increase in oil extraction ratio was reached at 350 bar. Pressing at higher pressures appeared to inhibit the subsequent process of oil extraction from dry SCG due to clogging of oil capillary channels. Solvent extraction with

ASE from wet and partially wet pressed SCG with hydrophobic hexane resulted in a significant decrease in extraction ratio relative to completely dry SCG. ASE extraction at elevated temperature conditions from wet and partially dried pressed SCG with ethanol showed significantly reduced sensitivity to SCG moisture content relative to ASE trials with hexane and Soxhlet experiments with ethanol, because of the synergistic effect of high temperature and solvent polarity.

The following chapter concentrates on the transesterification of extracted SCG oil and the subsequent utilization of the obtained biodiesel in combustion experiments, either pure or blended with fossil diesel, so as to investigate its performance as a fuel for modern diesel engines.

8. Transesterification of SCG lipids and engine tests

This chapter presents experimental results obtained from transesterification of SCG oil and subsequent combustion experiments with untreated SCG oil and SCG derived biodiesel in a single cylinder research compression-ignition engine.

8.1 Transesterification of SCG lipids

This section presents results from the acid-catalyzed esterification of SCG oil and subsequent base-catalyzed transesterification of pretreated oil, regarding the effect of parameters such as duration, temperature, alcohol-to-oil molar ratio and catalyst weight percentage relative to oil on the efficiency of the process.

8.1.1 Acid-catalyzed pretreatment

Acid-catalyzed pretreatment trials were performed according to the method described in section 3.2.7.1 in order to reduce the FFA content of lipids extracted from ICG2 at the NHE pilot plant from an initial measured level of 29.91 ± 0.51 % w/w to a value below 1.5 % w/w prior to base-catalyzed transesterification, and evaluate the effect of certain parameters on the efficiency of this process. Prior to esterification, the density of the ICG2 oil was found to be 0.927 g/ml (Appendix C), a value similar to those reported in previous studies (Table 2.6). In the acid esterification process, one FFA molecule reacts with one methanol molecule to yield a FAME and a water molecule, however, excessive methanol was used to ensure a successful FFA conversion since the reaction is reversible (Chai et al., 2014). The various conditions of process temperature, methanol-to-FFA molar ratio and catalyst-to-FFA weight percentage that were investigated are presented in Table 8.1 .

Table 8.1: Acid-catalyzed esterification experimental conditions.

Trial	Temperature (°C)	Methanol-to-FFA molar ratio	% w/w Catalyst-to- FFA
1	50	17.8:1	3.2
2	50	17.8:1	6.4
3	50	13:1	6.4
4	50	13:1	3.2
5	60	17.8:1	6.4
6	60	17.8:1	3.2
7	60	13:1	6.4
8	60	13:1	3.2
9	60	22.5:1	6.4

Figures 8.1 and 8.2 show the FFA content of the pretreated SCG oil against the duration of the process, with oil samples subjected to esterification at different conditions of temperature, methanol-to-FFA molar ratio and catalyst-to-FFA weight percentage (Table 8.1). In order to facilitate the evaluation of the effect of various parameters on the efficiency of esterification process, the obtained results are presented in two sets depending on the catalyst-to-FFA weight percentage used, with Figures 8.1 and 8.2 showing results obtained at constant catalyst-to-FFA weight percentages of 3.2 % w/w and 6.4 % w/w respectively.

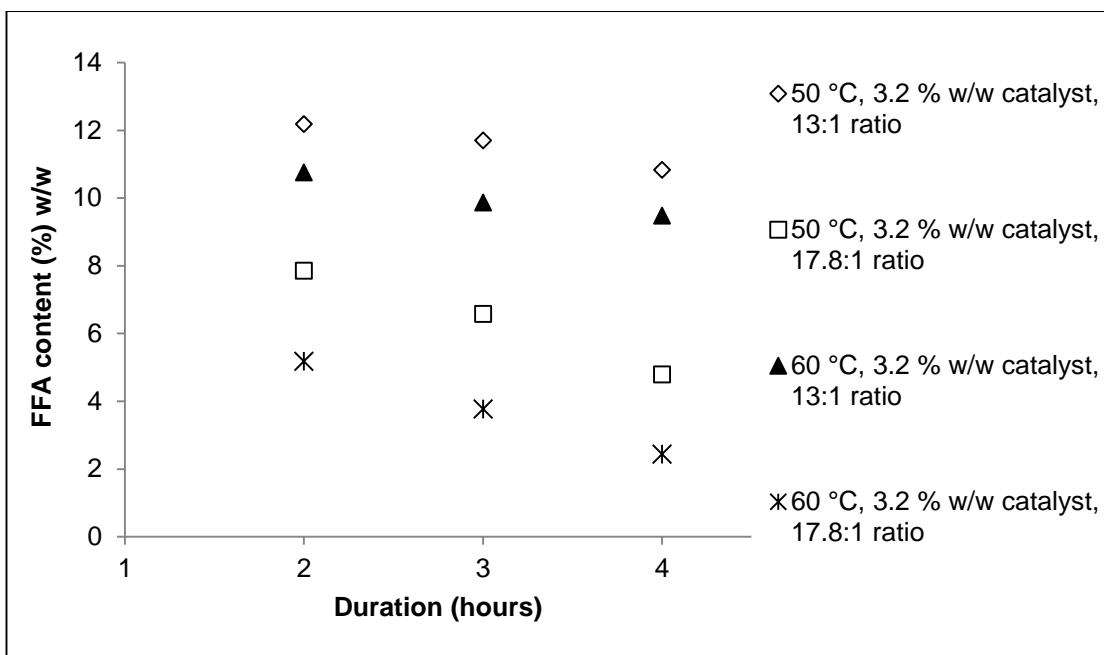


Figure 8.1: FFA content of ICG2 oil versus duration of acid-catalyzed esterification at a constant catalyst-to-FFA weight percentage of 3.2 % w/w. The standard deviation of each point was found to be 0.3 as calculated from three experimental repeats and a total of 27 titration measurements.

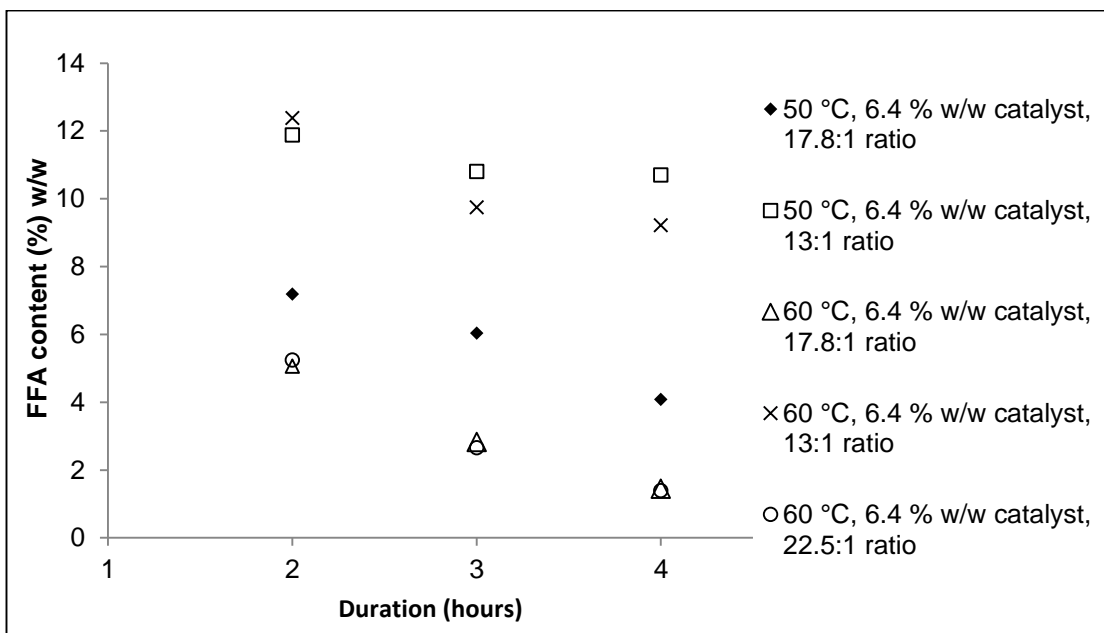


Figure 8.2: FFA content of ICG2 oil versus duration of acid-catalyzed esterification at a constant catalyst-to-FFA weight percentage of 6.4 % w/w. The standard deviation of each point was found to be 0.3 as calculated from three experimental repeats and a total of 27 titration measurements.

It can be seen in Figures 8.1 and 8.2 that an increase of process duration from 2 to 4 hours resulted in oil with reduced level of FFAs, regardless of the other experimental conditions. The obtained results showed that an acid-catalyzed esterification treatment of ICG2 oil at durations shorter than 4 hours was not sufficient for a successful conversion of FFAs into esters within the range of conditions investigated. An esterification duration of 4 hours was also found to be sufficient in previous studies that investigated the two-step transesterification of SCG oil, without the need for additional consecutive acid-catalyzed esterification steps for FFA reduction (Al-Hamamre et al., 2012; Vardon et al., 2013).

Furthermore, the temperature of the process had a significant impact on the efficiency of FFA esterification, with a higher temperature of 60 °C resulting in pretreated oil with lower FFA content relative to samples esterified at 50 °C in both Figures 8.1 and 8.2 and irrespective of the methanol-to-FFA molar ratio. The beneficial effect of increased esterification temperature, below the boiling point of methanol, on the efficiency of the process regardless of the lipid source has also been reported in previous studies (Eevera et al., 2009; Leung et al., 2010; Leung and Guo, 2006).

Regarding the effect of methanol-to-FFA molar ratio on the esterification of FFA, a ratio of 17.8:1 resulted in oil samples with lower FFA content compared to those esterified at a molar ratio of 13:1 in both of the examined temperatures and catalyst-to-FFA weight percentages (Figures 8.1 and 8.2). In particular, when the catalyst-to-FFA weight percentage used was 6.4 % w/w and the temperature set at 60 °C, a methanol-to-FFA molar ratio of 17.8:1 resulted in oil with 1.44 % w/w FFA content, below the required limit of 1.5 % w/w (Figure 8.2), and these were the experimental conditions used as the standard esterification method to provide pretreated oil suitable for the subsequent base-catalyzed transesterification.

Further increase of the methanol-to-FFA molar ratio from 17.8:1 to 22.5:1 at the same conditions of temperature and catalyst-to-FFA weight percentage did not significantly improve the efficiency of the process and only slightly reduced the FFA content of the oil to 1.39 % w/w, indicating that overly

excessive amounts of methanol did not further enhance the esterification reaction. The efficient conversion of FFAs into esters at methanol-to-FFA molar ratios of 17.8:1 and 22.5:1 is in agreement with previous studies that have suggested a molar ratio of approximately 20:1 as optimal for esterification pretreatment of lipid samples with high FFA content such as SCG oil (Caetano et al., 2014; Chai et al., 2014; Haile, 2014).

A comparison between Figures 8.1 and 8.2 shows that the use of a higher percentage of acidic catalyst relative to FFA (6.4 % w/w) led to oil samples with slightly reduced % w/w FFA contents, relative to those esterified with a catalyst-to-FFA weight percentage of 3.2 % w/w at the same conditions of temperature and methanol-to-FFA molar ratio. This is in agreement with the study of Chai et al. (2014) who reported that a catalyst-to-FFA percentage of approximately 5 % w/w is optimal for esterification of vegetable oils containing 15-35 % w/w FFA, while previous studies have reported that an increase in the amount of acid catalyst has a beneficial effect on the efficiency of the process (Canakci and Gerpen, 2001; Marchetti and Errazu, 2008). In particular, at the most favourable conditions of temperature and methanol-to-FFA molar ratio (Figures 8.1 and 8.2), different catalyst-to-FFA weight percentages of 6.4 % w/w and 3.2 % w/w resulted in pretreated oil with FFA contents of 1.44 and 2.43 % w/w respectively.

In general, the effect of methanol-to-FFA molar ratio on the conversion of FFAs during esterification process was found to be more crucial than that of sulfuric acid quantity within the range of investigated conditions (Figures 8.1 and 8.2). The experimentally determined optimal conditions of methanol-to-FFA molar ratio and catalyst-to-FFA weight percentage were somewhat similar to those reported in previous studies that investigated the esterification of vegetable oils with FFA content similar to that of ICG2 oil. In particular, sludge palm oil with 22.33-23.20 % w/w of FFAs (Hayyan et al., 2011, 2010) and waste cooking oil and tobacco seed oil with FFA contents of 37.96 % w/w and 35 % w/w respectively (Veljković et al., 2006; Wang et al., 2006) were reported to reach full FFA conversion into esters at a methanol-to-FFA molar ratio of between 13:1 to 18:1, and at a catalyst to weight percentage of 3.23%

w/w to 10.54 % w/w, with a tendency for higher optimal ratios when oil samples with higher FFA content were used.

In conclusion, the weight loss of pretreated SCG oil relative to initial untreated oil weight due to acid-catalyzed esterification pretreatment, when the process was carried out at optimal conditions (Trial 5 – Table 8.1), which was found to be 1.31 ± 0.73 % w/w, was likely attributable to the process of separating the excess methanol and water from the mixture, as small amounts of unreacted triglycerides and methyl esters can dissolve in the methanol and water mixture (Canakci and Gerpen, 2001; Kombe et al., 2012). This weigh loss is significantly lower than those observed by Haile (2014) and Berhe et al. (2013), who reported SCG oil losses of 6.8 % w/w and 8.67 % w/w respectively after acid-catalyzed pretreatment.

8.1.2 Base-catalyzed transesterification

Base-catalyzed transesterification experiments were performed with ICG2 oil previously subjected to acid-catalyzed esterification according to the method described in Section 3.2.7.2, while the specific experimental conditions of the pretreatment step were those presented in trial 5 of Table 8.1. The density of the pretreated oil was found to be 0.915 g/ml (Appendix C). Table 8.2 shows the different experimental conditions of methanol-to-pretreated oil molar ratio and catalyst-to-pretreated oil weight percentage, while process temperature and duration were kept constant at 60 °C and 4 hours respectively throughout the base-catalyzed transesterification experiments.

Table 8.2: Base-catalyzed transesterification experimental conditions.

Trial	Methanol-to-pretreated oil molar ratio	% w/w catalyst-to-pretreated oil
1	9:1	1
2	9:1	1.25
3	9:1	1.5
4	9:1	1.75
5	9:1	2
6	9:1	2.25
7	13.5:1	2.25
8	18:1	2.25
9	9:1	2.5
10	9:1	2.75

Figure 8.3 shows the effect of varying catalyst-to-pretreated oil weight percentage on the % w/w reaction yield expressed relative to initial pretreated oil weight, when the base-catalyzed transesterification was performed at a constant methanol-to-pretreated oil molar ratio of 9:1..

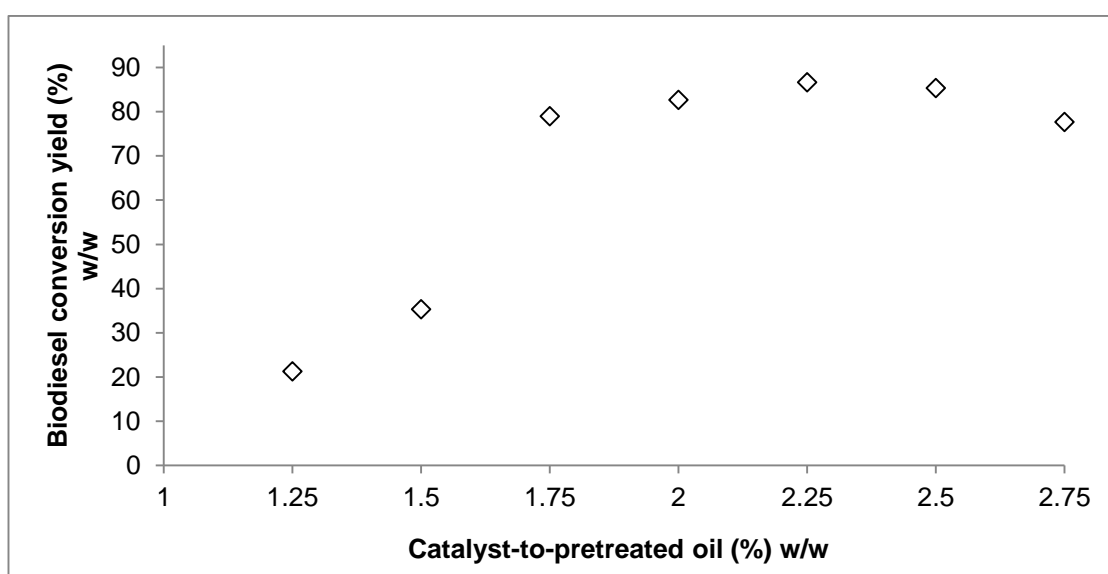


Figure 8.3: Base-catalyzed transesterification reaction yields against catalyst-to-pretreated oil weight percentage. The standard deviation (σ) was found to be 0.5 as calculated by a total of 9 experimental repeats.

It can be seen in Figure 8.3 that potassium hydroxide weight percentages up to 1.5 % w/w of the pretreated oil were not sufficient for successful conversion of oil into FAMEs, achieving low reaction yields. The low biodiesel reaction yields observed with potassium hydroxide percentages up to 1.5 % w/w can possibly be attributed to neutralization of the catalyst by unreacted acids that led to incomplete conversion of triglycerides into FAMEs. However, an increase of the catalyst percentage to 1.75 % w/w relative to oil resulted in significant increase of the conversion rate, with further increase to 2.25 % w/w resulting in the highest reaction yield of 86.66 % w/w.

Catalyst percentages higher than 2.25 % w/w led to a slight decrease of the reaction yield, potentially due to soap formation by the reaction of triglycerides with KOH, that reduced conversion rate and inhibited the separation of FAMEs from glycerol (Eevera et al., 2009; Leung et al., 2010). The pH of SCG biodiesel produced when the catalyst-to-oil weight percentage used ranged between 1.75 % w/w and 2.75 % w/w, was found to vary between 8.16 and 8.82 prior to FAME purification, with higher pH values corresponding to higher quantities of KOH used.

The optimal percentage of potassium hydroxide to pretreated oil weight of 2.25 % w/w was slightly higher than those reported in previous studies that investigated base-catalyzed transesterification of SCG oil, which ranged between 0.5 % w/w and 1.5 % w/w of the lipid weight (Berhe et al., 2013; Deligiannis et al., 2011; Haile, 2014; Kondamudi et al., 2008; Vardon et al., 2013). This difference in optimal quantity of base catalyst can possibly be attributed to the level of unreacted FFAs present in the ICG2 oil after the esterification pretreatment (1.44 ± 0.26 % w/w), which was higher than FFA levels of SCG oil samples in the aforementioned studies, thus requiring slightly higher catalyst amount. Furthermore, the initial reaction yield increase with % w/w catalyst-to-pretreated oil increase until an optimal value, with subsequent slight yield decrease with higher base catalyst amounts, has been also reported by studies that investigated the base-catalyzed transesterification of various vegetable oils such as coconut oil, palm oil, groundnut oil, rice bran oil, neem and cotton seed oil (Canakci and Gerpen, 2001; Eevera et al., 2009; Leung et al., 2010).

Figure 8.4 shows the effect of varying methanol-to-pretreated oil molar ratio on the efficiency of the base-catalyzed transesterification process, expressed through the % w/w reaction yield relative to initial pretreated oil weight. The experiments with different methanol-to-pretreated oil molar ratios were performed at a constant catalyst-to-pretreated oil weigh percentage of 2.25 % w/w.

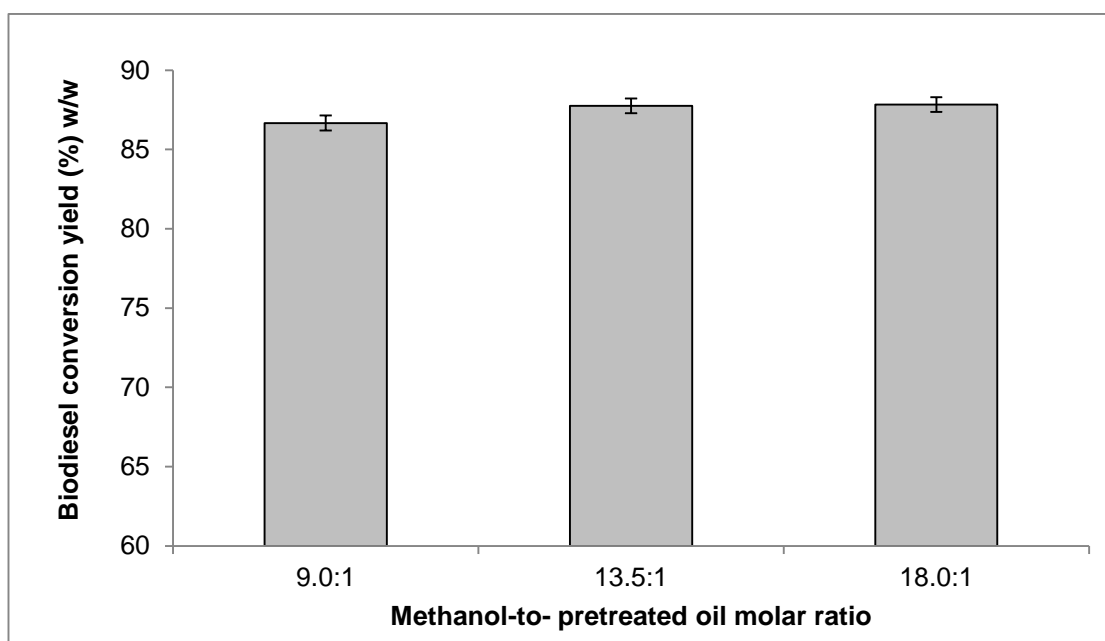


Figure 8.4: Base-catalyzed transesterification reaction yield against methanol-to-pretreated oil molar ratio. The error bars represent standard deviation ($\sigma=0.5$) that was calculated from three experimental repeats.

It can be seen in Figure 8.4 that an increase of the methanol-to-pretreated oil molar ratio from 9.0:1 to 13.5:1 resulted in slight increase of the process reaction yield, with further molar ratio increase to 18.0:1 having insignificant effect on the efficiency of base-catalyzed transesterification at the investigated conditions of duration, temperature and catalyst-to-oil weight percentage. The relationship found between methanol-to-oil molar ratio and reaction yield is in good agreement with previous studies that performed base-catalyzed transesterification of vegetable oils, which reported that increase of methanol-to-oil molar ratio above an optimal value had little effect on the reaction yield (Leung et al., 2010; Vyas et al., 2011). The slight increase of % w/w reaction yield with an increase of the methanol-to-oil molar ratio to 13.5:1 can be

possibly attributed to a decrease of pretreated oil viscosity due to increased alcohol quantity, which resulted in increased oil solubility in methanol and consequently higher FAME yield (Eevera et al., 2009).

The optimal methanol-to-pretreated oil molar ratio for base-catalyzed transesterification of vegetable oils including SCG oil has been reported to be 6:1 (Caetano et al., 2014; Eevera et al., 2009; Leung et al., 2010; Vardon et al., 2013), however, a molar ratio of 9:1 has been used in previous studies to achieve higher reaction yields from SCG oil (Al-Hamamre et al., 2012; Berhe et al., 2013; Deligiannis et al., 2011; Haile, 2014). Furthermore, previous studies that investigated the base-catalyzed transesterification of various vegetable oils such as jatropha oil, rubber seed oil and palm oil and have reported contradictory results of utilizing methanol-to-oil molar ratios higher than 9:1 (Vyas et al., 2011; Yusup and Khan, 2010). In particular, Yusup and Khan (2010) reporting a reduced conversion rate when a molar ratio of 10:1 was used due to enhanced saponification reaction caused by increase of alcohol quantity, while Vyas et al. (2011) achieved maximum conversion to FAMES with a methanol-to-oil molar ratio of 12:1, a finding that coincides with the relatively high conversion yield of SCG to FAMES obtained in this study with a slightly higher methanol-to-pretreated oil molar ratio of 13:5:1.

A comparison of the reaction yields obtained relative to catalyst-to-pretreated oil weight percentage and methanol-to-pretreated oil molar ratio presented in Figures 8.3 and 8.4 respectively, suggests that the amount of catalyst relative to oil weight has a more important effect on the efficiency of the process than the methanol-to-oil ratio within the investigated range. The relatively lower % w/w reaction yield obtained relative to previous studies that investigated base-catalyzed transesterification of SCG oil (Al-Hamamre et al., 2012; Deligiannis et al., 2011; Kondamudi et al., 2008; Vardon et al., 2013), can potentially be attributed to the FFA content of the pretreated oil that may have inhibited complete conversion into FAMES, and to the high methanol-to-oil molar ratios used which possibly enhanced emulsion and hindered the separation of FAMES from water (Eevera et al., 2009).

8.1.3 Oil and biodiesel properties

This section presents a compositional analysis of the SCG oil and biodiesel samples which were produced as described in Section 3.2.7, along with results related to their physical properties. Table 8.3 shows the elemental composition of ICG2 oil, acid-catalyzed ICG2 oil and biodiesel samples obtained at different conditions of methanol-to-pretreated oil molar ratio (Trials 6 and 8 – Table 8.2) on a weight basis, with the Carbon-Hydrogen-Nitrogen analysis (CE440 analyzer) and Oxygen analysis (MT/ELE/21) performed externally by Exeter Analytical Ltd. and Intertek Ltd. respectively (Appendix I). Elemental analyses of SCG oil and biodiesel from a previous study are also presented in Table 8.3 for comparison purposes.

Table 8.3: Elemental composition of SCG oil and biodiesel.

Sample	% w/w			
	C	H	N	O
ICG2 oil	76.72	11.83	0.05	11.9
Pretreated ICG2 oil	76.79	11.97	0	11.5
ICG2 biodiesel (Trial 6 - Table 8.2)	76.92	12.11	0.01	11.6
ICG2 biodiesel (Trial 8 - Table 8.2)	76.69	12.17	0	11.5
SCG oil (hexane-extracted) [1]	79.07	11.07	0.23	9.63
SCG biodiesel [1]	83.78	12.59	0.34	3.29

[1]: (Al-Hamamre et al., 2012).

It can be seen in Table 8.3 that the elemental composition of the ICG2 oil was not significantly affected by the acid-catalyzed esterification pretreatment and the subsequent base-catalyzed transesterification. No clear impact of oil processing for biodiesel production on the percentage of carbon contained in the intermediate and final products is apparent, while the percentage of hydrogen in the ICG2 biodiesel samples slightly increased relative to the initial ICG2 oil sample. The percentages of nitrogen and oxygen in treated oil and FAME samples were found to be marginally lower compared to raw oil. Furthermore, Table 8.3 shows a limited impact of the varying methanol-to-pretreated oil molar ratio on the elemental composition of the obtained

biodiesel, as very little difference is apparent in the analysis of trial 6 and trial 8 ICG2 biodiesel.

The small degree of difference found between samples can be attributed to the fact that the oxygen atoms, and the majority of carbon and hydrogen atoms present in the oil and biodiesel are associated with the fatty acid alkyl chains and ester groups common to both, while during transesterification the CH_2 groups belonging to glycerol are replaced by the CH_3 groups of methanol in FAMEs (Equation 2.2). This increase in molar hydrogen when triglycerides react with methanol to yield FAMEs is therefore plausibly responsible for the slight increase in the percentage of hydrogen in ICG2 biodiesel samples relative to untreated oil. It can also be seen in Table 8.3 that the elemental composition of ICG2 oil is similar to that of hexane-extracted SCG oil reported in a previous study. However, the elemental composition of SCG FAMEs reported by Al-Hamamre et al. (2012) significantly varied from the original SCG oil, an observation which is inconsistent with the findings of the present study.

Table 8.4 shows the fatty acid profile of ICG2 biodiesel samples produced at different base-catalyzed transesterification conditions of methanol-to-pretreated oil molar ratio (Table 8.2), along with those of soya and rapeseed biodiesel for comparison purposes. Regarding the biodiesel properties presented in Table 8.4, it should be noted that the different ICG2 biodiesel samples which were produced at varying conditions of base-catalyzed transesterification were subsequently mixed so as to increase the quantity of biodiesel available for engine testing (Section 8.2). Therefore, the acid value, density, kinematic viscosity and HHV of this mixture were determined and are shown in Table 8.4. The acid values, fatty acid profiles and HHVs of biodiesel samples were determined according to the methods described in Sections 3.2.6, 3.2.8 and 3.2.9 respectively. The kinematic viscosity and density of ICG2 biodiesel were calculated according to the methods described in Appendix J and C, while those of soya and rapeseed biodiesel were provided by the source of the fuels (BP Global Fuels, Appendix E). Table 8.4 also shows the properties of the reference fossil diesel (Appendix E) and the

generally applicable diesel quality requirements according to European standard EN 14214 (BSI Standard, 2014).

Table 8.4: Fatty acid profile and properties of SCG, soya and rapeseed biodiesel. The standard deviations in the case of Acid value and HHV were calculated from three experimental repeats.

Sample	% (w/w) Fatty acid/Total								Average chain length	Average number of double bonds	SFA	PUFA	Density at 15 °C (g/cm ³)	AV (mg _{KOH} /g)	KV at 40 °C (mm ² /s)	HHV (MJ/kg)
	C16:0	C18:0	C18:1	C18:2	C18:3n6	C18:3n3	C20:1	Unknown								
ICG2 biodiesel (Trial 6)	34.19	7.92	9.29	43.60	2.81	1.13	-	1.06	17.12	1.08	42.11	47.54	0.893	0.55 ± 0.06	6.26	39.72 ± 0.428
ICG2 biodiesel (Trial 7)	34.43	7.96	9.23	43.14	2.88	1.08	-	1.27	17.08	1.07	42.39	47.10				
ICG2 biodiesel (Trial 8)	34.24	7.92	9.22	43.40	2.90	1.11	-	1.19	17.10	1.08	42.17	47.42				
Soya biodiesel	10.32	4.36	26.80	50.69	-	6.75	-	1.08	17.60	1.48	14.69	57.44	0.885	0.18 ± 0.03	4.075	40.55 ± 0.221
Rapeseed biodiesel	4.80	1.78	61.24	21.52	-	7.82	1.25	1.59	17.87	1.29	6.59	29.34	0.883	0.27 ± 0.05	4.325	40.28 ± 0.184
Reference diesel					-								0.835	-	2.892	45.68
EN 14214 [1]					-								0.860-0.900	<0.5	3.5-5	-

SFA: Saturated fatty acids, PUFA: Polyunsaturated fatty acids, AV: Acid value, KV: Kinematic viscosity, [1]: (BSI Standard, 2014).

It can be seen in Table 8.4 that the main fatty acid esters in the ICG2 biodiesel are linoleic (C18:2), palmitic (C16:0), oleic (C18:1) and stearic (C18:0), with lower quantities of γ -linolenic (C18:3n6) and α -linolenic (C18:3n3) in decreasing order of magnitude. The variations in the percentages of the fatty acids present in ICG2 biodiesel samples are relatively small, suggesting that the transesterification process, and in particular the varying methanol-to-pretreated oil molar ratio of the base-catalyzed step, did not have a significant and systematic effect on the fatty acid profile of the resulting SCG biodiesel. Furthermore, the fatty acid profile of the obtained ICG2 biodiesel is similar to the fatty acid profile of ICG1 biodiesel (Table 5.2), while similarities can also be found with the fatty acid profiles of SCG FAMEs reported in previous studies (Table 2.5).

The density of the ICG2 biodiesel mixture was found to be slightly higher than the densities of soya and rapeseed FAMEs but within the standard EN 14214 limit of 0.860-0.900 g/cm³ (BSI Standard, 2014). In addition, the density of ICG2 biodiesel was lower than that of untreated ICG2 oil which was found to be 0.927 kg/m³ (Appendix C), and similar to that of SCG biodiesel samples reported in previous studies (Table 2.9).

The acid value of ICG2 was found to be slightly higher than the standard EN 14214 limit of 0.5 mg_{KOH}/g (BSI Standard, 2014), while the acid values of soya and rapeseed biodiesel were within the limit. The relatively high acid value of ICG2 biodiesel, which corresponds to a FFA content of 0.27 % w/w, can potentially be attributed to incomplete transesterification due to the relatively high FFA content of the acid-catalyzed pretreated oil (1.44 ± 0.27 % w/w).

The kinematic viscosity of the ICG2 biodiesel was significantly reduced relative to that of raw ICG2 oil which was found to be 45.7 mm²/s (Appendix J), but greater than that of soya and rapeseed biodiesel and above the standard EN 14214 limit of 3.5-5 mm²/s (BSI Standard, 2014). The high viscosity of ICG2 biodiesel can be possibly attributed to an incomplete transesterification reaction and/or inefficient purification process that may have not separated traces of glycerol from the ester phase. Furthermore, the

relatively high acid value of ICG2 biodiesel indicates the presence of FFAs which might also be responsible for the high kinematic viscosity.

The HHV of biodiesel derived from ICG2 oil through two-step transesterification was found to be higher than that of ICG2 oil (39.05 ± 0.15 MJ/kg, Table 4.1) and similar to SCG biodiesel HHVs measured in previous studies (Table 2.9). The HHVs of soya and rapeseed FAMEs were slightly higher than that of ICG2 biodiesel, possibly attributable to their longer average chain length due to higher presence of C18 chains in soya and rapeseed FAMEs compared to ICG2 FAMEs (Table 8.4).

8.2 Combustion experiments

Engine tests were performed with reference fossil diesel, neat ICG2, soya and rapeseed biodiesel and blends of 7 % v/v and 20 % v/v of each of the FAMEs with reference fossil diesel, while raw ICG2 oil was also used directly as a fuel after heating to 45 °C. All combustion experiments were performed in a compression-ignition research engine (Section 3.2.11) at constant engine speed of 1200 rpm and fuel injection pressure of 600 bar, while the injection duration was adjusted in each test in order to maintain a constant IMEP of 4 bar. In the experiments with raw ICG2 oil, the fuel injection pressure was initially increased to 860 bar at constant injection conditions and 940 bar at constant ignition conditions so as to ignite the sample before decreasing it to measurement conditions (600 bar) for the collection of in-cylinder pressure and exhaust emissions data. An injection timing of 5.0 CAD before TDC was selected in the case of constant injection tests, whereas the SOI was varied for each sample in the constant ignition timing experiments to ensure that the SOC always occurred at TDC. Table 8.5 shows the SOI timing that was selected for each sample in constant ignition timing experiments.

Table 8.5: Injection timings in constant ignition timing experiments.

Sample	Injection timing (CAD)
Reference fossil diesel	4.7-5.0
Raw ICG2 oil	5.2
ICG2 B7	5.0
ICG2 B20	4.4
ICG2 B100	4.2
Rapeseed B7	4.3
Rapeseed B20	4.3
Rapeseed B100	3.6
Soya B7	4.4
Soya B20	4.5
Soya B100	4.2

Figures 8.5 and 8.6 show the engine in-cylinder pressure during combustion of the various fuel samples and reference diesel at constant injection and constant ignition timing conditions respectively.

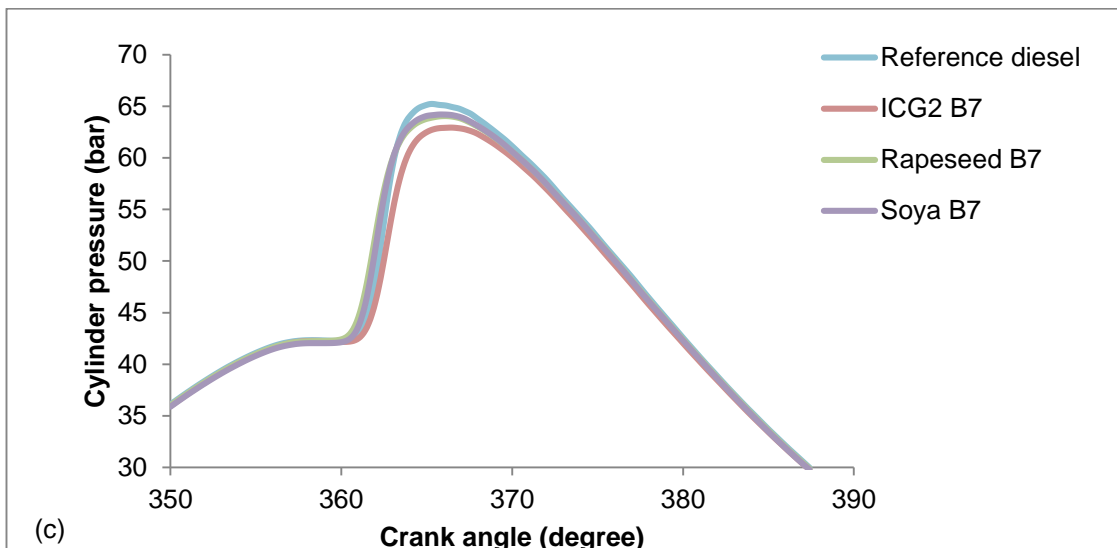
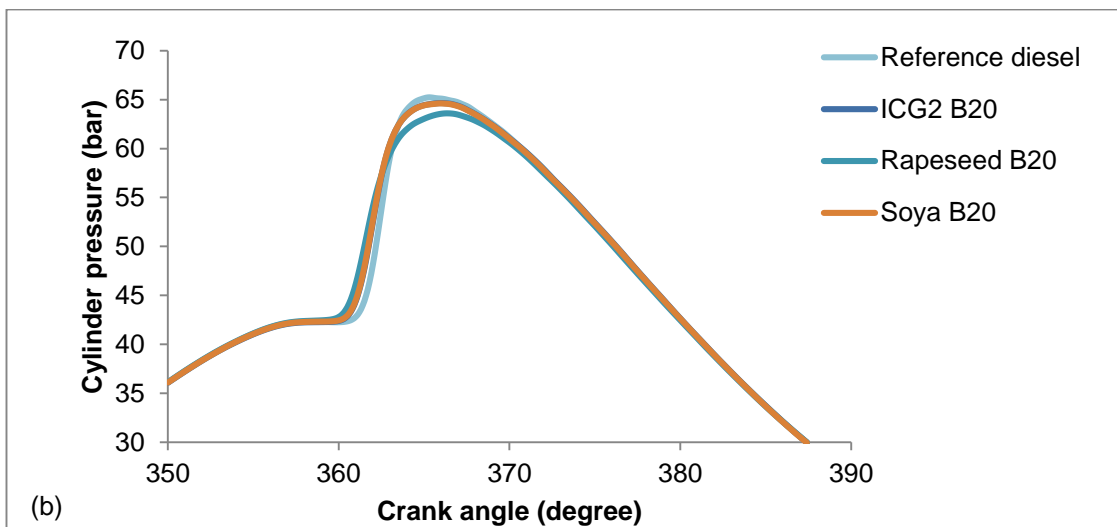
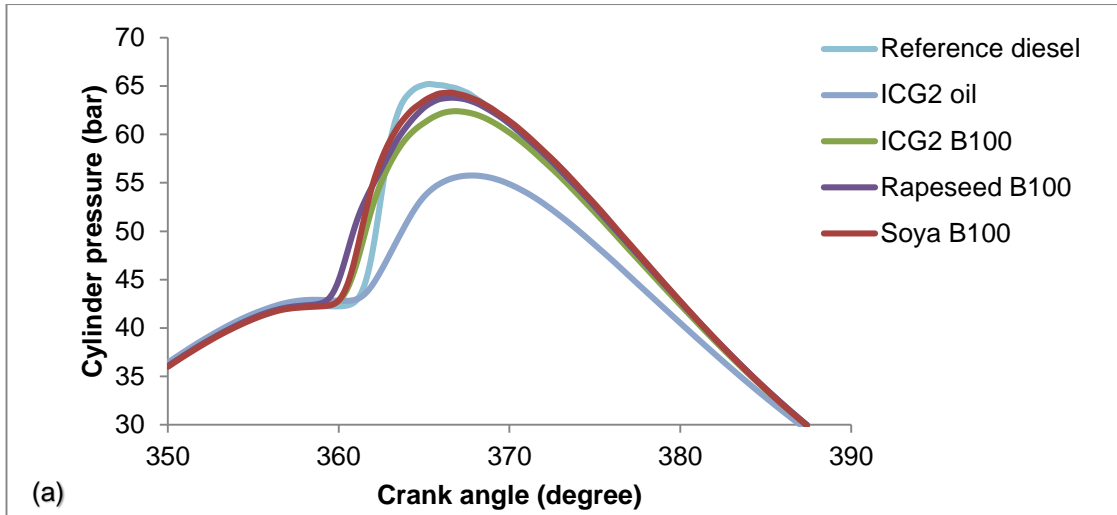


Figure 8.5: (a) In-cylinder pressure of ICG2 oil, reference diesel and 100 % v/v ICG2, soya and rapeseed FAMEs, (b) 20 % v/v FAME and fossil diesel blends, (c) 7 % v/v FAME and fossil diesel blends at constant injection timing.

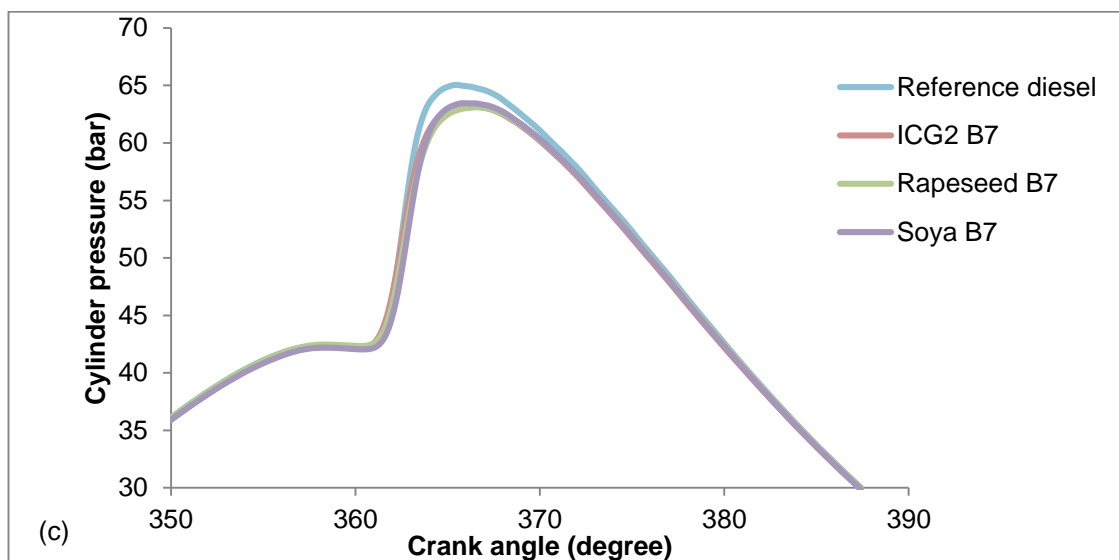
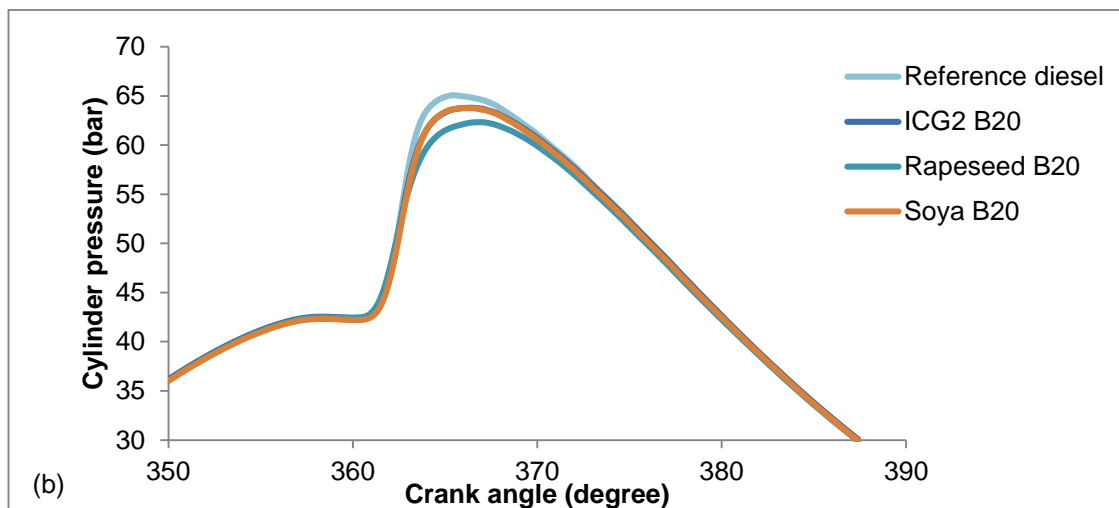
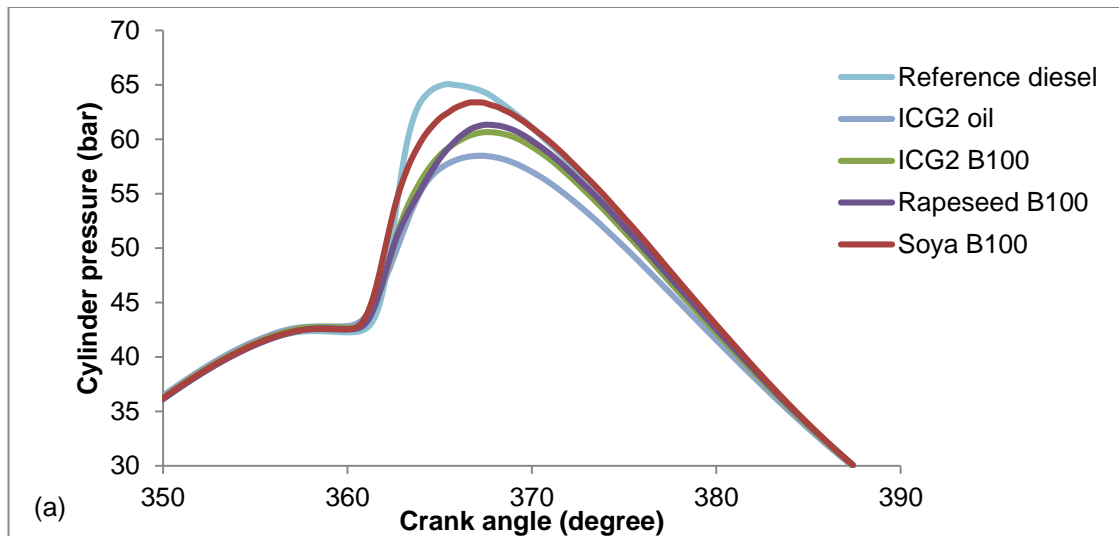


Figure 8.6: (a) In-cylinder pressure of ICG2 oil, reference diesel and 100 % v/v ICG2, soya and rapeseed FAMES, (b) 20 % v/v FAME and fossil diesel blends, (c) 7 % v/v FAME and fossil diesel blends at constant ignition timing.

It can be seen in Figures 8.5 and 8.6 that the lowest in-cylinder pressure occurred when ICG2 oil was used directly without transesterification or blending, while at both conditions the reference fossil diesel showed the highest in-cylinder pressures. The high in-cylinder pressure achieved with reference fossil diesel relative to other fuel samples used can be attributed to a larger amount of premixed fuel prior to ignition and hence a greater rate of initial heat release close to TDC. The lower peak in-cylinder pressure achieved with raw ICG2 oil and neat ICG2 biodiesel is likely attributable to reduced air mixing and subsequent lower rates of combustion resulting from poor fuel atomisation, due to the high viscosity of raw ICG2 oil ($45.7 \text{ mm}^2/\text{s}$ at $40 \text{ }^\circ\text{C}$ – Appendix J), and the relatively high viscosity of the neat ICG2 biodiesel compared to other biodiesel samples ($6.26 \text{ mm}^2/\text{s}$ at $40 \text{ }^\circ\text{C}$ - Table 8.4).

Of the various FAME samples tested at conditions of constant injection timing, neat ICG2 biodiesel showed the lowest peak in-cylinder pressure of all the neat or blended samples tested, while rapeseed biodiesel blends showed similar or lower peak pressures relative to ICG2 biodiesel blends at conditions of constant ignition timing. It can also be seen in Figure 8.5(a) that neat rapeseed biodiesel ignited earlier than the other samples at conditions of constant injection timing. In general, both Figure sets 8.5 and 8.6 show that the reduction in the amount of FAME present in the biodiesel and fossil diesel blends generally resulted in higher peak in-cylinder pressures.

Figures 8.7 and 8.8 show the apparent net heat release rate of neat and blended ICG2, soya and rapeseed FAMEs, ICG2 oil and reference diesel at constant injection and constant ignition timing conditions respectively.

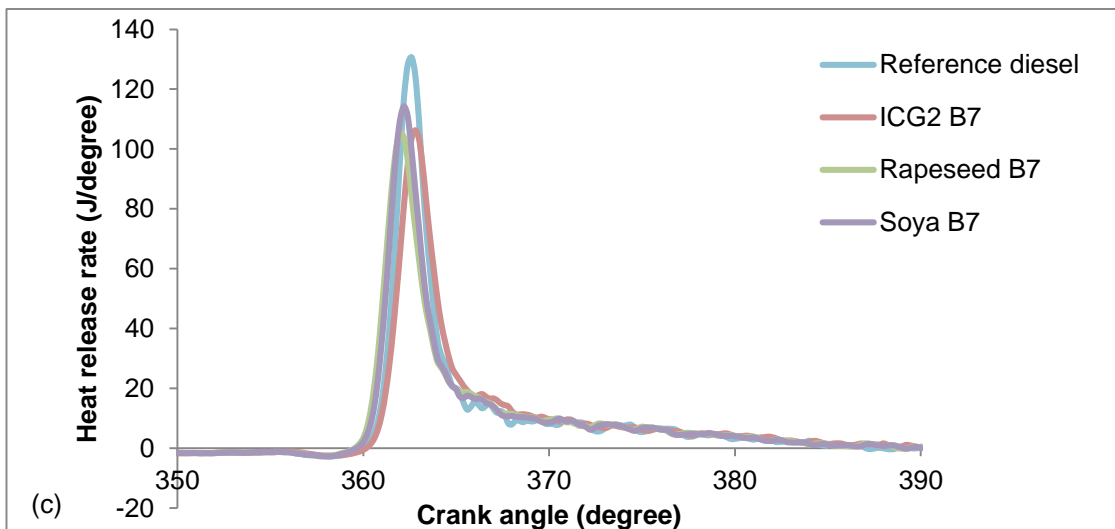
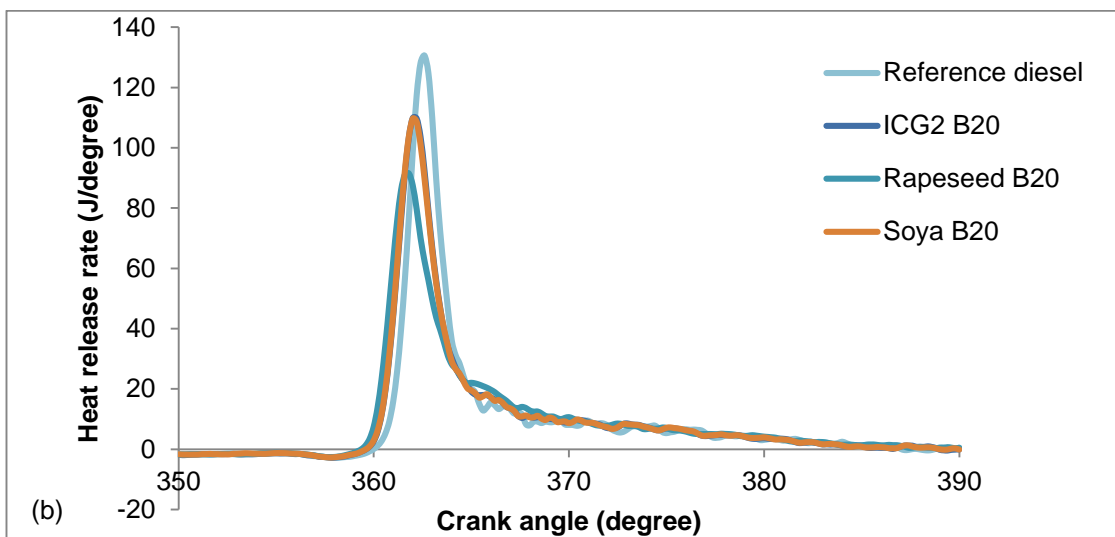
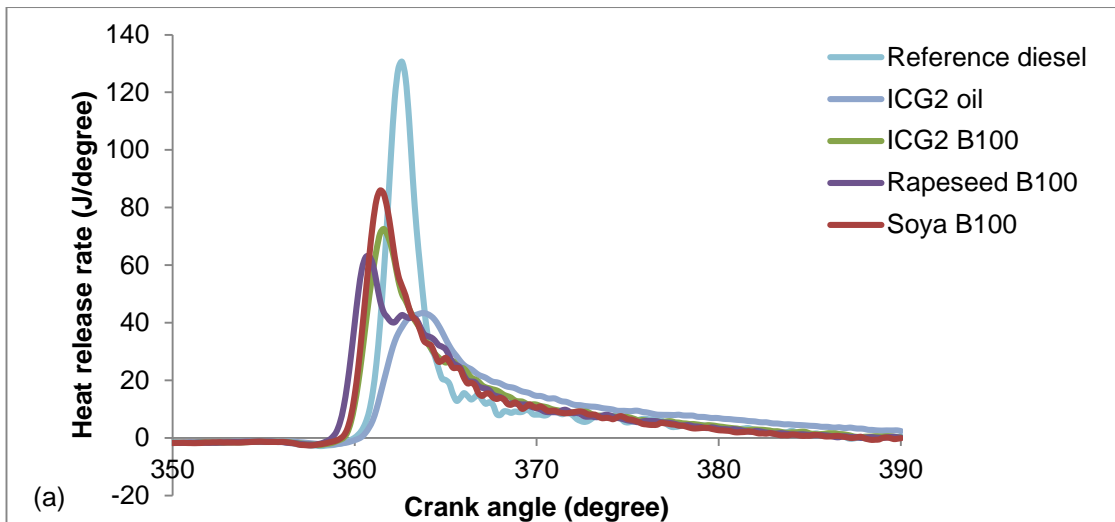


Figure 8.7: (a) Heat release rate of ICG2 oil, reference diesel and 100 % v/v ICG2, soya and rapeseed FAMES, (b) 20 % v/v FAME and fossil diesel blends, (c) 7 % v/v FAME and fossil diesel blends at constant injection timing.

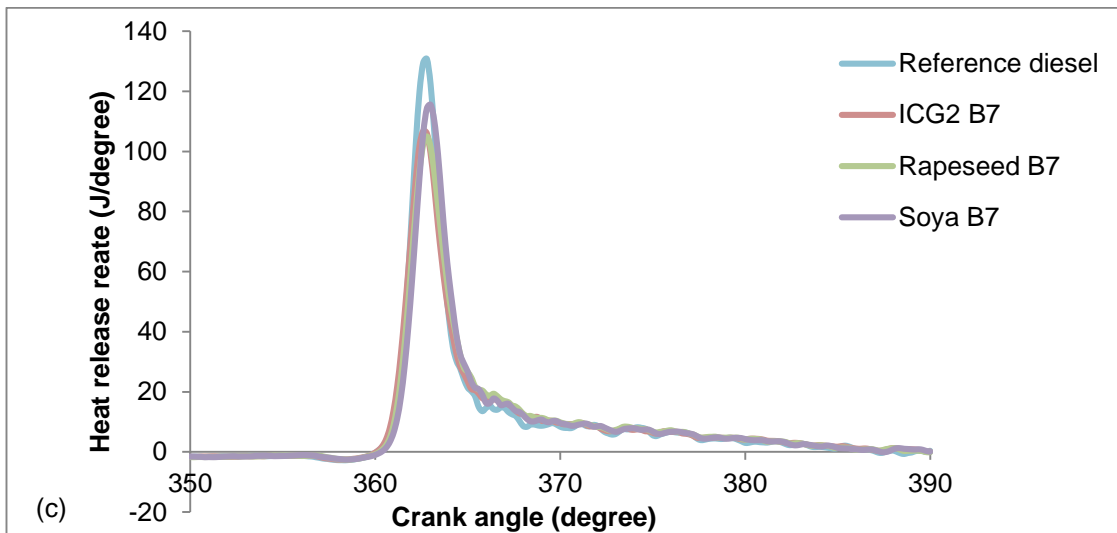
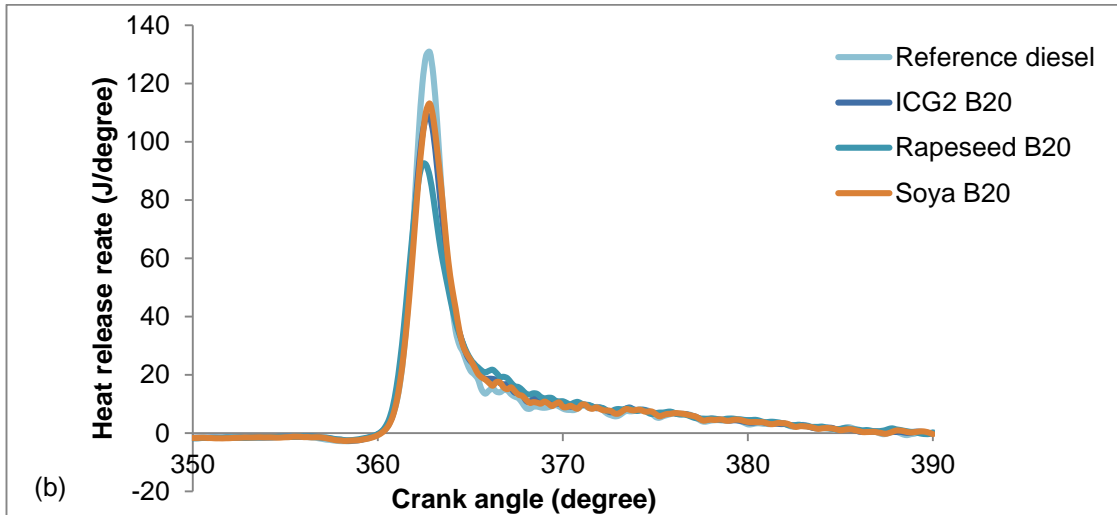
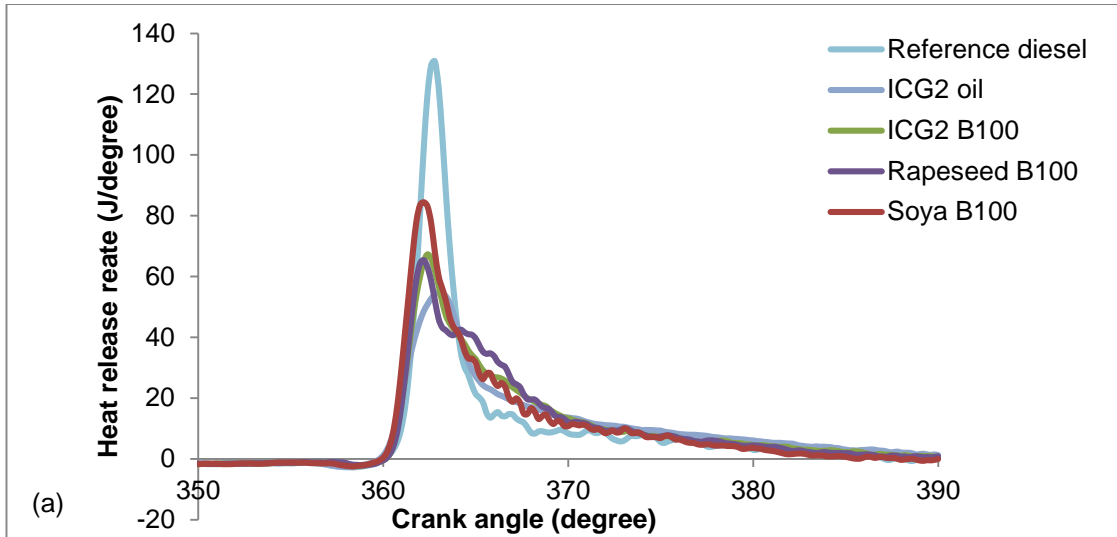


Figure 8.8: (a) Heat release rate of ICG2 oil, reference diesel and 100 % v/v ICG2, soya and rapeseed FAMES, (b) 20 % v/v FAME and fossil diesel blends, (c) 7 % v/v FAME and fossil diesel blends at constant ignition timing.

It can be seen in Figures 8.7 and 8.8 that for all the samples used, the apparent HRR reduced to values below zero just before ignition due to the fuel spray absorbing energy (enthalpy of vaporization) from the in-cylinder air to form the vapour/air mixture that subsequently ignited. In the case of reference fossil diesel and biodiesel blends, the majority of heat release occurred during premixed combustion, defined as the combustion of fuel and air that are mixed to combustible stoichiometry during the ignition delay period (Hellier et al., 2013), as signified by the rapid rise of heat release rates following SOC.

The significant change in the slope of the curves after premixed combustion, which occurred at 365 CAD in the case of fossil reference diesel (Figures 8.7(a) and 8.8(a)), indicates that the premixed amount of fuel/air mixture had been consumed and signals the transition of the combustion mode from premixed to diffusion burning dominated. Fuels with a small premixed burn fraction have more of the injected fuel burning in the diffusion-combustion mode, as is the case with the neat rapeseed biodiesel for which combustion became diffusion burning dominated at 361 CAD as shown in Figure 8.7(a).

The raw ICG2 oil showed a low heat release rate during premixed mode at both timing conditions, possibly due to poor mixing, followed by a subsequent higher rate of heat release compared to other samples during diffusion burning mode, from approximately 365 CAD onwards (Figure 8.7(a)). On the contrary, reference fossil diesel showed the highest peak heat release rate in both Figure sets 8.7 and 8.8, with the majority of heat release occurring during the premixed combustion. Consequently, fossil diesel shows a low HRR during diffusion burning mode as most of the injected fuel had already burned in the premixed mode.

Figures 8.9 and 8.10 show the ignition delay of the various samples used in the engine experiments against their biodiesel content, where 0 % v/v biodiesel is pure reference fossil diesel, at constant injection and constant ignition timing conditions respectively.

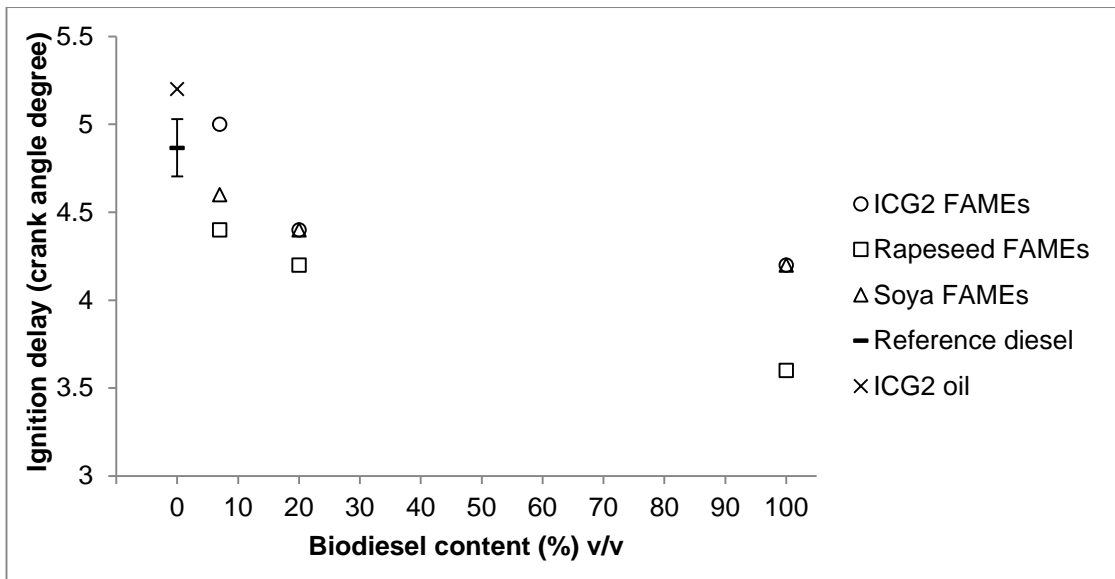


Figure 8.9: Ignition delay against biodiesel content at conditions of constant injection timing. The error bars shown represent standard deviation ($\sigma=0.16$) calculated by 6 experimental repeats with reference diesel.

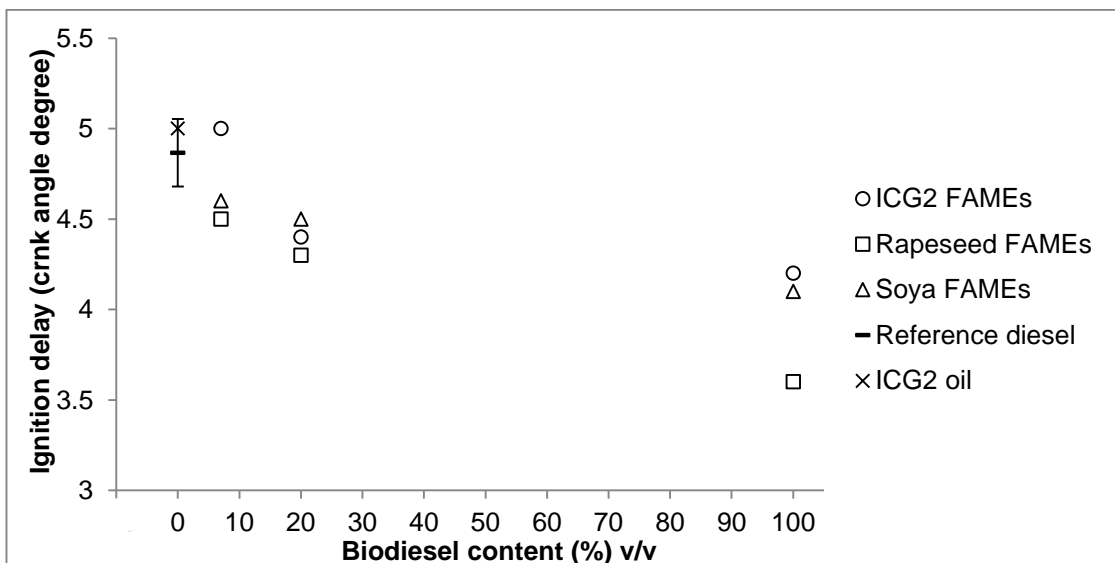


Figure 8.10: Ignition delay against biodiesel content at conditions of constant ignition timing. The error bars shown represent standard deviation ($\sigma=0.18$) calculated by 6 experimental repeats with reference diesel.

It can be seen in both Figures 8.9 and 8.10 that the neat biodiesel samples exhibited the shortest duration of ignition delay of all the samples tested, while reference fossil diesel and raw ICG2 oil had the longest delays. Also apparent is that in the case of all three varieties of FAMES tested (ICG2, soya,

rapeseed), an increase of the biodiesel content from 7 % v/v to 100 % v/v resulted in a decrease in the ignition delay time at both timing conditions.

In general, FAMEs tend to have shorter ignition delay relative to fossil diesel due to the presence of long alkyl carbon chains which can undergo hydrogen abstraction and break down more easily than some of the molecules present in fossil diesel (e.g. aromatic molecules, isomers and naphthenes in diesel are more difficult to ignite than the long alkyl chains of FAMEs) (Koivisto, 2016). In addition the aromatic molecules in fossil diesel can have hydrogen abstracted but subsequently absorb radicals to re-stabilize and thus reduce the radical pool which would otherwise accelerate the process of ignition.

Long ignition delays have been associated with low fuel cetane numbers and high degree of FAME unsaturation (Canakci and Sanli, 2008; Pinzi et al., 2009). Therefore, and drawing conclusions from the fatty acid profiles of ICG2, soya and rapeseed biodiesel presented in Table 8.4, the soya and rapeseed FAMEs might have been expected to exhibit longer ignition delays compared to ICG2 FAMEs which were more saturated. However, it can be seen in Figures 8.9 and 8.10 that ICG2 biodiesel exhibits a longer ignition delay than the rapeseed FAME blends, and equivalent or longer ignition delay than the soya FAME blends; this can potentially be attributed to the higher viscosity of the ICG2 biodiesel which may have caused a longer ignition delay due to prolonged fuel vaporization and formation of the fuel vapour and air mixture (Canakci and Sanli, 2008). This hypothesis is also supported by the long ignition delay of the viscous raw ICG2 oil.

Furthermore, while the ICG2 FAMEs possess a greater proportion of fully saturated components, the average alkyl chain length of the soya and rapeseed esters is slightly longer (Table 8.4). In addition, the higher presence of longer chain C18 FAMEs in rapeseed and soya biodiesel relative to ICG2 biodiesel (Table 8.4), the presence of which results in higher cetane number and consequently shorter ignition delay (Canakci and Sanli, 2008; Hellier and Ladommatos, 2015; Pinzi et al., 2009).

Figures 8.11 and 8.12 show the peak heat release rate (PHRR) of the samples used in combustion experiments against the biodiesel content at conditions of constant injection and constant ignition timing respectively.

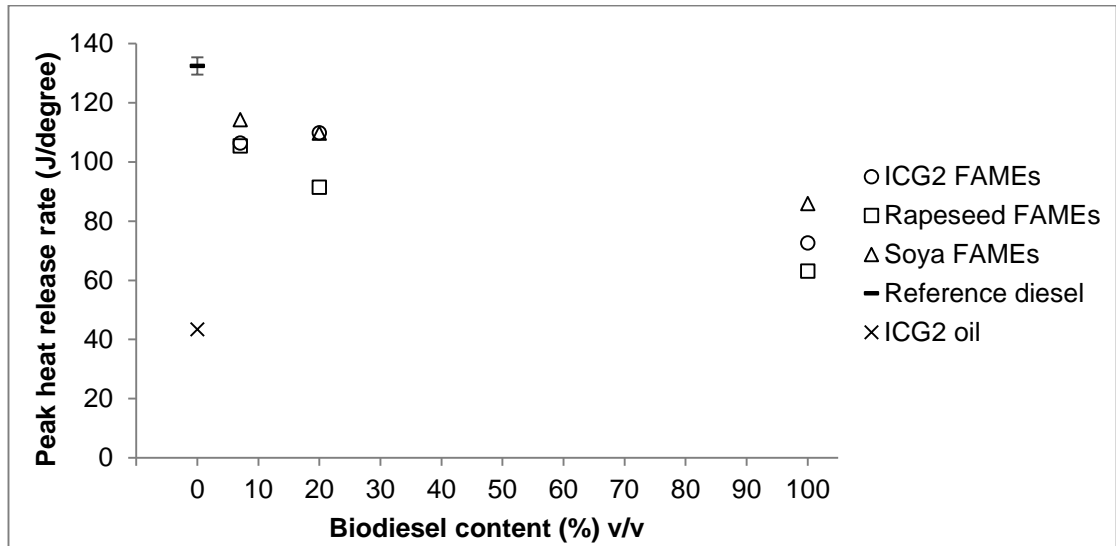


Figure 8.11: Peak heat release rate against biodiesel content at constant injection timing. The error bars shown represent standard deviation ($\sigma=2.9$) calculated by 6 experimental repeats with reference diesel.

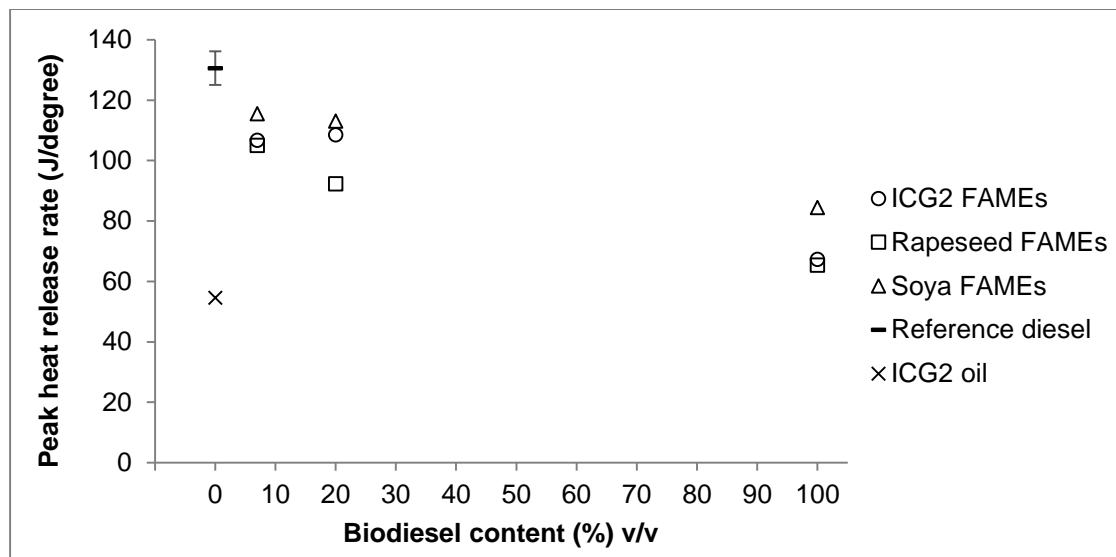


Figure 8.12: Peak heat release rate against biodiesel content at constant ignition timing. The error bars shown represent standard deviation ($\sigma=5.6$) calculated by 6 experimental repeats with reference diesel.

It can be seen in both Figures 8.11 and 8.12 that reference fossil diesel displayed the highest PHRR of all samples at both timing conditions, and raw ICG2 oil the lowest. The PHRRs of the neat and blended biodiesel samples were found to be in between those of fossil diesel and ICG2 oil, with neat biodiesel having a significantly lower PHRR relative to the blended samples (Figures 8.11 and 8.12).

PHRR and ignition delay are closely related and it has been previously observed that increased ignition delay time allows more time for fuel and air mixing prior to ignition, resulting in a larger premixed combustion fraction and therefore higher PHRR (Hellier et al., 2011). In the case of the reference diesel, the high PHRR observed might also be attributable to the presence of volatile components absent from biodiesel samples, which combined with the long ignition delay, helped form a large amount of premixed fuel/air mixture that then burned rapidly once ignition occurred.

However, raw ICG2 oil displays a low PHRR despite a long ignition delay duration similar to that of reference fossil diesel (Figures 8.9 and 8.10), suggesting that ignition delay is not the only limiting factor on the rate of fuel and air mixing. The low PHRR of the raw ICG2 oil can therefore possibly be attributed to its high viscosity (Table 8.4), which potentially inhibits the fuel and air mixing during the ignition delay period, thus reducing the extent of the premixed fuel fraction and consequently the PHRR.

Figures 8.13 and 8.14 show the exhaust gas NO_x emissions of the various fuel samples and reference fossil diesel at constant injection and constant ignition timings respectively.

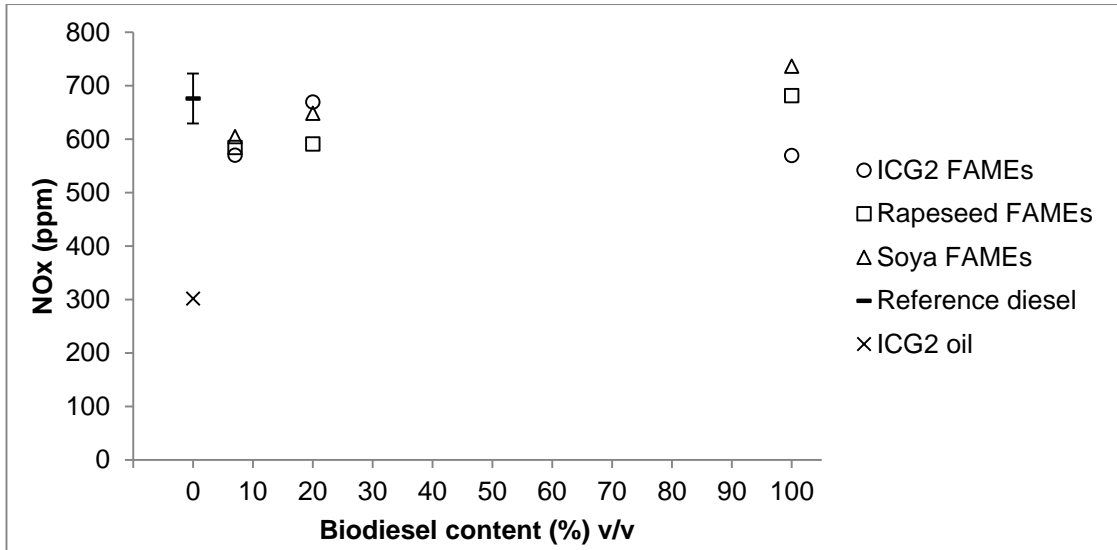


Figure 8.13: Exhaust gas NO_x emissions of fuel samples and reference fossil diesel against biodiesel content at constant injection timing. The error bars shown represent standard deviation ($\sigma=46.7$) calculated by 6 experimental repeats with reference diesel.

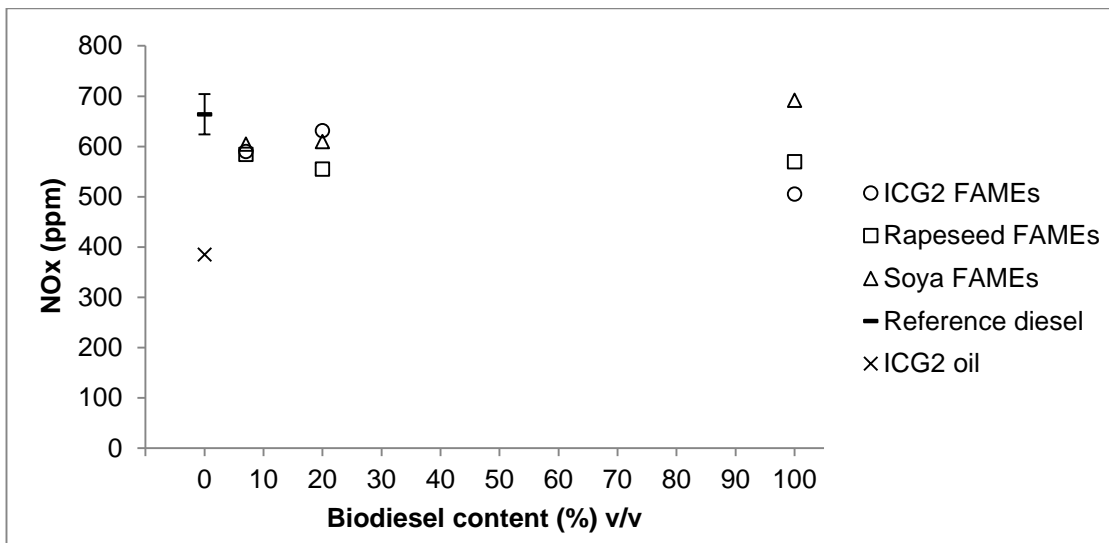


Figure 8.14: Exhaust gas NO_x emissions of fuel samples and reference fossil diesel against biodiesel content at constant ignition timing. The error bars shown represent standard deviation ($\sigma=40.2$) calculated by 6 experimental repeats with reference diesel.

Figures 8.13 and 8.14 show that at both timing conditions raw ICG2 oil emitted significantly lower levels of NO_x relative to all the other investigated fuel samples. Reference fossil diesel and neat soya biodiesel emitted the highest

NO_x levels of all fuel samples, while neat rapeseed biodiesel emitted a level of NO_x exhaust gases similar to that emitted by fossil diesel when the combustion experiments took place at constant injection timing. Of the biodiesel samples tested, the lowest levels of NO_x were emitted by pure ICG2 FAMES at both timing conditions.

Production of NO_x in compression ignition engines is primarily caused by the oxidation of nitrogen present in the intake air, with the reaction rate mainly dependent on in-cylinder temperature and residence time of the cylinder at elevated temperatures (Mueller et al., 2009; Schönborn et al., 2009; Szybist et al., 2005). Consequently, the level of NO_x emissions is also a function of the duration of ignition delay, as the subsequent in-cylinder temperature conditions are influenced by the extent of premixed burn fraction and the rates of peak heat release (Hellier and Ladommatos, 2015).

Therefore, the high NO_x emissions of the reference fossil diesel shown in Figures 8.13 and 8.14 are in agreement with the high peak heat release rates and long ignition delays observed in Figures 8.11-8.12 and Figures 8.9-8.10 respectively. The low NO_x emissions of raw ICG2 oil are in agreement with the low peak heat release rates observed in Figures 8.11 and 8.12, and can be attributed to poor mixing of air and fuel, despite the long ignition delay (Figures 8.9 and 8.10), and incomplete burning.

This relationship between ignition delay and NO_x emissions is less apparent in the case of the neat and blended biodiesel samples, with shorter ignition delays generally resulting in increased NO_x emissions, suggesting that the quality of combustion is not dominated by ignition delay but by the progressive replacement of fossil diesel with biodiesel. This can possibly be explained by the long alkyl chains of the FAME samples when compared to some of the diesel molecules, such as the aromatics, isomers and naphthenes. Furthermore, the presence of oxygen in FAME molecules can also result in relatively high NO_x emissions compared to fossil diesel (Song et al., 2016).

In addition, the production of NO_x exhaust gases from FAMES is known to increase with higher degree of unsaturation and decreasing chain length due to increasing adiabatic flame temperature (Hellier and Ladommatos, 2015;

Knothe, 2008; Pinzi et al., 2009), and therefore the high levels of NO_x emissions observed when rapeseed and soya FAMEs were used can be partly attributed to the high degree of unsaturation of these samples (Table 8.4).

Figures 8.15-8.16 and 8.17-8.18 show the CO and THC emissions of the various fuel samples and reference fossil diesel at conditions of constant injection and constant ignition timing.

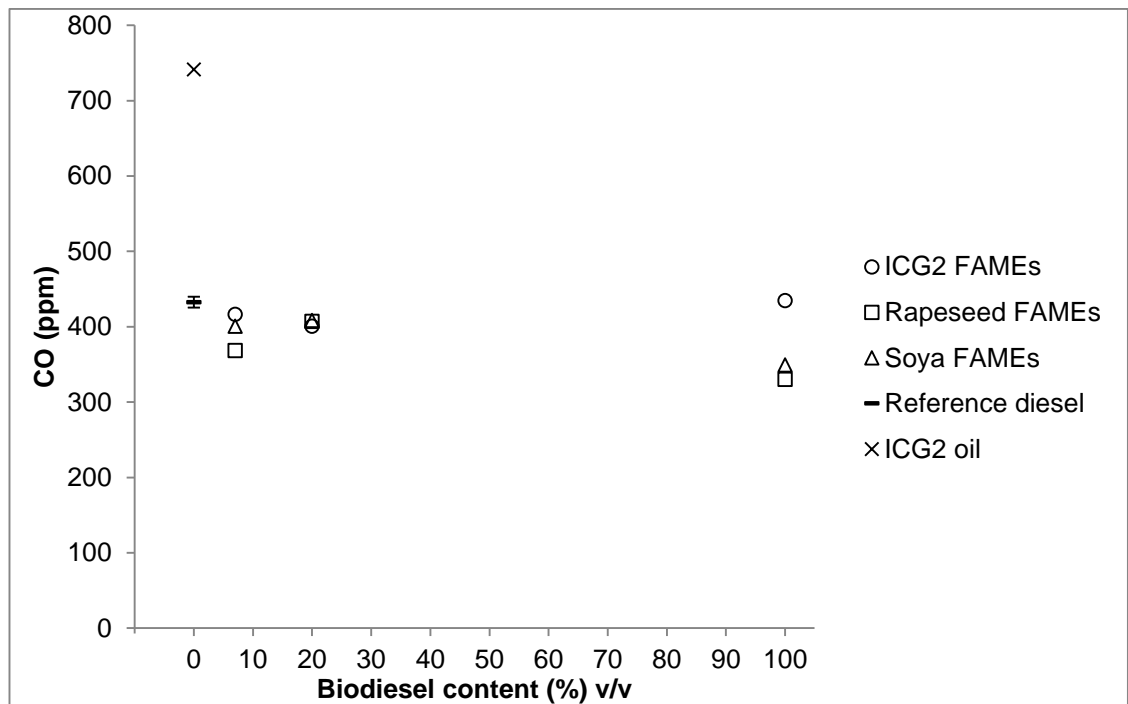


Figure 8.15: CO emissions against biodiesel content at constant injection timing. The error bars shown represent standard deviation ($\sigma=7.3$) calculated by 6 experimental repeats with reference diesel.

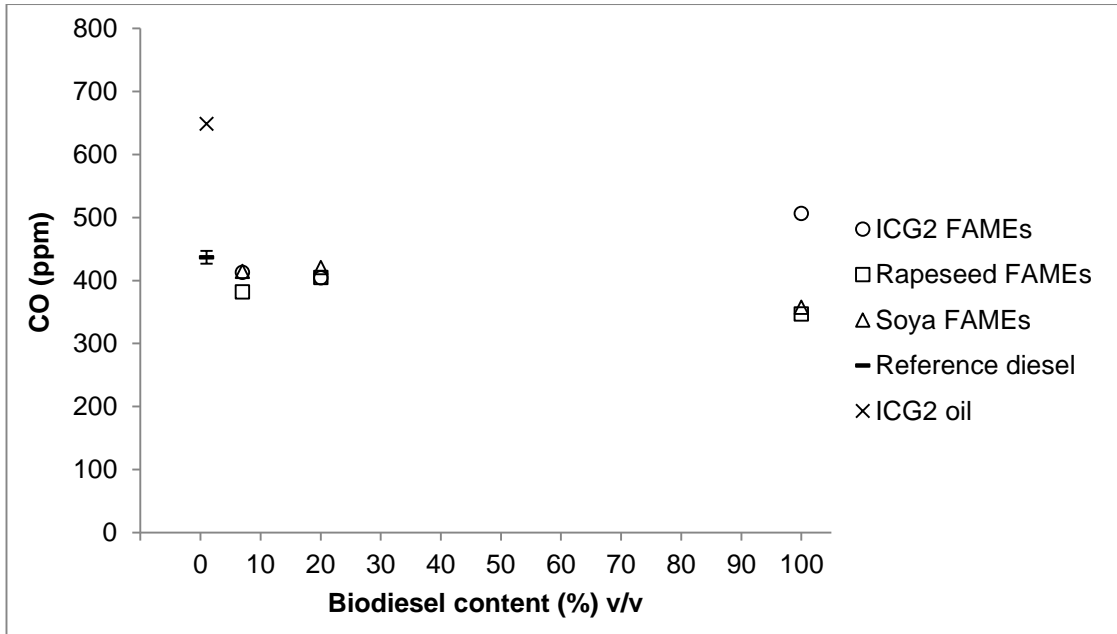


Figure 8.16: CO emissions against biodiesel content at constant ignition timing. The error bars shown represent standard deviation ($\sigma=10.1$) calculated by 6 experimental repeats with reference diesel.

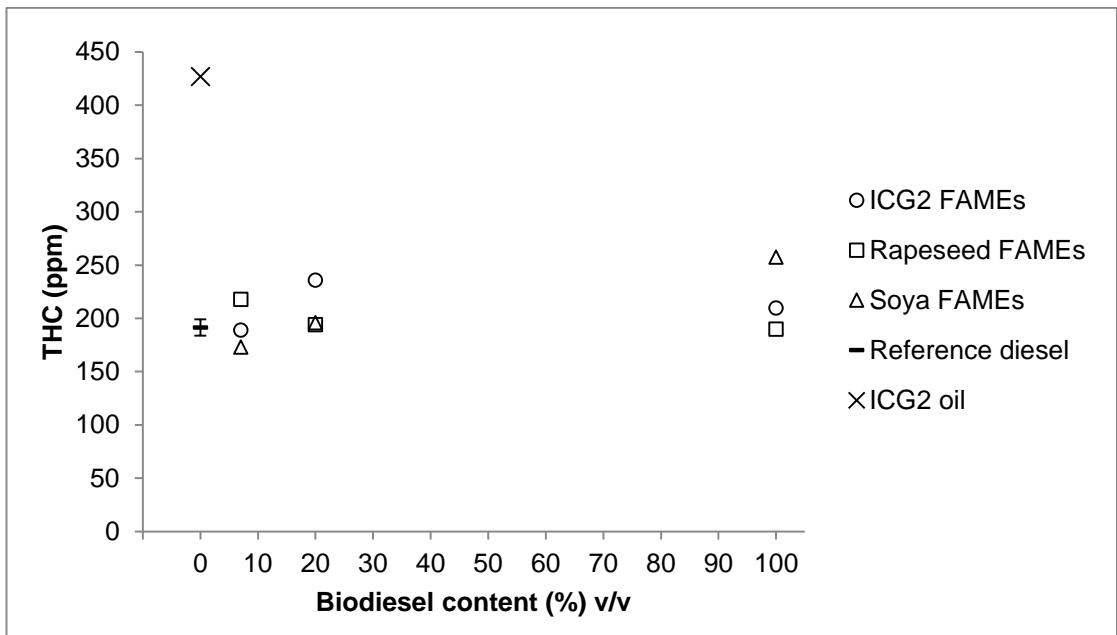


Figure 8.17: THC emissions against biodiesel content at constant injection timing. The error bars shown represent standard deviation ($\sigma=7.6$) calculated by 6 experimental repeats with reference diesel.

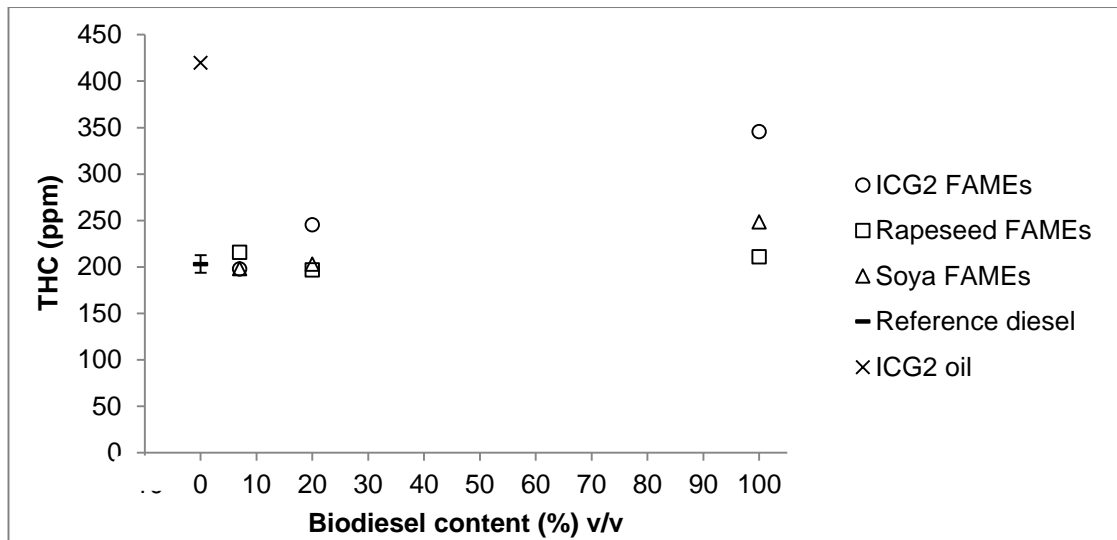


Figure 8.18: THC emissions against biodiesel content at constant ignition timing. The error bars shown represent standard deviation ($\sigma=9.5$) calculated by 6 experimental repeats with reference diesel.

It can immediately be seen in Figures 8.15-8.16 and 8.17-8.18 that raw ICG2 oil emitted very high levels of CO and THC relative to the other fuel samples tested. This observation, in conjunction with the low NO_x emissions produced when raw ICG2 oil was used as a fuel (Figures 8.13 and 8.14), further verifies the hypothesis that the ICG2 oil did not mix well with air, resulting in incomplete burning, as both CO and THC are known products of incomplete combustion (Hellier et al., 2015).

Furthermore, the CO emissions of neat and blended soya and rapeseed biodiesel show an overall tendency to decrease when the biodiesel content of the sample increased and the ignition delay decreased (Figures 8.9 and 8.10), while THC emissions tended to increase especially in the case of soya FAMES. A greater fraction of ICG2 biodiesel in the fuel sample resulted in higher emissions of CO and THC in most cases. This observation, along with the relatively high CO and THC emissions produced when neat ICG2 biodiesel was used at both timing conditions, suggests that the high viscosity of ICG2 biodiesel caused inefficient air-fuel mixing.

Figures 8.19 and 8.20 show the particulate emissions of the tested fuel samples and reference fossil diesel at constant injection and constant ignition timing respectively.

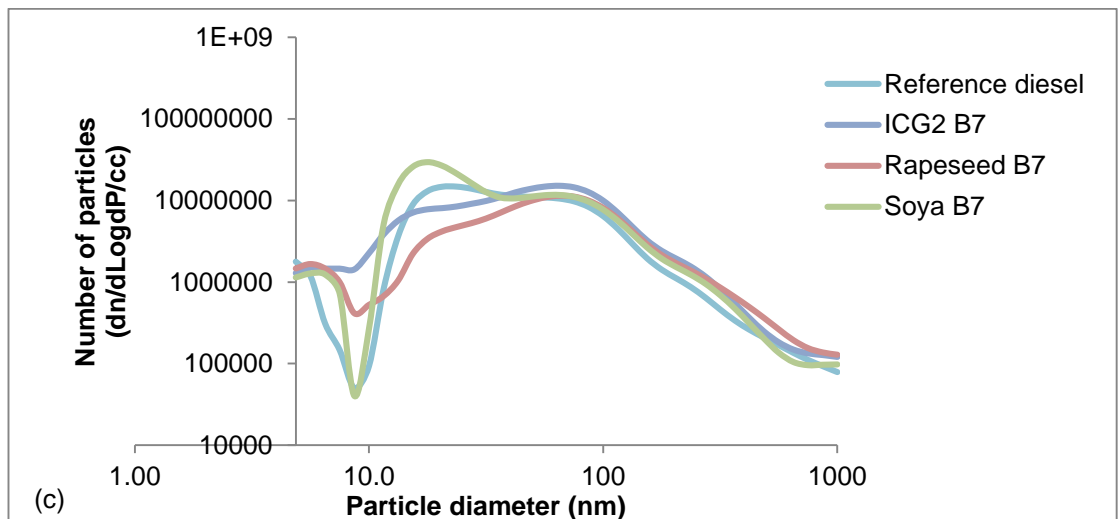
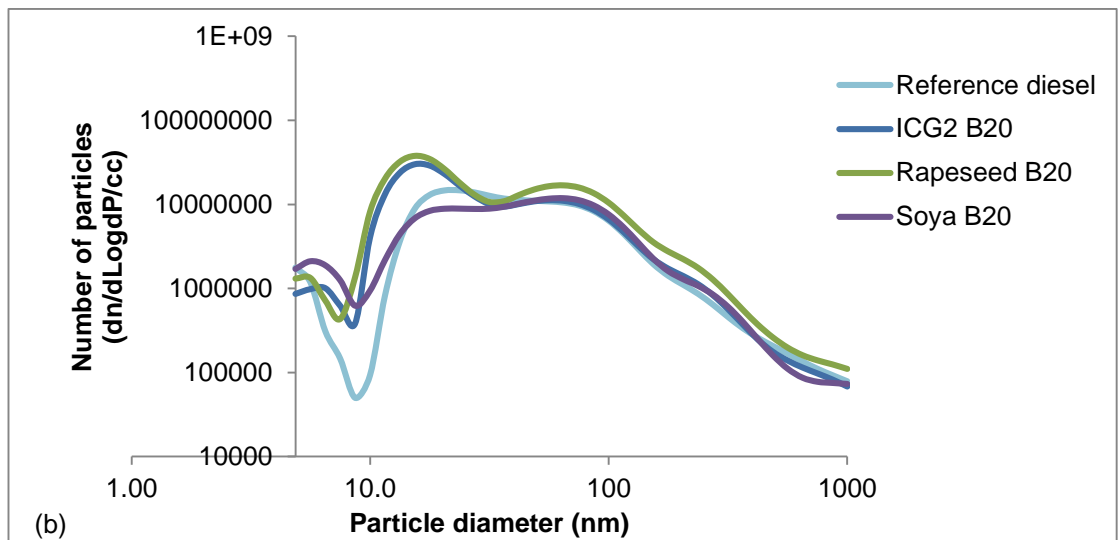
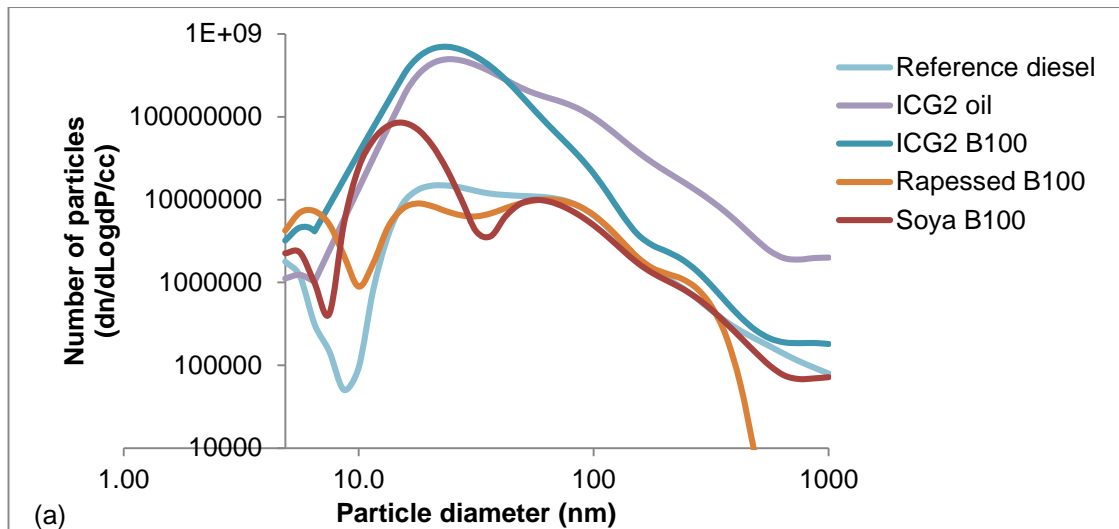


Figure 8.19: (a) Particulate emissions of ICG2 oil, reference diesel and 100 % v/v ICG2, soya and rapeseed FAMEs, (b) 20 % v/v FAME and fossil diesel blends, (c) 7 % v/v FAME and fossil diesel blends at constant injection timing.

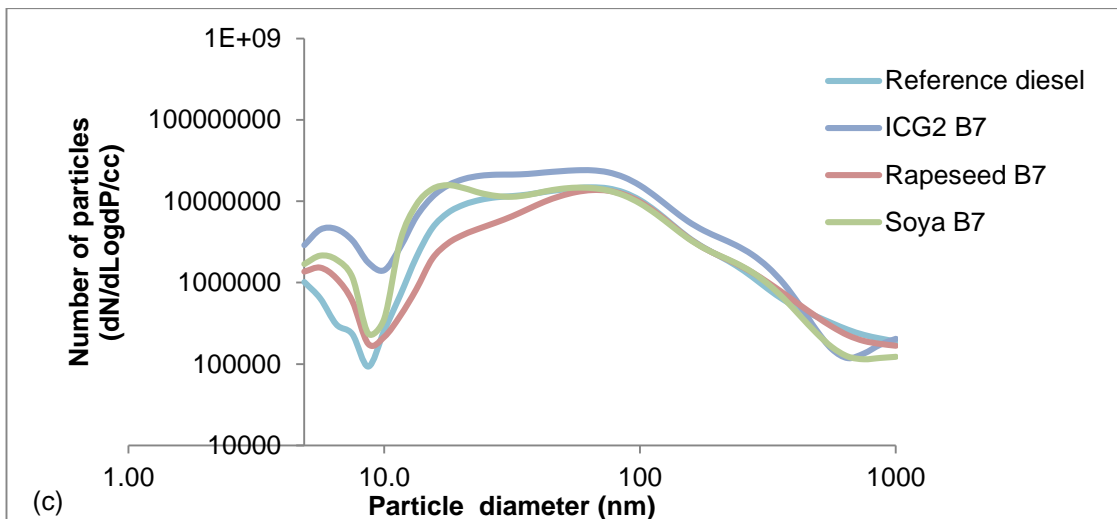
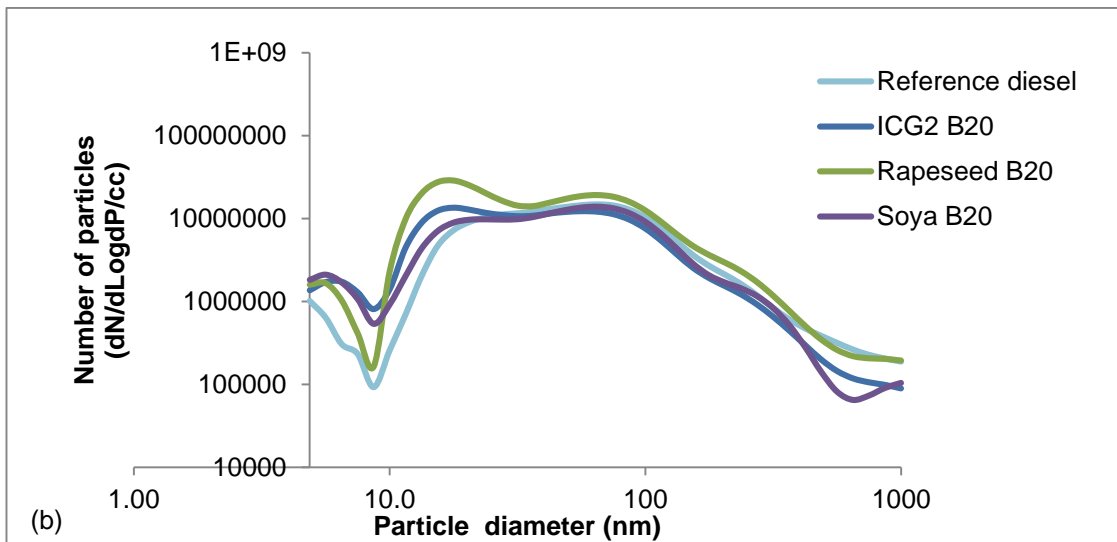
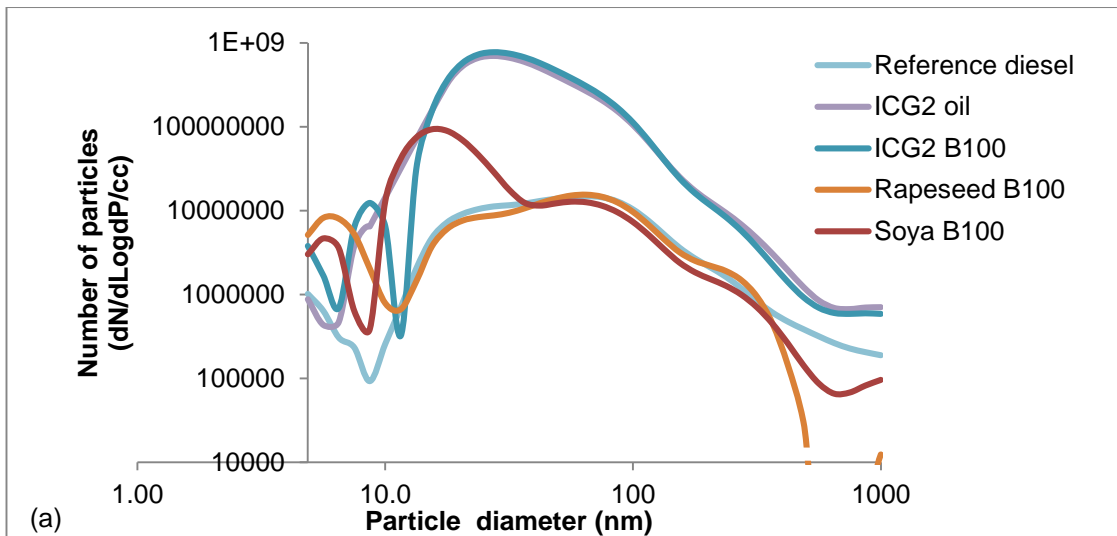


Figure 8.20: (a) Particulate emissions of ICG2 oil, reference diesel and 100 % v/v ICG2, soya and rapeseed FAMEs, (b) 20 % v/v FAME and fossil diesel blends, (c) 7 % v/v FAME and fossil diesel blends at constant ignition timing.

Figures 8.19 and 8.20 show that neat ICG2 biodiesel and raw ICG2 oil emit a much higher number of particles relative to the other fuel samples used at both conditions of constant injection and constant ignition timing. Figure 8.19(a) shows that raw ICG2 oil resulted in the production of a much higher number of particles greater than 50 nm in diameter relative to neat ICG2 biodiesel at conditions of constant injection timing, while both samples produced a similar number of particulates between 10 to 1000 nm when the experiments were performed at conditions of constant ignition timing (Figure 8.20).

This high amount of particulates produced from raw ICG2 oil is possibly a consequence of poor fuel atomization, attributable to the high viscosity of the oil, and incomplete burning conditions, as suggested by the elevated emissions of CO and THC (Figures 8.15-8.16 and 8.17-8.18), while the relatively low rates of heat release allowed more time for the continued production and agglomeration of smaller particles into large ones. The significantly higher amount of particulates produced by the combustion of neat ICG2 biodiesel relative to other biodiesel samples can similarly be partly attributed to the higher viscosity of this sample, however, this alone cannot justify the hundred times higher number of particulates produced by the neat ICG2 biodiesel. It is tentatively suggested that ICG2 biodiesel contained other unidentified compounds which resulted in an increase of the number of particles emitted upon combustion.

Figures 8.19(b, c) and 8.20(b, c) show that the combustion of blended samples with 20 % and 7 % biodiesel content emitted lower amounts of particulates relative to neat biodiesel samples at both experimental conditions, something attributed to the lower quantity of biodiesel in the samples, while small variations can be observed between samples.

Figures 8.21 and 8.22 show the total particulate mass emitted by the various fuel samples and reference fossil diesel at constant injection and constant ignition timing respectively.

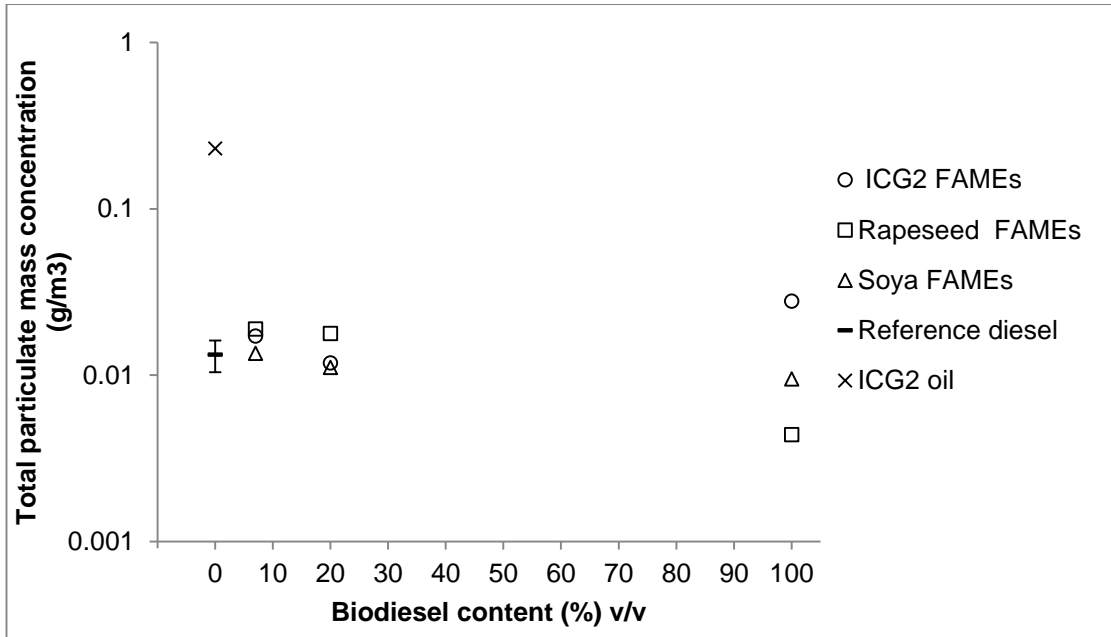


Figure 8.21: Total particulate mass emitted against biodiesel content at constant injection timing. The error bars shown represent standard deviation ($\sigma=0.002$) calculated by 6 experimental repeats with reference diesel.

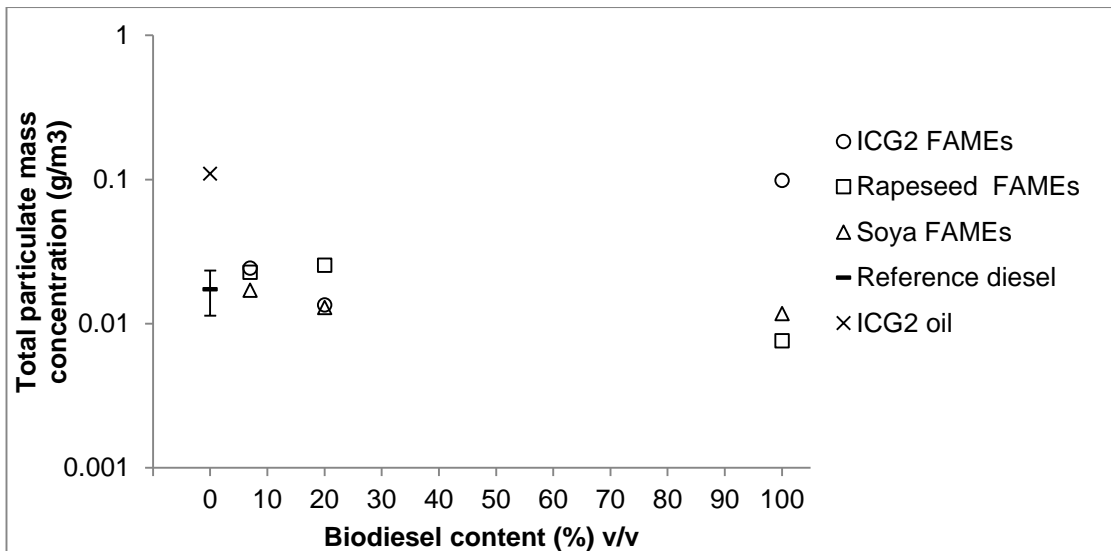


Figure 8.22: Total particulate mass emitted against biodiesel content at constant ignition timing. The error bars shown represent standard deviation ($\sigma=0.006$) calculated by 6 experimental repeats with reference diesel.

Figure 8.21 shows that the use of raw ICG2 oil as an engine fuel resulted in particulate mass emissions significantly higher than those observed when the neat and blended biodiesel samples were tested at conditions of constant injection timing, in agreement with the higher number of particles emitted

(Figure 8.19(a)). Figure 8.22 shows that raw ICG2 oil produced a much lower concentration of particulates at conditions of constant ignition timing, about half of that produced at constant injection, while the total mass of particulates produced by neat ICG2 biodiesel was similar to that of the raw ICG2 oil, an observation coinciding with the particle number distribution of the two fuels at this condition (Figure 8.20(a)).

8.3 Conclusions

An increase of acid-catalyzed pretreatment temperature up to 60 °C and a prolongation of the process duration to 4 hours were found to be beneficial in terms of FFA conversion into esters. The use of higher weight percentage of sulfuric acid relative to FFAs also resulted in pretreated oil with slightly lower FFA content, however, an increase of methanol-to-FFA molar ratio from 13:1 to 17.8:1 was found to be more significant in determining the efficiency of the process. At optimum esterification conditions, the FFA content of the oil was reduced to a value below 1.5 % w/w. In base-catalyzed transesterification of the pretreated oil, an increase of the potassium hydroxide weight percentage relative to oil up to 2.25 % was found to result in higher yields, with further increase slightly inhibiting the process due to soap formation. Increase of methanol-to-pretreated oil molar ratio from 9:1 to 18:1 was found to have little positive effect on the process yield.

The elemental composition of the obtained biodiesel was found to be similar to that of raw SCG oil, showing that the treatment of the oil to yield FAMES had little effect on the composition of the intermediate and end products, with the main difference being the slightly increased hydrogen content of pretreated oil and biodiesel relative to raw oil. The use of varying methanol-to-pretreated oil molar ratios was found to be insignificant for the elemental composition of the obtained FAMES.

Combustion of raw SCG oil resulted in the lowest in-cylinder pressure and PHRR relative to the other fuels samples despite exhibiting the longest ignition delay, indicating inadequate mixing and incomplete burning, possibly due to poor atomization and high viscosity, and suggesting the oil physical properties to be more important in determining the fuel premixed fraction than the

duration of ignition delay. These observations were supported by the low NO_x and high THC, CO and particulate emissions of raw ICG2 oil. Combustion characteristics of neat and blended SCG derived biodiesel were similar to those of the other vegetable biodiesel samples tested, and especially those of soya biodiesel. A relationship between increasing SCG biodiesel fraction in blended samples and higher CO and THC emissions suggested that the relatively high viscosity of SCG biodiesel compared to the other biodiesel samples inhibited the air-fuel mixing. The ignition delay of biodiesel blends was found to correlate well with the biodiesel content of the sample, with an increase of the biodiesel content from 7 % v/v to 100 % v/v resulting in decrease of the ignition delay time.

All of the examined fuel samples, with the exception of neat soya biodiesel, emitted significantly lower levels of NO_x compared to the reference fossil diesel, in agreement with the observed peak heat release rates. The high particulate emissions of neat ICG2 biodiesel can be partly attributed to the relatively high viscosity of this sample compared to other biodiesel fuels tested, which resulted in reduced in-cylinder pressures and therefore rates of soot oxidation, and poor atomization that increased the presence of fuel rich zones suitable for particulates formation within the cylinder.

9. Conclusions and recommendations for further work

This chapter summarizes the main conclusions drawn by the experiments performed in this study, including SCG characterization, water removal and lipid extraction from SCG, transesterification of SCG oil and subsequent engine tests.

9.1 Conclusions

The experimental studies presented in this work have shown that some SCG properties differ depending on the sample source, with SCG of the instant coffee industry, which had not been previously investigated in such depth, having higher lipid content, mean particle size and FFA content of SCG oil compared to RCG samples. Furthermore, SCG samples with larger particles were found to possess higher moisture levels, while a correlation between higher SCG moisture content and increasing FFA content of the oil was observed. Brewing of coffee in an espresso machine did not significantly affect the oil content of the grounds, but increased the FFA content of the oil and resulted in a slight increase of average dry particle diameter and a less homogeneous particle size distribution.

Solvent extraction experiments showed that lower SCG-to-solvent ratios, longer extraction durations, higher temperatures, low moisture presence (~2 % w/w) and mixed size SCG particles generally resulted in improved oil yields. The effect of pressure on SCG oil recovery efficiency was investigated for the first time and pressures up to 75 bar resulted in oil yield increase regardless of the extraction temperature, whereas the impact of process pressures higher than 75 bar and up to 110 bar was found to be related to the temperature of the extraction. In particular, higher pressures led to lower oil yields when the extraction was performed at 25 °C and 45 °C, potentially due to increased solvent viscosity and surface tension, while the obtained yield further increased with higher pressures when the extraction temperature was similar to the boiling point of the solvent, suggesting that any inhibitory effect of high pressure was balanced by the enhanced extraction kinetics and solubility. In

addition, longer durations of extraction were correlated with reduced FFA content, while higher extraction temperatures, including temperatures above the boiling point of the solvent that had not been previously examined in SCG oil extraction, showed an increased presence of mono- and diglycerides in the recovered oil. The solvent selection significantly affected the composition of the obtained SCG oil, with polar solvents extracting higher amounts of FFAs, while ethanol showed reduced sensitivity to moisture presence, and a significantly higher oil extraction ratio relative to hexane, when the extraction was performed at a temperature of 125 °C.

Soxhlet method was found to be more efficient relative to ASE and the prototype pressurized vessel solvent extraction in terms of absolute SCG oil yield extracted, however, was the least efficient on the basis of yield per time and required larger solvent quantities. Pilot plant scale extractions were investigated for the first time with SCG and were found to be successful in extracting SCG oil quantities directly comparable to those recovered by Soxhlet extraction at similar durations, while the pilot plant trials showed a reduced sensitivity to water presence in terms of obtained oil yield and no systematic effect of moisture level on the oil fatty acid profile. The obtained results demonstrate that SCG oil extraction can be efficiently undertaken at a large scale through a continuous process.

The various solvent extraction methods used for oil removal from SCG generally required drying of the grounds prior to extraction, while mechanical pressing had been scarcely investigated as a processing method for SCG water removal and/or oil recovery. Mechanical pressing was used in this study as a method of processing residues of the coffee industry and was found to be efficient in removing part of the moisture residing in SCG (42 % w/w of the total) with increase of pressure, temperature and duration generally resulting in higher rates of water removal. However, mechanical expression was only successful in removing oil from whole RDCB, with the densely packed formation of SCGs being possibly responsible for the ineffective oil expression from SCG samples. In addition, solvent extraction with pre-pressed and thermally dried SCGs was examined and the pre-pressing of SCG up to 350 bar prior to thermal drying was found to be beneficial for subsequent lipid

extraction, potentially due to distortion of the SCG matrix that facilitated solvent penetration and oil diffusion. Pre-pressing at higher pressures up to 550 bar was found to slightly inhibit the subsequent solvent extraction due to compaction of particles that impeded oil removal. Furthermore, the level of moisture removal achieved with mechanical pressing was found to be sufficient for efficient solvent extraction when ethanol was used at elevated temperature and pressure conditions through ASE, suggesting pressing to be an effective moisture processing strategy provided that the solvent extraction method had also been optimized.

Transesterification of SCG oil was successfully conducted despite the high FFA content through a two-step process with limited influence on elemental composition and fatty acid profile. The acid-catalyzed pretreatment of SCG reduced the FFA content below 1.5 % w/w with minor losses (1.31 ± 0.73 % w/w of the initial untreated oil weight) and the subsequent base-catalyzed transesterification achieved a maximum FAME conversion yield of 87.83 ± 0.47 % w/w relative to pretreated oil weight.

Engine tests with SCG biodiesel and oil were performed for the first time showing that SCG biodiesel had similar combustion and emission characteristics to other commercial vegetable biodiesel samples, both as a pure biodiesel and when blended with fossil diesel. Moreover, the relatively high viscosity of the SCG biodiesel relative to soya and rapeseed biodiesel resulted in higher CO, THC and particulate matter emissions, despite exhibiting a similar duration of ignition delay. In addition, a correlation was found between increasing biodiesel content in blended fuel samples from 7 % v/v to 100 % v/v and decreasing ignition delay duration, possibly attributable to the presence of long alkyl carbon chains that can break down more easily than some molecules present in fossil diesel.

Finally, raw SCG oil showed the lowest in-cylinder pressure, PHRR, and NO_x emissions, and the highest THC, CO and particulate matter emissions relative to other fuel samples used, and these observations, along with the long ignition delay of raw SCG oil, suggested that the high viscosity of the oil

resulted in incomplete mixing with air and burning, and justified the use of transesterification to improve the SCG oil fuel properties.

9.2 Recommendations for future work

While this work has identified the effect of solvent extraction conditions on the yield and quality of oil recovered from SCG, further understanding on the impact of the use of different solvents on the quality of extracted oil is required. In Section 5.1.3 an unidentified peak was apparent in the ^1H NMR spectra of the oil extracted with long chained alcohols through the Soxhlet method, which was suggested to correspond to alkyl esters arising from transesterification reactions between FFAs and/or glycerides and alcohol solvent despite the absence of a catalyst, and possibly due to the long duration and relatively high temperature of the process. Therefore, it would be of interest to identify the compound responsible for this peak and investigate the potential consequences of its presence on the composition of the extracted oil and on its intended use. Furthermore, if the aforementioned compound is an alkyl ester, the use of long chained alcohols for direct transesterification of SCG without a catalyst could be a possible route for biodiesel synthesis from this feedstock.

In Sections 6.1.1 and 7.3 the use of polar ethanol for extraction of oil from dried and wet SCG respectively at temperatures above its boiling point through ASE resulted in oil extraction ratios significantly higher than those obtained with non-polar solvents at the same conditions. It was suggested that ethanol removed compounds other than FFAs and glycerides due to its highly polar character, and identifying these compounds, one of which was found to be caffeine but at quantities that cannot fully explain such high extraction ratios, would be useful in understanding the composition of the extracted oil and the possible impact that they might have on its utilization.

The study of the effect of pressure on the solvent extraction of lipids from dried SCG (Section 6.2.1) showed that an increase of hexane pressure up to 110 bar was beneficial in terms of oil extraction ratio when the extraction was performed at a temperature close to the boiling point of the solvent, however, higher pressures and temperatures were not explored due to equipment

limitations. It would be of interest to investigate higher temperatures and pressures so as to check whether the observed oil yield trend will persist at more extreme conditions, while the use of other polar and non-polar solvents would be useful in understanding their impact on extracted oil yield and quality.

In addition, while the present study has determined the effect of SCG oil transesterification conditions such as temperature, duration, catalyst to oil ratio and methanol-to-oil ratio on the efficiency of the process (Section 8.1), ultrasound-assisted or high pressure transesterification experiments were not considered in this work. An investigation of ultrasound-assisted and/or pressurized transesterification might reduce the duration of the process and optimize the biodiesel conversion rate.

Finally, combustion experiments with pure SCG biodiesel showed that the level of particulate matter emissions was significantly higher than those produced from other vegetable biodiesel samples tested, something that cannot be solely attributed to the slightly higher viscosity of SCG biodiesel (Section 8.2). Therefore, it would be interesting to further investigate the combustion of SCG biodiesel under varying conditions of engine speed, injection pressure and ignition timing in order to better understand its emission characteristics. Additionally, further analysis of the SCG derived biodiesel might identify the presence of other compounds at ppm level that could possibly account for the elevated particulate matter emissions.

A. Pressure vessel design

A.1 Determination of minimum wall thickness requirements

Table A.1: Pressure vessel specifications.

Maximum pressure (P)	20 MPa
Maximum temperature (T)	200 °C
Stainless steel 304 tensile strength (f)	216 MPa
Inside diameter (D _i)	52 mm
Factor for circular ends (C)	0.41
Top plate compressed fluid opening diameter (d _{e1})	12 mm
Top plate pressure transducer opening diameter (d _{e2})	1.5 mm
Top plate thermocouple opening diameter (d _{e3})	1.5 mm

Cylinder wall thickness calculation: $e = \frac{PD_i}{2f-P} = 2.52 \text{ mm}$

Bottom plate thickness: $e = CD \sqrt{\frac{P}{f}} = 6.48 \text{ mm}$

Parameter for compressed fluid opening: $Y_1 = \sqrt{\frac{D_i}{D_i - d_{e1}}} = 1.14$

Parameter for pressure transducer opening: $Y_2 = Y_3 = \sqrt{\frac{D_i}{D_i - d_{e2}}} = 1.01$

Top plate thickness: $e = CD \sqrt{\frac{P}{f}} \times Y_1 \times Y_2 \times Y_3 = 7.54 \text{ mm}$

The pressurized vessel was designed in accordance with the British standard 5500 (BSI Standard, 2006). The cylinder walls were thicker than the minimum required for safety purposes.

A.2 O-ring

Table A.2: O-ring specifications.

O-ring BS code	229
O-ring inside diameter (d_1)	59.92 mm
O-ring cross section diameter (d_2)	3.53 mm
Outside diameter of housing for axial sealing (d_7)	66.98 mm
Width of the O-ring axial housing (b_4)	5.3 mm
Height of O-ring axial housing (h)	2.7 mm
Housing radius (f)	0.4 mm
Lead-in chamfer ($^\circ$)	20

The O-ring specifications were taken from BSI Standard (2008).

A.3 Threads

Table A.3: Thread specifications.

Major diameter (d)	76 mm
Pitch (p)	2.5 mm
Maximum pressure (P)	20 MPa
Stainless steel 304 tensile strength (f)	216 MPa

Pitch diameter: $d_p = d - 0.649519 p = 0.07293 \text{ m}$

Minor diameter: $d_r = d - 1.226869 p = 0.07437 \text{ m}$

Tensile stress area: $A_t = \frac{\pi}{4} \times \left(\frac{d_p + d_r}{2}\right)^2 = 0.004259 \text{ m}^2$

Shear stress area: $A_s = 0.8 \pi d_r p = 0.000458 \text{ m}^2$

Shear stress for thread stripping: $\tau_s = \frac{F}{A_s} = \frac{P A_c}{A_s} = \frac{P \pi \left(\frac{d}{2}\right)^2}{A_s} = 197.99 \text{ N/mm}^2$

Minimum number of threads required to avoid stripping: $n = \frac{\tau_s}{f} = 0.9166$

Minimum length of thread required: $n \times p = 2.291 \text{ mm}$

The selected number of threads was higher than the minimum for safety purposes. All specifications and equations used were taken from Oberg et al. (2004).

A.4 Catia Drawings

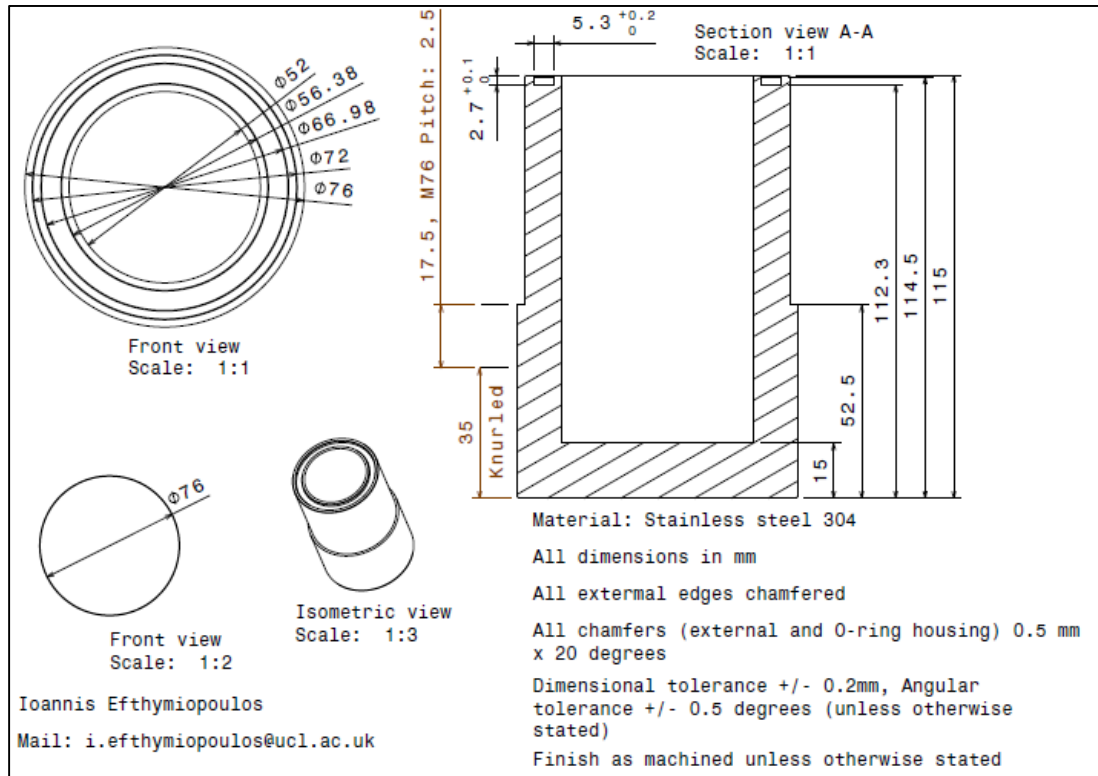


Figure A.1: Internal cylinder drawing.

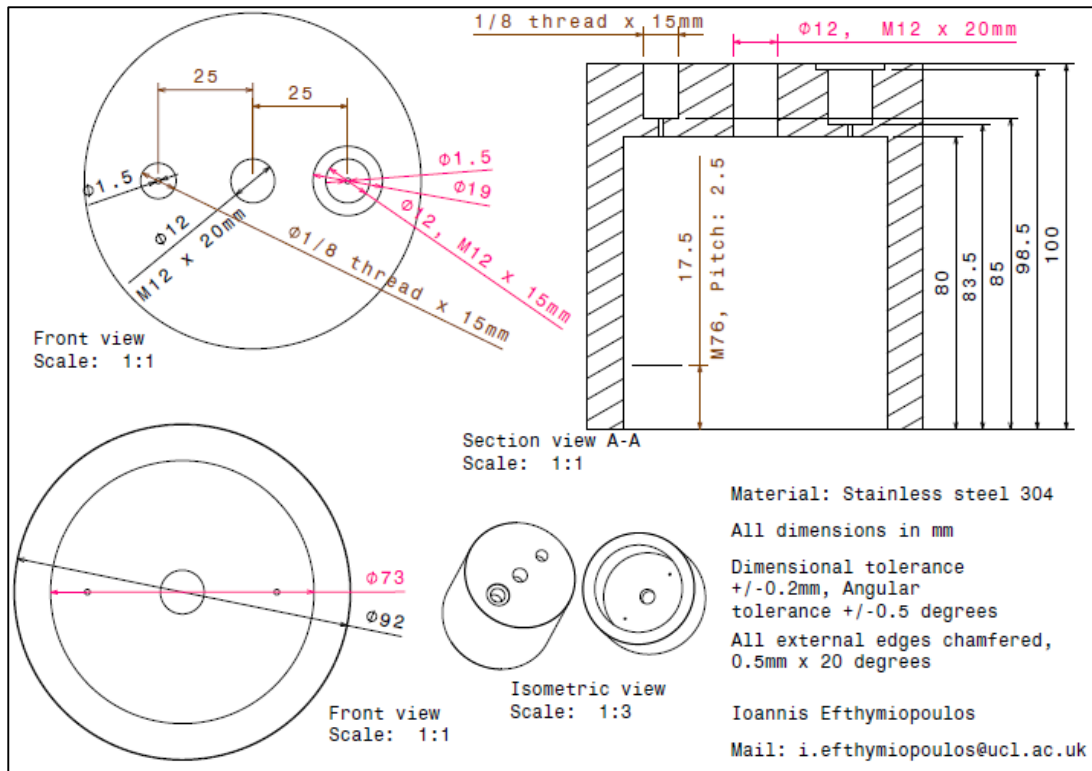


Figure A.2: External cylinder drawing.

B. Mechanical ram press design

B.1 Determination of minimum wall thickness requirements

Table B.1: Ram press specifications.

Maximum pressure (P)	60 MPa
Maximum temperature (T)	200 °C
Stainless steel 304 tensile strength (f)	216 MPa
Inside diameter (D _i)	99.46 mm
Factor for circular ends (C)	0.41
Top plate compressed fluid opening diameter (d _{e1})	12 mm
Top plate pressure transducer opening diameter (d _{e2})	1.5 mm

Cylinder wall thickness calculation: $e = \frac{PD_i}{2f-P} = 16.04 \text{ mm}$

Bottom plate thickness: $e = CD \sqrt{\frac{P}{f}} = 21.49 \text{ mm}$

Parameter for compressed fluid opening: $Y_1 = \sqrt{\frac{D_i}{D_i - d_{e1}}} = 1.06$

Parameter for pressure transducer opening: $Y_2 = \sqrt{\frac{D_i}{D_i - d_{e2}}} = 1.00$

Top plate thickness: $e = CD \sqrt{\frac{P}{f}} \times Y_1 \times Y_2 = 22.93 \text{ mm}$

The mechanical press was designed in accordance with the British standard 5500 (BSI Standard, 2006). The cylinder walls were thicker than the minimum required for safety purposes.

B.2 O-rings

B.2.1 Piston O-rings

Table B.2: Piston O-ring specifications.

O-ring BS code	341
O-ring inside diameter (d_1)	88.27 mm
O-ring cross section diameter (d_2)	5.33 mm
Piston diameter (d_4)	99.36 mm
Housing inside diameter (d_3)	90.88 mm
Housing width without extrusion rings (b_1)	7.2 mm
Lead-in chamfer ($^\circ$)	20
Length of lead-in chamfer (z)	2.1 mm
Housing radius (f)	0.4 mm
Depth available for O-rings (a)	50 mm
Number of O-rings (N)	2

Spacing between O-rings: $\frac{a-(N \times b_1)}{N+1} = 11.86$ mm

B.2.2 Internal cylinder O-rings

Table B.3: Internal cylinder O-ring specifications.

O-ring BS code	047	159
O-ring inside diameter (d_1)	114.02	126.67 mm
O-ring cross section diameter (d_2)	1.78 mm	2.62 mm
Outside diameter of housing for axial sealing (d_7)	117.52 mm	131.90 mm
Width of the O-ring axial housing (b_4)	3.2 mm	4 mm
Height of O-ring axial housing (h)	1.3 mm	2 mm
Housing radius (f)	0.4 mm	0.4 mm
Lead-in chamfer ($^\circ$)	20	20
Depth available for O-rings (a)	20.09 mm	
Number of O-rings (N)	2	

Spacing between O-rings: $\frac{a-b_{4,047}-b_{4,159}}{N+1} = 4.29 \text{ mm}$

The equations and O-ring specifications were taken from BSI Standard (2008).

B.3 Threads

Table B.4: Threads specifications.

Major diameter (d)	140 mm
Pitch (p)	4 mm
Maximum pressure (P)	60 MPa
Stainless steel 304 tensile strength (f)	216 MPa

Pitch diameter: $d_p = d - 0.649519 p = 0.13509 \text{ m}$

Minor diameter: $d_r = d - 1.226869 p = 0.13740 \text{ m}$

Tensile stress area: $A_t = \frac{\pi}{4} \times \left(\frac{d_p + d_r}{2}\right)^2 = 0.014572 \text{ m}^2$

Shear stress area: $A_s = 0.8 \pi d_r p = 0.001018 \text{ m}^2$

Shear stress for thread stripping: $\tau_s = \frac{F}{A_s} = \frac{P A_c}{A_s} = \frac{P \pi \left(\frac{d}{2}\right)^2}{A_s} = 456.74 \text{ N/mm}^2$

Minimum number of threads required to avoid stripping: $n = \frac{\tau_s}{f} = 2.114$

Minimum length of thread required: $n \times p = 8.458 \text{ mm}$

The selected number of threads was higher than the minimum for safety purposes. All specifications and equations used were taken from Oberg et al. (2004).

B.4 Catia Drawings

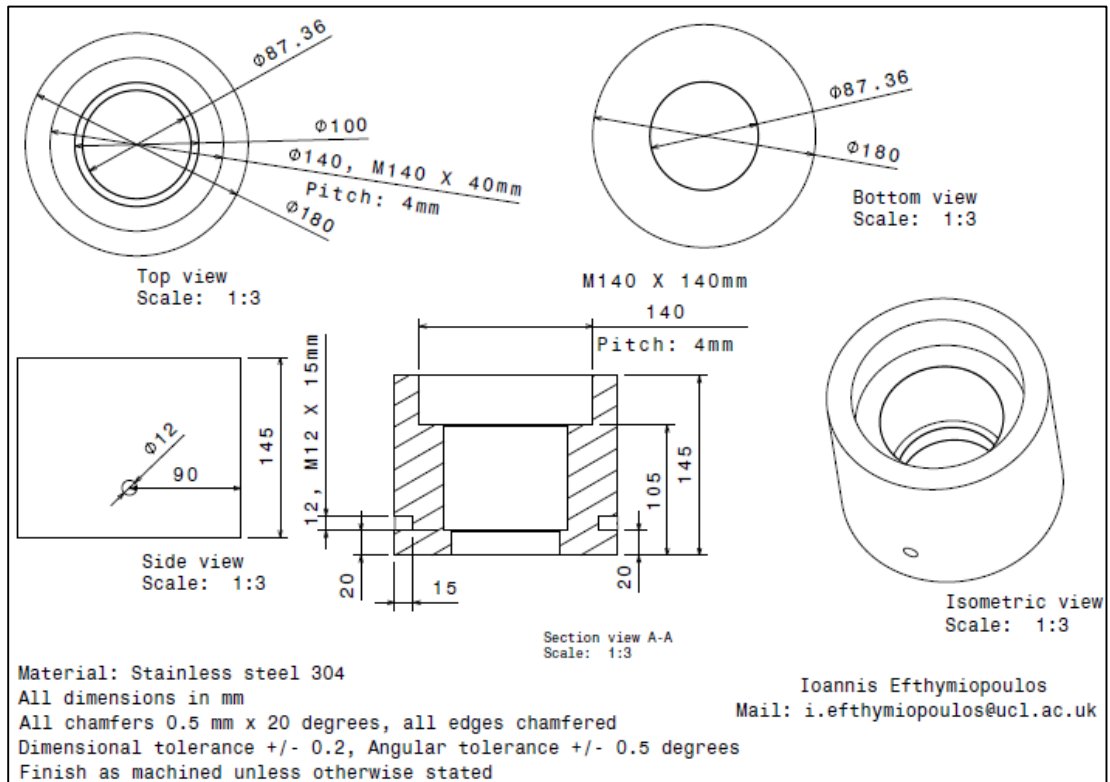


Figure B.1: External cylinder drawing.

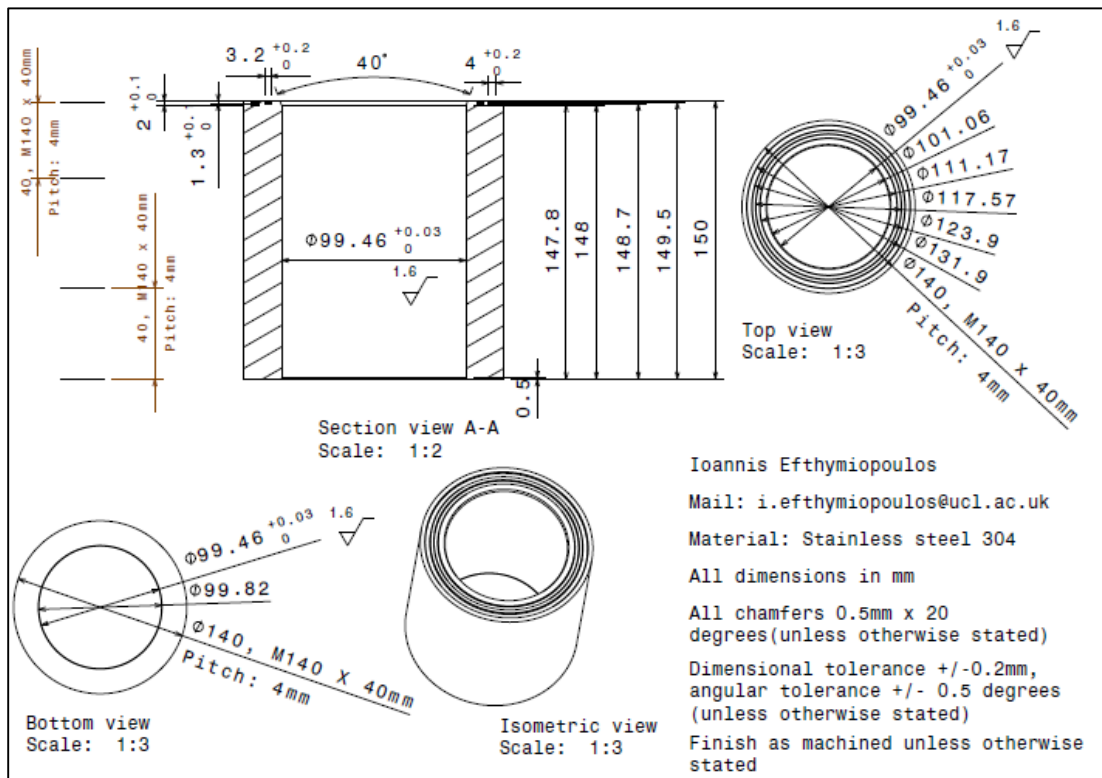


Figure B.2: Internal cylinder drawing.

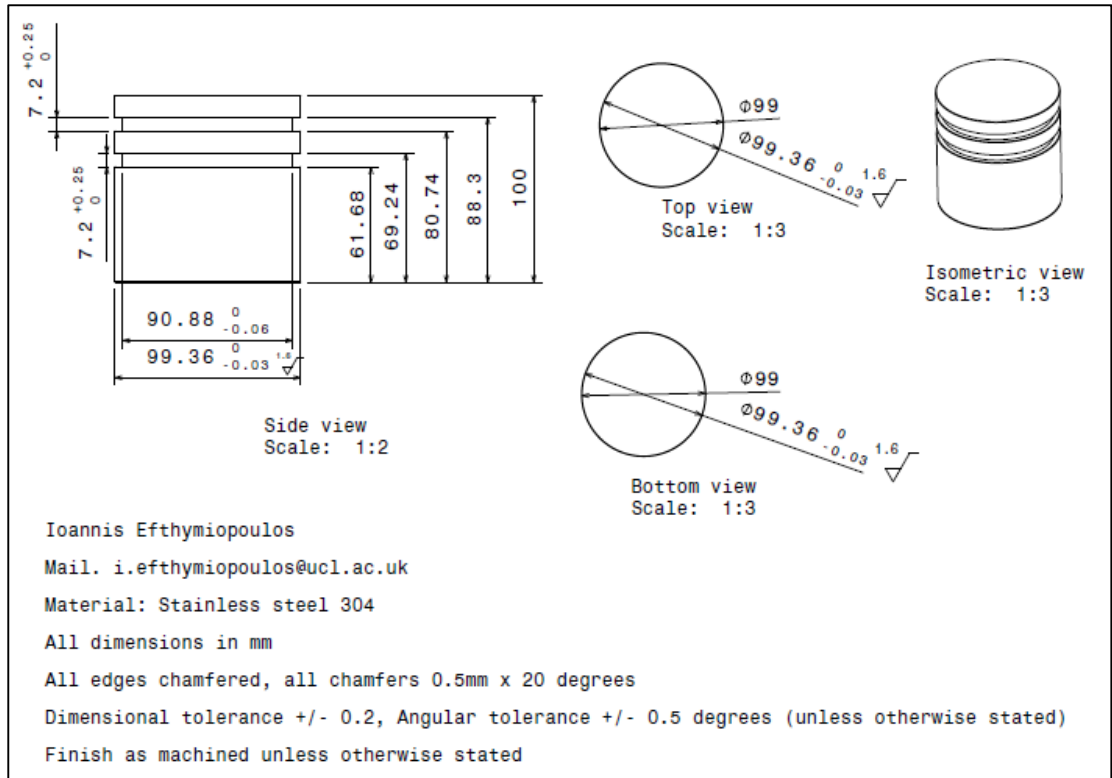


Figure B.3: Piston drawing.

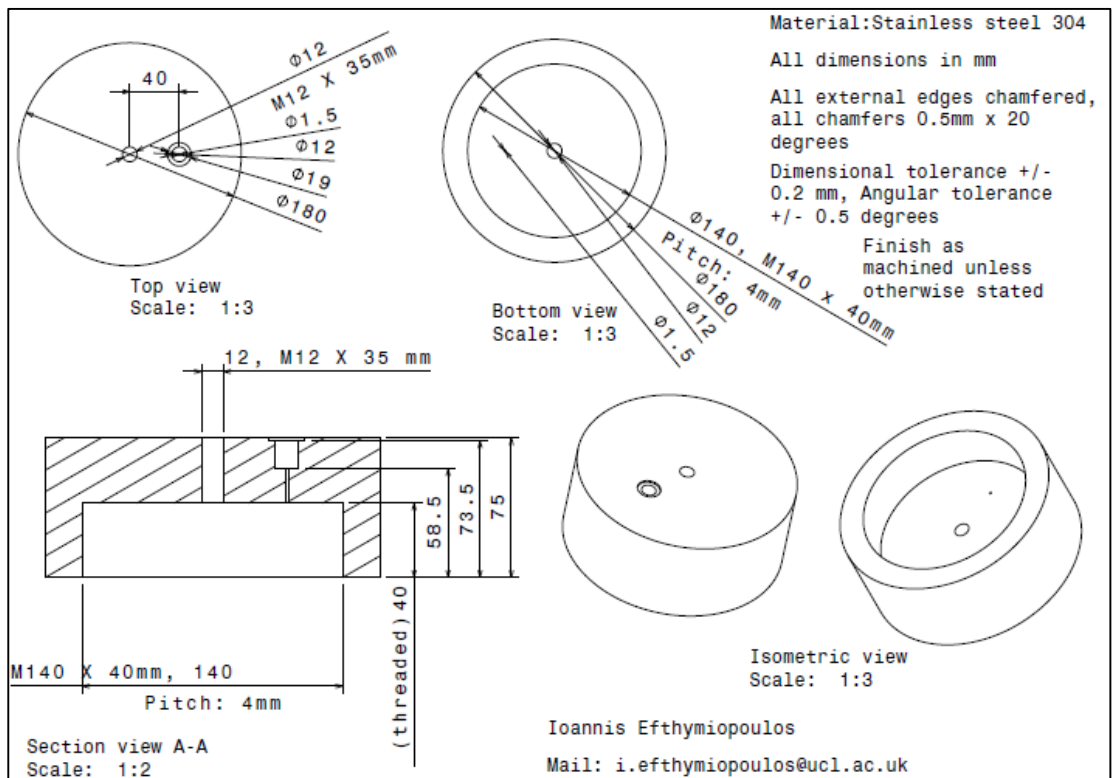


Figure B.4: Upper cap drawing.

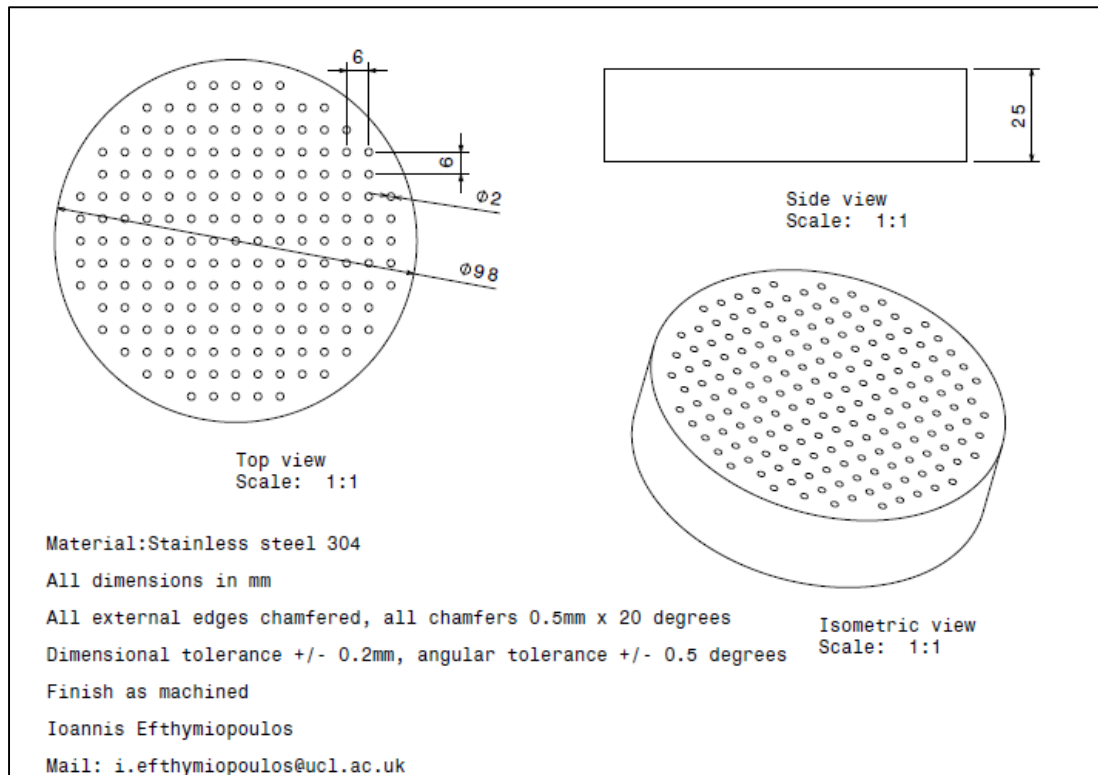


Figure B.5: Supporting plate drawing.

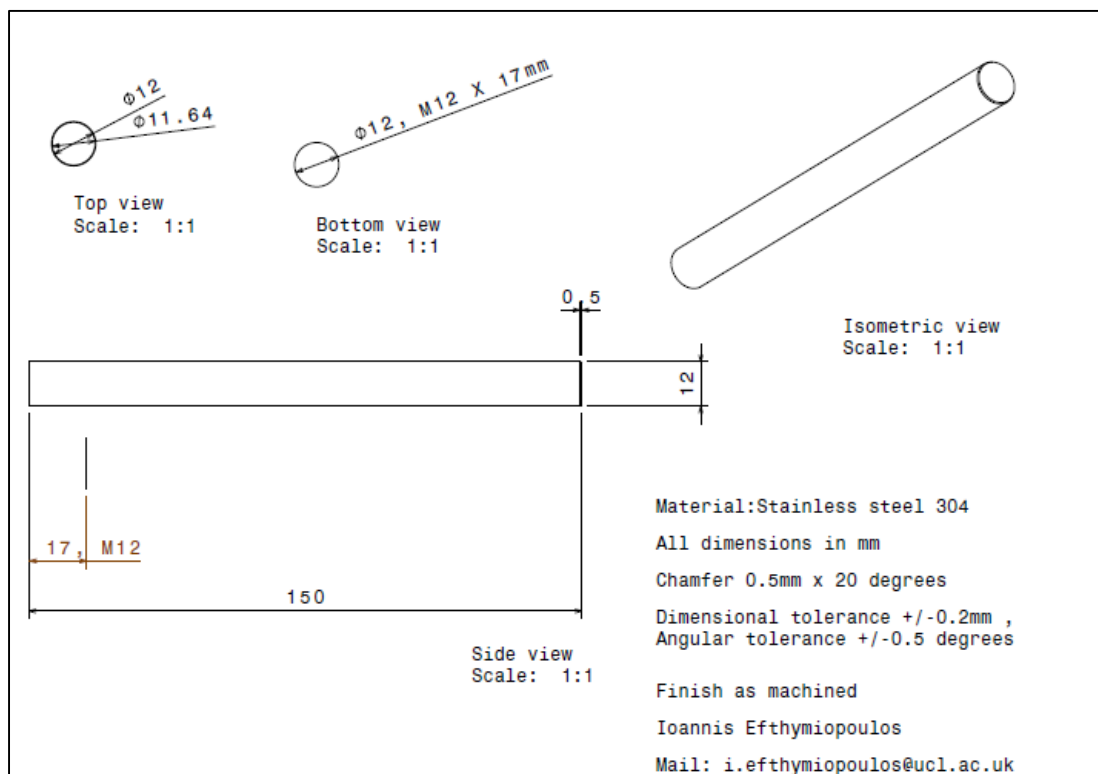


Figure B.6: Handle drawing.

C. Density calculation

The density of ICG2 oil and biodiesel was determined by adding quantities of 1 ml in a 10 ml volumetric cylinder, plotting a mass against volume graph and taking the gradient of the straight best fit line. Figures C.1, C.2 and C.3 show the graphs used for the determination of the density of ICG2 oil, ICG2 pretreated oil and ICG2 biodiesel respectively.

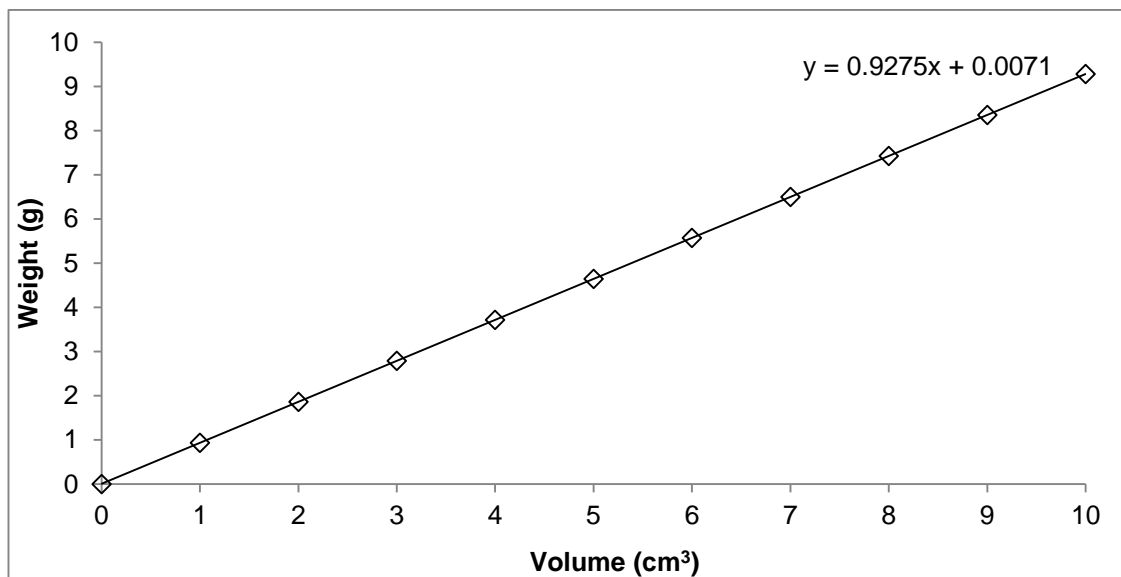


Figure C.1: ICG2 oil density determination.

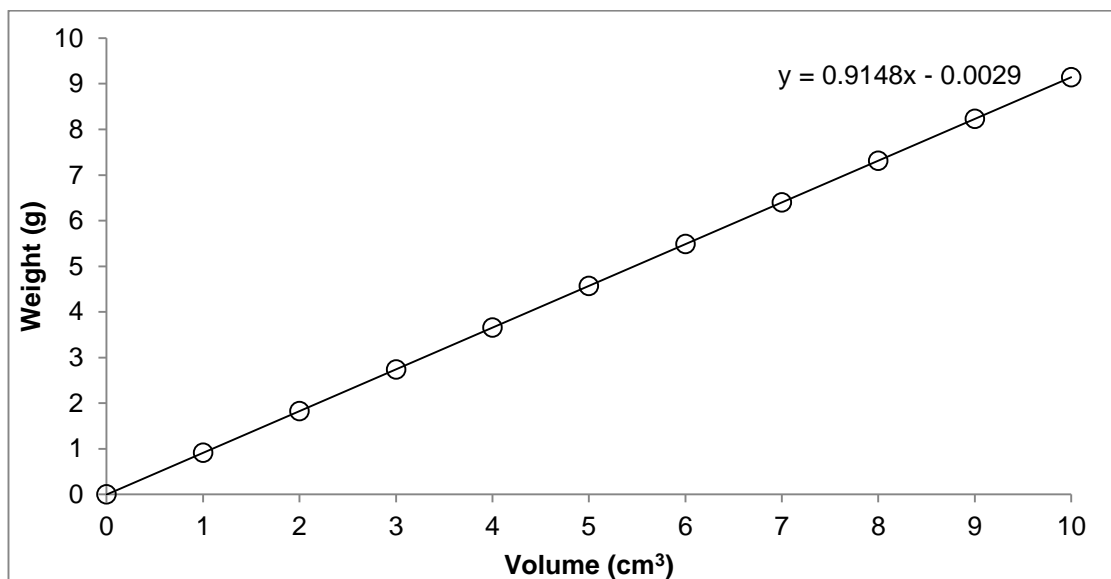


Figure C.2: ICG2 pretreated oil density determination (conditions of acid-catalyzed pretreatment can be found in Table 8.1 - Trial 5)

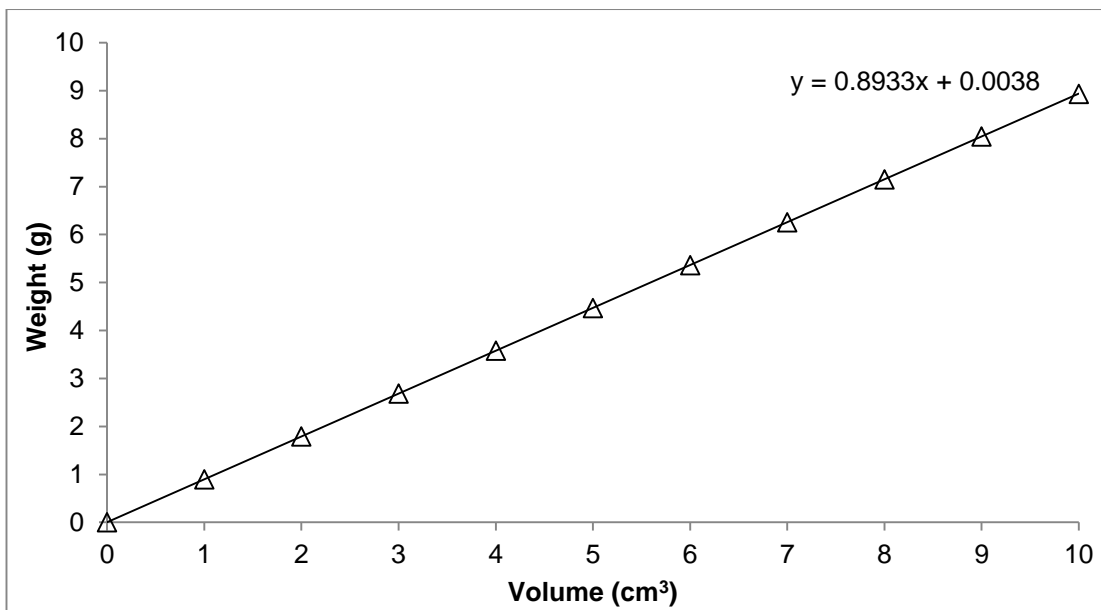


Figure C.3: ICG2 biodiesel density determination.

D. NHE methods and molecular weight of SCG oil fatty acids

D.1 NHE transesterification method

The procedure followed at NHE for transesterification of an oil sample with FFA content greater than 4 % w/w prior to gas chromatography is described here:

1. Label test tubes clearly.
2. Add 4 drops of sample to a test tube.
3. Add 4.0 ml of methanol with 3-5 sulfuric acid drops and shake.
4. Warm sample in heating block @ 80 °C for 20 minutes.
5. Remove from heat.
6. Add 3.0 ml of demineralized water.
7. Add 3.0 ml of hexane.
8. Place the sample into the centrifuge @ 3500 rpm for 2 minutes.
9. Remove from heat and pipette the top layer to a clearly labelled second test tube.
10. Add 2.0 ml of dimethylcarbonate: hexane (50:50 mixture) to second test tube.
11. Add 2.0 ml of sodium methoxide and shake.
12. Warm sample in heating block @ 60 °C for 20 minutes.
13. Remove from heat and add 3.0 ml of demineralized water.
14. Place the sample into the centrifuge @ 3500 rpm for 2 minutes.
15. Cut the top off a Pasteur pipette at the 2 ml mark.

16. Plug the bottom end of the pipette with a small piece of cotton wool.
17. Place the pipette filter into the top of the CG vial.
18. Pipette off the top layer into the pipette filter and allow to drop filter into the vial.
19. Discard the remaining sample and filter once the GC vial is full.
20. Seal sample in a vial ready for analysis via the gas chromatograph and label.

D.2 NHE GC method

The parameters listed in Table D.1 were used to carry out the analysis of FAMEs using an Agilent Capillary column CP-Wax 52 CB FS.

Table D.1: NHE gas chromatography settings.

Injector temperature	230 °C
Detector temperature	300 °C
Measured flow rate	5.0 ml/min
Carrier flow rate	0.80 ml/min
Split ratio	15:1
Range	1
Attenuation	2
Response	200
Oven temperature	170 °C
Time 1	3 min
Ramp 1	4 °C /min
Temperature 2	220 °C
Time 2	15 min
Ramp 2	End

D.3 Percentage and molecular weight of SCG oil fatty acids

Table D.2 shows the average fatty acid profile of ICG1 oil determined at the NHE site, along with the molecular weight of each fatty acid.

Table D.2: Fatty acid profile of ICG1 oil and molecular weight of individual fatty acids.

C _n	Fatty acid	% w/w Average composition	Standard deviation	Molecular weight (g/mol)
14:0	Myristic	0.06	0	228
16:0	Palmitic	33.13	1.27	256
16:1	Palmitoleic	0.1	0	254
17:0	Heptadecanoic	0.06	0	270
18:0	Stearic	7.9	0.34	284
18:1	Oleic	9.86	0.49	282
18:1	cis-vaccenic	0.5	0	282
18:2	Linoleic	41.83	1.20	280
18:3 α	α -linolenic	1	0.1	278
20:0	Eicosanoic	3.63	0.47	312
20:1	Eicosenoic	0.2	0.17	310
20:2	Eicosadienoic	0.1	0	308
22:0	docosanoic	0.63	0.05	340
22:1	docosenoic	0.1	0	338
24:0	tetracosanoic	0.33	0.05	368

E. Fuel samples specifications

Table E.1 shows the known properties of the reference fossil diesel and vegetable biodiesel samples used in the engine tests.

Table E.1: Properties of reference fossil diesel and biodiesel samples.

Property	Reference fossil diesel	Rapeseed biodiesel	Soya biodiesel
Density at 15 °C (kg/m ³)	835.4	883.1	884.9
Kinematic viscosity at 40 °C (mm ² /s)	2.892	4.325	4.075
Cetane number	53.3	52	52
HHV (MJ/kg)	45.68	-	-

F. GC-FID

Table F.1 shows the 37 component FAME mix used in the CG-FID analysis with FAMES ranging from C4:0 to C24:1 (Supelco, 1996).

Table F.1: Composition of Supelco 37 Component FAME mix.

Peak ID	Component (acid methyl esters)	Weight (%)
1	C4:0 (Butyric)	4
2	C6:0 (Caproic)	4
3	C8:0 (Caprylic)	4
4	C10:0 (Capric)	4
5	C11:0 (Undecanoic)	2
6	C12:0 (Lauric)	4
7	C13:0 (Tridecanoic)	2
8	C14:0 (Myristic)	4
9	C14:1 (Myristoleic)	2
10	C15:0 (Pentadecanoic)	2
11	C15:1 (cis-10-Pentadecenoic)	2
12	C16:0 (Palmitic)	6
13	C16:1 (Palmitoleic)	2
14	C17:0 (Heptadecanoic)	2
15	C17:1 (cis-10-Heptadecenoic)	2
16	C18:0 (Stearic)	4
17	C18:1n9c (Oleic)	4
18	C18:1n9t (Elaidic)	2
19	C18:2n6c (Linoleic)	2
20	C18:2n6t (Linolelaidic)	2
21	C18:3n6 (γ -Linolenic)	2
22	C18:3n3 (α -Linolenic)	2
23	C20:0 (Arachidic)	4
24	C20:1n9 (cis-11-Eicosenoic)	2
25	C20:2 (cis-11,14-Eicosadienoic)	2

Peak ID	Component (acid methyl esters)	Weight (%)
26	C20:3n6 (cis-8,11,14-Eicosatrienoic)	2
27	C20:3n3 (cis-11,14,17-Eicosatrienoic)	2
28	C20:4n6 (Arachidonic)	2
29	C20:5n3 (cis-5,8,11,14,17-Eicosapentaenoic)	2
30	C21:0 (Henicosanoic)	2
31	C22:0 (Behenic)	3
32	C22:1n9 (Erucic)	2
33	C22:2 (cis-13,16-Docosadienoic)	2
34	C22:6n3 (cis-4,7,10,13,16,19-Docosahexaenoic)	2
35	C23:0 (Tricosanoic)	2
36	C24:0 (Lignoceric)	4
37	C24:1n9 (Nervonic)	2

Figure F.1 shows the 37 component FAME mix chromatogram obtained with a SP-2380 Column (Supelco, 1996), the same used in the GC-FID analysis performed in this study. The numbers aligned with each peak shown in Figure F.1 correspond to the FAMEs presented in Table F.1.

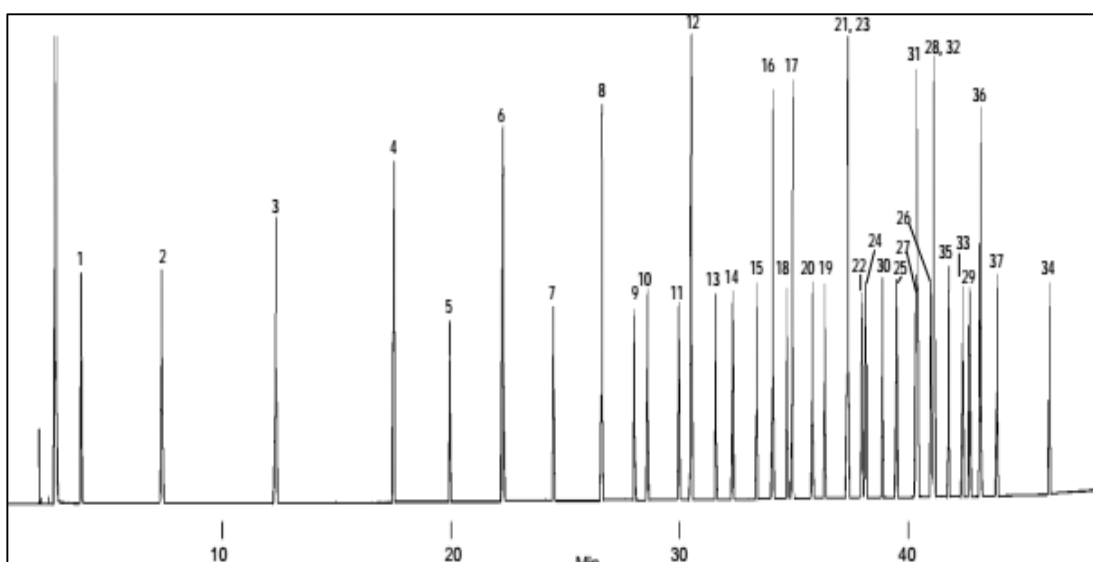


Figure F.1: Supelco 37 Component FAME Mixture on SP-2380 Column.

Figures F.2, F.3, F.4 and F.5 show the chromatograms obtained when the 37 FAME component mixture, ICG2 biodiesel (Table 8.2 – trial 6), soya biodiesel and rapeseed biodiesel were analyzed respectively. All the samples were diluted in dichloromethane at a concentration of 5000 ppm.

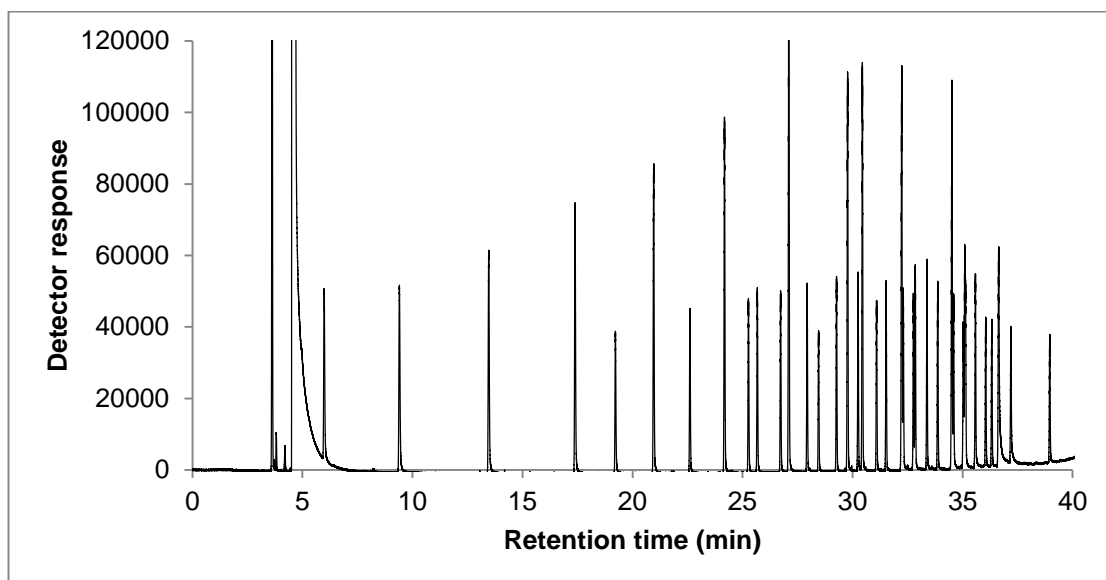


Figure F.2: GC-FID chromatogram obtained with 37 FAME component mixture.

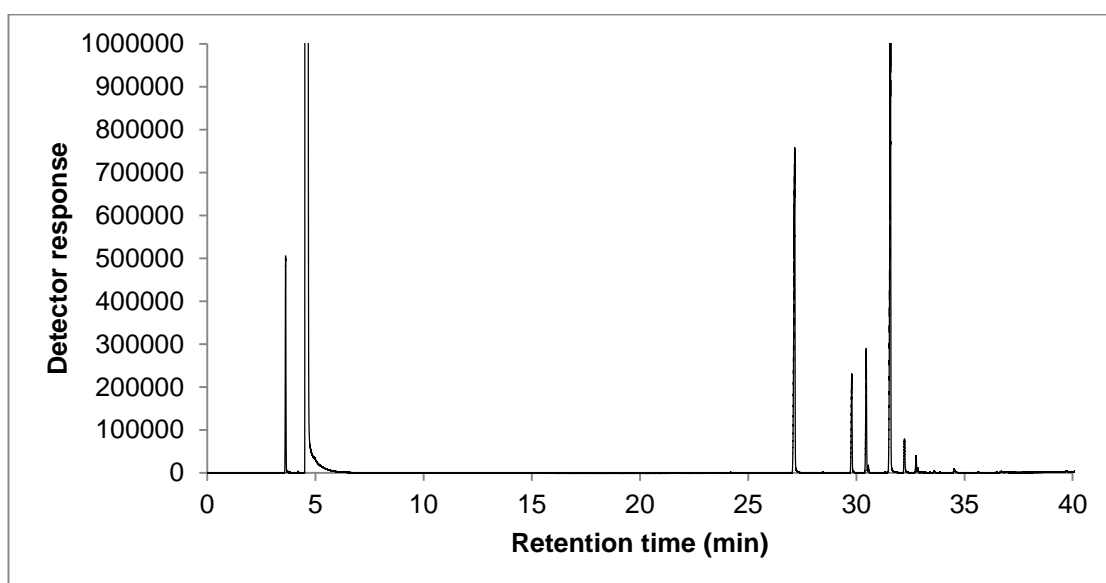


Figure F.3: GC-FID chromatogram obtained with ICG2 biodiesel ((Table 8.2 – trial 6).

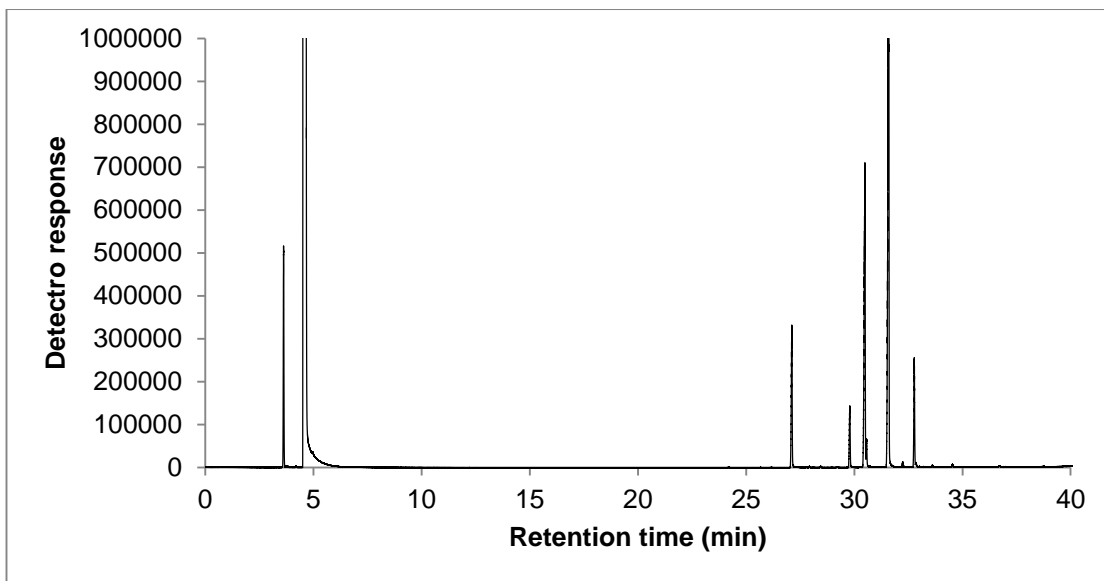


Figure F.4: GC-FID chromatogram obtained with soya biodiesel.

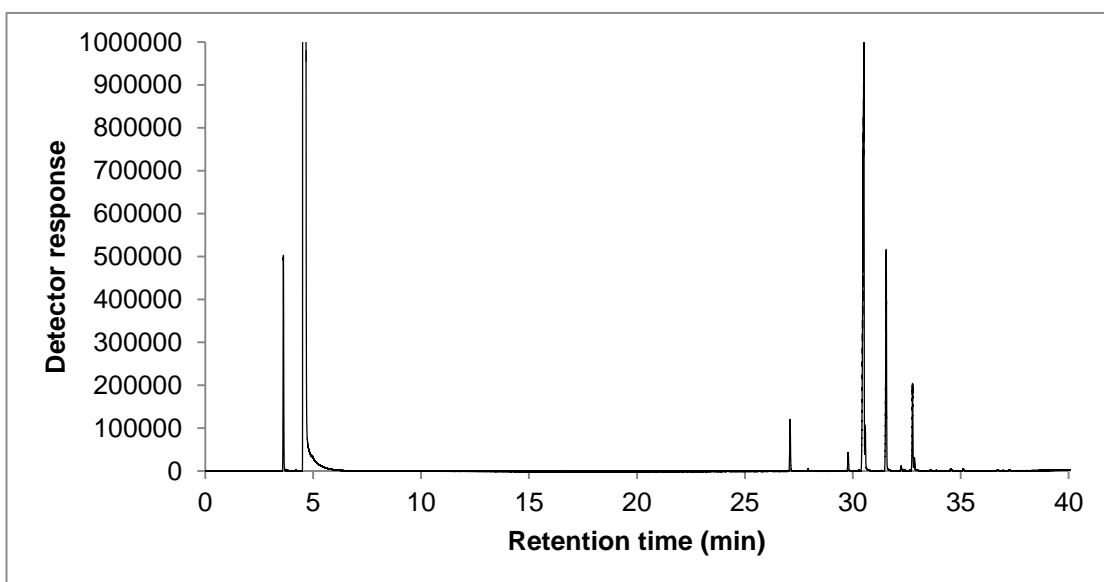


Figure F.5: GC-FID chromatogram obtained with soya biodiesel.

Tables F.2, F.3, F.4, F.5 and F.6 show the calculations used for fatty acid profile determination.

Table F.2: ICG2 biodiesel (Table 8.2 - trial 6).

Trendline	Type	Area	Component concentration (µg/mL)	Component percentage (%)
$y = 853.2x - 142265$	C16:0	1316367.79	1709.60	34.19
$y = 497.72x - 41119$	C18:0	155937.88	395.91	7.92
$y = 580.11x - 108375$	C18:1	161077.96	464.48	9.29
$y = 797.05x - 24884$	C18:2	1712707.62	2180.02	43.60
$y = 568.54x - 33768$	C18:3n6	49000.53	140.39	2.81
$y = 793.5x - 24351$	C18:3n3	20536.44	56.56	1.13
SUM of FAME identified				98.94
Unknown				1.06

Table F.3: ICG2 biodiesel (Table 8.2 - trial 7).

Trendline	Type	Area	Component concentration (µg/mL)	Component percentage (%)
$y = 853.2x - 142265$	C16:0	1326562.68	1721.55	34.43
$y = 497.72x - 41119$	C18:0	157094.10	398.24	7.96
$y = 580.11x - 108375$	C18:1	159310.69	461.43	9.23
$y = 797.05x - 24884$	C18:2	1694298.69	2156.93	43.14
$y = 568.54x - 33768$	C18:3n6	52615.35	144.32	2.88
$y = 793.5x - 24351$	C18:3n3	18506.97	54.01	1.08
SUM of FAME identified				98.73
Unknown				1.27

Table F.4: ICG2 biodiesel (Table 8.2 - trial 8).

Trendline	Type	Area	Component concentration (µg/mL)	Component percentage (%)
$y = 853.2x - 142265$	C16:0	1318708.68	1712.34	34.24
$y = 497.72x - 41119$	C18:0	156042.57	396.12	7.92
$y = 580.11x - 108375$	C18:1	159116.29	461.10	9.22
$y = 797.05x - 24884$	C18:2	1704965.34	2170.31	43.40
$y = 568.54x - 33768$	C18:3n6	53022.97	145.00	2.90
$y = 793.5x - 24351$	C18:3n3	19588.21	55.60	1.11
SUM of FAME identified				98.81
Unknown				1.19

Table F.5: Soya biodiesel.

Trendline	Fatty acid	Area	Component concentration (µg/mL)	Component percentage (%)
$y = 853.2x - 142265$	C16:0	298249.13	516.30	10.32
$y = 497.72x - 41119$	C18:0	67574.28	218.38	4.36
$y = 580.11x - 108375$	C18:1	669262.45	1340.50	26.80
$y = 797.05x - 24884$	C18:2	1995216.37	2534.47	50.69
$y = 793.5x - 24351$	C18:3n3	243439.86	337.48	6.75
SUM of FAME identified				98.92
Unknown				1.08

Table F.6: Rapeseed biodiesel.

Trendline	Type	Area	Component concentration (µg/mL)	Component percentage (%)
$y = 853.2x - 142265$	C16:0	62752.18	240.29	4.80
$y = 497.72x - 41119$	C18:0	3345.84	89.33	1.78
$y = 580.11x - 108375$	C18:1	1667921.82	3062.00	61.24
$y = 797.05x - 24884$	C18:2	832948.67	1076.26	21.52
$y = 793.5x - 24351$	C18:3n3	285990.63	391.10	7.82
$y = 436.86x - 25036$	C20:1	2390.33	62.78	1.25
SUM of FAME identified				98.41
Unknown				1.59

G. Engine specifications

Table G.1: Research engine specifications

Engine head model	Ford Duratorq
Number of cylinders	1
Cylinder bore (mm)	86
Crankshaft stroke (mm)	86
Displacement (cc)	499.56
Compression ratio	18.2:1
Piston bowl design	Central ω -bowl in piston
Maximum cylinder pressure (MPa)	15
High pressure fuel system	160 MPa common rail (BOCH CRS2)
Injector type	6-hole (DELPHI DF1 1.3)
Injector control	1 μ s accuracy (EMTRONIX EC-GEN 500)
Shaft encoder	0.2 CAD resolution
Coolant water temperature	80 \pm 2.5 $^{\circ}$ C
Engine oil temperature	80 \pm 2.5 $^{\circ}$ C

H.NMR method

A range of oils extracted from the SCG were selected for analysis by ^1H NMR; these were the oils obtained from Soxhlet extraction, and oils extracted by ASE using ethanol and hexane at various temperatures. For NMR analysis, the oil samples were diluted into chloroform-d (CDCl_3), typically 0.025 mL of oil into 1 mL of CDCl_3 . The samples were transferred into 0.5mm NMR tubes.

NMR spectroscopic analysis of oil samples was carried out at 298 K using a Bruker Advance III 600 spectrometer, operating at 600.13 MHz, and equipped with a cryoprobe. The acquisition parameters were as follows: spectral width 12335 Hz, relaxation delay 1 s, acquisition time 4 s, 32 scans, flip angle of 30° deg. A 0.3 Hz line broadening was applied prior to Fourier transform, and the spectra were referenced to residual CHCl_3 in the solvent at (δ , 7.26 ppm). Data was processed manually using Bruker TOPSPIN-NMR software (version 3.5.6). The method of evaluating NMR spectra to give the apparent ratios of the various lipid components was adapted from that of Nieva-Echevarría et al. (2014). Estimations of component mass percentage were made using an assumed molecular weight for all lipid chains, corresponding to that of palmitic acid which is broadly representative of lipids found in oil from SCG (Jenkins et al., 2014).

The spectra obtained from NMR analysis of the SCG oils were broadly similar in their apparent composition; and were similar to those reported by other researchers (Döhlert et al., 2016; Jenkins et al., 2014). An example spectra which highlights some of the main spectral peaks and assignments is given in Figure H.1.

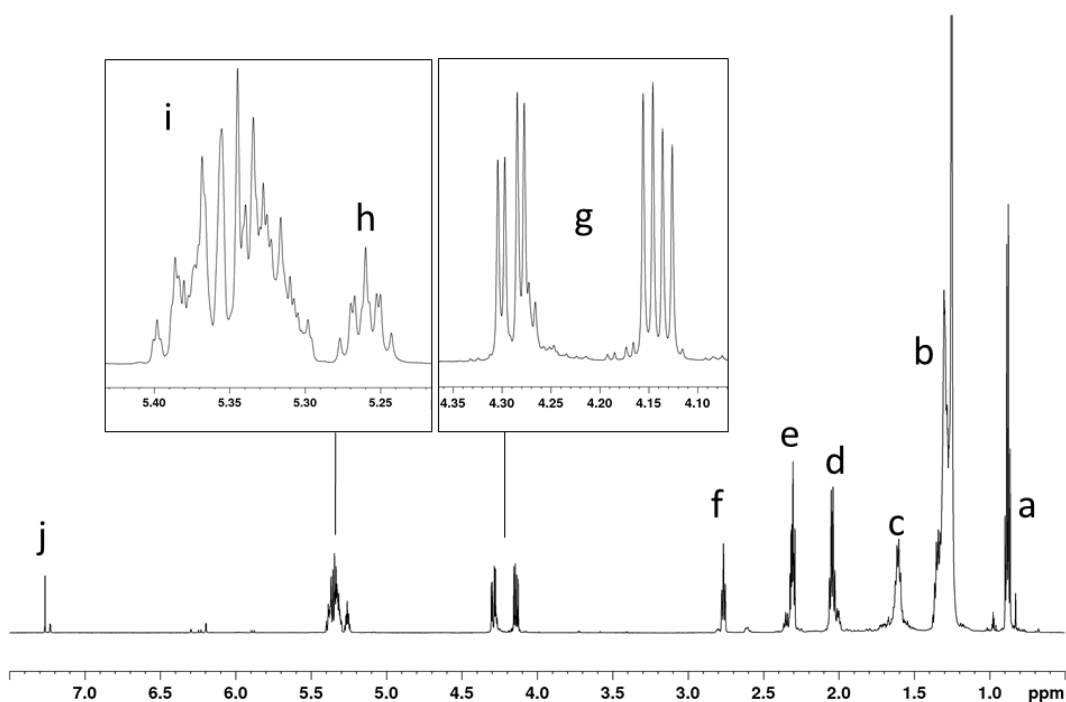


Figure H.1: Example ¹H NMR spectrum highlighting some main spectral peaks and their assignments. Spectrum shown is of the oil extracted from SCG using ASE with hexane solvent at 125 °C. (a) -CH₃, (b) -(CH₂)_n-, (c) -OCO-CH₂-CH₂-, (d) CH₂-CH=CH, (e) -OCO-CH₂-, (f) =HC-CH₂-CH=, (g) R'OCH₂-CH(OR')-CH₂OR", (h) R'OCH₂-CH(OR')-CH₂OR", (i) -CH=CH-, (j) residual solvent CHCl₃.

Using the spectral peaks particular to FFAs, triglycerides, 1-monoglycerides, 1,2-diglycerides, and 1,3-diglycerides, estimations were made using the peak areas of the molar ratios of these various constituent components of the oils. The COOH peak could provide a unique signal in the ¹H spectrum for FFA, however, fast proton exchange processes with water in CDCl₃ result in the broadening of the signal arising from the carboxylic acid group (COOH) at around 12 ppm, such that is not apparent in the spectrum. Skiera et al. (2014) investigated the FFA content in pharmaceutical lipids using NMR spectroscopy. Their method involved the addition of small amounts of deuterated dimethyl sulfoxide (DMSO-d₆) to the fatty oils in CDCl₃, which slowed the proton transfer sufficiently to allow the detection of the COOH signal. Addition of DMSO-d₆ was also trailed in the present work; however, addition of DMSO at various levels resulted in the visible precipitation of some

of the oil. Instead, a method was adopted that used the signal arising from the acyl group (COOH-CH₂-) of the FFAs, which is distinguishable from the ester functional group in glycerides. An unidentified peak was apparent in the spectra of oils obtained with long chained alcohols through Soxhlet extraction. A two-dimensional COSY NMR experiment was carried out on the propanol sample, and the peak was seen to be coupled to -OCO-CH₂- (i.e. peak C in Figure H.1)

Due to the complex composition of the oils analyzed in this work (including mono-, di and triglycerides), previously reported methods (e.g. (Satyarthi et al., 2009; Skiera et al., 2014, 2012)) needed to be adapted to take account of each of these components. Part of the method used in this paper relied on making an assumption of the average molecular masses of each component. Small variations in the actual molecular compositions, and overlapping spectral peaks, therefore lead to error in the NMR method. A detailed appraisal of the absolute accuracy of the quantitative results obtained by the NMR analysis is beyond the scope of this work, and is left to future studies.

Table H.1 shows the apparent molar ratios of the identified constituents of the oils (normalized to the triglyceride component), and the estimated percentage composition by mass.

Table H.1: Composition of oils obtained from Soxhlet extraction using different extraction solvents, using ^1H NMR spectra. Estimations were made of the apparent molar ratios of the components (using adjusted peak integral values), and derived estimates of mass concentration.

Solvent	Apparent molar ratio					Estimated mass (%)				
	TAG	1-MAG	1,2-DAG	1,3-DAG	FFAs	TAG	1-MAG	1,2-DAG	1,3-DAG	FFAs
Dichloromethane	1.00	0.00	0.08	0.19	1.50	61%	0%	3%	8%	27%
Toluene	1.00	0.01	0.07	0.20	1.21	64%	0%	3%	9%	23%
Pentane	1.00	0.00	0.10	0.22	0.52	72%	0%	5%	11%	11%
Hexane	1.00	0.00	0.07	0.22	0.79	69%	0%	3%	11%	16%
Heptane	1.00	0.00	0.08	0.19	0.52	74%	0%	4%	10%	12%
Ethanol	1.00	0.03	0.09	0.44	2.33	48%	1%	3%	15%	33%
Propanol	1.00	0.11	0.17	0.57	1.92	47%	2%	5%	19%	27%
Butanol	1.00	0.01	0.15	0.41	1.68	53%	0%	6%	15%	26%
Pentanol	1.00	0.26	0.22	0.72	1.66	44%	5%	7%	22%	22%
Hexanol	1.00	0.36	0.29	0.83	2.01	39%	6%	8%	23%	24%

TAG: Triglyceride, 1,2-DAG: 1,2-diglyceride, 1,3-DAG: 1,3-diglyceride, 1-MAG: 1-monoglyceride.

I. Elemental analysis of oil and biodiesel samples



Warwick Analytical Service

Warwick Analytical Service is the analytical division of Exeter Analytical (UK) Ltd

Page 1 of 1

Ioannis Efthymiopoulos
UCL Department Of Mechanical
Engineering
Department Of Mechanical Engineering

Report No. 32039
Ref: F45-2347878
Date In: 22-May-17
Date Out: 24-May-17

TEST REPORT		
WAS: 32039	Sample ID: 1-Biodiesel	Sample Type: Liquid

Technique	Element	Units	Result	Date
SOP 31	Carbon	%wt/wt	76.92	23-May-17
	Hydrogen		12.11	
	Nitrogen		0.01	

Test Report prepared by:

Kiran Bhamber - Quality Assistant

All samples are tested "as received".
 Methods indicated ▼ are not covered by the scope of UKAS 17025 accreditation
 Elements indicated * have been generated within the bounds of the Laboratory's UKAS Flexible Scope accreditation
 Methods indicated ♦ are carried out by a sub-contracted Laboratory
 Any expression of opinion or interpretation of results is outside the scope of accreditation
 Results shall not be reproduced except in full without written approval of Warwick Analytical Service
 Warwick Analytical Service- The Venture Centre – University of Warwick Science Park – Coventry – CV4 7EZ



FM010-2



Warwick Analytical Service

Warwick Analytical Service is the analytical division of Exeter Analytical (UK) Ltd

Page 1 of 1

Ioannis Efthymiopoulos
UCL Department Of Mechanical
Engineering
Department Of Mechanical Engineering

Report No. 32040
Ref: F45-2347878
Date In: 22-May-17
Date Out: 24-May-17

TEST REPORT		
WAS: 32040	Sample ID: 2-Biodiesel	Sample Type: Liquid

Technique	Element	Units	Result	Date
SOP 31	Carbon	%wt/wt	76.69	23-May-17
	Hydrogen		12.17	
	Nitrogen		0	

Test Report prepared by:

Kiran Bhamber - Quality Assistant

All samples are tested "as received".
Methods indicated ▼ are not covered by the scope of UKAS 17025 accreditation
Elements indicated * have been generated within the bounds of the Laboratory's UKAS Flexible Scope accreditation
Methods indicated + are carried out by a sub-contracted Laboratory
Any expression of opinion or interpretation of results is outside the scope of accreditation
Results shall not be reproduced except in full without written approval of Warwick Analytical Service
Warwick Analytical Service- The Venture Centre - University of Warwick Science Park - Coventry - CV4 7EZ



FM010-2



Warwick Analytical Service

Warwick Analytical Service is the analytical division of Exeter Analytical (UK) Ltd

Page 1 of 1

Ioannis Efthymiopoulos
UCL Department Of Mechanical
Engineering
Department Of Mechanical Engineering

Report No. 32041
Ref: F45-2347878
Date In: 22-May-17
Date Out: 24-May-17

TEST REPORT		
WAS: 32041	Sample ID: 3-Biodiesel	Sample Type: Liquid

Technique	Element	Units	Result	Date
SOP 31	Carbon	%wt/wt	76.79	24-May-17
	Hydrogen		11.97	
	Nitrogen		0	

Test Report prepared by:

Kiran Bhamber - Quality Assistant

All samples are tested "as received".
Methods indicated ▼ are not covered by the scope of UKAS 17025 accreditation
Elements indicated * have been generated within the bounds of the Laboratory's UKAS Flexible Scope accreditation
Methods indicated + are carried out by a sub-contracted Laboratory
Any expression of opinion or interpretation of results is outside the scope of accreditation
Results shall not be reproduced except in full without written approval of Warwick Analytical Service
Warwick Analytical Service - The Venture Centre - University of Warwick Science Park - Coventry - CV4 7EZ



2763

FM010-2



Warwick Analytical Service

Warwick Analytical Service is the analytical division of Exeter Analytical (UK) Ltd

Page 1 of 1

Ioannis Efthymiopoulos
UCL Department Of Mechanical
Engineering
Department Of Mechanical Engineering

Report No. 32042
Ref: F45-2347878
Date In: 22-May-17
Date Out: 24-May-17

TEST REPORT		
WAS: 32042	Sample ID: 4-Coffee Oil	Sample Type: Liquid

Technique	Element	Units	Result	Date
SOP 31	Carbon	%wt/wt	76.72	23-May-17
	Hydrogen		11.83	
	Nitrogen		0.05	

Test Report prepared by:

Kiran Bhambher - Quality Assistant

All samples are tested "as received".
Methods indicated ▼ are not covered by the scope of UKAS 17025 accreditation
Elements indicated * have been generated within the bounds of the Laboratory's UKAS Flexible Scope accreditation
Methods indicated ♦ are carried out by a sub-contracted Laboratory
Any expression of opinion or interpretation of results is outside the scope of accreditation
Results shall not be reproduced except in full without written approval of Warwick Analytical Service
Warwick Analytical Service- The Venture Centre - University of Warwick Science Park - Coventry - CV4 7EZ



FM010-2

To: Ioannis Efthymiopoulos Department of Mechanical Engineering - UCL Roberts Building Torrington Place London WC1E 7JE UK	Report No. RT/ELE/17190 Date: 30/06/2017 Phoenix No. UK760-0023616 Order No. F45 2347290 Quote No. QT/SUN/17/D98 Date Samples Received 24/05/2017 Total Cost for Analysis £460
E-Mail: i.efthymiopoulos@ucl.ac.uk	

Oxygen Content of Biodiesel

Sample Summary

SAMPLE NUMBERS	SAMPLE DESCRIPTION
ELE-300056	1 Biodiesel
ELE-300057	2 Biodiesel
ELE-300058	3 Biodiesel
ELE-300059	4 Coffee OIP

Disclaimer

This report was made with due care within the limitation of a defined scope of work and on the basis of information, materials received from the Customer or its nominated third parties or collected by Intertek in accordance with the Customer's instructions. Intertek is under no obligation to refer to or report upon any facts or circumstances which are outside the specific instructions received and accepts no responsibility to any parties whatsoever, following the issue of the report, for any matters arising outside the agreed scope of the works. The tests results are not intended to be a recommendation for any particular course of action. Customer is responsible for acting as it sees fit on the basis of such results. The reported result(s) relate specifically to the sample(s) that were drawn and delivered by the Customer or their nominated third party. The reported result(s) provide no warranty or verification on the sample(s) representing any specific goods, material and/or shipment and only relate to the sample(s) as received and tested. Intertek will not be responsible for any damages caused to the samples during their transit to Intertek's facilities and Customer acknowledges that the conditions surrounding the samples during the transit may impact the results. This report does not discharge or release the factory/sellers/suppliers from their commercial, legal or contractual obligations with buyers or end-users in respect of products provided by the factory/sellers/suppliers. This report by itself does not imply that the material, product, or service is or has ever been under an Intertek certification program. Any use of the Intertek name or one of its marks for the sale or advertisement of the tested materials or product must first be approved in writing by Intertek.

Lab Sample No: ELE-300056
 Sample Description: 1 Biodiesel

METHOD	ANALYSIS	RESULT	UNITS
Oxygen Analysis (MT/ELE/21)*	Oxygen Content	11.6	% wt/wt

Lab Sample No: ELE-300057
 Sample Description: 2 Biodiesel

METHOD	ANALYSIS	RESULT	UNITS
Oxygen Analysis (MT/ELE/21)*	Oxygen Content	11.5	% wt/wt

Lab Sample No: ELE-300058
 Sample Description: 3 Biodiesel

METHOD	ANALYSIS	RESULT	UNITS
Oxygen Analysis (MT/ELE/21)*	Oxygen Content	11.5	% wt/wt

Lab Sample No: ELE-300059
 Sample Description: 4 Coffee OIP

METHOD	ANALYSIS	RESULT	UNITS
Oxygen Analysis (MT/ELE/21)*	Oxygen Content	11.9	% wt/wt

* Test not UKAS accredited


Analysis has been carried out on samples as received, independent of sampling procedure, using the latest versions of all test methods.

Samples will be disposed of after 1 month unless alternative arrangements have been made in agreement with the customer.

¥ Opinions and interpretations expressed herein are outside the scope of UKAS accreditation.

Reported By:  _____

Mark Sykes
 Analytical Chemist

Checked By:  _____

Rachel Inkster
 Analyst

Contact No.: +44(0)1932 732 118

J. Viscosity measurement

Viscosity measurements were conducted on the steady state mode using a rotational hybrid rheometer (DHR-3, TA Instruments) equipped with a 60 mm cone geometry (1 deg) at a gap of 27 μm . A 6 minutes equilibration time was applied before each measurement to ensure that the sample had reached the desired temperature (40 °C). Tables J.1 and J.2 show the results obtained from the viscosity measurement of raw ICG2 oil and ICG2 biodiesel.

Table J.1: Viscosity measurement of raw ICG2 oil.

Stress (Pa)	Shear rate (1/s)	Viscosity (Pa.s)	Step time (s)	Temperature (°C)	Normal stress (Pa)	Gap (μm)	Axial force (N)	Torque (μN.m)
0.423146	10.0004	0.042313	41.0935	40.021	-69.8617	300.022	-0.0439	5.31741
0.670428	15.8498	0.042299	82.2805	40.006	-67.4663	300.011	-0.04239	8.42484
1.06376	25.118	0.042351	123.406	40	-67.7291	300.039	-0.04256	13.3677
1.68736	39.8109	0.042384	164.484	39.993	-65.449	300.025	-0.04112	21.204
2.67542	63.0928	0.042405	205.593	39.997	-66.7946	300.04	-0.04197	33.6204
4.24353	99.9963	0.042437	246.671	39.995	-66.6751	300.037	-0.04189	53.3258

Table J.2: Viscosity measurement of ICG2 biodiesel.

Stress (Pa)	Shear rate (1/s)	Viscosity (Pa.s)	Step time (s)	Temperature (°C)	Normal stress (Pa)	Gap (μm)	Axial force (N)	Torque (μN.m)
0.373629	63.0961	0.005922	591.739	39.997	-47.9638	27.0124	-0.06781	21.1282
0.56786	100	0.005679	632.898	40.005	-49.8804	27.0262	-0.07052	32.1117
0.883154	158.489	0.005572	674.073	39.999	-52.2431	27.0283	-0.07386	49.9412
1.38252	251.189	0.005504	715.238	40.01	-55.5638	27.0323	-0.07855	78.1796
2.17502	398.108	0.005463	756.365	40.012	-62.0212	27.0339	-0.08768	122.995
2.70678	500	0.005414	797.524	40.011	-69.1522	27.0521	-0.09776	153.065

The average dynamic viscosity was used for the determination of the kinematic viscosity:

$$\text{Kinematic viscosity of raw ICG2 oil at } 40\text{ }^{\circ}\text{C} \left(\frac{\text{mm}^2}{\text{s}} \right) = \frac{\text{Dynamic viscosity (mPa s)}}{\text{Density} \left(\frac{\text{g}}{\text{cm}^3} \right)} =$$

$$\frac{42.365}{0.927} = 45.70 \text{ mm}^2/\text{s}$$

$$\text{Kinematic viscosity of ICG2 biodiesel at } 40\text{ }^{\circ}\text{C} \left(\frac{\text{mm}^2}{\text{s}} \right) = \frac{5.592 \text{ (mPa s)}}{0.893 \left(\frac{\text{g}}{\text{cm}^3} \right)} = 6.26$$

mm²/s

References

- Abdullah, M., Bulent Koc, A., 2013. Oil removal from waste coffee grounds using two-phase solvent extraction enhanced with ultrasonication. *Renew. Energy* 50, 965–970. doi:10.1016/j.renene.2012.08.073
- Acevedo, F., Rubilar, M., Scheuermann, E., Cancino, B., Uquiche, E., Garcés, M., Inostroza, K., Shene, C., 2013. Spent coffee grounds as a renewable source of bioactive compounds. *J. Biobased Mater. Bioenergy* 7, 420–428. doi:10.1166/jbmb.2013.1369
- Adeeko, K.A., Ajibola, O.O., 1990. Processing factors affecting yield and quality of mechanically expressed groundnut oil. *J. Agric. Eng. Res.* 45, 31–43. doi:10.1016/S0021-8634(05)80136-2
- Adesina, And Bankole, Y.O., 2013. Effects of Particle Size, Applied Pressure and Pressing Time on the Yield of Oil Expressed from Almond Seed. *Niger. Food J. Off. J. Niger. Inst. Food Sci. Techonology* www.nifst.org NIFOJ 31, 98–105. doi:10.1016/S0189-7241(15)30082-5
- Agarwal, D., Singh, M., 2016. iscometric studies of molecular interactions in binary liquid mixtures of nitromethane with some polar and non-polar solvents at 298.15 K. *J. Indian Chem. Soc.* 81, 850–859.
- Aguilera, J.M., Stanley, D.W., 1999. Microstructural principles of food processing and engineering, *Microstructural Principles of Food Processing and Engineering*. doi:10.1016/0924-2244(90)90115-F
- Ahangari, B., Sargolzaei, J., 2013. Extraction of lipids from spent coffee grounds using organic solvents and supercritical carbon dioxide. *J. Food Process. Preserv.* 37, 1014–1021. doi:10.1111/j.1745-4549.2012.00757.x
- Ahmad, N., Rehana, N., 1980. Solvent and temperature effect on the dipole moment of dichloroethane. *J.Chem.Soc.Pak* 2.
- Akgün, N.A., Bulut, H., Kikic, I., Solinas, D., 2014. Extraction behavior of lipids obtained from spent coffee grounds using supercritical carbon dioxide. *Chem. Eng. Technol.* 37, 1975–1981. doi:10.1002/ceat.201400237

- Akoh, C.C., 2005. Handbook of Functional Lipids. CRC Press.
- Al-Hamamre, Z., Foerster, S., Hartmann, F., Kröger, M., Kaltschmitt, M., 2012. Oil extracted from spent coffee grounds as a renewable source for fatty acid methyl ester manufacturing. *Fuel* 96, 70–76. doi:10.1016/j.fuel.2012.01.023
- Alajmi, F.S.M.D.A., Hairuddin, A.A., Adam, N.M., Abdullah, L.C., 2017. Recent trends in biodiesel production from commonly used animal fats. *Int. J. Energy Res.* n/a--n/a. doi:10.1002/er.3808
- Ali, M., Watson, I.A., 2014. Comparison of oil extraction methods, energy analysis and biodiesel production from flax seeds. *Int. J. Energy Res.* 38, 614–625. doi:10.1002/er.3066
- Anisa Aris, N.I., Morad, N.A., 2014. Effect of extraction time on degradation of bioactive compounds (*Zingiber officinale roscoe*). *J. Teknol. (Sciences Eng.* 67, 63–66. doi:10.11113/jt.v67.2800
- Athankar, K.K., Wasewar, K.L., Varma, M.N., Shende, D.Z., 2016. Reactive extraction of gallic acid with tri-n-caprylylamine. *New J. Chem.* 40, 2413–2417. doi:10.1039/C5NJ03007B
- Ballesteros, L.F., Teixeira, J.A., Mussatto, S.I., 2014. Chemical, Functional, and Structural Properties of Spent Coffee Grounds and Coffee Silverskin. *Food Bioprocess Technol.* 7, 3493–3503. doi:10.1007/s11947-014-1349-z
- Bargale, P.C., Ford, R.J., Sosulski, F.W., Wulfsohn, D., Irudayaraj, J., 1999. Mechanical oil expression from extruded soybean samples. *J. Am. Oil Chem. Soc.* 76, 223–229. doi:10.1007/s11746-999-0222-0
- Barratt, M.D., 1995. A quantitative structure-activity relationship for the eye irritation potential of neutral organic chemicals. *Toxicol. Lett.* 80, 69–74. doi:10.1016/0378-4274(95)03338-L
- Baumgarten, H.E., 1989. Mechanism and Theory in Organic Chemistry, Third Edition (Lowry, T. H.; Richardson, K. S.), *Journal of Chemical Education.*

doi:10.1021/ed066pA131.2

- Berchmans, H.J., Hirata, S., 2008. Biodiesel production from crude *Jatropha curcas* L. seed oil with a high content of free fatty acids. *Bioresour. Technol.* 99, 1716–1721. doi:10.1016/j.biortech.2007.03.051
- Berhe, M.H., Asfaw, A., Asfaw, N., 2013. Investigation of Waste Coffee Ground as a Potential Raw Material for Biodiesel Production. *Int. J. Renew. Energy Res.* 3, 854–860.
- Berk, Z., 2013. Chapter 8 - Filtration and Expression BT - Food Process Engineering and Technology (Second Edition), in: *Food Science and Technology*. pp. 217–240. doi:http://dx.doi.org/10.1016/B978-0-12-415923-5.00008-3
- Berk, Z., 2009. 11 Extraction. *Food Process Eng. Technol.*
- Bertrand, B., Guyot, B., Anthony, F., Lasherme, P., 2003. Impact of the *Coffea canephora* gene introgression on beverage quality of *C. arabica*. *Theor. Appl. Genet.* 107, 387–394. doi:10.1007/s00122-003-1203-6
- Bok, J.P., Choi, H.S., Choi, Y.S., Park, H.C., Kim, S.J., 2012. Fast pyrolysis of coffee grounds: Characteristics of product yields and biocrude oil quality. *Energy* 47, 17–24. doi:10.1016/j.energy.2012.06.003
- Bolotnikov, M.F., Neruchev, Y.A., 2004. Relative permittivity for 1-chlorohexane, 1-iodohexane, 1-iodoheptane, and 1-chlorononane from (293.15 to 373.15) K and hexane + 1-chlorohexane from (293.15 to 333.15) K. *J. Chem. Eng. Data* 49, 895–898. doi:10.1021/je034205+
- Borém, F.M., Marques, E.R., Alves, E., 2008. Ultrastructural analysis of drying damage in parchment Arabica coffee endosperm cells. *Biosyst. Eng.* 99, 62–66. doi:10.1016/j.biosystemseng.2007.09.027
- Borrelli, R.C., Esposito, F., Napolitano, A., Ritieni, A., Fogliano, V., 2004. Characterization of a new potential functional ingredient: coffee silverskin. *J. Agric. Food Chem.* 52, 1338–1343. doi:10.1021/jf034974x
- BP, 2017. BP Statistical Review of World Energy 2017. *Br. Pet.* 1–52.

doi:<http://www.bp.com/content/dam/bp/en/corporate/pdf/energy-economics/statistical-review-2017/bp-statistical-review-of-world-energy-2017-full-report.pdf>

Brando, C.H.J., 2004. Harvesting and Green Coffee Processing, in: Wintgens, J.N. (Ed.), *Coffee: Growing, Processing, Sustainable Production: A Guidebook for Growers, Processors, Traders, and Researchers*. pp. 604–715. doi:10.1002/9783527619627.ch24

Bresciani, L., Calani, L., Bruni, R., Brighenti, F., Del Rio, D., 2014. Phenolic composition, caffeine content and antioxidant capacity of coffee silverskin. *Food Res. Int.* 61, 196–201. doi:10.1016/j.foodres.2013.10.047

Brown, W., Foote, C., Iverson, B., Anslyn, E., 2008. Nucleophilic Substitution and β -Elimination, in: *Organic Chemistry*. Cengage Learning, p. 335.

BSI Standard, 2014. BS EN 14214:2012+A1:2014.

BSI Standard, 2008. BS ISO 3601 - Fluid power systems - O-rings.

BSI Standard, 2006. BS 5500 - Specification for unfired fusion welded pressure vessels.

Budryn, G., Nebesny, E., Zyzelewicz, D., Oracz, J., Miśkiewicz, K., Rosicka-Kaczmarek, J., 2012. Influence of roasting conditions on fatty acids and oxidative changes of Robusta coffee oil. *Eur. J. Lipid Sci. Technol.* 114, 1052–1061. doi:10.1002/ejlt.201100324

Bulent Koc, A., Fereidouni, M., 2011. Soybeans processing for biodiesel production, in: Ng, T.-B. (Ed.), *Soybean - Applications and Technology*. doi:10.5772/14216

Caetano, N.S., Silva, V.F.M., Melo, A.C., Martins, A.A., Mata, T.M., 2014. Spent coffee grounds for biodiesel production and other applications. *Clean Technol. Environ. Policy* 16, 1423–1430. doi:10.1007/s10098-014-0773-0

Caetano, N.S., Silvaa, V.F.M., Mata, T.M., 2012. Valorization of coffee grounds for biodiesel production, in: *Chemical Engineering Transactions*.

pp. 267–272. doi:10.3303/CET1226045

Calixto, F., Fernandes, J., Couto, R., Hernández, E.J., Najdanovic-Visak, V., Simões, P.C., 2011. Synthesis of fatty acid methyl esters via direct transesterification with methanol/carbon dioxide mixtures from spent coffee grounds feedstock. *Green Chem.* 13, 1196.
doi:10.1039/c1gc15101k

Camel, V., 2001. Recent extraction techniques for solid matrices—supercritical fluid extraction, pressurized fluid extraction and microwave-assisted extraction: their potential and pitfalls. *Analyst* 126, 1182–1193.
doi:10.1039/b008243k

Campos-Vega, R., Loarca-Piña, G., Vergara-Castañeda, H., Oomah, B.D., 2015. Spent coffee grounds: A review on current research and future prospects. *Trends Food Sci. Technol.* 45, 24–36.
doi:10.1016/j.tifs.2015.04.012

Canakci, M., Gerpen, J. Van, 2001. Biodiesel production from oils and fats with high free fatty acids. *Trans. ASAE* 44, 1429–1436.
doi:10.1016/j.fuel.2013.09.020

Canakci, M., Sanli, H., 2008. Biodiesel production from various feedstocks and their effects on the fuel properties. *J. Ind. Microbiol. Biotechnol.*
doi:10.1007/s10295-008-0337-6

Carabias-Martínez, R., Rodríguez-Gonzalo, E., Revilla-Ruiz, P., Hernández-Méndez, J., 2005. Pressurized liquid extraction in the analysis of food and biological samples. *J. Chromatogr. A.* doi:10.1016/j.chroma.2005.06.072

Chai, M., Tu, Q., Lu, M., Yang, Y.J., 2014. Esterification pretreatment of free fatty acid in biodiesel production, from laboratory to industry. *Fuel Process. Technol.* 125, 106–113. doi:10.1016/j.fuproc.2014.03.025

Chang, N., Gu, Z.Y., Yan, X.P., 2010. Zeolitic imidazolate framework-8 nanocrystal coated capillary for molecular sieving of branched alkanes from linear alkanes along with high-resolution chromatographic separation of linear alkanes. *J. Am. Chem. Soc.* 132, 13645–13647.

doi:10.1021/ja1058229

Clarke, R.J., 1985. Green Coffee Processing, in: Clifford, M.N., Willson, K.C. (Eds.), *Coffee: Botany, Biochemistry and Production of Beans and Beverage*. Springer US, Boston, MA, pp. 230–250. doi:10.1007/978-1-4615-6657-1_10

Clarke, R.J., Vitzthum, O.G., 2008. *Coffee: Recent Developments*. doi:10.1002/9780470690499

Clayton, S. a., Scholes, O.N., Hoadley, a. F. a., Wheeler, R. a., McIntosh, M.J., Huynh, D.Q., 2006. Dewatering of Biomaterials by Mechanical Thermal Expression. *Dry. Technol.* 24, 819–834. doi:10.1080/07373930600733093

Corrêa, J., Johnson, S., Fonseca, B.E., da Silva Carvalho, A., 2014. Drying of spent coffee grounds in a cyclonic dryer. *Coffee Sci.* 9, 68–76.

Corrêa, P.C., Oliveira, G.H.H. de, Oliveira, A.P.L.R. de, Vargas-Elías, G.A., Santos, F.L., Baptestini, F.M., 2016. Preservation of roasted and ground coffee during storage Part 1: Moisture content and repose angle. *Rev. Bras. Eng. Agrícola e Ambient.* 20, 581–587. doi:10.1590/1807-1929/agriambi.v20n6p581-587

Couto, R.M., Fernandes, J., da Silva, M.D.R.G., Simões, P.C., 2009. Supercritical fluid extraction of lipids from spent coffee grounds. *J. Supercrit. Fluids* 51, 159–166. doi:10.1016/j.supflu.2009.09.009

Crisafulli, P., Navarini, L., Silizio, F., Pallavicini, A., Illy, A., 2014. Ultrastructural Characterization of Oil Bodies in Different *Coffea* Species. *Trop. Plant Biol.* 7, 1–12. doi:10.1007/s12042-013-9132-2

Cruz, R., Cardoso, M.M., Fernandes, L., Oliveira, M., Mendes, E., Baptista, P., Morais, S., Casal, S., 2012. Espresso coffee residues: A valuable source of unextracted compounds. *J. Agric. Food Chem.* 60, 7777–7784. doi:10.1021/jf3018854

de Azevedo, A.B.A., Kieckbush, T.G., Tashima, A.K., Mohamed, R.S.,

- Mazzafera, P., Melo, S.A.B.V. de, 2008. Extraction of green coffee oil using supercritical carbon dioxide. *J. Supercrit. Fluids* 44, 186–192. doi:10.1016/j.supflu.2007.11.004
- Deligiannis, A., Papazafeiropoulou, A., Anastopoulos, G., Zannikos, F., 2011. Waste Coffee Grounds as an Energy Feedstock. *Proceeding 3rd Int. CEMEPE SECOTOX Conf.* 617–622.
- Demirbas, A., 2011. Competitive liquid biofuels from biomass. *Appl. Energy*. doi:10.1016/j.apenergy.2010.07.016
- Demirbas, A., 2009. Biofuels securing the planet’s future energy needs. *Energy Convers. Manag.* 50, 2239–2249. doi:10.1016/j.enconman.2009.05.010
- Dias, E.C., Borém, F.M., Pereira, R.G.F.A., Guerreiro, M.C., 2012. Amino acid profiles in unripe Arabica coffee fruits processed using wet and dry methods. *Eur. Food Res. Technol.* 234, 25–32. doi:10.1007/s00217-011-1607-5
- Döhlert, P., Weidauer, M., Enthaler, S., 2016. Spent coffee ground as source for hydrocarbon fuels. *J. Energy Chem.* 25, 146–152. doi:10.1016/j.jechem.2015.11.012
- Duarte, G., Pereira, A., Farah, A., 2009. Chemical Composition of Brazilian Green Coffee Seeds Processed by Dry and Wet Post-Harvesting Methods, in: *22ème Colloque Scientifique International Sur Le Café*. pp. 593–596.
- Duarte, S.M. da S., Abreu, C.M.P. de, Menezes, H.C. de, Santos, M.H. dos, GouvÃ\textordfemeninea, C.M.C.P., 2005. Effect of processing and roasting on the antioxidant activity of coffee brews. *Food Sci. Technol.* 25, 387–393.
- Duroudier, J.-P., 2016. 4.1 Fundamentals of extraction and solid-liquid washing. *Liq. Solid-Liquid Extr.*
- Eevera, T., Rajendran, K., Saradha, S., 2009. Biodiesel production process

optimization and characterization to assess the suitability of the product for varied environmental conditions. *Renew. Energy* 34, 762–765.

doi:10.1016/j.renene.2008.04.006

Energy and Climate Change committee, 2017. 2020 renewable heat and transport targets. House of Commons, Second report of Session 2016-17 (published on 9 September 2016), <https://publications.parliament.uk/pa/cm201617/cmselect/cmenergy/173/173.pdf>

Farah, A., 2012. Coffee Constituents, in: Chu, Y.F. (Ed.), *Coffee: Emerging Health Effects and Disease Prevention*. Wiley-Blackwell, Oxford, UK, pp. 21–58. doi:10.1002/9781119949893.ch2

Fassinou, W.F., 2012. Higher heating value (HHV) of vegetable oils, fats and biodiesels evaluation based on their pure fatty acids' HHV. *Energy* 45, 798–805. doi:10.1016/j.energy.2012.07.011

Fernando, W.J.N., Hewavitharana, L.G., 1990. Effect of drying on the formation of free fatty acids in rice bran. *Dry. Technol.* 8, 609–612. doi:10.1080/07373939008959902

Ferrario, V., Veny, H., De Angelis, E., Navarini, L., Ebert, C., Gardossi, L., 2013. Lipases immobilization for effective synthesis of biodiesel starting from coffee waste oils. *Biomolecules* 3, 514–534. doi:10.3390/biom3030514

Fiol, N., Escudero, C., Villaescusa, I., 2008. Re-use of Exhausted Ground Coffee Waste for Cr(VI) Sorption. *Sep. Sci. Technol.* 43, 582–596. doi:10.1080/01496390701812418

Folstar, P., Pilnik, W., de Heus, J.G., van der Plas, H.C., 1976. The composition of fatty acids in coffee oil and wax. *VII Intern. Sci. Colloq. Coffee* 253–258.

Franca, A.S., Oliveira, L.S., 2008. Chemistry of defective coffee beans, *Progress in Food Chemistry*.

- Franca, A.S., Oliveira, L.S., Ferreira, M.E., 2009. Kinetics and equilibrium studies of methylene blue adsorption by spent coffee grounds. *Desalination* 249, 267–272. doi:10.1016/j.desal.2008.11.017
- Franca, A.S., Oliveira, L.S., Mendonça, J.C.F., Silva, X.A., 2005. Physical and chemical attributes of defective crude and roasted coffee beans. *Food Chem.* 90, 89–94. doi:10.1016/j.foodchem.2004.03.028
- Franca, S.A., Oliveira, L.S., 2009. *Coffee Processing Solid Wastes: Current Uses and Future Perspectives, Agricultural Wastes.*
- Freedman, B., Pryde, E.H., Mounts, T.L., 1984. Variables affecting the yields of fatty esters from transesterified vegetable oils. *J. Am. Oil Chem. Soc.* 61, 1638–1643. doi:10.1007/BF02541649
- Freeman, S., Harrington, M., Sharp, J., 2011. Lipids, Membranes, and the First Cells. *Biol. Sci.* 99–124. doi:10.1021/mp9000662.Biophysical
- Ghanadzadeh, A., Ghanadzadeh, H., Sariri, R., Ebrahimi, L., 2005. Dielectric study of molecular association in the binary mixtures (2-ethyl-1-hexanol + alcohol) and (cyclohexane + alcohol) at 298.2 K. *J. Chem. Thermodyn.* 37, 357–362. doi:10.1016/j.jct.2004.09.017
- Giergielewicz-Mozajska, H., Dabrowski, L., Namieśnik, J., 2001. Accelerated solvent extraction (ASE) in the analysis of environmental solid samples - Some aspects of theory and practice. *Crit. Rev. Anal. Chem.* 31, 149–165.
- Go, A.W., Conag, A.T., Cuizon, D.E.S., 2016. Recovery of Sugars and Lipids from Spent Coffee Grounds: A New Approach. *Waste and Biomass Valorization* 7, 1047–1053. doi:10.1007/s12649-016-9527-z
- Gómez-De La Cruz, F.J., Cruz-Peragón, F., Casanova-Peláez, P.J., Palomar-Carnicero, J.M., 2015. A vital stage in the large-scale production of biofuels from spent coffee grounds: The drying kinetics. *Fuel Process. Technol.* 130, 188–196. doi:10.1016/j.fuproc.2014.10.012
- Gross, G., Jaccaud, E., Huggett, A.C., 1997. Analysis of the content of the

- diterpenes cafestol and kahweol in coffee brews. *Food Chem. Toxicol.* 35, 547–554. doi:10.1016/S0278-6915(96)00123-8
- Gui, M.M., Lee, K.T., Bhatia, S., 2008. Feasibility of edible oil vs. non-edible oil vs. waste edible oil as biodiesel feedstock. *Energy*. doi:10.1016/j.energy.2008.06.002
- Gunstone, F., 1996. *Fatty Acid and Lipid Chemistry, Fatty Acid and Lipid Chemistry*. doi:10.1007/978-1-4615-4131-8
- Haile, M., 2014. Integrated volarization of spent coffee grounds to biofuels. *Biofuel Res. J.* 2, 65–69. doi:10.18331/BRJ2015.1.2.6
- Hanai, T., Koizumi, N., Gotoh, R., 1961. Temperature dependence of dielectric constant and dipole moment in polar liquids. *Bull. Inst. Chem. Res. Kyoto Univ.* 39, 195–201.
- Harwood, L.M., Moody, C.J., Percy, J.M., 1998. *Experimental organic chemistry : standard and microscale. Exp. Org. Chem. Stand. microscale 2nd*, 127–132.
- Hayyan, A., Alam, M.Z., Mirghani, M.E.S., Kabbashi, N.A., Hakimi, N.I.N.M., Siran, Y.M., Tahiruddin, S., 2011. Reduction of high content of free fatty acid in sludge palm oil via acid catalyst for biodiesel production. *Fuel Process. Technol.* 92, 920–924. doi:10.1016/j.fuproc.2010.12.011
- Hayyan, A., Alam, M.Z., Mirghani, M.E.S., Kabbashi, N.A., Hakimi, N.I.N.M., Siran, Y.M., Tahiruddin, S., 2010. Sludge palm oil as a renewable raw material for biodiesel production by two-step processes. *Bioresour. Technol.* 101, 7804–7811. doi:10.1016/j.biortech.2010.05.045
- Hellier, P., Ladommatos, N., 2015. The influence of biodiesel composition on compression ignition combustion and emissions. *Proc. Inst. Mech. Eng. Part A J. Power Energy* 229, 714–726. doi:10.1177/0957650915598424
- Hellier, P., Ladommatos, N., Allan, R., Payne, M., Rogerson, J., 2011. The Impact of Saturated and Unsaturated Fuel Molecules on Diesel Combustion and Exhaust Emissions. *SAE Int. J. Fuels Lubr.* 5, 106–122.

doi:10.4271/2011-01-1922

Hellier, P., Ladommatos, N., Allan, R., Rogerson, J., 2013. Combustion and emissions characteristics of toluene/n-heptane and 1-octene/n-octane binary mixtures in a direct injection compression ignition engine. *Combust. Flame* 160, 2141–2158.
doi:10.1016/j.combustflame.2013.04.016

Hellier, P., Ladommatos, N., Allan, R., Rogerson, J., 2012. The Influence of Fatty Acid Ester Alcohol Moiety Molecular Structure on Diesel Combustion and Emissions. *Energy & Fuels* 26, 1912–1927.
doi:10.1021/ef2017545

Hellier, P., Ladommatos, N., Yusaf, T., 2015. The influence of straight vegetable oil fatty acid composition on compression ignition combustion and emissions. *Fuel* 143, 131–143. doi:10.1016/j.fuel.2014.11.021

<http://docslide.us/documents/thermochemical-equations-calorimetry-at-the-end-of-this-lesson-you-should.html> (accessed on 30/6/2017).

<http://sachiacidbase.weebly.com/titrations.html> (accessed on 30/6/2017).

<http://www.chemguide.co.uk/physical/acidbaseeqia/indicators.html> (accessed on 30/6/2017).

<http://www.chempro.in/fattyacid.htm> accessed on 24/5/2016.

http://www.ika.com/owa/ika/catalog.product_detail?iProduct=10002170 (accessed on 30/6/2017).

http://www.keison.co.uk/nabertherm_tr.shtml (accessed on 30/6/2017).

<http://www.stenutz.eu/chem/solv6.php?name=octane> (accessed on 11/1/2018).

<https://www.laboratory-equipment.com/calorimeters/c1-calorimeter-ika.php> (accessed on 30/6/2017).

https://www.researchgate.net/figure/275480639_fig1_Figure-2-Schematic-diagram-of-soxhlet-extractor-7 (accessed on 29/08/2017).

- IEA, 2017. CO2 emissions from fuel combustion-Highlights. IEA Stat.
- IKA Calorimeter C1, Operating instructions (accessed on 31/3/2017). URL http://www.ika.com/owa/ika/catalog.product_downloads?iProduct=3825000&iProductgroup=&iSubgroup=&iCS=1&iAcc=&iCon=
- International Coffee Association, 2016. International Coffee Organization - The Current State of the Global Coffee Trade | #CoffeeTradeStats. Cofffee Trade Status. URL http://www.ico.org/monthly_coffee_trade_stats.asp
- Iwunze, M., 2009. The solvent system, in: Equilibrium Concept in Analytical Chemistry. AuthorHouse, p. 40.
- Jalilvand, M., Kamali, H., Nematollahi, A., 2013. Pressurized Fluid Extraction of Rice Bran Oil Using a Modified Supercritical Fluid Extractor and a Central Composite Design for Optimization. J. Liq. Chromatogr. Relat. Technol. 36, 1562–1574. doi:10.1080/10826076.2012.692152
- Jenkins, R.W., Stageman, N.E., Fortune, C.M., Chuck, C.J., 2014. Effect of the type of bean, processing, and geographical location on the biodiesel produced from waste coffee grounds. Energ.Fuels 28, 1166–1174. doi:10.1021/ef4022976
- Jham, G.N., Velikova, R., Vidal Muller, H., Nikolova-Damyanova, B., Cecon, P.R., 2001. Lipid classes and triacylglycerols in coffee samples from Brazil: Effects of coffee type and drying procedures. Food Res. Int. 34, 111–115. doi:10.1016/S0963-9969(00)00137-X
- Joët, T., Laffargue, A., Descroix, F., Doulebeau, S., Bertrand, B., Kochko, A. de, Dussert, S., 2010. Influence of environmental factors, wet processing and their interactions on the biochemical composition of green Arabica coffee beans. Food Chem. 118, 693–701. doi:10.1016/j.foodchem.2009.05.048
- Johnson, L.A., Lusas, E.W., 1983. Comparison of alternative solvents for oils extraction. J. Am. Oil Chem. Soc. 60, 229–242. doi:10.1007/BF02543490
- Kamali, H., Aminimoghadamfarouj, N., Nematollahi, A., 2014. Optimization of

variables for pressurized fluid extraction of essential oil from *Lavandula angustifolia* using Box-Behnken design. *Int. J. ChemTech Res.* 6, 4844–4852.

Kang, D., Dai, J., Yuan, J., 2011. Changes of structure and dipole moment of water with temperature and pressure: A first principles study. *J. Chem. Phys.* 135, 24505. doi:10.1063/1.3608412

Kante, K., Nieto-Delgado, C., Rangel-Mendez, J.R., Bandosz, T.J., 2012. Spent coffee-based activated carbon: Specific surface features and their importance for H₂S separation process. *J. Hazard. Mater.* 201–202, 141–147. doi:10.1016/j.jhazmat.2011.11.053

Kaufmann, B., Christen, P., 2002. Recent extraction techniques for natural products: Microwave-assisted extraction and pressurised solvent extraction. *Phytochem. Anal.* 13, 105–113. doi:10.1002/pca.631

Kaufmann, B., Christen, P., Veuthey, J.-L., 2001. Study of factors influencing pressurised solvent extraction of polar steroids from plant material. Application to the recovery of withanolides. *Chromatographia* 54, 394–398. doi:10.1007/BF02492690

Kawamura, F., Kikuchi, Y., Ohira, T., Yatagai, M., 1999. Accelerated solvent extraction of paclitaxel and related compounds from the bark of *Taxus cuspidata*. *J. Nat. Prod.* 62, 244–247. doi:10.1021/np980310j

Kelkar, S., Saffron, C.M., Chai, L., Bovee, J., Stuecken, T.R., Garedew, M., Li, Z., Kriegel, R.M., 2015. Pyrolysis of spent coffee grounds using a screw-conveyor reactor. *Fuel Process. Technol.* 137, 170–178. doi:10.1016/j.fuproc.2015.04.006

Kemper, T.G., 2005. Oil Extraction, in: John Wiley & Sons, Inc. pp. 57–98. doi:10.1002/047167849X.bio013

KerbalaUniversity, 2010. Factors Affecting the Extraction Process of Oil-bearing flakes of Sunflower , Cotton and Soybean seeds. *J. Kerbala Univ.* 8, 32–47.

- Khan, L.M., Hanna, M.A., 1983. Expression of oil from oilseeds-A review. *J. Agric. Eng. Res.* doi:10.1016/0021-8634(83)90113-0
- Knopp, S., Bytof, G., Selmar, D., 2006. Influence of processing on the content of sugars in green Arabica coffee beans. *Eur. Food Res. Technol.* 223, 195–201. doi:10.1007/s00217-005-0172-1
- Knothe, G., 2008. “Designer” biodiesel: Optimizing fatty ester composition to improve fuel properties. *Energ. Fuels* 22, 1358–1364. doi:10.1021/ef700639e
- Knothe, G., 2007. Some aspects of biodiesel oxidative stability. *Fuel Process. Technol.* doi:10.1016/j.fuproc.2007.01.005
- Knothe, G., 2005. Dependence of biodiesel fuel properties on the structure of fatty acid alkyl esters. *Fuel Process. Technol.* 86, 1059–1070. doi:10.1016/j.fuproc.2004.11.002
- Knothe, G., Van Gerpen, J.H., Krahl, J.J., Gerpen, J.H. Van, 2005. *The Biodiesel Handbook*, Applied Sciences. doi:10.1201/9781439822357
- Knowles, J., Watkinson, C., 2014. Extraction of omega-6 fatty acids from speciality seeds. *Lipid Technol.* 26, 107–110. doi:10.1002/lite.201400021
- Koivisto, E., 2016. Ignition and combustion of future oxygenated fuels in compression-ignition engines.
- Koivisto, E., Ladommatos, N., Gold, M., 2016. Compression ignition and pollutant emissions of large alkylbenzenes. *Fuel* 172, 200–208. doi:10.1016/j.fuel.2016.01.025
- Koivisto, E., Ladommatos, N., Gold, M., 2015a. Systematic study of the effect of the hydroxyl functional group in alcohol molecules on compression ignition and exhaust gas emissions. *Fuel* 153, 650–663. doi:10.1016/j.fuel.2015.03.042
- Koivisto, E., Ladommatos, N., Gold, M., 2015b. The influence of various oxygenated functional groups in carbonyl and ether compounds on compression ignition and exhaust gas emissions. *Fuel* 159, 697–711.

doi:10.1016/j.fuel.2015.07.018

Kombe, G.G., Temu, A.K., Rajabu, H.M., Mrema, G.D., 2012. High Free Fatty Acid (FFA) Feedstock Pre-Treatment Method for Biodiesel Production. Second Int. Conf. Adv. Eng. Technol. 176–182.

Kondamudi, N., Mohapatra, S.K., Misra, M., 2008. Spent coffee grounds as a versatile source of green energy. J. Agric. Food Chem. 56, 11757–11760. doi:10.1021/jf802487s

Kumar Tiwari, A., Kumar, A., Raheman, H., 2007. Biodiesel production from jatropha oil (*Jatropha curcas*) with high free fatty acids: An optimized process. Biomass and Bioenergy 31, 569–575. doi:10.1016/j.biombioe.2007.03.003

Kwon, E.E., Yi, H., Jeon, Y.J., 2013. Sequential co-production of biodiesel and bioethanol with spent coffee grounds. Bioresour. Technol. 136, 475–480. doi:10.1016/j.biortech.2013.03.052

Lago, R.C.A., Antoniassi, R., Freitas, S.C., 2001. Centesimal composition and amino acids of raw, roasted and spent ground of soluble coffee, in: II Simpósio de Pesquisa Dos Cafés Do Brasil Vitoria. pp. 1473–1477.

Lajara, J.R., 1990. Solvent extraction of oil from oilseeds: the real basics, in: Erickson, D.R. (Ed.), Edible Fats and Oils Processing: Basic Principles and Modern Practices. The American Oil Chemists Society, pp. 51–52.

Lawson, O., Oyewumi, A., Ologunagba, F., Ojomo, A.O., 2010. Evaluation of the Parameters Affecting the Solvent Extraction of Soybean Oil. APRN J. Eng. Appl. Sci. 5, 51–55.

Leung, D.Y.C., Guo, Y., 2006. Transesterification of neat and used frying oil: Optimization for biodiesel production. Fuel Process. Technol. 87, 883–890. doi:10.1016/j.fuproc.2006.06.003

Leung, D.Y.C., Wu, X., Leung, M.K.H., 2010. A review on biodiesel production using catalyzed transesterification. Appl. Energy. doi:10.1016/j.apenergy.2009.10.006

- Liu, Y., Tu, Q., Knothe, G., Lu, M., 2017. Direct transesterification of spent coffee grounds for biodiesel production. *Fuel* 199, 157–161. doi:10.1016/j.fuel.2017.02.094
- Luthria, D., Vinjamoori, D., Noel, K., Ezzell, J., 2004. Accelerated Solvent Extraction, in: *Oil Extraction and Analysis*. doi:10.1201/9781439822340.ch3
- Luthria, D.L., Noel, K., D., V., 2004. Effect of Moisture Content, Grinding, and Extraction Technologies on Crude Fat Assay, in: Luthria, D.L. (Ed.), *Oil Extraction and Analysis, Critical Issues and Comparative Studies*. AOCS Publishing.
- Ma, F., Hanna, M.A., 1999. Biodiesel production: A review. *Bioresour. Technol.* doi:10.1016/S0960-8524(99)00025-5
- Marchetti, J.M., Errazu, A.F., 2008. Esterification of free fatty acids using sulfuric acid as catalyst in the presence of triglycerides. *Biomass and Bioenergy* 32, 892–895. doi:10.1016/j.biombioe.2008.01.001
- Martín, M.J., Pablos, F., González, A.G., Valdenebro, M.S., León-Camacho, M., 2001. Fatty acid profiles as discriminant parameters for coffee varieties differentiation. *Talanta* 54, 291–297. doi:10.1016/S0039-9140(00)00647-0
- Matthäus, B., Brühl, L., 2001. Comparison of different methods for the determination of the oil content in oilseeds. *J. Am. Oil Chem. Soc.* 78, 95–102. doi:10.1007/s11746-001-0226-y
- Meher, L.C., Dharmagadda, V.S.S., Naik, S.N., 2006. Optimization of alkali-catalyzed transesterification of *Pongamia pinnata* oil for production of biodiesel. *Bioresour. Technol.* 97, 1392–1397. doi:10.1016/j.biortech.2005.07.003
- Mercier, C., Charbonniere, R., Grebaut, J., de la Gueriviere, J.F., 1980. Formation of Amylose-Lipid Complexes by Twin-Screw Extrusion Cooking of Manioc Starch. *Cereal Chem.* 57, 4–9.

- Mezger, T.G., 2006. The Rheology Handbook. Hann. Curt R Vincentz Verlag 27–28. doi:10.1108/prt.2009.12938eac.006
- Moreau, R. a., Powell, M.J., Singh, V., 2003. Pressurized liquid extraction of polar and nonpolar lipids in corn and oats with hexane, methylene chloride, isopropanol, and ethanol. *J. Am. Oil Chem. Soc.* 80, 1063–1067. doi:10.1007/s11746-003-0821-y
- Moser, B.R., 2009. Biodiesel production, properties, and feedstocks. *Vitr. Cell. Dev. Biol. - Plant* 45, 229–266. doi:10.1007/s11627-009-9204-z
- Moussa, A.I., Bahnasy, A.F., El-Marakby, F., Ahmed, A.I., Gawady, A.A., 2014. The influence of additives on diesel engine performance and the ecological parameters. *J. Soil Sci. Agric. Eng., Mansoura Univ* 5, 847–858.
- Mueller, C.J., Boehman, A.L., Martin, G.C., 2009. An Experimental Investigation of the Origin of Increased NO_x Emissions When Fueling a Heavy-Duty Compression-Ignition Engine with Soy Biodiesel. *SAE Int. J. Fuels Lubr.* 2, 2009-01–1792. doi:10.4271/2009-01-1792
- Murthy, P.S., Madhava Naidu, M., 2012. Sustainable management of coffee industry by-products and value addition - A review. *Resour. Conserv. Recycl.* doi:10.1016/j.resconrec.2012.06.005
- Mussatto, S.I., Carneiro, L.M., Silva, J.P.A., Roberto, I.C., Teixeira, J.A., 2011a. A study on chemical constituents and sugars extraction from spent coffee grounds. *Carbohydr. Polym.* 83, 368–374. doi:10.1016/j.carbpol.2010.07.063
- Mussatto, S.I., Machado, E.M.S., Martins, S., Teixeira, J.A., 2011b. Production, Composition, and Application of Coffee and Its Industrial Residues. *Food Bioprocess Technol.* doi:10.1007/s11947-011-0565-z
- Mustafa, A., Turner, C., 2011. Pressurized liquid extraction as a green approach in food and herbal plants extraction: A review. *Anal. Chim. Acta.* doi:10.1016/j.aca.2011.07.018

- Najdanovic-Visak, V., Lee, F.Y.L., Tavares, M.T., Armstrong, A., 2017. Kinetics of extraction and in situ transesterification of oils from spent coffee grounds. *J. Environ. Chem. Eng.* 5, 2611–2616. doi:10.1016/j.jece.2017.04.041
- Narita, Y., Inouye, K., 2014. Review on utilization and composition of coffee silverskin. *Food Res. Int.* doi:10.1016/j.foodres.2014.01.023
- Nhu, N. Van, Iglesias, G.A., Kohler, F., 1989. Correlation of Third Virial Coefficients to Second Virial Coefficients. *Berichte der Bunsengesellschaft für Phys. Chemie* 93, 526–531. doi:10.1002/bbpc.19890930418
- Nielsen, S.S., 2014. *Food Analysis*, 4th ed. doi:10.1038/1841347a0
- Nieva-Echevarría, B., Goicoechea, E., Manzanos, M.J., Guillén, M.D., 2014. A method based on ¹H NMR spectral data useful to evaluate the hydrolysis level in complex lipid mixtures. *Food Res. Int.* 66, 379–387. doi:10.1016/j.foodres.2014.09.031
- Novaes, F.J.M., Oigman, S.S., De Souza, R.O.M.A., Rezende, C.M., De Aquino Neto, F.R., 2015. New approaches on the analyses of thermolabile coffee diterpenes by gas chromatography and its relationship with cup quality. *Talanta* 139, 159–166. doi:10.1016/j.talanta.2014.12.025
- Oberg, E., Jones, F.D., Horton, H.L., Ryffel, H.H., 2004. *Machinery's Handbook (27th Edition) & Guide to Machinery's Handbook*. Ind. Press 260 ff. doi:10.1017/CBO9781107415324.004
- Oliveira, L.S., Franca, A.S., Camargos, R.R.S., Ferraz, V.P., 2008. Coffee oil as a potential feedstock for biodiesel production. *Bioresour. Technol.* 99, 3244–3250. doi:10.1016/j.biortech.2007.05.074
- Oliveira, L.S., Franca, A.S., Mendonça, J.C.F., Barros-Júnior, M.C., 2006. Proximate composition and fatty acids profile of green and roasted defective coffee beans. *LWT - Food Sci. Technol.* 39, 235–239. doi:10.1016/j.lwt.2005.01.011

- Park, J., Kim, B., Lee, J.W., 2016. In-situ transesterification of wet spent coffee grounds for sustainable biodiesel production. *Bioresour. Technol.* 221, 55–60. doi:10.1016/j.biortech.2016.09.001
- Park, K., Kittelson, D.B., Zachariah, M.R., McMurry, P.H., 2004. Measurement of inherent material density of nanoparticle agglomerates. *J. Nanoparticle Res.* 6, 267–272. doi:10.1023/B:NANO.0000034657.71309.e6
- Perry, R.H., Green, D.W., Maloney, J.O., 1997. *Perry's Chemical Engineers' Handbook*, McGrawhill.
- Picard, H., Guyot, B., Vincent, J., 1984. Study on the sterol compounds of coffee *Coffea canephora* oil. *Inst. Rech. du Cafe du Cacao, Montpellier (France). Lab. Chim. Technol.* 28, 47–62.
- Pichai, E., Krit, S., 2015. Optimization of solid-to-solvent ratio and time for oil extraction process from spent coffee grounds using response surface methodology. *ARPN J. Eng. Appl. Sci.* 10, 7049–7052.
- Pieruccini, M., Saija, F., 2004. A mean field analysis of the static dielectric behavior of linear lower alcohols. *J. Chem. Phys.* 121, 3191–3196. doi:10.1063/1.1773386
- Pilipczuk, T., Kusznierevicz, B., Zielińska, D., Bartoszek, A., 2015. The influence of roasting and additional processing on the content of bioactive components in special purpose coffees. *J. Food Sci. Technol.* 52, 5736–5744. doi:10.1007/s13197-014-1646-6
- Pinzi, S., Garcia, I.L., Lopez-Gimenez, F.J., DeCastro, M.D.L., Dorado, G., Dorado, M.P., 2009. The ideal vegetable oil-based biodiesel composition: A review of social, economical and technical implications. *Energ. Fuels* 23, 2325–2341. doi:10.1021/ef801098a
- Predojević, Z.J., 2008. The production of biodiesel from waste frying oils: A comparison of different purification steps. *Fuel* 87, 3522–3528. doi:10.1016/j.fuel.2008.07.003
- Preethu, D.C., Prakash, B.N.U.H., Srinivasamurthy, C.A., Vasanthi, B.G.,

2007. Maturity indices as an index to evaluate the quality of compost of coffee waste blended with other organic wastes. *Proc. Int. Conf. Sustain. Solid Waste Manag.* 270–275.
- Pujol, D., Liu, C., Gominho, J., Olivella, M.À., Fiol, N., Villaescusa, I., Pereira, H., 2013. The chemical composition of exhausted coffee waste. *Ind. Crops Prod.* 50, 423–429. doi:10.1016/j.indcrop.2013.07.056
- Quinn, P.J., 1988. Effects of temperature on cell membranes. *Symp. Soc. Exp. Biol.* 42, 237–58.
- Ramos, L., Kristenson, E.M., Brinkman, U.T., 2002. Current use of pressurised liquid extraction and subcritical water extraction in environmental analysis. *J. Chromatogr. A* 975, 3–29. doi:10.1016/S0021-9673(02)01336-5
- Ramos, M.J., Fernández, C.M., Casas, A., Rodríguez, L., Pérez, Á., 2009. Influence of fatty acid composition of raw materials on biodiesel properties. *Bioresour. Technol.* 100, 261–268. doi:10.1016/j.biortech.2008.06.039
- Rao, D.G., 2009. Chapter 20:Extraction, in: *Fundamentals of Food Engineering*. pp. 364–368.
- Ratnayake, W.M.N., Hollywood, R., O'Grady, E., Stavric, B., 1993. Lipid content and composition of coffee brews prepared by different methods. *Food Chem. Toxicol.* 31, 263–269. doi:10.1016/0278-6915(93)90076-B
- Reh, C.T., Gerber, A., Prodolliet, J., Vuataz, G., 2006. Water content determination in green coffee - Method comparison to study specificity and accuracy, in: *Food Chemistry*. pp. 423–430. doi:10.1016/j.foodchem.2005.02.055
- Reichardt, C., Welton, T., 2010a. Solute-Solvent Interactions, in: *Solvents and Solvent Effects in Organic Chemistry*. pp. 7–64. doi:10.1002/9783527632220.ch2
- Reichardt, C., Welton, T., 2010b. Classification of Solvents, in: *Solvents and*

- Solvent Effects in Organic Chemistry. pp. 65–106.
doi:10.1002/9783527632220.ch3
- Reichardt, C., Welton, T., 2010c. Empirical Parameters of Solvent Polarity, in: Solvents and Solvent Effects in Organic Chemistry. pp. 425–508.
doi:10.1002/9783527632220.ch7
- Reichardt, C., Welton, T., 2010d. Appendix A. Properties, Purification, and Use of Organic Solvents, in: Solvents and Solvent Effects in Organic Chemistry. pp. 549–586.
- REN21, 2017. Renewables 2017: global status report, Renewable and Sustainable Energy Reviews. doi:10.1016/j.rser.2016.09.082
- Reverchon, E., De Marco, I., 2006. Supercritical fluid extraction and fractionation of natural matter. *J. Supercrit. Fluids*.
doi:10.1016/j.supflu.2006.03.020
- Ribeiro, H., Marto, J., Raposo, S., Agapito, M., Isaac, V., Chiari, B.G., Lisboa, P.F., Paiva, A., Barreiros, S., Simões, P., 2013. From coffee industry waste materials to skin-friendly products with improved skin fat levels. *Eur. J. Lipid Sci. Technol.* 115, 330–336. doi:10.1002/ejlt.201200239
- Richter, B.E., Jones, B. a, Ezzell, J.L., Porter, N.L., 1996. Accelerated Solvent Extraction : A Technique for Sample Preparation. *Anal. Chem.* 68, 1033–1039. doi:10.1021/ac9508199
- Rocha, M.V.P., de Matos, L.J.B.L., Lima, L.P. de, Figueiredo, P.M. da S., Lucena, I.L., Fernandes, F.A.N., Gonçalves, L.R.B., 2014. Ultrasound-assisted production of biodiesel and ethanol from spent coffee grounds. *Bioresour. Technol.* 167, 343–348. doi:10.1016/j.biortech.2014.06.032
- Romeiro, G.A., Salgado, E.C., Silva, R.V.S., Figueiredo, M.K.K., Pinto, P.A., Damasceno, R.N., 2012. A study of pyrolysis oil from soluble coffee ground using low temperature conversion (LTC) process. *J. Anal. Appl. Pyrolysis* 93, 47–51. doi:10.1016/j.jaap.2011.09.006
- Routray, W., Orsat, V., 2012. Microwave-Assisted Extraction of Flavonoids: A

- Review. Food Bioprocess Technol. doi:10.1007/s11947-011-0573-z
- Rusanov, A.I., Prokhorov, V.A., 1996. Interfacial Tensiometry. Stud. Interface Sci. 3, 328–350. doi:10.1016/S1383-7303(96)80031-7
- Sacchetti, G., Di Mattia, C., Pittia, P., Mastrocola, D., 2009. Effect of roasting degree, equivalent thermal effect and coffee type on the radical scavenging activity of coffee brews and their phenolic fraction. J. Food Eng. 90, 74–80. doi:10.1016/j.jfoodeng.2008.06.005
- Sadeghi, R., Azizpour, S., 2011. Volumetric, compressibility, and viscometric measurements of binary mixtures of poly(vinylpyrrolidone) + water, + methanol, + ethanol, + acetonitrile, + 1-propanol, + 2-propanol, and + 1-butanol. J. Chem. Eng. Data 56, 240–250. doi:10.1021/je100818t
- Sadrameli, S.M., Seames, W., Mann, M., 2008. Prediction of higher heating values for saturated fatty acids from their physical properties. Fuel 87, 1776–1780. doi:10.1016/j.fuel.2007.10.020
- Saenger, M., Hartge, E.U., Werther, J., Ogada, T., Siagi, Z., 2001. Combustion of coffee husks. Renew. Energy 23, 103–121. doi:10.1016/S0960-1481(00)00106-3
- Santoso, H., Iryanto, Ingrid, M., 2014. Effects of Temperature, Pressure, Preheating Time and Pressing Time on Rubber Seed Oil Extraction Using Hydraulic Press. Procedia Chem. 9, 248–256. doi:10.1016/j.proche.2014.05.030
- Sastry, N.V., Valand, M.K., 1998. Excess volumes and relative permittivity increments of $\{ x\text{H}_2\text{C}=\text{CHCO}_2\text{CH}_3 + (1-x)\text{C}_n\text{H}_{2n+2} \}$ ($n=5, 6, 7, 10,$ and 12). J. Chem. Thermodyn. 30, 929–938.
- Satyarthi, J.K., Srinivas, D., Ratnasamy, P., 2009. Estimation of Free Fatty Acid Content in Oils, Fats, and Biodiesel by ^1H NMR Spectroscopy. Energ. Fuels 23, 2273–2277. doi:10.1021/ef801011v
- Sayyar, S., Abidin, Z.Z., Yunus, R., Muhammad, A., 2009. Extraction of oil from Jatropha seeds-optimization and kinetics. Am. J. Appl. Sci. 6, 1390–

1395. doi:10.3844/ajassp.2009.1390.1395

- Schenker, S., Handschin, S., Frey, B., Perren, R., Escher, F., 2000. Pore Structure of Coffee Beans affected by roasting conditions. *J. Food Sci.* 65, 452–457. doi:10.1111/j.1365-2621.2000.tb16026.x
- Scholte, T.G., de Vos, F.C., 2010. The determination of molecular polarisabilities and effective RADII of some normal alkanes. *Recl. des Trav. Chim. des Pays-Bas* 72, 625–642. doi:10.1002/recl.19530720712
- Schönborn, A., Ladommatos, N., Williams, J., Allan, R., 2007. Effects on diesel combustion of the molecular structure of potential synthetic bio-fuel molecules effects on diesel combustion of the molecular structure of potential synthetic bio-fuel molecules. SAE Tech Pap 24.
- Schönborn, A., Ladommatos, N., Williams, J., Allan, R., Rogerson, J., 2009. The influence of molecular structure of fatty acid monoalkyl esters on diesel combustion. *Combust. Flame* 156, 1396–1412. doi:10.1016/j.combustflame.2009.03.011
- Schwartzberg, H.G., 1997. Expression of fluid from biological solids. *Sep. Purif. Rev.* 26, 1–47. doi:10.1080/03602549708014156
- Scully, D., Jaiswal, A., Abu-Ghannam, N., 2016. An Investigation into Spent Coffee Waste as a Renewable Source of Bioactive Compounds and Industrially Important Sugars. *Bioengineering* 3, 33. doi:10.3390/bioengineering3040033
- Selmar, D., Bytof, G., Knopp, S.E., 2008. The storage of green coffee (*Coffea arabica*): Decrease of viability and changes of potential aroma precursors. *Ann. Bot.* 101, 31–38. doi:10.1093/aob/mcm277
- Sheibani, A., Ghaziaskar, H.S., 2008. Pressurized fluid extraction of pistachio oil using a modified supercritical fluid extractor and factorial design for optimization. *LWT - Food Sci. Technol.* 41, 1472–1477. doi:10.1016/j.lwt.2007.09.002
- Shitov, O.P., Korolev, V.L., Tartakovskiy, V.A., 2009. Synthesis of 1,2,4-

- triazolium 4-nitrimides with polyfunctionalized substituents. *Russ. Chem. Bull.* 58, 2347–2355. doi:10.1007/s11172-009-0326-6
- Shrestha, D., Gerpen, J. van, 2010. Biodiesel from oilseed crops., in: *Industrial Crops and Uses*. pp. 140–156.
doi:10.1079/9781845936167.0140
- Silva, M.A., Nebra, S.A., Machado Silva, M.J., Sanchez, C.G., 1998. The use of biomass residues in the Brazilian soluble coffee industry. *Biomass and Bioenergy* 14, 457–467. doi:10.1016/S0961-9534(97)10034-4
- Singh, J., Bargale, P.C., 2000. Development of a small capacity double stage compression screw press for oil expression. *J. Food Eng.* 43, 75–82.
doi:10.1016/S0260-8774(99)00134-X
- Skiera, C., Steliopoulos, P., Kuballa, T., Diehl, B., Holzgrabe, U., 2014. Determination of free fatty acids in pharmaceutical lipids by ¹H NMR and comparison with the classical acid value. *J. Pharm. Biomed. Anal.* 93, 43–50. doi:10.1016/j.jpba.2013.04.010
- Skiera, C., Steliopoulos, P., Kuballa, T., Holzgrabe, U., Diehl, B., 2012. Determination of free fatty acids in edible oils by ¹H NMR spectroscopy. *Lipid Technol.* 24, 279–281. doi:10.1002/lite.201200241
- Skinner, J.F., Cussler Jr., E.L., Fuoss, R.M., 1968. Pressure dependence of dielectric constant and density of liquids. *J. Phys. Chem.* 72, 1057–1064.
doi:10.1021/j100849a048
- Smallwood, I.M., 1996. Handbook of Organic Solvent Properties. *Handb. Org. Solvent Prop.* 149–151. doi:10.1016/B978-0-08-052378-1.50026-8
- Somnuk, K., Eawlex, P., Prateepchaikul, G., 2017. Optimization of coffee oil extraction from spent coffee grounds using four solvents and prototype-scale extraction using circulation process. *Agric. Nat. Resour.* 51, 181–189. doi:https://doi.org/10.1016/j.anres.2017.01.003
- Song, H., Quinton, K., Peng, Z., Zhao, H., Ladommatos, N., 2016. Effects of Oxygen Content of Fuels on Combustion and Emissions of Diesel

- Engines. *Energies* 9, 28. doi:10.3390/en9010028
- Sorin-Stefan, B., Ionescu, M., Voicu, G., Ungureanu, N., Vladut, V., 2013. Calculus Elements for Mechanical Presses in Oil Industry, in: Muzzalupo, I. (Ed.), *Food Industry*. InTech, Rijeka. doi:10.5772/53167
- Speer, K., Kölling-Speer, I., 2006. The lipid fraction of the coffee bean. *Brazilian J. Plant Physiol.* doi:10.1590/S1677-04202006000100014
- Supelco, 1996. Comparison of 37 Component FAME Standard on Four Capillary GC Columns. *Bull.* 907 4.
- Swanepoel, W., Karmee, S.K., Marx, S., 2016. Biocatalytic Production of Biodiesel from Spent Coffee Grounds, in: *International Conference on Advances in Science, Engineering, Technology and Natural Resources (ICASETNR-16)*. Parys (South Africa).
- Szybist, J.P., Boehman, A.L., Taylor, J.D., McCormick, R.L., 2005. Evaluation of formulation strategies to eliminate the biodiesel NO_x effect. *Fuel Process. Technol.* 86, 1109–1126. doi:10.1016/j.fuproc.2004.11.006
- T. Toledo, R., 1993. Extraction. In: *Fundamentals of Food Process Engineering*. Springer, Boston, MA. doi:https://doi.org/10.1007/978-1-4615-7052-3_14
- Tayar, N. El, Tsai, R. -S, Testa, B., Carrupt, P. -A, Leo, A., 1991. Partitioning of solutes in different solvent systems: The contribution of hydrogen-bonding capacity and polarity. *J. Pharm. Sci.* 80, 590–598. doi:10.1002/jps.2600800619
- ThermoFisher, 2011. Dionex ASE 150 Accelerated Solvent Extractor Operator β€™ s Manual. Available from <http://www.canitec.com.mx/doc/ASE150.pdf> (accessed 30/6/2017).
- Todaka, M., Kowhakul, W., Masamoto, H., Shigematsu, M., 2016. Thermal analysis and dust explosion characteristics of spent coffee grounds and jatropa. *J. Loss Prev. Process Ind.* 44, 538–543. doi:10.1016/j.jlp.2016.08.008

- Toschi, T.G., Cardenia, V., Bonaga, G., Mandrioli, M., Rodriguez-Estrada, M.T., 2014. Coffee silverskin: Characterization, possible uses, and safety aspects. *J. Agric. Food Chem.* 62, 10836–10844. doi:10.1021/jf503200z
- Tsai, W.T., Liu, S.C., Hsieh, C.H., 2012. Preparation and fuel properties of biochars from the pyrolysis of exhausted coffee residue. *J. Anal. Appl. Pyrolysis* 93, 63–67. doi:10.1016/j.jaap.2011.09.010
- Tuntiwiwattanapun, N., Monono, E., Wiesenborn, D., Tongcumpou, C., 2017. In-situ transesterification process for biodiesel production using spent coffee grounds from the instant coffee industry. *Ind. Crops Prod.* 102, 23–31. doi:10.1016/j.indcrop.2017.03.019
- U.S. Energy Information Administration, 2017. International Energy Outlook 2017. *Int. Energy Outlook IEO2017*.
- Vardon, D.R., Moser, B.R., Zheng, W., Witkin, K., Evangelista, R.L., Strathmann, T.J., Rajagopalan, K., Sharma, B.K., 2013. Complete utilization of spent coffee grounds to produce biodiesel, bio-oil, and biochar. *ACS Sustain. Chem. Eng.* 1, 1286–1294. doi:10.1021/sc400145w
- Varzakas, T., Tzia, C., 2015. *Handbook of Food Processing: Food Safety, Quality, and Manufacturing Processes*. CRC Press.
- Veggi, P.C., Martinez, J., Meireles, M.A.A., 2013. Fundamentals of Microwave Extraction, in: Chemat, F., Cravotto, G. (Eds.), *Microwave-Assisted Extraction for Bioactive Compounds: Theory and Practice*. Springer US, Boston, MA, pp. 15–52. doi:10.1007/978-1-4614-4830-3_2
- Veljković, V.B., Lakićević, S.H., Stamenković, O.S., Todorović, Z.B., Lazić, M.L., 2006. Biodiesel production from tobacco (*Nicotiana tabacum* L.) seed oil with a high content of free fatty acids. *Fuel* 85, 2671–2675. doi:10.1016/j.fuel.2006.04.015
- Vincent, J.-C., 1987. Green Coffee Processing, in: Clarke, R.J., Macrae, R. (Eds.), *Coffee: Volume 2: Technology*. Springer Netherlands, Dordrecht, pp. 1–33. doi:10.1007/978-94-009-3417-7_1

- Vyas, A.P., Verma, J.L., Subrahmanyam, N., 2011. Effects of Molar Ratio, Alkali Catalyst Concentration and Temperature on Transesterification of Jatropha Oil with Methanol under Ultrasonic Irradiation. *Adv. Chem. Eng. Sci.* 1, 45–50. doi:10.4236/aces.2011.12008
- Wang, Y., Ou, S., Liu, P., Xue, F., Tang, S., 2006. Comparison of two different processes to synthesize biodiesel by waste cooking oil. *J. Mol. Catal. A Chem.* 252, 107–112. doi:10.1016/j.molcata.2006.02.047
- Willems, P., Kuipers, N.J.M., de Haan, A.B., 2008a. Gas assisted mechanical expression of oilseeds: Influence of process parameters on oil yield. *J. Supercrit. Fluids* 45, 298–305. doi:10.1016/j.supflu.2008.01.010
- Willems, P., Kuipers, N.J.M., De Haan, A.B., 2008b. Hydraulic pressing of oilseeds: Experimental determination and modeling of yield and pressing rates. *J. Food Eng.* 89, 8–16. doi:10.1016/j.jfoodeng.2008.03.023
- Williamson, K.L., 2003. *Macroscale and microscale organic experiments*, 4th ed. Houghton Mifflin, Boston.
- Yao, L., Schaich, K.M., 2015. Accelerated Solvent Extraction Improves Efficiency of Lipid Removal from Dry Pet Food While Limiting Lipid Oxidation. *J. Am. Oil Chem. Soc.* 92, 141–151. doi:10.1007/s11746-014-2568-1
- Yen, W.J., Wang, B. Sen, Chang, L.W., Duh, P. Der, 2005. Antioxidant properties of roasted coffee residues. *J. Agric. Food Chem.* 53, 2658–2663. doi:10.1021/jf0402429
- Yusup, S., Khan, M.A., 2010. Base catalyzed transesterification of acid treated vegetable oil blend for biodiesel production. *Biomass and Bioenergy* 34, 1500–1504. doi:10.1016/j.biombioe.2010.04.027
- Zhang, Y., Dubé, M.A., McLean, D.D., Kates, M., 2003. Biodiesel production from waste cooking oil: 2. Economic assessment and sensitivity analysis. *Bioresour. Technol.* 90, 229–240. doi:10.1016/S0960-8524(03)00150-0
- Zuorro, A., Lavecchia, R., 2012. Spent coffee grounds as a valuable source of

phenolic compounds and bioenergy. *J. Clean. Prod.* 34, 49–56.
doi:10.1016/j.jclepro.2011.12.003